POLITECNICO
MILANO 1863

SCUOLA DI INGEGNERIA INDUSTRIALE
E DELL'INFORMAZIONE

Modelling of Ultrasound Accelerated Whisky Maturation Process

TESI DI LAUREA MAGISTRALE IN
FOOD ENGINEERING
INGEGNERIA ALIMENTARE

Authors: **Beatrice Fontana, Patrick Victor Nerito**

Student ID: 10628842, 10671653
Advisor: Professor Maurizio Masi
Academic Year: 2023-2024

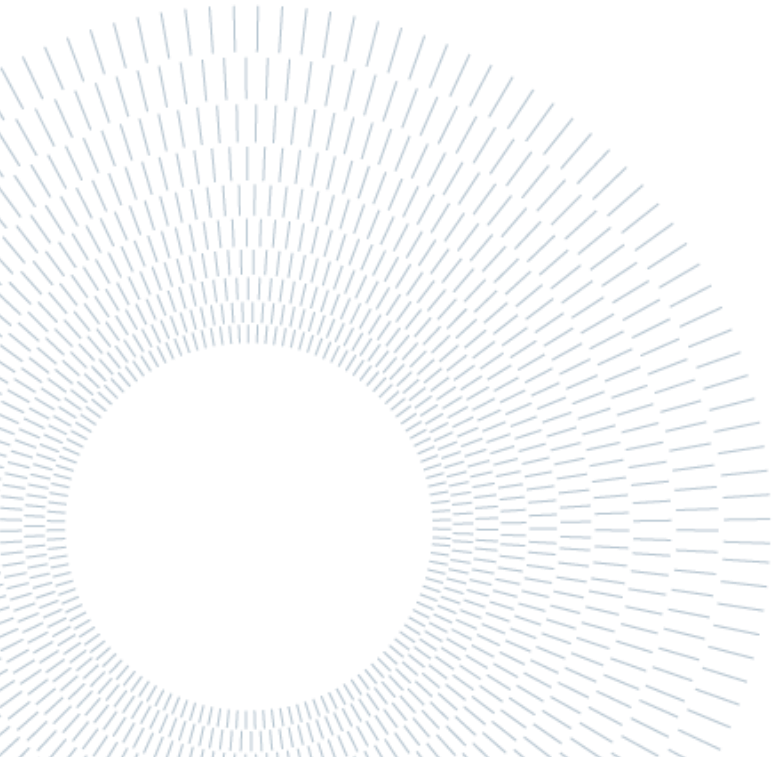

Abstract

Whisky maturation is one of the most critical stages of the entire production chain, as it contributes significantly to the development of the sensory profile in terms of flavour, colour and overall quality. However, the conventional techniques for this process have been shown to be expensive and time-consuming, raising interest worldwide in the search for alternative technologies that can speed up the distillate's ageing process while maintaining its characteristic properties.

This thesis explores the potential of ultrasound technology as a promoter of the ageing process. The specific objective is to develop a mathematical model that can reproduce the evolution over time of some of the most important lignin and tannins derived congeners in a sonicated system, such as syringaldehyde, syringic acid, conifer aldehyde, vanillin, vanillic acid, and gallic acid.

The work starts with a careful analysis of the experimental data obtained from the work of De Taddeo and Ramirez, referred to samples subjected to an accelerated ultrasonic ageing process conducted under different operating conditions.

Thorough bibliography research about the distillate's main features and the maturation stage under ultrasound effects led to the formulation of a model that incorporates both diffusive and kinetic phenomena typical of a hybrid regime, well represented by the Shrinking Core Model, usually employed for describing non-catalytic surface reactions between solids and fluids.

The manipulation of the significant parameters of the process, resulted in diffusivities and kinetic constants, allowed the derived systems to replicate the profile of experimental concentrations over time. The final proposal accurately depicts the species evolutionary tendencies, showing a higher relevance in diffusion processes over the kinetic ones, but underestimates the numerical value of some parameters.

The study provides a good starting point for describing and predicting the dynamics of the accelerated whisky maturation process and highlights the critical issues to be taken into account for future improvements.

Key-words: whisky, maturation, ultrasound, mathematical model, Shrinking Core Model.

Abstract in italiano

La maturazione del whisky è uno dei passaggi più critici di tutta la linea di produzione, in quanto risulta essere il principale contribuente dello sviluppo del profilo sensoriale in termini di aroma, colore e qualità complessiva. Tuttavia, i tradizionali metodi impiegati per questo processo sono stati dimostrati essere molto dispendiosi sia in termini di tempo sia per quanto riguarda i costi, trascinando l'intero scenario globale ad accrescere interesse verso la scoperta di tecnologie alternative in grado di accelerare l'invecchiamento del distillato preservandone le caratteristiche finali.

Questa tesi esplora il potenziale della tecnologia ad ultrasuoni come promotore delle complesse interazioni chimico-fisiche che governano la maturazione ed ha come particolare obiettivo lo sviluppo di un modello matematico in grado di descrivere l'evoluzione nel tempo di alcuni tra i composti chiave del processo, tra cui siringaldeide, acido siringico, coniferaldeide, vanillina, acido vanillico e acido gallico.

Il seguente lavoro si sviluppa a partire da un'attenta analisi dei dati sperimentali raccolti da De Taddeo e Ramirez, riferiti a campioni soggetti al processo accelerato di maturazione tramite ultrasuoni e condotti al variare di alcune condizioni operative.

Una completa ricerca bibliografica sulle principali caratteristiche del whisky e sul processo di maturazione condotto con la tecnologia ad ultrasuoni ha portato alla formulazione di un sistema che considerasse sia i fenomeni diffusivi sia l'aspetto cinetico tipici di un regime ibrido, ben approssimati dal modello Shrinking Core, tipicamente utilizzato per descrivere reazioni superficiali non catalitiche tra un solido e un fluido.

La manipolazione dei principali parametri che influenzano il processo, risultati essere costanti cinetiche e coefficienti di diffusione, ha portato alla derivazione di un sistema capace di replicare l'andamento delle concentrazioni nel tempo dei dati sperimentali e che evidenzia un maggiore contributo diffusivo rispetto a quello cinetico; tuttavia, i valori numerici di alcuni di questi parametri risultano essere notevolmente sottostimati.

Questo studio fornisce un buon punto di partenza per descrivere e prevedere le dinamiche del processo di maturazione accelerata del whisky ed evidenzia le criticità di cui tener conto per futuri miglioramenti.

Parole chiave: whisky, maturazione, ultrasuoni, modello matematico, modello Shrinking Core.

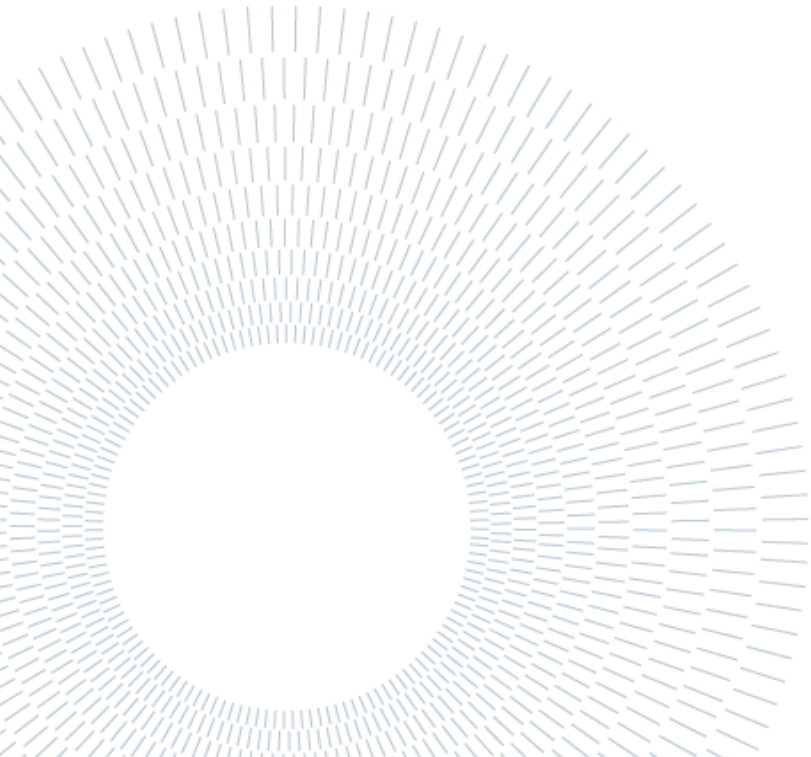

Contents

Abstract ..... **i**
Abstract in italiano ..... **iii**
Contents ..... **vii**
1 Whisky **3**
1.1. Whisky origin 3
1.2. Whisky market 6
1.3. Whisky production process 8
1.3.1. Raw materials selection 10
1.3.2. Malting 10
1.3.3. Mashing 11
1.3.4. Fermentation 11
1.3.5. Distillation 12
1.3.6. Maturation 14
1.4. Maturation 15
1.4.1. Maturation influencing factors 15
1.4.2. Wood composition 19
1.4.3. Maturation associated costs 24
1.4.4. Accelerated maturation 25
2 Ultrasound **30**
2.1. Ultrasound definition 30
2.2. Ultrasound mechanism: cavitation 31
2.3. Ultrasound effects and applications 32
2.4. Ultrasound food industry applications 35
2.4.1. Ultrasound-accelerated whisky maturation 36
3 Aim of the thesis **38**
4 Materials and methods **39**
4.1. Materials 39
4.1.1. Experimental set-up 39
4.1.2. High-performance liquid chromatography (HPLC) 40
4.2. Methods 41

4.2.1. Kinetic models 42
4.2.2. Mathematical approach 48
5 Model development 51
5.1. Data analysis 51
5.1.1. Data inspection 53
5.1.2. Data visualization 54
5.1.3. Data cleaning and selection 57
5.2. Model formulation 64
5.2.1. Coniferyl and Syringil families 65
5.2.2. Gallic acid 87
5.3. Results and discussion 91
5.3.1. Syringil family 91
5.3.2. Coniferyl family 101
5.3.3. Gallic Acid 111
5.4. Further development 117
6 Conclusions 119
Bibliography 121
A Appendix 133
A.1. Data visualization 133
A.2. Data collection and calculations 137
A.2.1. Solution characterization 137
A.2.2. Headspace characterization 139
A.2.3. Wood matrix characterization 140
A.2.4. Surface to volume parameter 141
A.2.5. Theoretical diffusion coefficients 142
A.3. Residence times evaluation 143
A.4. Step-charts 144
List of Figures 149
List of Tables 153
List of symbols 154
Acknowledgments 161

1 Whisky

Whisky is one of the most renowned distilled spirits in the world, moreover, it boasts a complex history and deep-rooted traditions.

The following chapter will explore the origins of whisky and its development into a worldwide product with a competitive global market.

The main defining steps of its industrial manufacturing process, malting, mashing, fermentation, distillation, and maturation, will next be briefly explained in a comprehensive view of its production.

The chapter will conclude with an in-depth look of the maturation step investigating its main influencing factors. Following this, the characterization of chemical-physical processes will be described, and lastly, novel approaches to improve process efficiency will be introduced.

1.1. Whisky origin

As stated by the Food and Agricultural Organization (FAO) [1]:

"Whisky is a spirit drink produced by the distillation of a mash of cereals, saccharified by the diastase of the malt contained therein, with or without other natural enzymes, fermented by the action of yeast, distilled at less than 94,8 % vol so that the distillate has an aroma and taste derived from the raw materials used and matured for at least three years in wooden casks not exceeding 700 litres capacity."

Etymologically, the word 'whisky' is thought to be derived from the Gaelic word for 'water of life', 'uisge beatha' or 'usquebaugh', that represents how Irish and Scots monks called their distilled barley beer. In this sense, all distilled alcoholic beverages were once thought to have significant therapeutic, even mystical, qualities, and their recipes were left to the clerics of the day [2].

Despite the fact that nowadays whisky has become one of the trademarks of Scottish, its production is most likely an Irish invention that has been carried across to Scotland by monks between the years 1100 and 1300 [2]. Irish Christian monks obtained the

secrets of distilling from the Moors of Spain during their voyages to the Mediterranean in the 11th century; in 1405 in the Annals of Clonmacnoise appeared their first recipe: a distilled alcohol based on essential oils and herbs, known as aqua vitae. Irish whisky saw its peak in the early 1900s with 88 distilleries exporting 12 million cases annually [3]. However, political unrest, economic policies, and the reluctance to adopt column still technology led to the industry's decline, giving Scottish producers a competitive edge [4].

The earliest documentation of Scottish whisky is the Exchequer Rolls of 1494, written by order of the King James IV, to commission the monk Friar John Cor 'eight bolls of malt' to produce aqua vitae. The King was the first to famously appreciate aqua vitae [5]. Even if more than its taste, he recognized its potential utility as a component in gunpowder production. This is probably due to the fact that early distillation practices involved just two stages [6], fermentation and single distillation leading to a raw spirit: strong and harsh in flavour [7].

Whisky became more widely known as a beverage by the 16th century, when the first production regulations were also established[8]. The introduction of stringent rules and taxation caused a series of conflicts between authorities and producers in the 17th century which resulted in an illicit market [9], which only ended in 1823 following a tax reduction [10].

The 19th century marked the rapid global rise of Scotch whisky, driven by entrepreneurial innovation, technological advancements, and favourable circumstances. The invention of continuous stills by Aeneas Coffey in 1830, for example, revolutionized whisky industry enabling the distillation of grain whisky and allowing the production of variegate and innovative whisky blends [7]. The phylloxera epidemic in Europe 1880-1900, France mainly, created a shortage of wine, brandy and cognac [5], allowing whisky to dominate the market. The formation of trade associations and the consolidation of distilleries under the Distillers Company Ltd (DCL) in 1877 brought stability to the industry [7]. Nowadays, the Scotch whisky industry has evolved into a global symbol of tradition, craftsmanship, and quality.

The history of American whisky traces its roots to Ireland and Scotland. European immigrants in the 17th and 18th centuries brought the tradition of producing distillates to North America, with early spirits likely derived from local resources like berries, fruits, vegetables, and grains: Applejack, a distilled apple cider, is credited to Scottish immigrant William Laird around 1700 [11]. Even though American grains like maize and rye were hard to separate from the mash, which typically resulted in burned

whisky aromas, distilling became feasible in the New World because of the abundance of grain output: it often happened that Whisky was produced unnecessarily to address practical challenges such as grain storage losses due to spoilage, rodents, and insects [11].

Whisky remained a marginal spirit until the late 18th century, period in which commercial distilling began to increase and therefore in which the first taxes and rules began to be imposed leading to rebellions [6].

Rebellions became a political challenge for President George Washington who offered incentives to distillers in order to relocate westward to the fertile land of Kentucky [12]. Here American whisky become to be called Bourbon denoting one of the first port from which it was traded [13]. For the same reasons mentioned above, the 19th century was a period of innovation and growth for American whiskey, which however was short-lived due to the arrival of Prohibition in the 20th century. Puritan influence banned alcohol production and consumption: distilleries were dismantled, and stocks destroyed, only limited production of "Prohibition Whiskey" was allowed for medicinal purposes [14]. The industry began recovering in the 1930s through exports, since 1933 when Prohibition was repealed, and legal alcohol production and consumption was resumed [7]. But even this time the stability lasted due to the Second World War.

Following the repeal of Prohibition and with the end of the War, federal regulations were established to ensure quality and consistency both in Scottish and American whisky and with the aim of avoiding counterfeiting to which the spirit has always been very susceptible. To qualify as bourbon, also nowadays, whisky must follow the guidelines reported in The Code of Federal Regulations 27 [11]: it needs to be made from a mash containing at least 51% maize (corn, rye, wheat, malted barley, or malted rye grain), aged for a minimum of two years in charred new oak barrels, and meet specific standards of quality. On the other hand, Scotch Whisky Act of 1988 and the 2009 Regulations, defined Scotch production standards [5] and its five distinct categories: single malt, single grain, blended, blended malt, blended grain [15].

By the early 2000s, Scotch whisky has solidified its position as a top global whisky, with American whisky serving as its primary rival to this day [14].

1.2. Whisky market

Whisky industry has evolved significantly in the last few centuries in response to geopolitical challenges and evolving consumer preferences [16].

Despite the many difficulties of periods such as the Prohibition period and the World Wars, the whisky industry is now thriving, driven by trends, such as globalization, that lead to a growing export market, by the demand for experiential consumption, denoting the interest of consumers in researching rare and collectible bottles, tastings and brand heritage [17], and by the growing popularity of craft distilleries due to the increase interest in unique and artisanal products [18].

Nowadays the global whiskey market is categorized based on product type, country of origin, and quality standards [17].

The latest categorization sees the market segmented into premium, super-premium, and high-end premium products [19], that mainly depends on price, craftsmanship, accessibility and brand reputation. In general, to define a product as premium it must meet four criteria: easy sippability, quality ingredients, a unique and full-bodied flavour, and be aged for longer than the minimum requirement according to The Distilled Spirits Council of the United States (DISCUS) [20]. High-end and super-premiums, on the other hand, are often rare, small batches produced in limited quantities.

As it is possible to observe from Figure 1.1, the premium whisky segment led the global market in 2024, driven by customers demand for high-quality at affordable prices. Meanwhile, the super-premium segment is expected to grow the fastest, fuelled by premiumization trends, rising disposable income, and strong branding strategies [19].

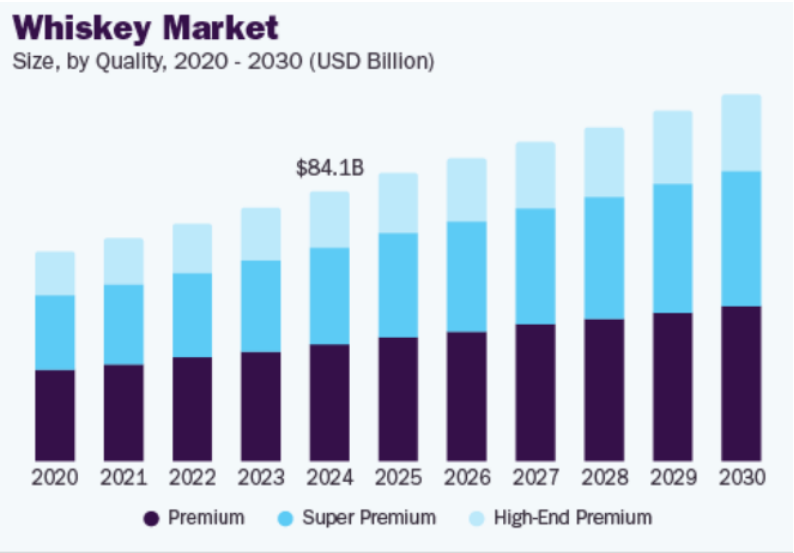

Figure 1.1: Whisky market fragmentation into premium, super-premium and high-end premium.

The main contenders in the global whiskey scenario are Scotch whisky, American whisky, Canadian whisky, Irish whisky and others of less importance coming from Japan, Thailand, France, China, and India. It remains not to be underestimated that new whisky-producing countries are continuously emerging powered by the rising of craft whisky movement. It is the case of Switzerland, Austria, Argentina, Belgium, Brazil, the Czech Republic, Denmark, Israel, Italy, Liechtenstein, Finland, Germany, Iceland, the Netherlands, New Zealand, Norway, Russia, and South Africa [21].

In 2024 the Scotch whisky industry dominated the market, followed by American bourbon, Canadian and Irish one as it is shown in Figure 1.2 [22].

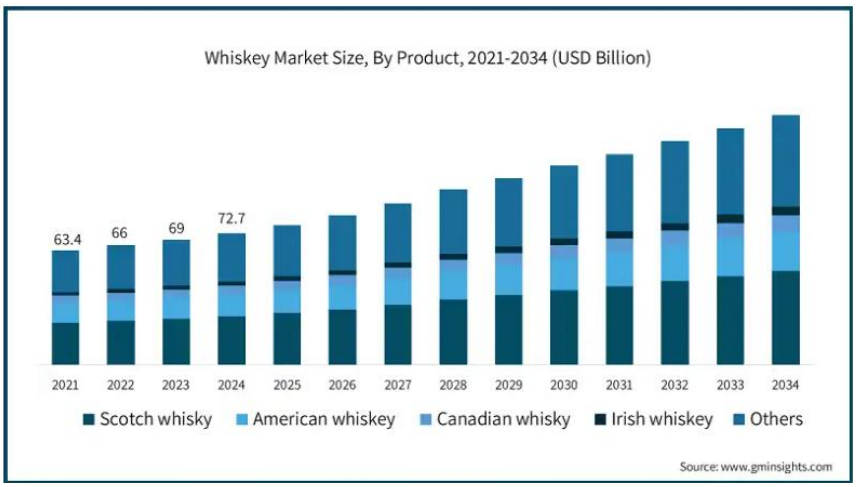

Figure 1.2: Whisky market fragmentation and size.

Its global popularity stems from rich traditions, diverse flavours, and strict production standards accomplishing the growing preference for high quality spirits.

Scotch industry has developed different array of brands and typologies to meet customer's demand diversification: single-malt Scotch, single-grain Scotch, blended-malt Scotch, blended-grain Scotch, and blended Scotch whisky are the main five recognized [21].

Malt whisky is crafted exclusively from malted barley using the pot still method, a batch process consisting of malting, mashing, fermenting, and distilling. The last step is usually carried out two to three times, after which the distillate remains to mature in casks for a minimum of three years [7].

In contrast grain whisky can either be made with 100% maize, wheat, or rye, or more commonly mixed in combination with malted barley and it is produced using a continuous distillation process. This method imparts the product paler and lighter character compared to previous one [3].

Blended whiskies make up most of the Scotch whisky market as they are viewed as more uniform and commercial thanks to their affordable pricing and consistent quality [23]. A blended Scotch Whisky is a blend of at least one single malt and one single grain whisky [15], this allows a wide variety of flavours resulting particularly attractive in young consumers.

The presence of grain whisky, usually in percentage around 40-60% of the blend, helps to unify the mixture. Most whisky experts instead focus on the single malts produced by Scottish distilleries which are often considered more authentic and distinctive in flavour [23].

1.3. Whisky production process

Whisky production involves three main ingredients: water, cereal (barley, rye, wheat, corn) and yeast, following a fundamental process that varies across styles, distilleries, and regions [24] [25].

Variations in whisky treatment such as the selection of raw materials, the equipment employed, and the duration of each processing step play a critical role in shaping its

chemical composition [3]. Thus, since each compound contributes distinct aromas, differences in production significantly influences the spirit's overall flavour profile. This is crucial for the whisky industry as flavour, along with colour [26], is a key indicator of product quality [25] and a primary factor in consumer enjoyment [27].

Volatile compounds must be present in sufficient quantities to trigger a response in consumers' receptors. This highlights the importance of controlling and regulating the whisky production process in order to achieve desired product specifications [28].

The whisky-making process involves many distinct phases such as cereal processing, milling, mashing, cooking, fermentation, distillation and maturation depending on the selection of raw ingredients, as it is shown in Figure 1.3 [29].

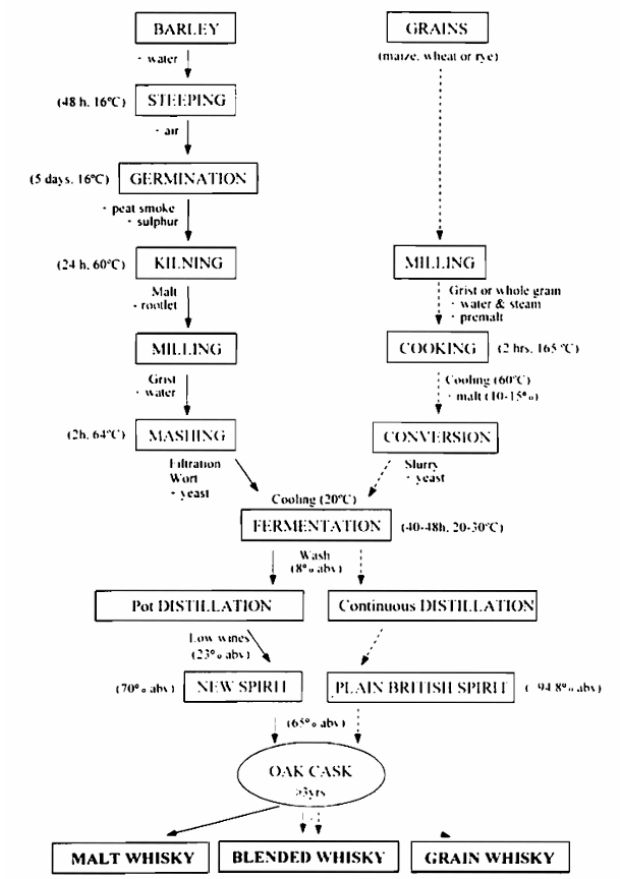

Figure 1.3: Whisky production process scheme.

The following paragraphs will only explain the most crucial steps of the industrial process that are commonly performed to make every variation of whisky.

1.3.1. Raw materials selection

Water and cereals are the two fundamental components used in the production of whiskey. The type of cereal adopted depends on the product that is being manufactured; typically, malt distillers use malted barley, while grain distillers use un-malted cereals such wheat, maize, and rye.

Referring uniquely to Scotch whisky being currently, as mentioned in the previous paragraph, the most popular worldwide, production mainly relies on wheat and barley depending on whether one is considering malt, grain or blended types.

The quality in finished whisky is obtained starting with the selection of quality raw ingredients.

In order to achieve a certain whisky distilling quality, the proper grains are bred and chosen using defined protocols and put through stringent testing and controlling processes [30].

The selected varieties must meet specific critical traits [31]which are categorised according to two different priority levels [8]:

- High priority accounts for resistance to splitting, rapid water uptake, high starch content, vigorous germination and low glycosidic nitrile potential.
- Medium priority, on the other hand, accounts for barley's specific and uniform size, low dormancy, good husk appearance.

Sustainability is now a key focus and mainly depends on a stable, high-quality cereal supply chain; an accurate selection of raw ingredients can also minimize environmental impact and reduce the industry's carbon footprint [32].

Water, besides being essential for most steps in the production process, constitutes between 40 % and 60 % of the product itself contributing to its final characteristics [33]. This is why an efficient supply of water is essential for whisky industry together with the choice of its source that strongly influences mineral salt and microbiological content [9]. Differences in salt concentrations affect whisky organoleptic properties and its pH, in particular the presence of salts helps to keep the pH down, for this reason most of Scotch distillers favours soft water [34].

1.3.2. Malting

After the selection of raw materials, with barley being the most widely used cereal source, the first real step in whisky production is malting. This process has the task of converting the starch in the grain into sugars essential for the fermentation process

with yeast. Malt formation occurs following three steps: steeping, germination and kilning [35].

Steeping is the process of soaking barley in warm water until its moisture content reaches 45 - 47%. A sequence of enzymes is activated after the target value is attained, preparing the barley seeds for germination [9]. During this stage, important enzymes as limit-dextrinase, proteases, α-amylase, and β-glucanase break down protein, starch, and cell wall linkages; these will only stabilize during the last kilning step. The malt is now dried, the water content is quickly lowered, and Maillard reactions are initiated, resulting in the production of the first aromatic compounds, such as pyrazines and furfurals, which give the liquor its caramel, toasted, or fatty flavours [3].

1.3.3. Mashing

Before the mashing process is started, the malt undergoes a milling stage where it is broken down into small particles of a size that depends solely on the mill being used [3]. This step gives the starch properties such as pasting, swelling, solubility, and digestibility, and also makes the enzymes involved largely more accessible [9].

Mashing is another fundamental step in the production of spirits; it is here that the malt is converted into a sugar-rich wort by the action of enzymes. The compound coming out of the milling process is mixed with hot water, due the contact with water starch undergoes gelatinisation, loses its crystalline structure and becomes amorphous. At this point, enzymes convert it into sugars in a process called saccharification. The last step is lautering and filtration and involves separating the must from the residual materials in order to make it ready for the next step [6].

A portion of the whisky's sensory profile develops during the mashing process influencing the blend aroma with vanilla, apple, hay, and herbal notes; congeners such phenolic compounds, aldehydes, and volatile sulphur compounds are observed in addition to the pyrazines and furans that are already present [21].

1.3.4. Fermentation

Fermentation in whisky industry is a stage similar to that of other alcoholic beverages, where yeast converts sugars into ethanol and carbon dioxide. However, a wide variety of organisms, such as other yeasts and bacteria, can be found in the malt or other cereals used to obtain the wort and can take part to the fermentation process [36].

Yeast produces a range of compounds, including acids, esters, aldehydes, ketones, other alcohols and sulphur-containing compounds, which significantly contribute to

the sensory character; moreover, the specific yeast strain used in the fermentation can have a considerable effect on the spirit's flavour profile, largely due to the varying secondary metabolites produced by different yeasts, and this is the peculiarity notable when aiming for a high alcohol yield [37].

Several factors affect the congener profile during fermentation, such as, as just said, the choice of the yeast strain and the mix of yeasts used, but also the design of the fermenter, aeration, duration of fermentation, wort composition and the potential presence of contaminating bacteria; another key factor is given by temperature; the fermentation process typically occurs at temperatures between 20 and 32 °C, resulting in an alcohol content of 5 – 10 % by volume as the yeast converts the soluble sugars; anyway, the heat released during the fermentation of sugars to ethanol causes the temperature to increase to 33 °C (or more during the early stage of fermentation, when the fermentation rate is greater), meaning that variations in temperature must be monitored to avoid undesirable changes in the spirit's quality [38].

1.3.5. Distillation

A crucial procedure for raising a generic liquid's alcohol content and concentrating the presence of specific volatile chemicals, both desired and undesirable, is distillation [35]. This is precisely the function assigned to this stage in the whisky production process; at the outlet, the distillate will have a greater alcohol content per volume of solution and will be concentrated with congeners that enhance the final sensory profile while eliminating unwanted components [9].

The process must be conducted at precise temperatures to avoid the production of undesirable compounds, so it is essential that a good heating system is coupled to the column also guaranteeing the initiation of chemical reactions that produce new congeners [39].

Depending on the whisky typology being processed, distillation can be conducted using a pot or a column still, each characterized by precise operative methods.

1.3.5.1. Pot still distillation

Pot stills, depicted in Figure 1.4, are commonly used in the production of malt whisky. It refers to a batch procedure where successive distillations are often performed.

Most of the times, the process can be broken down into two primary steps, known as wash and spirit distillations. In the first, undesirable chemicals are first skimmed, and

in the second, the final product is obtained in order to proceed to the next maturation step.

A third distillation may occur for enhancing the purity of the distillate which typically needs to achieve an alcohol content between 60 % and 70 % alcohol by volume [40] [41].

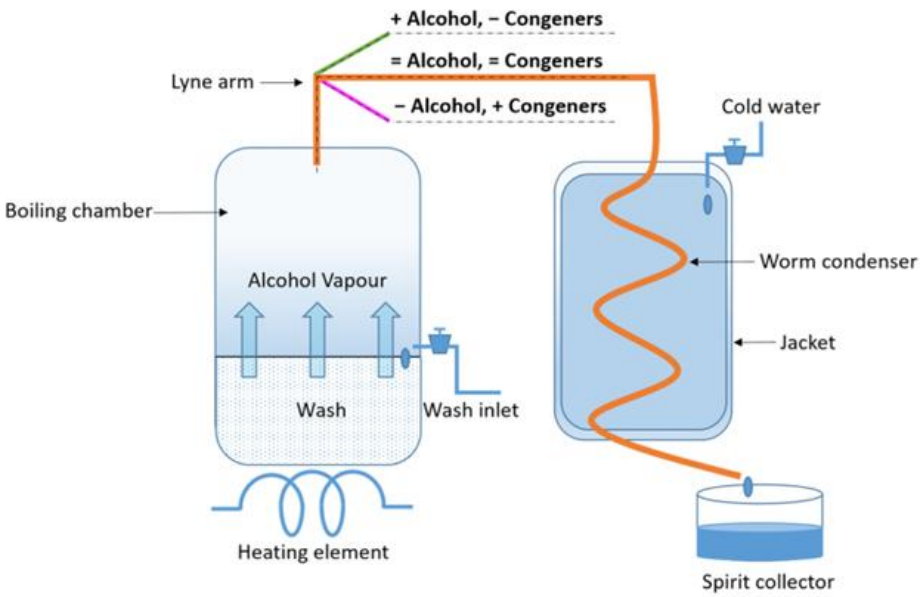

Figure 1.4: Pot still distillation configuration [41].

1.3.5.2. Column still distillation

Conversely, most American whiskeys, including bourbon, as well as plain grain whiskeys from any nation, are produced using column stills. Part of the reason this method is so much more effective than the last one is that it runs continually. The fermenting liquid is introduced from above and forced to descend each of the perforated plates that make up the distillation column. This stepped structure shown in Figure 1.5 combined with heated vapor jets that rise from below, firstly allows the separation of the liquid from undesired solid and guarantees the more volatile substances to ascend the column [40]. Through this process, the alcohol concentration increases until it approaches 95% ABV [41].

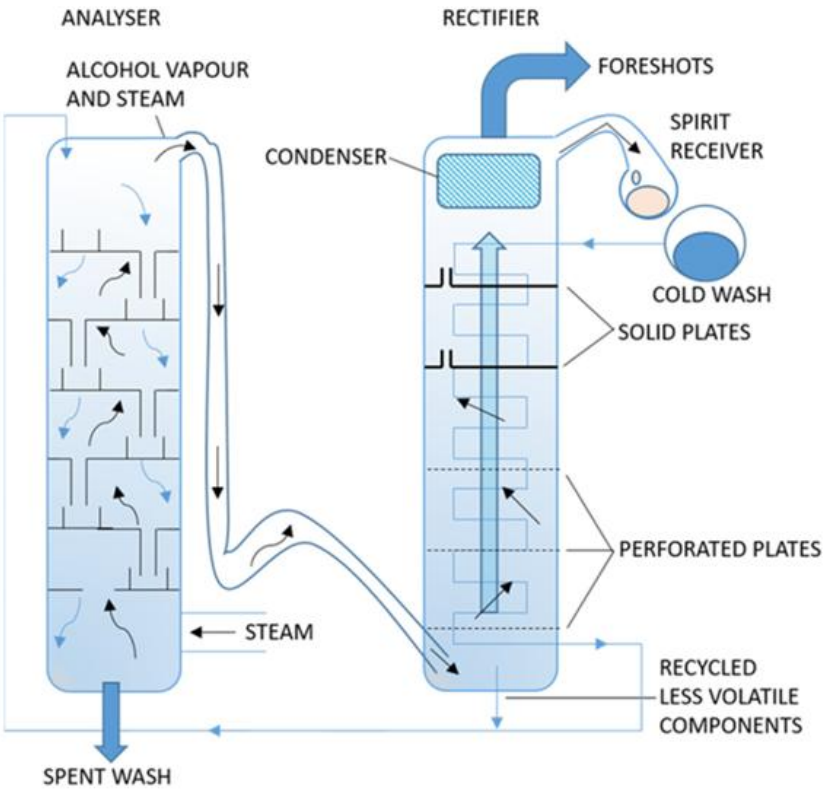

Figure 1.5: Column still distillation configuration [41].

1.3.6. Maturation

Freshly distilled spirits derived from the fermentation process are usually rather colourless and harsh in taste and possess an overpowering alcoholic content [42]; for these reasons, distilled spirits undergo maturation, a unique process that allows to obtain a more mature, mellow and smoother product, together with the development of the colour typical of each beverage. As for the other distillates, the typical flavour and colour of whisky are obtained after the maturation process, that accounts up to the 60 % of its final quality and taste [6]. Such modifications are the outcome of several physical and chemical processes that take place between the distilled matrix and the wooden barrels in which maturation is conducted; in particular, these phenomena include direct extraction of wood components, decomposition of macromolecules shaping the wood, reactions between the wood compounds and the liquid matrix, reactions involving only the wood compounds, reaction involving only distillate compounds, absorption or vaporization of unpleasant flavours [43], reduction of ethanol pungency and formation of stable clusters between ethanol and water [25].

Three types of reactions happen in the wooden cask: additive, interactive or subtractive. Additive reactions introduce new compounds to the spirit or elevate their concentrations, such as when extracting compounds from the wood; interactive is when oxygen diffuses into the casks, resulting in reactions between the molecules in the spirit and between these molecules and molecules from wood; subtractive reactions correspond to where compounds are lost through evaporation, desorption and oxidation [3].

To obtain the desired results and maintain its authenticity and reputation [44], whisky must be aged in wooden barrels for a period of at least 3 years, during which the final beverage will be influenced by several parameters that characterize the ageing process [45].

1.4. Maturation

The previous section provided a concise overview of each of the primary steps in the whisky production process, emphasizing the significance of ageing in forming the final product's sensory profile. This study focuses on this same stage; hence the next section will go into extensive detail on the physical and chemical processes involved, the key factors that affect it, and its overall significance in the production process. Finally, the associated challenges of a competitive market will be explored.

1.4.1. Maturation influencing factors

Maturation is a crucial process in whisky production as it is mainly responsible for the changes achieved in the final flavour, smell and colour profiles of the product [46]. Because of this, it is imperative that the working conditions under which this critical phase is carried out are closely monitored.

Actually, several factors, such as the kind of wood characterising casks, the composition of the recipe, the environmental conditions and the ageing time have an important influence on sensory and physico-chemical composition of the spirit [47]:

- Alcohol content

Whisky, as explained in Chapter 1 paragraph 1, consists of only three ingredients: water, ethanol and a cereal source. Therefore, precise amounts of each element must be used in order to get a balanced composition of the mixture.

In particular, ethanol plays a crucial role in the maturation of distilled spirits, influencing both the extraction of wood compounds and the final whisky's chemical and sensory features.

Depending on the category of whisky considered, the percentage of alcohol by volume of solution (ABV) lays in the range of 40 - 75%, which for Scotch is reduced to 63 - 67% [43].

This compound evolves as the process progresses and it undergoes evaporation, oxidation and definitely interacts with the wooden barrel. Oxidation causes the production of acetaldehyde, which negatively alters the taste of the final product [48].

Ethanol acting as a solvent for the extraction of wood-derived compounds plays a key role in the kinetic reactions involved and thus in ensuring the adequate presence of congeners in the final product. Due this it is partly responsible for the spirit's flavour and colour profile; in this latter case, it has been demonstrated that higher concentrations of ethanol will give mature whisky darker, redder hues because of an increase in the extraction of wood pigments, whereas lower concentrations will result in more brownish-yellow hues [43].

The changes it makes to the blend's physical characteristics are equally significant. As the ABV increases, the density of the whisky decreases in favour of its ability to penetrate the woody matrix, the viscosity decreases in the same way, simplifying its passage through the pores. On the other hand, this causes a lowering of the surface tension of the mixture, which leads to a limitation in the depth of penetration [49].

- Oxygen

Between the free surface of whiskey and the upper wall of the barrel there is a layer of air called headspace which is crucial for maturation [9]. It has in fact been demonstrated that completely full and hermetically sealed containers do not lead to any evolution of the sensorial profile of the product [50]. The headspace increases as the process progresses and due to the evaporation of volatile compounds allowing oxygen to diffuse into the spirit. Upon contact with the mixture this triggers a series of oxidation reactions which contribute to the removal of unwanted aromas and the formation of new shades of colour and flavour. Examples to cite are the conversion of ethanol to acetaldehyde, the breakdown of sulfur compounds, the oxidation of phenolic alcohols to give their respective aldehydes and acids and of tannins [51]. Concretely, studies have shown that higher concentrations of oxygen correspond to

higher contents of lignin derived congeners which give an intense flavour; vice versa, lower concentrations will lead to a whiskey with more harmonious and less astringent notes [50].

- Environmental conditions

The environmental conditions to which the ageing process is subjected, including temperature, pressure and humidity, play an important role on the final characteristics of the product.

In general, it is widely known that high temperatures increase chemical reaction rates, coherently it has been demonstrated that congeners level increases with storage temperatures [42]. In addition, reference is made to the portion of whisky that is lost through evaporation during the process. In the presence of high temperatures and low relative humidity, water tends to evaporate more quickly causing an overall loss of product, as a consequence an increase in ABV over time is expected which, on one hand can cause negative alteration in final sensorial whisky profile, on the other hand confers an enhancement in the release of wood congeners accelerating the overall maturation process [52].

Although using conditions of this type could result in a curious and explorable way to reduce total maturation times, the traditional Scottish method prefers long times and slow maturation processes conducted at room temperature and in humid environments in order to limit the evaporation of water and obtain a gradual slow reduction in ABV [53].

- Ageing time

Traditionally, whisky is matured in barrels for a minimum of three years before consumption, nonetheless, this procedure can be carried up till 18 years. Whisky sensory properties are known to improve over time and with the completion of complex series of chemical reactions that alter its composition. In particular, some studies found that most of chemical changes occur between 10 – 12 years and 14 – 16 [54]. After the sixteenth year the composition of spirit seems to be stabilising. In conclusion, the sensorial profile of whisky improves as the ageing time increases.

- Wooden barrels

One of the most relevant aspects to take into account are the characteristics of the barrel used throughout the process [55]. Although there are other ways to carry out the maturation process, like using stainless steel containers, wooden casks are still the preferred method. This because through its interaction with the spirit, it can enhance whisky complexity and quality.

When deciding which barrel to utilize, there are numerous factors to take into account. The selection of the wood's source plant is essential because it must give the barrel the mechanical and physical characteristics needed for the process and for the entire duration of the barrel's life, moreover the precise chemical composition of the wood, including all of its compounds, determines the final whisky's flavour and colour profiles [9].

Oak wood is currently the most widely used in its two American and European variants due to its strong characteristics in terms of durability, permeability and chemical composition [43].

American oak is characterized by low porosity and permeability, its structure guarantees that oxidation processes occur slowly and controlled [47]. Its composition is rich in compounds derived from lignin which are mainly responsible for the flavor profile of whisky. European oak, on the other hand, is richer in tannins, favoring a rapid development of the whisky color profile but making the development of an intense flavor slower [49].

Other types of wood explored and used in different regions of the world are acacia, chestnut, cherry, mulberry, and Brazilian wood [42].

During the maturation stage the wood undergoes major changes as a result of the impregnation with the solution it comes in touch. It is common practice to reuse the barrels for other maturation processes in which can also be involved a different spirit [56].

Compared to barrels that have already been used in previous maturation processes, unused barrels result in higher concentrations of lignin, tannins, and aromatic aldehydes. These substances diminish with increasing utilization until they are present in nearly insignificant amounts, at which time the barrel is deemed exhausted and hence no longer useable. Since each maturation cycle results in a very slight loss of each of the compounds listed, it has been luckily proven that this is a very slow depletion [56].

Lastly, using a cask that has already been impregnated with a particular spirit also contributes to the whiskey's flavour profile. This technique is called secondary maturation and it is widely used for whisky ageing processes [3].

1.4.2. Wood composition

Wood is a fibrous, porous and hard substance composed of cellular and intracellular components; the three main organic polymers responsible for the cell structure of wood are cellulose, hemicellulose and lignin, distinguished by their long chain and sugar unit composition [42]; these components have the most impact on the whisky flavour, where lignin being the most relevant since, as will be discussed soon, its degradation leads to the formation of congeners that confer the typical organoleptic features to whisky. Another class of key compounds is represented by phenolic compounds among which a major contribute is assigned to tannins, that add bitterness and astringency to the beverage, as well as affecting its colour; moreover, they are helpful in removing unwanted sulphur notes [3].

In the following paragraph a brief insight of each compound is reported:

- Cellulose

Cellulose is the most abundant component and the structurally key component, accounting for about 40-50% of the entire cell volume; this component is a linear polymer made up of glucose units connected by β-(1,4)-glycosidic linkages. The hydrogen bonding of the cellulose chains results in the development of fibrils which contribute to the formation of a structure on which the other wood constituents are built [57]. The hydroxy groups also determine the physical and chemical behaviour, since they can form two types of hydrogen bonds depending on their location in the glucose units. Moreover, cellulose is rather difficult to isolate from wood in its native intact state because it is intimately associated with hemicellulose and lignin.

- Hemicellulose

Another major constituent of wood is called hemicellulose, which serves as the matrix substance for the cellulose superstructure, so it provides structural integrity to wood. In general, hemicellulose constitutes between 20 and 35 % by weight of wood, has a lower molecular weight than cellulose and may contain short side chains. The

carbohydrate composition of hemicellulose can vary and is usually composed of a combination of 5-carbon sugars such as xylose and arabinose, and 6-carbon sugars typified by glucose, mannose, and galactose. Hemicellulose is closely associated with cellulose via hydrogen bonding and van der Waal's forces. Compared to cellulose, it is susceptible to chemical degradation due to its solubility and instability [58].

- Lignin

Lignin is the third major component of wood, with mature wood containing between 18% and 38%. It is a three-dimensional, highly branched, polyphenolic molecule of complex structure and high molecular weight; it serves as a cementing material that assists in binding wood cells together. Lignin is one of the most complex natural compounds, making its separation and identification particularly difficult. Differently from cellulose and hemicellulose, it is water insoluble and requires covalent bond cleavage prior to hydrolysis [3].

Based on the phenylpropane units, lignin can be classified as G-lignin (with coniferyl units), H-lignin (with p-hydroxyphenyl units) and S-lignin (with syringil units), as can be seen in Figure 1.6. For the maturation of whisky, a wood with a high concentration of S and G-type lignin wood is employed [6].

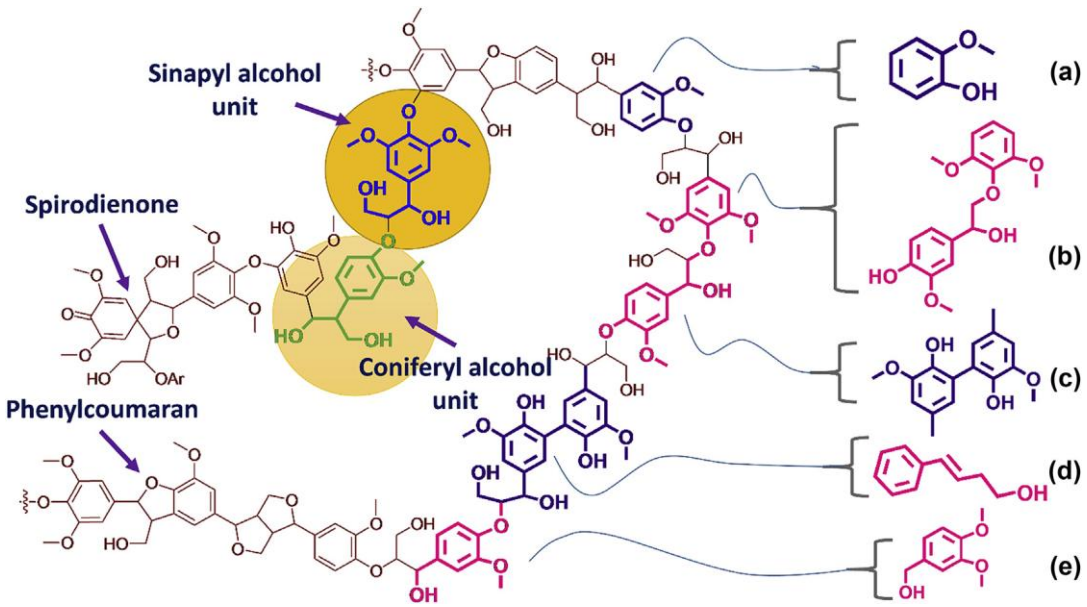

Figure 1.6: Lignin representation and its phenylpropane units [59].

- Tannins

The term tannin is widely applied to a complex large biomolecule of polyphenolic nature having sufficient hydrolysis and other suitable groups, such as carboxyl, to form strong complexes with various macromolecules [60].

Tannins can be subdivided into two main groups: hydrolysable tannins and condensed tannins. Hydrolysable tannins are composed of ellagic acid and gallic acid with a sugar core of mainly glucose; condensed tannins, instead, are composed of flavonoids without a sugar core [61]. The acid hydrolysis of hydrolysable tannins leads to the formation of gallic acid, ellagic acid or other similar species [62].

1.4.2.1. Lignin-derived congeners

One of the main mechanisms among the multiple chemical pathways that contribute to the development of flavour and generally to the quality of whisky is the degradation of lignin.

Two main pathways are differentiated, one involves the direct extraction of phenolic compounds from the wood that enter directly into the distillate, the other is the breakdown of lignin through interaction with ethanol to give an ethanol-lignin complex that tends to degrade into simpler phenolic compounds later in the course [48].

This process, known as ethanolysis, follows distinct kinetic patterns and leads to the release of various phenolic compounds evolving over time and that have a major impact on the final sensory profile of the aged whisky.

The sensory profile of distillates is given by the simultaneous participation of numerous chemical compounds that are formed throughout the steps of their industrial processes. It is therefore complicated to attribute a specific aroma to each single chemical, but sensory attributes such as smoke, woody, spicy and toasted are associated with phenolic compounds [3].

Lignin-derived congeners are divided into two main broad categories the coniferyl and syringil groups [48]. Both show similar chemical pathways that follow a clear kinetic sequence in which firstly the alcohols rapidly degrade into cinnamaldehyde, followed by benzaldehyde formation and finally the respective benzoic acid which may esterify in the presence of alcohol [63].

Studies have revealed that the concentrations of these two classes of aromatic compounds increase throughout the ageing process following a hyperbolic trend. This suggests that a more rapid extraction will take place during the early stages, destined to gradually settle over time [43].

Syringil - group

The syringil group includes the compounds sinapyl alcohol ($C_{11}H_{14}O_4$), sinapaldehyde ($C_{11}H_{12}O_4$), syringaldehyde ($C_9H_{10}O_4$), syringic acid ($C_9H_{10}O_5$) and the ester ethyl syringate ($C_{11}H_{14}O_5$). Their kinetic scheme is simple and involves the formation of the above-mentioned compounds in series through repeated reactions as illustrated on the right in Figure 1.7. Sinapyl alcohol derives from lignin degradation by ethanol, which is rapidly oxidized into sinapaldehyde. The reaction that leads to the formation of syringaldehyde is a retroaldol cleavage involving water as main reactant [64]. Another oxidation brings to syringic acid, which in ethanol presence can undergo esterification giving ethyl syringate compound.

Coniferyl - group

The coniferyl group includes the compounds coniferyl alcohol ($C_{10}H_{12}O_3$), coniferaldehyde ($C_{10}H_{10}O_3$), vanillin ($C_8H_8O_3$), vanillic acid ($C_8H_8O_4$) and its ester ethyl vanillate ($C_{10}H_{12}O_4$).

The reaction scheme as for the case of syringil is illustrated in Figure 1.7 on the left. Coniferyl alcohol is the product of ethanolysis of lignin, which quickly oxidizes to give coniferaldehyde. The reaction that leads to the production of vanillin is instead retroaldol cleavage, which takes place in the presence of a water molecule. Vanillin then oxidizes into vanillic acid, which in the presence of ethanol can undergo esterification with the formation of ethyl vanillate [64] [65] .

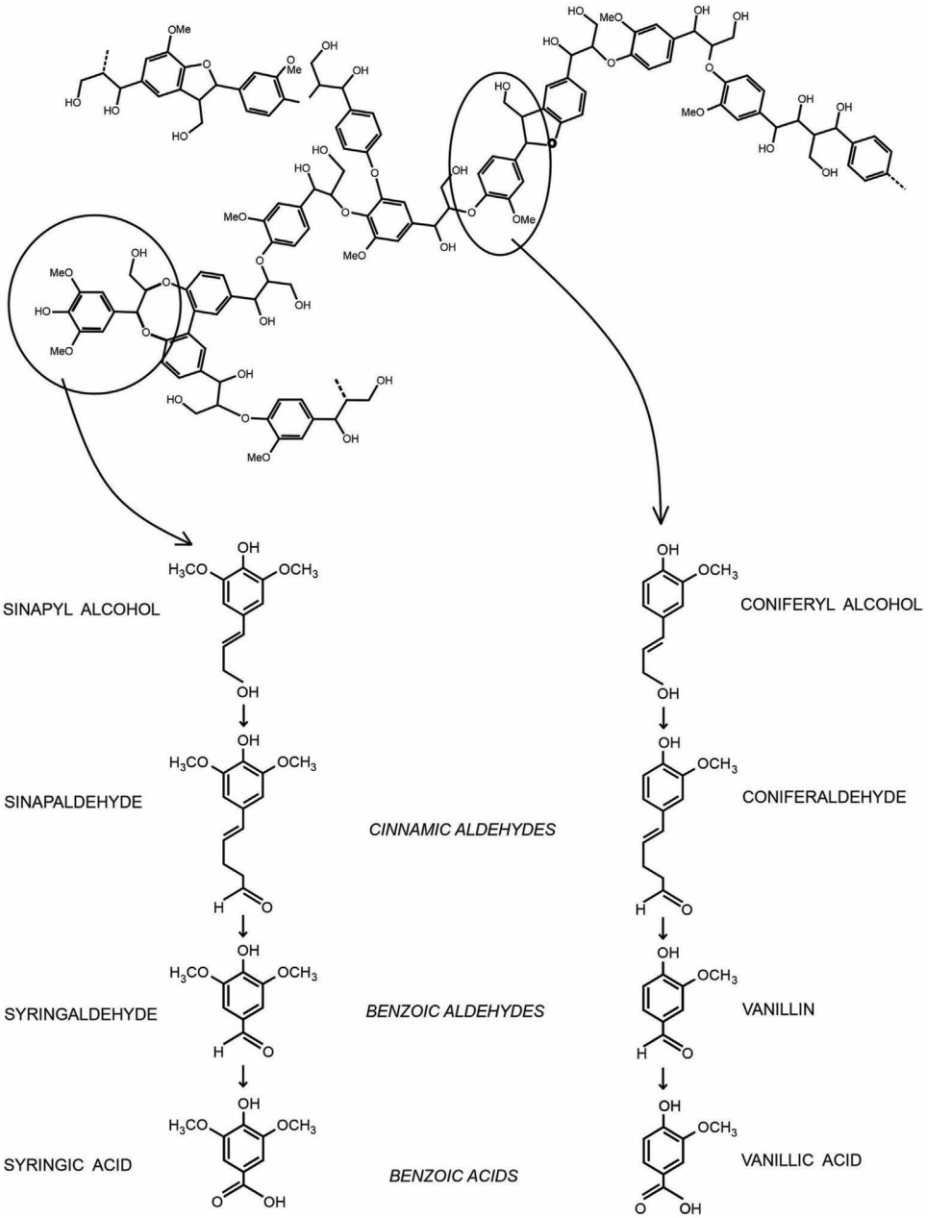

Figure 1.7: Syringil and Coniferyl reaction scheme [55].

1.4.2.2. Tannins - derived congeners

As already mentioned before, the heterogeneous nature of tannins implies that there are many possible chemical reactions paths these compounds can undergo; however, the field of interest regards the only hydrolysable tannins. The hydrolysis of gallotannins and ellagitannins, in fact, is a very well-known reaction that produces gallic acid and ellagic acid [66].

In particular, the hydrolysis of gallotannins has been found to be dependent on the pH and temperature of the solution and on the liquid matrix in which the reaction is

conducted, with particularly favourable conditions in a water-methanol and water-ethanol mixtures [67].

The proposed reaction scheme for the hydrolysis of gallotannins is reported in Figure 1.8:

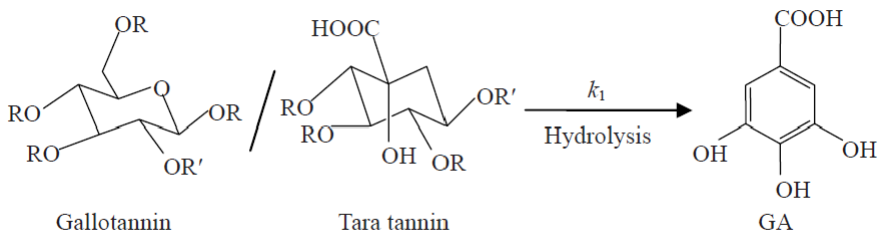

Figure 1.8: Hydrolysis of tannins [66].

However, gallotannins are characterized by an extremely complex kinetic scheme, and their hydrolysis in some cases, differently from what is represented above, is reversible, meaning that the reaction of gallic acid molecules with water leads to the original compounds, that are gallotannins [68].

1.4.3. Maturation associated costs

As already discusses, whisky is an important spirit that can be classified in many classes and types, according to the production region, the raw materials selected and the production process [69]. Despite the several differences existing between whisky's typologies, producers of whisky always must deal production costs, that include all the costs across the whole supply chain: raw materials costs, equipment costs, energy costs, labour costs, warehousing costs for both raw materials and finished products, financing costs.

The ageing phase accounts for a sizeable portion of the total expenses that each business must bear [8]. Whisky, in fact, as other distilled spirits, needs to be stored for a such number of years, and this implies a relevant impact both on the total production costs and the price the final consumer has to pay. Referring to the former, the issue is not related to the delay between the manufacturing time and the time of sale, because there is an adequate capital available to finance a company's production cost while waiting for the sale of the produced stock. The additional costs are given, instead, by wood costs and warehousing costs: wood costs are related to the casks used during maturation, in addition to regeneration and other treatments after their second use,

while warehousing costs concern the maintenance costs of the facilities where the barrels are placed during ageing and additional costs related to insurance on the maturing batches. These costs greatly depend on the region, the size of the company and the quality of the final product; anyway, despite the difficulty in providing a precise estimation, it can be concluded that a shortening of the ageing period through the novel technologies that will be discussed later on could also lead to a reduction in the total production costs [70]. This justifies the effort to develop new techniques that will enable the production of a beverage with the same intricate sensory profile as traditional approaches, but in a shorter amount of time.

1.4.4. Accelerated maturation

Most whisky's sensory qualities are imparted through aging, making it a crucial step in the whole production. Nevertheless, it is a slow process that, according to rules and regulations, requires at least three years for the product to meet stringent quality criteria.

In this regard and in order to find more efficient alternatives both in terms of process costs and time invested, several scientific studies have been advanced concerning innovative technologies capable of accelerating the chemical-physical processes characterising maturation.

Beginning with straightforward modifications to the conventional process of storing the distillate in casks, like adding barrel pretreatments or wood fragments to the mixture, alternative physical techniques that call for the use of specialized equipment have been put forth to change the process's operating conditions and thereby interfere with the chemical reactions that are the main players in maturation.

1.4.4.1. Wood fragments

The introduction of wood fragments into stainless steel barrels is an alternative maturation technique approved by the European Union in 2006. The technique is based on the concept of maximizing the contact surface between wood and liquid, thus promoting the release of congeners [71].

There are several factors to take into account in order to maximize the effectiveness of the technique including the size and shape of the chips, the level of toasting and the type of wood used. Small fragments lead to faster extractions, vice versa, the release

of congeners will occur more gradually; the level of toasting and the preferential choice of a specific wood composition directly impact the final aroma of whisky, contributing to different flavours [72].

It has been demonstrated that with this technique the sensorial characteristics of samples aged according to the traditional method for 70 days can be imitated in just 35 days [73].

Although the use of wood fragments brings the following advantages, compared to the traditional method a substantial difference has been identified in the concentrations of volatile compounds which therefore leads to variations in the sensory profiles of the finished product which make perfect replication difficult. Some, such as vanillin, are detected in larger quantities, others, such as acetovanillone, do not reach the same standards [47].

1.4.4.2. Charring

Charring is a pre-treatment that can be done in a barrel. It involves exposing the wood to a direct flame, which creates a layer of burned wood that has a big impact on how the wood interacts with the liquid. This method enhances the release of aromatic compounds like vanillin, syringaldehyde, coniferaldehyde, and sinapaldehyde, all of which are already known to be important contributors to whisky's sensory profile, in addition to enriching the liquid with new compounds that would not exist without it. Charring changes some of the spirit's physical properties, such as adding oily and resinous qualities that make it smoother and deeper on the palate, in addition to changing the spirit's overall aroma [42].

1.4.4.3. Micro-oxygenation

Micro-oxygenation (MOX) is an efficient and scientific method to emphasize the maturation of alcoholic beverages while maintaining the traditional characteristics of the process. This technique consists of introducing small doses of oxygen into the distillates in order to accentuate the aromatic and color profile and improve their texture. Specifically, MOX improves the vitality of yeasts, increases color stability and polymerization of tannins, reduces astringency and herbaceous notes, minimizes the odor related to the presence of sulphites and certainly promotes oxidation reactions between congeners. This is a valid alternative which however requires further research into the consistency in the quality of the finished product obtained compared to the traditional method [71].

1.4.4.4. RSLDE

Rapid Solid–Liquid Dynamic Extraction is a particular innovation in the field of techniques for accelerating the maturation process [74]. This consists in creating a negative pressure gradient from inside the solid matrix to the outside which facilitates the extraction of the main aging compounds. The advantages of this technique, in addition to the reduction in the time required by the process, are the possibility of conducting everything at room temperature without the risk of degrading specific thermolabile compounds [39].

1.4.4.5. High temperature technique

Aging whiskey at high temperatures is one of the most classic acceleration techniques in existence. It is based on the fundamental principle that stands out in the Arrhenius equation which states that the speed of chemical reactions usually increases as the temperature does. However, the ability of this technique to reliably replicate the natural mimicry of traditional barrel aging is strongly debated. Firstly due to the presence of compounds susceptible to high temperatures and secondly because a sudden alteration of the process environment could alter the balance of the liquid-wood interaction [75].

1.4.4.6. High-pressure processing

High-pressure processing (HPP), also known as High Hydrostatic Pressure (HHP) is a non-thermal accelerated aging method which consists of applying pressures of around 100 and 600 MPa to the distillate using water as a compression medium [72]. By significantly reducing the characteristic times of the process, it is an efficient technique in terms of costs and energy as well as environmentally friendly. There are numerous advantages that it brings to the final quality of the product including a greater quantity of esters in the composition of the mixture which improve the flavor and odor profile, improvements to the density of the liquid and an overall reduction in acidity. The main limitation lies in the possible alteration of the distillate at a molecular level which requires further investigations [71].

1.4.4.7. Pulsed electric fields technology

Another technology used to accelerate maturation is that of pulsed electric fields (PEF), as can be seen from the name, it is a non-thermal method which instead exploits the application of short bursts of high-voltage electric fields. This physical process is known as electroporation and concretely leads to the increase of the membrane permeability of the wood cells by improving the extraction of key congeners [71].

In addition, to shortening maturation timeframes without altering the dynamics of the conventionally carried out process, PEF technology produces a number of benefits concerning the physical properties of the distillate, including as stability, clarity, and palatability [72]. Additionally, it causes some microbial species to become inactive and lowers the levels of contaminants like sulphur dioxide.

1.4.4.8. Gamma irradiation

Gamma irradiation (GI) is another non-thermal method for speeding up the maturation process. Its original use is to improve the shelf-life of the treated product by eliminating any contamination from microbes such as harmful yeasts and fungi, as well as insects [71].

In spirits' industry it uses gamma radiation to change the distillate's composition. Specifically, a notable increase in esters' concentrations was noted, which improves the processed beverage's flavour and taste. The concentrations of alcohol, volatile acids, and aldehydes also cause the sensorial profile to deviate from the traditional method [76].Customers' apprehension about the likelihood of discovering any radioactive remains in the final product is one of the primary drawbacks, notwithstanding the accompanying benefits. Tests have already been conducted to confirm that there are no traces to address this issue [72].

1.4.4.9. Microwave technology

In addition to being widely employed in the food business, microwave technology has the potential to improve the extraction of flavour components from wood and minimize ripening times.

The technique uses electromagnetic non-ionized waves, this generates heat quickly and uniformly through the migration of ions and the molecular rotation of the medium being used. In particular, the microwave action dilates the wooden barrel's pores, which promotes oxygen diffusion and speeds up the release of congeners into the mixture enhancing whisky's sensory profile. The primary cause of limitations is the challenge of implementing the technology on a large scale [71].

1.4.4.10.Nanogold photocatalysis and UV radiation

The combination of nanogold particles in presence of UV radiation act as catalysts for oxidation reactions occurring in maturation process. This technique generates free radicals that break down harsh sulphur compounds and aldehydes promoting the formation of key compounds such as acetic acid and ethyl acetate of big relevance in

shaping aroma profiles and spirits complexity. This method guarantees for time, costs and product quality optimization. The main challenge is regulatory and consumer acceptance due to the materials involved in the practice [77].

1.4.4.11. Ultrasound technology

Ultrasound is a low cost, non-hazardous technique in which cyclic sound waves generate cavitation phenomena, with the aim to accelerate reaction rates to obtain the same aromatic and colour profile in a shorter time; in order to make this technology effective, it needs a combination with wood fragments and an economic feasibility.

All the explanations of the phenomena induced by ultrasounds and the implications they have on production processes will be widely discussed in the next chapter.

2 Ultrasound

The last paragraph of the previous chapter highlighted several novel techniques that have been applying to accelerate the process of ageing of wine spirits and distilled beverages, among this whisky. The last cited technique indicates the ultrasound technology as a prominent and innovative method to obtain the desired beverage in a reduced period of time. Due to their peculiarity and versatility in different application fields, this chapter wants to give an insight about ultrasounds, starting from a generic description of the nature and the phenomena induced by them, to the physical and chemical processes they impact on, with a specific focus on the ageing of whisky.

2.1. Ultrasound definition

Ultrasound (US) is a low-cost, non-hazardous, and environmentally friendly technique that consists of cyclic sound waves with a frequency above 20 kHz that lie beyond the upper limit of human hearing [78]. Although the range of ultrasonic frequencies can be extended up to 100 MHz, it is customary to divide ultrasound into three distinct frequency regions: conventional power ultrasound, between 20 and 100 kHz, that especially affects chemical reactivity in liquids (although higher frequencies can also do so), high frequency or extended range for sonochemistry, between 20 kHz and 2 MHz, and diagnostic ultrasound, above 1 MHz and up to 10 MHz, with applications in both medicine and materials processing. The Figure 2.1 summarizes what has been just explained [79].

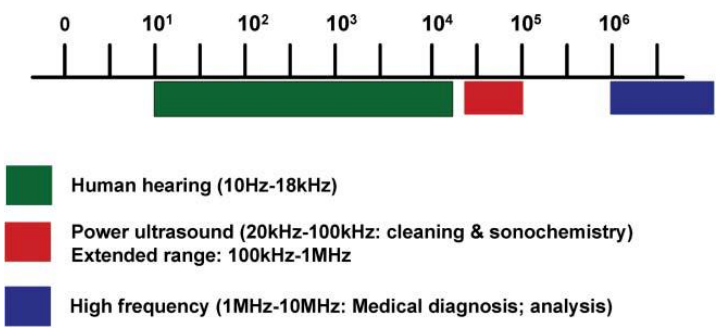

Figure 2.1: Ultrasound applications in different frequencies range [79].

In accordance with the subject matter of this paper, reference will be made to the first range mentioned as being specific to sonochemistry, a branch of chemical research

dealing with the chemical and physical effects and applications of ultrasonic waves [80].

2.2. Ultrasound mechanism: cavitation

Sound waves are acoustic pressure waves that consist of alternate compressions and rarefactions in the transmitting medium along the wave propagation direction [80]. Unlike light, sound waves do not directly interact with molecules to cause chemical reactions due to their large wavelengths, which are much greater than molecular sizes and ineffective to influence chemical bonds directly. Additionally, the energy contained in sound waves is far smaller than the energy required to break chemical bonds [81].

In this regard, the origin of sonochemical effects is cavitation, a phenomenon that occurs when high energy ultrasound is applied in a liquid having elastic properties [82]. When a large negative pressure is applied to a liquid, intermolecular Van der Waals forces are not strong enough to maintain cohesion and small cavities or gas-filled microbubbles are formed. Then, the bubble lifetime can be divided into four stages: creation, rectified diffusion, implosion and reaction [80].

During creation, the bubble nucleates due to ultrasound, typically starting small in size; the rectified diffusion describes the slow growth of the bubble as gas diffuses into it during the acoustic cycle; larger bubbles can grow when the liquid is supersaturated with gas, particularly when they oscillate in synchronisation with the acoustic field. Then, the cavitation bubble collapses violently after reaching a critical size, resulting in its implosion; this generates extremely high local temperatures (from 1500 K up to 5000 K) and pressures (thousands of bars), which contribute to chemical reactions. The life of bubble ends with the reaction, the final phase that includes the energy release from the collapse, which significantly impacts the surrounding liquid, potentially inducing chemical reactions due to the extreme local conditions created [83]. The Figure 2.2 shows the four stages explored in this paragraph.

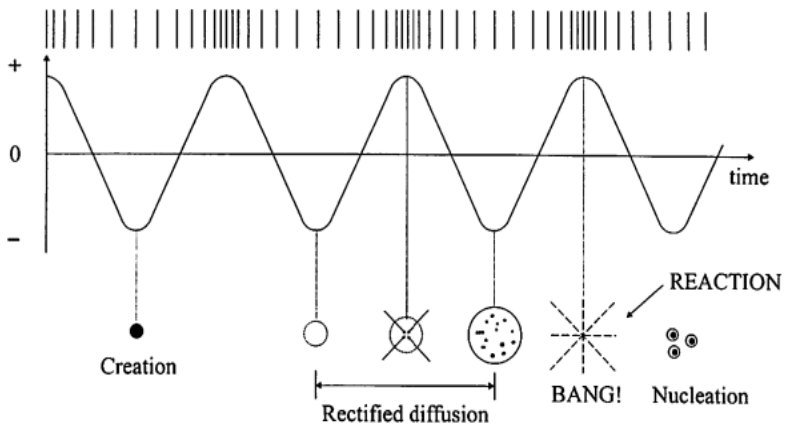

Figure 2.2: Schematic representation of the lifetime of a cavitation bubble [83].

A last consideration is about the distinction between two types of cavitation: stable and transient. Stable cavitation takes place when microbubbles mainly contain a gas (e.g. air) and their mean life is very much longer than a cycle of the ultrasound. During their growth, as long as their resonance frequency is higher than that of the ultrasound, they are driven into pressure antinodes, where they induce chemical reactions. Conversely, transient cavitation is a phenomenon of shorter duration: a cavity is rapidly formed which contains mainly vapor of the liquid and vigorously collapses after a few cycles [82].

2.3. Ultrasound effects and applications

Ultrasound technology is versatile for use in various industrial processes thanks to the mechanical and chemical contributions it induces as a consequence of the cavitation phenomenon [84]. This paragraph will explore the effects given by the ultrasound and the main processes in which their effectiveness has been validated, distinguishing the mechanical effect caused by microbubbles explosion from the chemical one caused by the generated hotspot areas.

Ultrasounds play an important role in various physical processes by speeding up mass transfer and diffusion phenomena. Several studies, such as the one on textile dyeing [85] or generical on drying food processes [86], have verified that the diffusion coefficient perceives an increase when processed at high frequencies of ultrasonic waves [87].

In practice, the mechanical effect caused by the phenomenon of cavitation generates intense microjets, shock waves and localised pressure fluctuations that are decisive on the interaction between particles. By accentuating the mobility of molecules, ultrasound improves the time, energy and cost efficiency of processes in which these diffusive phenomena are involved.

On the other hand, US action is decisive in all those systems and processes in which chemical reactions occur. Conventional approaches to perform synthesis reactions typically have drawbacks in terms of requirement of longer reaction times, unsatisfactory yields, use of large amounts of toxic or expensive reagents and high temperatures, giving an unsafe and sometimes uneconomical approach. Other disadvantages that fall back on chemical reactions are given by mass transfer resistances in the heterogeneous systems and by the agglomeration of particles, resulting into lower surface area and deposition of impurities on the solid surface [88].

In chemical processes, the main benefit derived from the use of US is the acceleration of reaction rates [89]: the observed increase in the kinetic rate constant is mostly attributed to this intense local heating and the other mechanisms, such as changes in activation energies, free radical mechanisms or the enhanced transport processes, that also contribute to some extent depending on the specific reactions. Another relevant benefit is the replacement of the role of phase transfer catalysts; phase transfer catalysts are popular among organic chemists for conducting two phase reactions, when the reactants are insoluble in each other. The phase transfer catalyst carries the reagent from one phase to another, where it reacts easily. Lastly, ultrasounds enable the change of reaction products (the so-called ultrasonic switching): perhaps the most surprising influence is that for some reactions the products obtained by ultrasonication are entirely different from the ones obtained by simple stirring [88].

The Table 2.1 below reports some examples of industrial processes that benefit from the mechanical, chemical or both ultrasound effects, together with short qualitative description rather than a quantitative, since the modelling of these phenomena is complex and not well documented [89].

Table 2.1: Examples of sonicated industrial processes

Processes	Ultrasound effects
Emulsification	Two immiscible liquids are easily emulsified by subjecting them to high power ultrasonication.
Degassing	Ultrasound quickly degasses solvents, likely due to rectified diffusion.
Crystallization	Ultrasound modifies crystallization and precipitation; it enhances nucleation, yielding cleaner, higher quality crystals and uniform-sized crystals in fluidized beds, likely due to convection from microjets.
Cell Disruption	Commonly used in biological labs for breaking cells, similar to its emulsifying effect.
Surface Cleaning	Ultrasound instantly cleans surfaces and generates new surface areas, influencing reaction rates, likely due to microjets from collapsing bubbles.
Particle Fusion	It has been reported by Suslick that under high intensity power ultrasonication, particles suspended in the medium move towards each other at very high velocities (of the order of 150 m/s). When these particles collide with each other, so much heat is generated that local melting occurs and particles get welded to each other. Once again, micro jets seem to be the cause of the high velocities attained by the particles [90].
Agglomeration	The convection caused by ultrasound is likely to increase the collision between particles and may lead to increased rates of coagulation.

Full extraction	It can be completed in minutes with high reproducibility, reducing the consumption of solvent, simplifying manipulation and work-up, giving higher purity of the final product, eliminating post-treatment of wastewater and consuming only a fraction of the fossil energy normally needed for a conventional extraction method.
Preparations of amorphous metal powders	/
Formation and degradation of polymers	/

2.4. Ultrasound food industry applications

US technology is considered an emerging and promising alternative in the food industry, since it produces permanent mechanical, chemical and biochemical changes in liquids due to intense cavitation, and gases due to generation of high intensity acoustic fields.

Since the 1990s the use of US has become a technological alternative applicable on a large scale in the processing industry [91]. As mentioned before the introduction of US technology favours a reduction in processing times and an improvement in the management of operative conditions, both strictly linked to obtaining high-quality products preserving their natural characteristics. Moreover, the use of US implies a reduction of the energy requirements of the processes limiting both environmental and economic costs [92].

In food industry, the application of US can be grouped into two categories, namely, replacing traditional technologies and assisting traditional technologies. In the latter case, US introduction increases process efficiency and limits the disadvantages caused by traditional technologies [93].

US are applied in numerous food processes, that can be group into two categories depending on whether they are affected mechanically or chemically/biochemically. In the first group there is crystallization of fats and sugars, degassing and destruction of foams, extraction of aromas [94]u, filtration and drying, freezing [95], mixing and homogenization, precipitation of airborne powders, meat tenderization. In the second group, instead, it is found wastewater treatments, modification of growth of living cells, alteration of enzymatic activities, sterilization of equipment and bactericidal actions.

Although all these physical and chemical processes occur at the microscopic level, the consumer really perceives these changes in the food's consistency, colour, flavour, and taste at the macroscopic level.

2.4.1. Ultrasound-accelerated whisky maturation

Among all the above-mentioned applications, the field of interest of this work regards the application of US technology for the acceleration of the ageing process in wine brandies and spirits, due to the fact that is a non-thermal, low cost and environmentally friendly technology [96]. The ageing of high-quality products, in fact, can take several years, and producers started to look for novel processes that allowed them to obtain a similar beverage in a faster way, in order to develop new products or to improve the characteristics of the existing ones. Several authors have published about accelerated methods of ageing that involve the using of ultrasound energy to improve the extraction of the cask compounds with the aim of producing wines and brandies, with positive results [82]. Most of the methods of wine and brandy ageing by US take place in a continuous way, meaning that the initial beverage and the oak chips are introduced in a tank where the ultrasound energy is applied without interruptions. This system is simple and effective when used on a laboratory scale, but it is difficult to scale if we age large quantities of wine brandy [73].

Anyway, this is a novel technique since there is still no specific literature dealing with the US technology applied to the ageing process of Whisky.

In the specific case of this work, the cavitation phenomena operate enhancing the maturation in three different mechanisms in which are involved both mechanical and chemical effects [97]:

1. The violent agitation generated by the process allows the mixing of reactants and enhances the oxidation reaction in the liquid phase.

2. The collapse of the microbubbles creates hotspots that drastically accelerate chemical reactions.
3. Microjets generated by the high pressure and temperature near the solid phase facilitate the disruption of the latter surface improving the diffusion of reactants.

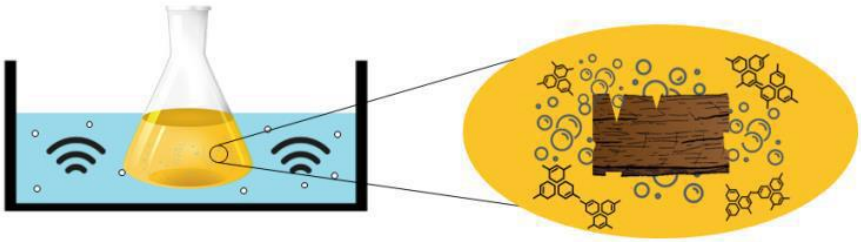

Figure 2.3: Sonicated whisky ageing representation [97].

3 Aim of the thesis

The objective of this thesis work is the development of a mathematical model capable of representing the evolution over time of the concentration of some of the main compounds involved in the whisky maturation process.

The ageing system in question is subjected to the action of an ultrasound technology, with the aim of evaluating its presumably advantageous contribution in comparison with the traditional method in wood barrels.

Before the development of an appropriate mathematical model, it has been necessary to deeply understand the science and chemistry of whisky, its manufacturing process, with a particular focus on the maturation stage, and the techniques already applied in accelerating the ageing of the beverage.

The research for an appropriate model starts with a careful analysis of the experimental data collected for samples subjected to different operating conditions, in which most relevant compounds characterizing the final taste, aroma and colour of whisky have been targeted, in particular, syringaldehyde, syringic acid, coniferaldehyde, vanillin, vanillic acid and gallic acid.

For each compound's behaviour, various process mechanisms are then proposed, in which the possibility of considering a hybrid regime instead of a purely kinetic or diffusive one was not ruled out. Once identified the most reliable mechanism, the purpose is to write the system of the equations that describe the concentration profiles of the above-mentioned compounds, finding the values of the parameters (kinetic constants and diffusivities) that better allow to fit the experimental data.

4 Materials and methods

The purpose of this chapter is to provide a description of the methods and materials used in the development of the kinetic model for the accelerated maturation of whisky.

A first section will be devoted to the description of the structure of the experimental set up designed for testing the samples, followed by the explanation of the techniques needed for the collection of congeners concentrations measurements.

The second paragraph, instead, will be dedicated to the theoretical background and the mathematical methods employed for the formulation of the kinetic model.

The goal of this section is to establish a strong basis for more accurate interpretation of experimental data and comprehension of the mechanics underlying the aging process of whisky.

4.1. Materials

4.1.1. Experimental set-up

The setup used to simulate the ageing process with ultrasound technology is shown in Figure 4.1.

A 2 L vessel is connected through a peristaltic pump to a 3 cm^3 fixed bed immersed in an ultrasonic bath. The volumetric flow at the outlet of the pump is 56 mL/min. The reactor is a cylinder characterized by a diameter of 19 mm and a length of 105 mm, it is filled with wood fragments in form of chips or cubes surrounded by a water-ethanol mixture at 63 % or 45 % alcohol by volume.

In order to maintain the temperature as constant or within an acceptable range a cooling system is linked to the bath. Consequently, even with the cavitation-induced heat effect, this system can be presumed to be isothermal.

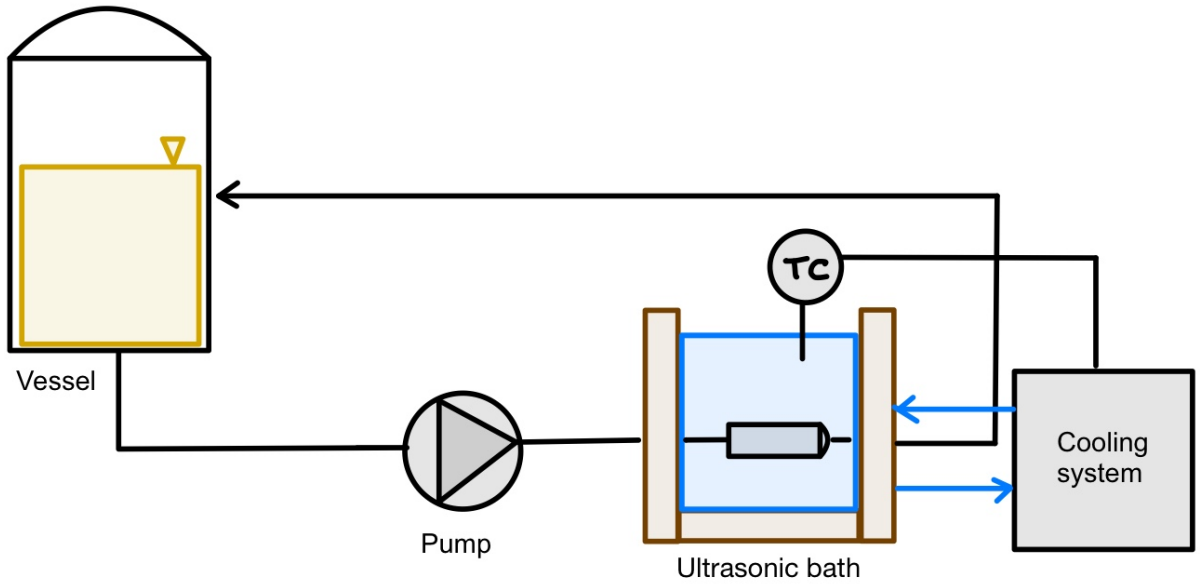

Figure 4.1: Experimental set-up representation.

The ultrasonic field was established using a Branson 2510 ultrasonic bath, which has an interior tank dimension of 24 cm x 14 cm x 10 cm and a maximum power of 130 W at a frequency of 40 kHz. The plug of the ultrasonic bath was connected to the Xiaomi Mi Smart plug, which is a programmable switch that can be controlled remotely via Wi-Fi allowing to perform the tests constantly, even all night long.

The programmable switch is set up for cycle periods of 5 or 9 minutes. On one side, 9-minute cycles offer 3 minutes of on-time and 6 minutes of off-time; on the other, 5-minute cycles offer 1 minute of active sonication and 4 minutes of off time. The smart plug, which was set to sonication mode without heating, controlled all aspects of the switching of the Branson 2510 ultrasonic bath.

4.1.2. High-performance liquid chromatography (HPLC)

The experimental values of concentration obtained from the work of Taddeo e Ramirez are related to chemical components in Whisky that give the alcoholic beverage its distinct taste, flavour and colour. Given this, without entering in detail about the preparation and collection of the samples and the working conditions that will be briefly discussed in the chapter data analysis, it has been necessary to introduce, only from a qualitative perspective, how the chemical compounds have been identified. Among the various techniques and technologies available for the detection and measurement of organic substances, HPLC have been used to carry out a quantitative evaluation of wood congeners.

High-performance liquid chromatography is a chemical method that performs three distinct tasks: separation, identification, and quantification of liquid mixture components [98]. Here, only compounds dissolved in solvents can be analysed in a quantitative and also qualitative manner.

HPLC technique entails the mobile and stationary phases, which are incompatible with each other, as well as the sample of interest. The mobile phase transports the sample through the stationary phase, that is a solid or a liquid film supported by an inert solid [99]. The retention and separation of each component of the mixture is governed by chemical and physical forces that operate between them; in particular, London dispersion forces, dipole interactions, hydrogen bond interactions, dielectric interactions, and electrostatic interactions [100]. Components with a higher affinity for the stationary phase move at a slower rate than those with a lower affinity and the separation of the components occurs when variances in velocities are observed.

4.2. Methods

As previously said, the ageing process consists of complex mechanisms that implies several chemical reactions and physical processes occurring simultaneously and involving many different components. In this regard, the research for kinetic laws capable to describe the maturation process becomes very challenging, in addition to the fact that literature about the kinetics of ageing of spirits is scarce.

Some papers studied the extraction phenomena of phenolic compounds obtained from wood in different alcoholic matrixes, while others detailed the kinetics of extraction of phenolic compounds from wood chips using wine model solutions as extractants [101] [102]. In this context, four mathematical models have been found to be good candidates for predicting the concentration over time of phenolic compounds: Lagergren's exponential first-order model, Peleg's hyperbolic pseudo-second order model, intra-particle diffusion model and parabolic diffusion model [26].

Despite some studies return good results in fitting the experimental values of phenolic compounds extracted from an alcoholic matrix with these four models, none of them has been found to be able to describe the phenomena occurring during the maturation of whisky. Lagergren and Peleg's models are applied with the purpose of determining the theoretical kinetic order of extraction procedures, but their main limitation is the inability to return specific information about the nature of these mechanisms, in particular for diffusion phenomena. The intra-particle diffusion model and parabolic diffusion model, instead, offer solid information about the extraction and diffusion of

the compounds from the solid matrix to the liquid phase, but they both assume that there are not chemical reactions taking place in system [103].

It can be concluded that, among the already explored models to describe the concentration profiles of some relevant compounds during the ageing process, all of them face limitations when it is necessary to deal with a hybrid regime.

Coming to the purpose of the following work, for the development of an alternative model describing Whisky maturation it was necessary to build a solid theoretical background to discover the most appropriate mechanism. In this section it will be discussed the main concepts of final formulation together with the mathematical approach necessary to demonstrate its validity.

4.2.1. Kinetic models

In the following, the basic concepts of the theories used in the model formulation are explained, with particular reference to the rate law model used to describe the reaction rates in the first purely kinetic attempts and the shrinking core model for the final one.

4.2.1.1. Rate Law kinetics model

Rate laws or rate equations are mathematical expressions that describes the relationship between the rate of a chemical reaction and the concentration of its reactants.

Their general formulation, reported in Equation 4.1, makes them adaptable for modelling in a variety of fields [104].

$$rate = k * C_i^m * C_j^n \ldots \tag{4.1}$$

In this expression k is the kinetic constant of the reaction, described by the Arrhenius Law (Equation 4.2), responsible for the dependence of the rate on temperature.

$$k = k_0 * \exp\left(-\frac{E_{att}}{RT}\right) \tag{4.2}$$

C_i and C_j are the concentrations of the involved species, and the exponents m and n are usually positive integers experimentally derived that define the reaction order.

In this regard, if m or n is equal to 1 or 2, the reaction rate is first or second order with respect to that reactant, instead, if the exponent is zero, it means that the rate is not affected by the concentration of that component. The overall reaction order is given by the sum of the orders of each reactant [105].

The units of measure of the kinetic constant depends on the reaction order, the Table 4.1 outlines the different alternatives for the most common types.

Table 4.1: Units of kinetic constants for different reaction orders.

Reaction order	Units of k
Zero	[mol/L/s]
First	[1/s]
Second	[L/mol/s]

- Zero order reactions

In a zero-order reaction the rate is apparently independent of reactants concentrations, but this is usually a consequence of the conditions under which the reaction is carried out. For this reason, it is more accurate to refer to this type of reactions as pseudo-zero-order.

There are two general conditions under which is reliable to consider a reaction as a zero-order type:

1. There is only a small portion of reactants participating in the reaction, but their presence is continuously replenished maintaining a steady reaction rate.
2. There is an excess of one or more reactants compared to the others. This creates a scenario in which the reaction rate becomes independent on the concentrations and proceeds at a constant value [106].

The reaction rate expressed by the rate law is reported in the Equation 4.3:

$$rate = \frac{dC_i}{dt} = -k = constant \tag{4.3}$$

Integrating both sides of Equation 4.3 can be obtained its linearized representation (Equation 4.4) that allows to visualize the evolution of the concentration of a certain reactant I along time:

$$C_i(t) = C_i^{\circ} - kt \tag{4.4}$$

The kinetic constant represents the slop of the function, while the concentration at t=0 is the intercept.

- First order reactions

A first order reaction is a reaction that proceeds with a rate that linearly depends on only one reactant concentration and can be expressed by Equation 4.5:

$$rate = \frac{dC_i}{dt} = -kC_i \tag{4.5}$$

By integrating both the terms of the Equation 4.6 the linearized expression assumes the shape of equation !! capable of describing the trend of concentration i along time:

$$\ln(C_i) = \ln\left(C_i^{\circ}\right) - kt \tag{4.6}$$

Where kinetic constant represents the slope of the function and the logarithm of the concentration at the starting point is the intercept.

- Second order reactions

Second order reactions are specific of kinetics in which the sum of the exponents in the rate law equations are equal to two: in some cases, the reaction rate may be non-linearly dependent on the concentration of a single reactant (Equation 4.7), in other cases it may depend on the concentration of several compounds (Equation 4.8).

$$rate = kC_iC_i \tag{4.7}$$

$$rate = kC_iC_j \tag{4.8}$$

The Equation 4.9 shows the second-order rate for a generical reactant [107].

$$rate = \frac{dC_i}{dt} = -kC_i^2 \tag{4.9}$$

Integrating both sides of the Equation 4.9 as in the previous cases, it is possible to obtain the linearized expression of the rate law:

$$\frac{1}{C_i} = \frac{1}{C^{\circ}} + kt \tag{4.10}$$

Where the kinetic constant is again the slope of the linearized function and $\frac{1}{C^{\circ}}$ the intercept.

4.2.1.2. Shrinking core model (SCM)

The shrinking core model accounts for both kinetic and mass transfer processes and it is usually used to describe and predict the gas-solid or liquid-solid non catalytic reactions occurring at an ideal interface and after the diffusion of the reactants through a layer of reacted products, called 'ash layer' [108].

This model is a powerful tool that has already been applied in several processes in very different contexts, widely used especially in chemical and metallurgical industries [109].

The shrinking core model outlines five different steps between fluids and solid particles [110], as well represented in Figure 4.2:

a. The external diffusion of reactants from the bulk to the solid surface.
b. The internal diffusion of reactants through the solid layer.
c. The reaction on an unreacted core surface with formation of products.
d. The retro-diffusion of the products to the solid surface.
e. The external diffusion from the solid surface to the bulk.

However, in most cases, it is possible to neglect the external mass transport processes due to the fact that they are usually faster than the diffusion through the solid media and the surface reaction. Accordingly, the rate determining step of the entire process is usually one of last two mentioned steps.

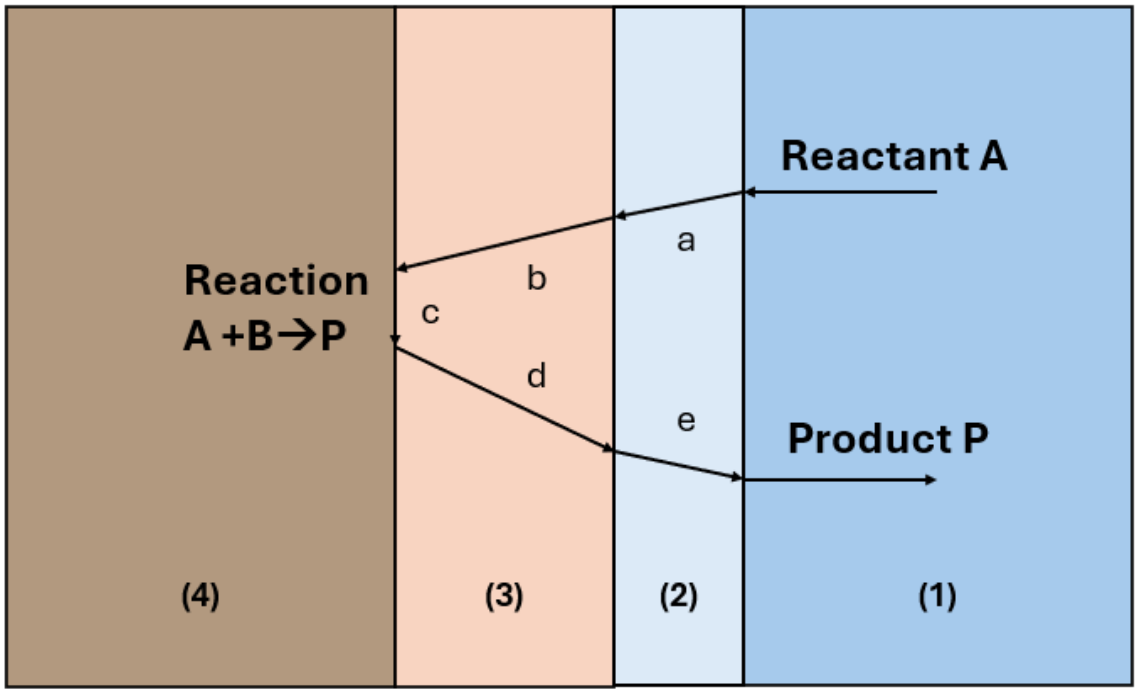

Figure 4.2: Shrinking core system and its five distinctive steps.

The Figure 4.2 clearly presents the generical shrinking core system where the layer 4 in brown represents the unreacted core of the solid, while the layer 3, in red, is the already reacted part, the so-called ash layer, through which the reactant diffuses and that increases with time as the surface reaction proceeds. Between them there is the interface, that is where the reaction between a generic reactant and some solid component takes place. In many situations, the reaction interface's movement is sufficiently slow to make the pseudo-steady-state approximation reliable.

Despite its potential in describing several processes, the shrinking core model is usually a simplified version of the real phenomena that occur and can face limitations. It was originally created to describe very simple systems, characterised by a single

heterogeneous reaction controlled by the transport of a single reactant, and, as a consequence, it is not so accurate and reliable when dealing with more complex systems [111]. Its applicability is indeed strictly limited by the introduction of several assumptions, one of the strongest being certainly the fact of having a single and very thin reaction front separating the unreacted core of the system from the reactive one. Other limitations concerning this model regard the assumption of a non-porous structure for the solid and the idealization of complex geometries in elementary ones. Lastly, it is well-suited for diffusion-limited reactions, but fails in describing transitions between kinetic, intermediate and diffusion-controlled regimes [112] [113].

Shrinking Core Model mechanism

Considering a generic system with the features previously explained the expression of the mass flux through the ash layer can be written as:

$$N_A = \frac{D_{S,A}}{\delta}\,(C_A^{\circ} - C_A^I) \tag{4.11}$$

Where $D_{S,A}$ is the diffusivity coefficient of the generic reactant A through the solid, δ is the thickness of the ash layer that varies with time according to the theory of the model, C_A° is the concentration of reactant A in the bulk, that can be assumed equal to the one at the external surface, and C_A^I is the concentration of A at the interface where the reaction takes place.

Considering the simplest case of a single heterogeneous reaction controlled by the transport of a single reactant, the surface reaction can be assumed second order with respect to the generic reactant A and to the generic reactant B inside the solid matrix, and takes the form illustrated by the Equation 4.12.

$$r_S = k_S * C_A^I * C_B \tag{4.12}$$

Where k_S is the kinetic constant of the reaction, C_A^I is the concentration of A at the interface and C_B is the concentration of the component inside the solid matrix.

For the reason discussed in the paragraph above, assuming steady state conditions at interface, the reactant consumed by the reaction must be supplied by its diffusion through the ash layer. In this way it is possible the express the concentration of A at the interface as a function of the other parameters, as derived below:

$$N_A = \frac{D_{S,A}}{\delta}\left(C_A^{\circ} - C_A^I\right) = r_S = k_S * C_A^I * C_B \tag{4.13}$$

$$C_A^I = \frac{C_A^{\circ}\frac{D_{S,A}}{\delta}}{k_S C_B + \frac{D_{S,A}}{\delta}} \tag{4.14}$$

The objective is to describe the evolution in time of the concentration of reactant A, thus it is possible to write the mass balance (Equation 4.15) on A by considering that its reaction rate reflects the presence of two contributions: the diffusion through the ash layer and the reaction on the surface interface:

$$\frac{dC_A}{dt} = r_{S,A} = k_S C_A^I C_B = k_S C_B \frac{C_A^\circ \frac{D_{S,A}}{\delta}}{k_S C_B + \frac{D_{S,A}}{\delta}} \tag{4.15}$$

In the present work a system with a water-ethanol mixture in contact with a porous wood matrix is discussed. The limited results that were achieved since today in modelling kinetic reactions involving wood components made challenging the research for a suitable model for whisky ageing [114]. However, despite a lack in literature on this topic, some studies employed the shrinking core model to describe the transformation of wood derived compounds, such as lignocellulose hydrolysis under dilute-acid conditions as well as the sulfuric acid-catalysed delignification of sugarcane bagasse [115]. This supported the choice of relying on this model.

Based on the previous considerations, a simplified scheme of the phenomena occurring in the system has been considered, for which there is a representation below; the main assumptions adopted for the development of the model are:

- liquid-solid reaction limited to a single interface (outer surface of the wood);
- separating the solid substance;
- pseudo steady state at the interface;
- wood structure comparable to a porous matrix with uniform porosity in each layer;
- negligible external mass transfer.

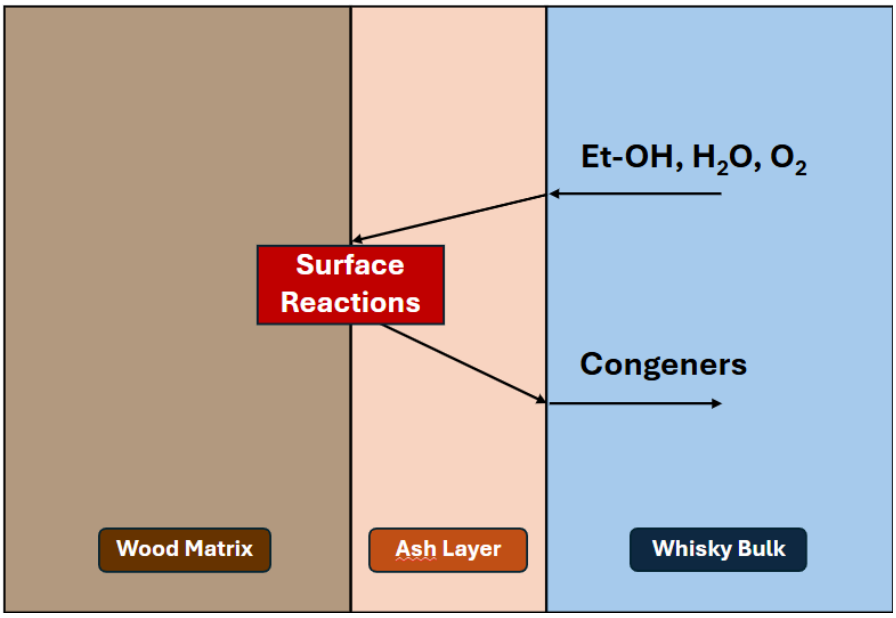

Figure 4.3: Shrinking core system applied to the key study.

4.2.2. Mathematical approach

4.2.2.1. Forward Euler theory

The application of the shrinking core model leads to the formulation of a non-linear ordinary differential equation (ODE) system that needs to be solved by implementing certain numerical integrators. At this purpose Forward Euler Method has been adopted.

It is the simplest numerical technique characterized by the basic idea of predicting the value of a function at a certain future time t by only knowing the values of previous steps and applying a simple formula. This research follows an iterative method, it starts from an initial condition and step-by-step, by repeatedly applying the update formula, it generates a sequence of approximated values till reaching the final one at the desired time. [116]

This concept can also be visualized graphically, each step is represented by small straight segments along the direction of the function's slope as it is shown in Figure 4.4.

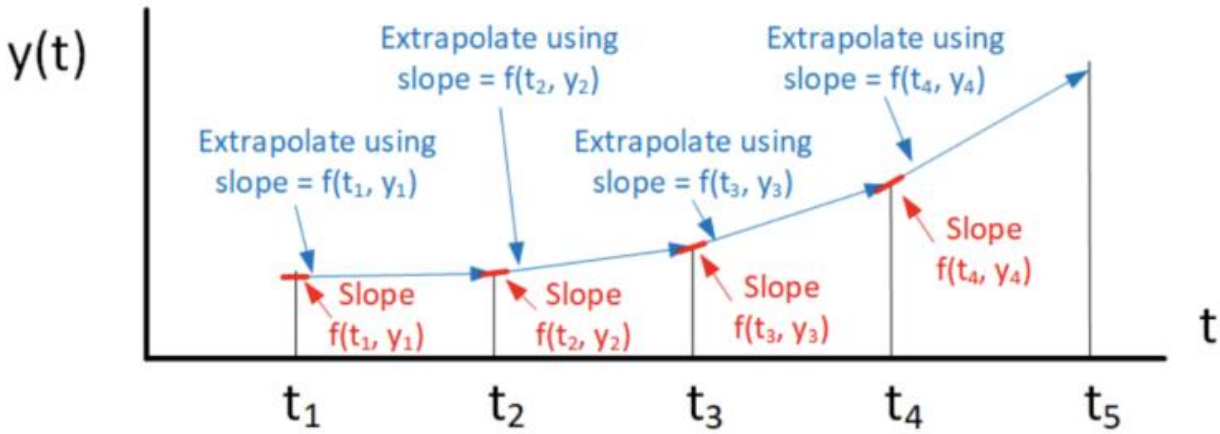

Figure 4.4: Representation of Forward Euler method [116].

The fragmentation of the solution is a possible source of error: the fact of considering only the initial slope of the curve at each step can lead the overall approximation away from the final result. This happens more frequently at larger step size and with stiff equations [117].

4.2.2.2. Forward Euler formulation

Given a generical first-order ODE (Equation 4.16) and fixed an initial condition (Equation 4.17) Euler Forward Method returns an explicit function $yy(t)$ that describes the evolution of the variable y for times $t > 0$.

$$\frac{dy}{dt} = f(t, y) \tag{4.16}$$

$$y\ (t = 0) = y_0 \tag{4.17}$$

The algorithm is derived directly from the discretization of Equation 4.16. This means to substitute a sampled function $y_n = y(t_n)$ (Equation 4.18) defined on discrete times t_n for the function $y(t)$ defined on a continuous time. Ideally, the time step between samples (h) is small and shaped by Equation 19:

$$\frac{y_{(t+h)} - y_t}{h} \approx f(t_n, y_n) \tag{4.18}$$

$$h = t_{n+1} - t_n \tag{4.19}$$

Making explicit the term $y_{(t+h)}$, the final formulation of the Euler Forward algorithm is represented by Equation 4.20:

$$y_{(t+h)} = y_t + h * f(t_n, y_n) \tag{4.20}$$

The Euler Forward method is an explicit method, meaning that all the calculations needed to define the next steps can be isolated on the right side of the examined equation.

5 Model development

The following chapter discusses the methodology employed in the development of the kinetic model for whisky maturation under ultrasound.

In this regard, two primary phases will be explained: the first will include gathering and analysing data, and the second will be dedicated to highlighting the most significant steps in developing the final model that will be used to characterize the concentration profiles over time of the primary congeners.

5.1. Data analysis

The initial phase of the project intends to depict and interpret the experimental data. These represent concentration measurements over time acquired by, as described in the previous section, the HPLC technique. Several whisky samples were analysed, with an emphasis on important chemicals like syringaldehyde, syringic acid, conifer aldehyde, vanillin, vanillic acid and gallic acid that were found to bring significant contributions to the maturation process (Chapter 1.4.2).

Different operating conditions were applied to each sample to understand how the concentration profiles varied. The distinguishing parameters and corresponding values for each studied sample are shown in the Table 5.1

.

Table 5.1: Samples operative parameters.

Sample	ABV	Type of wood	Wood origin	Volurne [ml]	Charring	Ultrasound time	Surface/Volume	Oxygenation	Temperature Range [°C]	Sonication time [min]
G-000	45%	chips	Barrel staves	289	No	1:4	7,96	No	15-20	1702
G-100	63%	chips	Barrel staves	289	No	1:4	7,94	No	15-20	1702
G-200	63%	cubes	Whisky barrel	289	Yes	3:6	8,55	No	15-20	2869
G-300	63%	chips	Barrel staves	289	No	3:6	7,96	No	15-20	2869
G-400	63%	cubes	Whisky barrel	289	Yes	1:4	7,44	No	15-20	3715
G-500	63%	chips	Barrel staves	289	Yes	1:4	7,95	No	15-20	3715
G-600	63%	cubes	Whisky barrel	289	Yes	3:6	10,32	No	15-20	3315
G-700	63%	cubes	Cognac barrel	289	Yes	3:6	19,11	No	15-20	3315
G-800	63%	cubes	Whisky barrel	289	Yes	3:6	8,58	Yes	15-20	3318
G-900	63%	cubes	Cognac barrel	289	Yes	3:6	19,11	No	15-20	3318
M-000	63%	cubes	Cognac barrel	289	Yes	3:6	14,92	No	35	1947
M-100	63%	cubes	Bourbon barrel	289	Yes	3:6	15,07	No	35	1947
M-200	63%	cubes	Whisky barrel	289	Yes	3:6	30,61	No	17-35	2010
M-300	63%	cubes	Cognac barrel	289	Yes	3:6	19,07	No	17-35	2010
M-400	63%	cubes	Cognac barrel	510	Yes	3:6	18,71	No	15-20	3315
M-500	63%	cubes	Whisky barrel	289	Yes	3:6	26,12	No	15-20	3315

Alcohol by volume, or ABV, shows the proportion of ethanol in the volume of the entire solution. Since 63% has been proved to be the ideal value for spirits' composition (Chapter 1.4.1), it was maintained at this level for all experiments except for sample G-000, enabling to observe the impact of ABV fluctuation on concentrations.

The wood utilized in the experimental trials varies in the geometry of the chosen wood pieced, being sometimes cube-shaped and other times chip-shaped, as well as in origin. Moreover, whisky is frequently matured in barrels that were previously used to age other spirits, as discussed in Chapter 1.4.1, since this affects the presence of specific chemicals of interest. Among the types used, it is then possible to distinguish between unused barrel wood and wood soaked in whisky, cognac or bourbon. Lastly, the pre-treatment of charring has also been applied to the wood of some samples, aiming at accelerating maturation (Chapter 1.4.4).

The parameter surface area of wood divided by the volume of solution, where the latter was maintained at 289 mL, accounts for the quantity of wood utilized for each trial. The M-400 sample is the only one with a different volume, which is 510 mL.

Chemical reactions are significantly influenced by temperature. The maturation process of whisky is conducted at a consistent and ideal temperature of about 20°C, as detailed in Chapter 1.4.1. Replicating these identical conditions was the goal of the

experimental trials. Experimental error affects samples where the temperature deviates significantly from the ideal value. This can be caused by operator mistake in measurement control or instrument faults.

An additional oxygenation treatment was performed on sample G-800 in order to evaluate its effects, as the majority of the processes that take place throughout the whisky ageing are oxidation reactions (Chapter 1.4.1).

The contribution of ultrasound is accounted for by two parameters. The exact minutes that the sample was exposed to the ultrasound effect are shown by the sonication time. The ratio under "ultrasound time" indicates the proportion of active versus inactive ultrasound intervals over the course of the trial. A (3:6) ratio, for instance, indicates that, of nine one-minute cycles, three were completed with the ultrasound equipment running and six with it off. The (1:4) ratio follows the same reasoning.

5.1.1. Data inspection

The unit of measurement for the experimental concentrations is ppm, which is equivalent to mg/L. It was thought reasonable to convert each of these into mmol/L, using the formula shown by Equation 5.1, in advance of a thorough kinetic investigation.

$$C_i \left[\frac{mmol}{L}\right] = C_i \left[\frac{mg}{L}\right] * \frac{1}{PM_i \left[\frac{mg}{mmol}\right]} \tag{5.1}$$

The duration of the experimental trials is approximately one to two weeks. In a traditional maturation process without ultrasound acceleration, this timeframe would not be sufficient to observe any noticeable changes in the reacting system. For this reason, each measurement refers solely to the sonication time. Essentially, the entire experiment is considered as if it corresponds only to the active cycles of the ultrasound machine, while the inactive periods are treated as negligible.

In the following discussion, it was decided to expand the sonication time to encompass the entire duration of the experiment and to consider for the development of the model, with the appropriate adjustments, also those moments of inactivity that keep the system at constant concentration.

The transformation of sonication time into actual real time was carried out by applying Equation 5.2.

$$time_{TOT} = \frac{time_{US}}{NC_{ON}} * NC_{TOT} \tag{5.2}$$

Where NC_{TOT} denotes the total number of on and off cycles and NC_{ON} denotes the cycles of ultrasound activity, respectively, based on the two ratios under "ultrasound time."

5.1.2. Data visualization

Graphs illustrating the concentrations over time were created for every sample and component, taking into account all aspects that have been discussed at this point. Some examples are shown in Figure from 5.1 to 5.5, the graphs of the remaining samples can be viewed in Annex A.1. This preliminary analysis demonstrated that, generally, and regardless of operating conditions, all of the compounds under study exhibit increasing concentration profiles over time and follow a function that resembles a logarithmic function in shape, with a distinct growth in the first few minutes before reaching a plateau-like state.

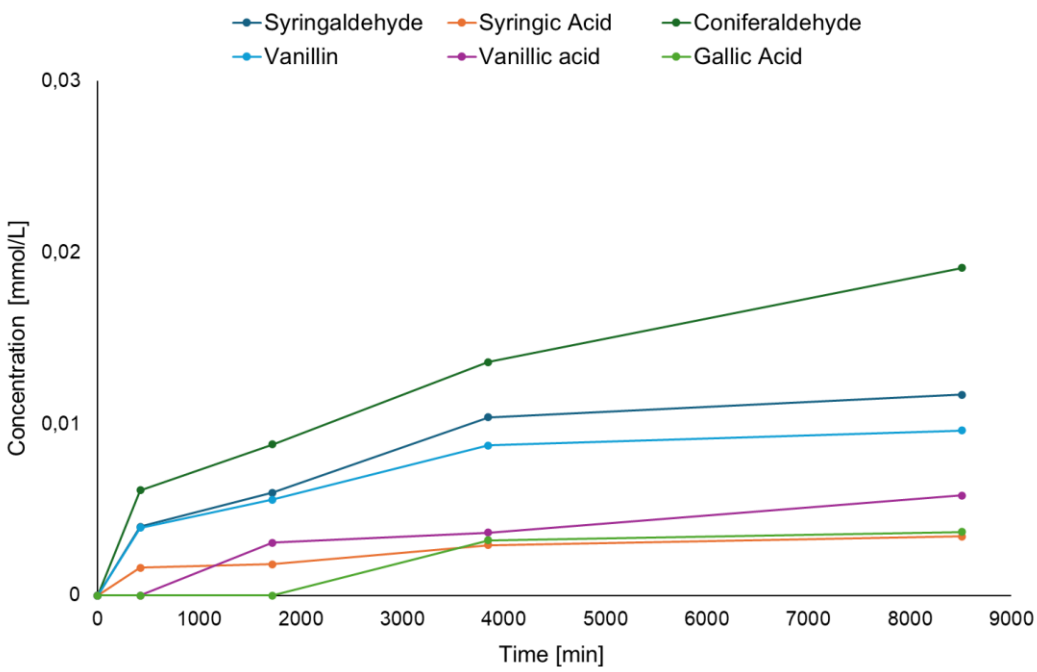

Figure 5.1: Sample G-000, experimental concentrations trends.

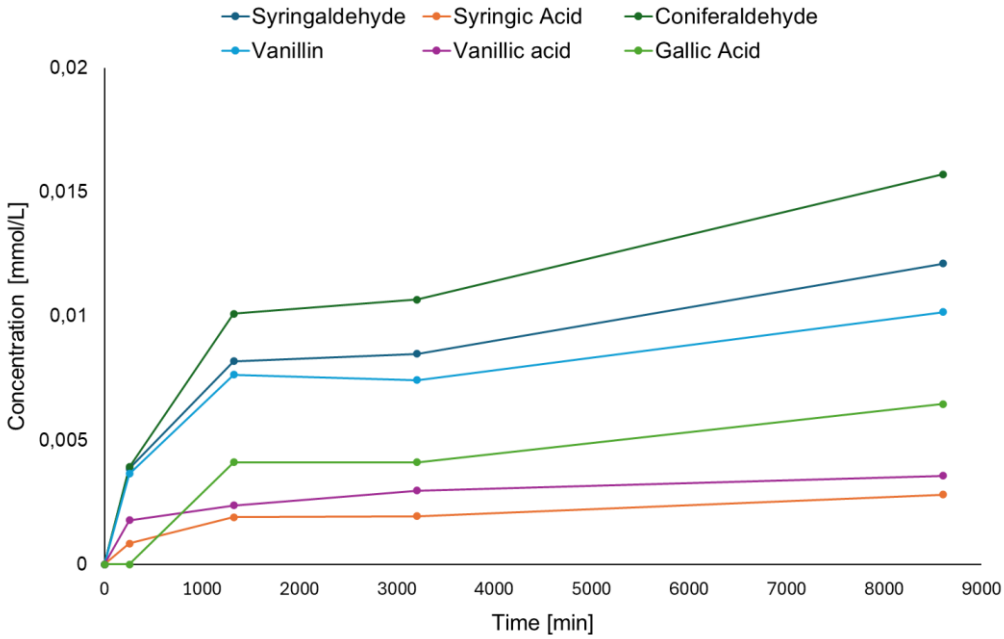

Figure 5.2: Sample G-300, experimental concentrations trends.

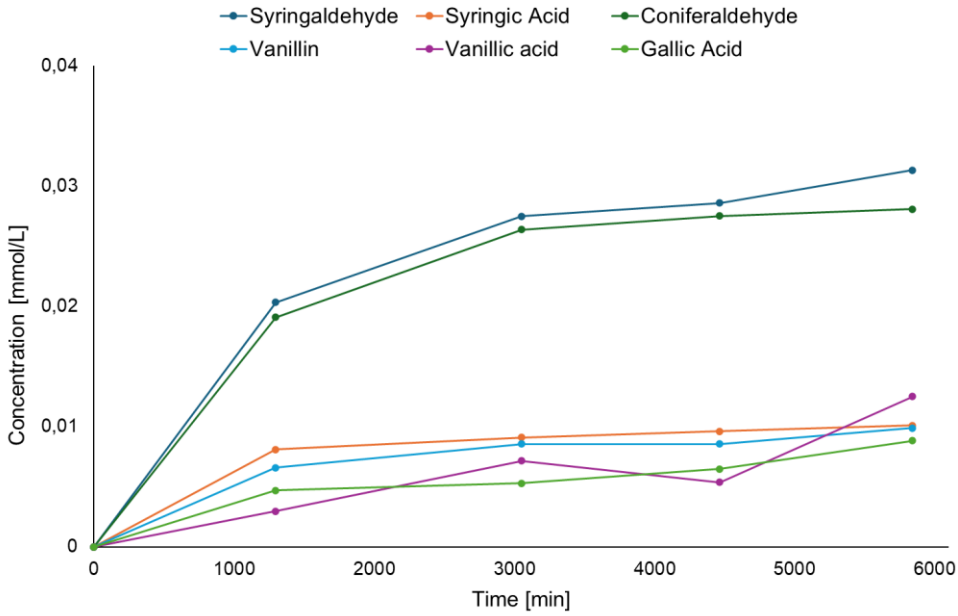

Figure 5.3: Sample M-000, experimental concentrations trends.

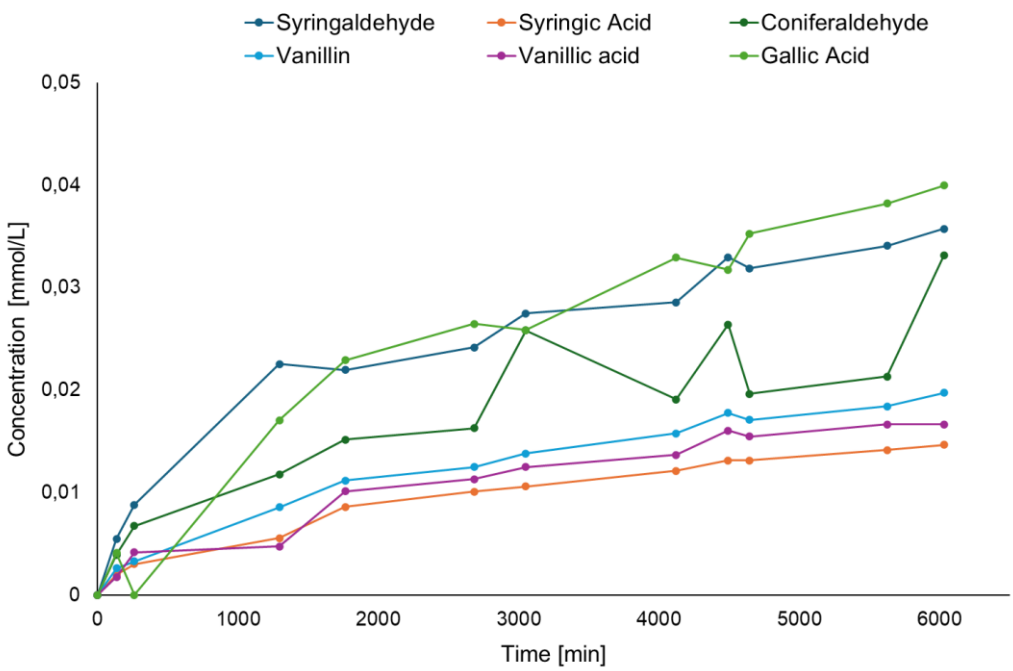

Figure 5.4: Sample M-300, experimental concentrations trends.

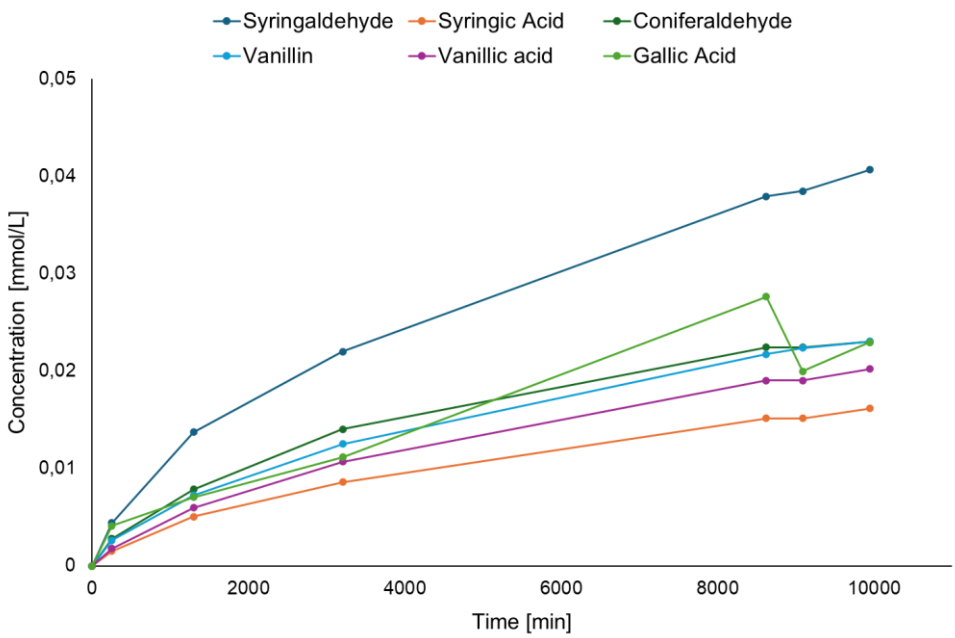

Figure 5.5: Sample M-500, experimental concentrations trends.

5.1.3. Data cleaning and selection

5.1.3.1. Samples exclusion

Laboratory measurements, especially when dealing with extremely small numbers, are typically susceptible to experimental error. At this regard, in the following figures (from Figure 5.6 to Figure 5.9) it is possible to observe some examples of samples displaying more asymmetrical curves than others and clear outliers marked by a red circle, including abruptly rising and declining peaks or a series of zero measurements, which create anomalies in trends.

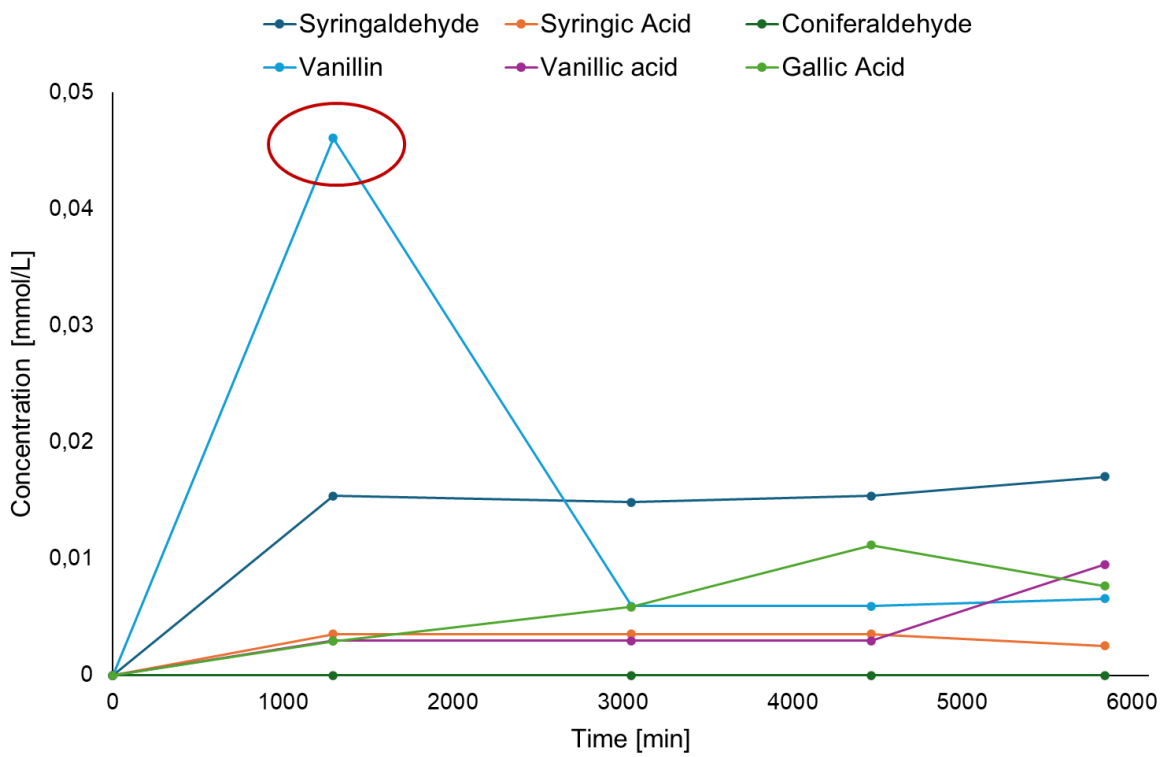

Figure 5.6: Sample M-100, experimental concentrations trends with evident outliers.

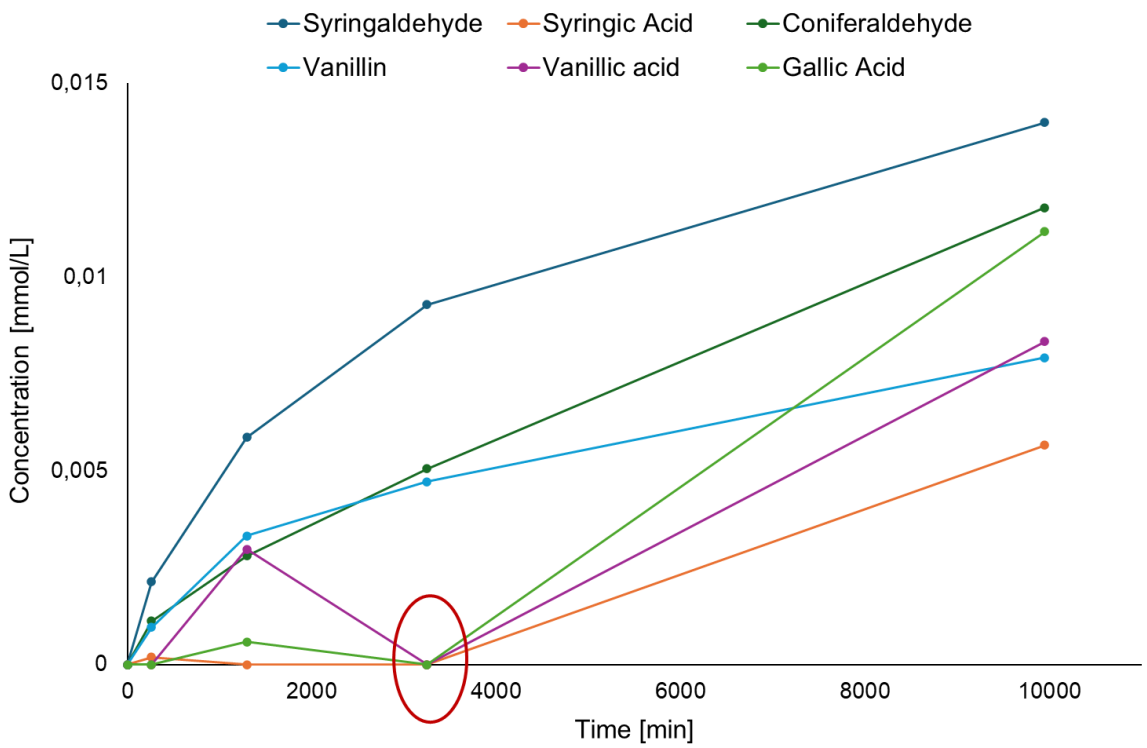

Figure 5.7: Sample G-600, experimental concentrations trends with evident outliers.

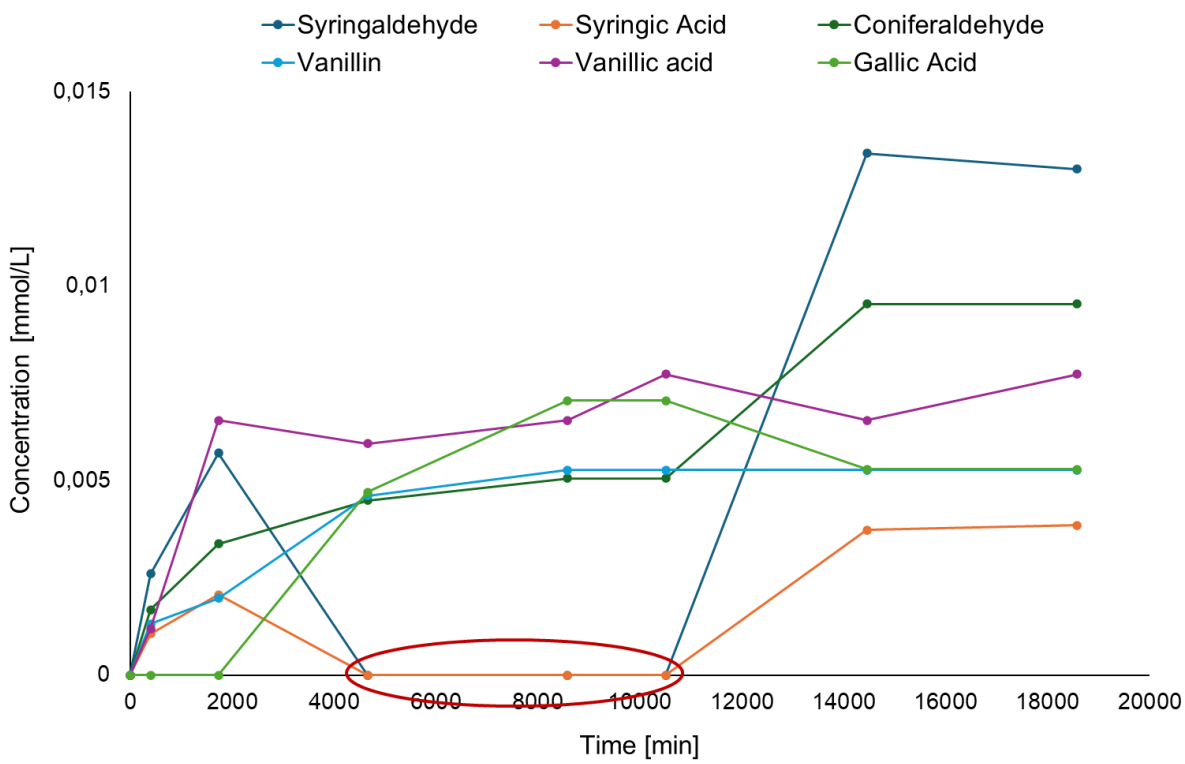

Figure 5.8: Sample G-400, experimental concentrations trends with evident outliers.

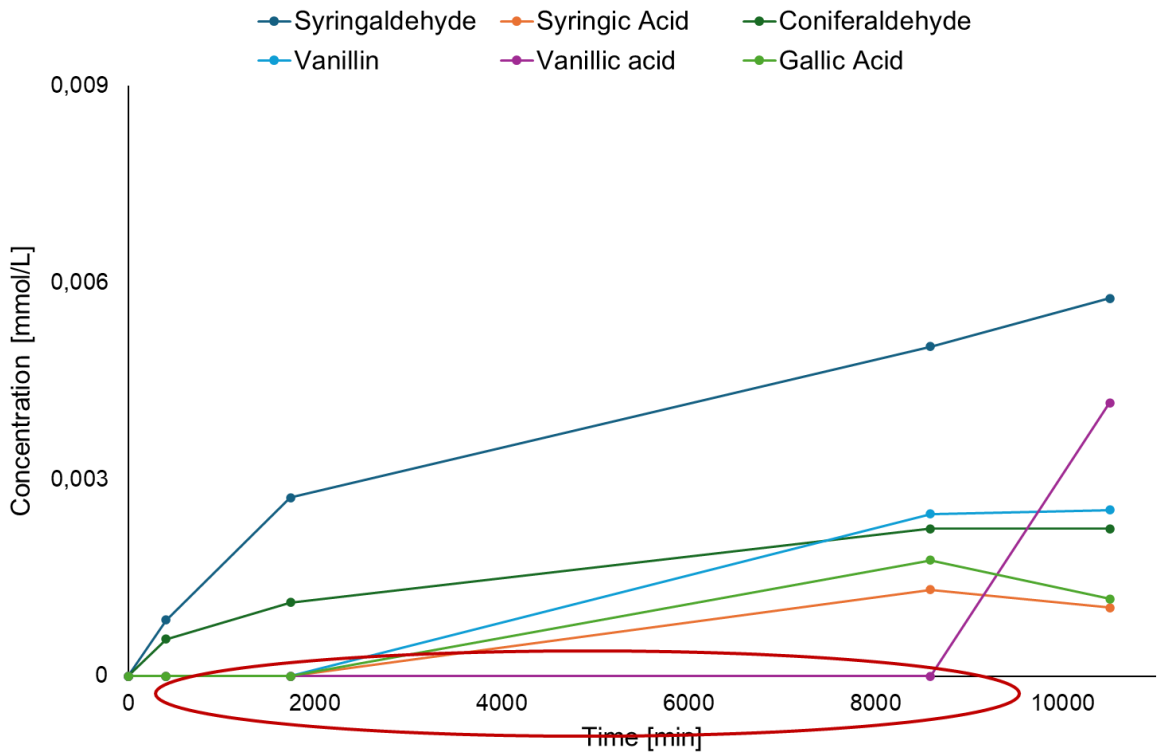

Figure 5.9: Sample G-500, experimental concentrations trends with evident outliers

It was therefore appropriate to proceed with a data cleaning and data selection phase in order to increase the reliability of the data and facilitate the search for a mathematical model capable of describing the real behaviour of compounds subjected to ultrasonic accelerated maturation.

The selection of invalid samples was done by referring to compounds belonging to the same kinetic scheme (Chapter 1.4.2) because imprecise measurements in reactants and products of the same reaction interfere and can cause error propagation.

The Table 5.2 shows the considered (⊆) and excluded (×) samples for each congeners group.

Table 5.2: Samples exclusion for each congeners group.

Samples	Syringil group	Coniferyl group	Gallic Acid
G-000	⊆	⊆	⊆
G-100	⊆	⊆	⊆
G-200	⊆	⊆	×
G-300	⊆	⊆	⊆
G-400	⊆	⊆	⊆
G-500	⊆	×	×
G-600	×	×	×
G-700	⊆	⊆	⊆
G-800	×	⊆	×
G-900	⊆	×	×
M-000	⊆	⊆	⊆
M-100	×	×	×
M-200	⊆	⊆	⊆
M-300	⊆	⊆	⊆
M-400	⊆	⊆	⊆
M-500	⊆	⊆	×

5.1.3.2. Normalization of data with respect to ABV percentage

Samples G-000 and G-100 are almost identical in terms of their operating conditions, with the exception of the alcohol content, which is 45% for the former and 63% for the latter. To investigate the effect of this parameter on the concentration profile, each component of both samples were plotted in the same Cartesian axis system as shown in Figures from 5.10 to 5.15 .

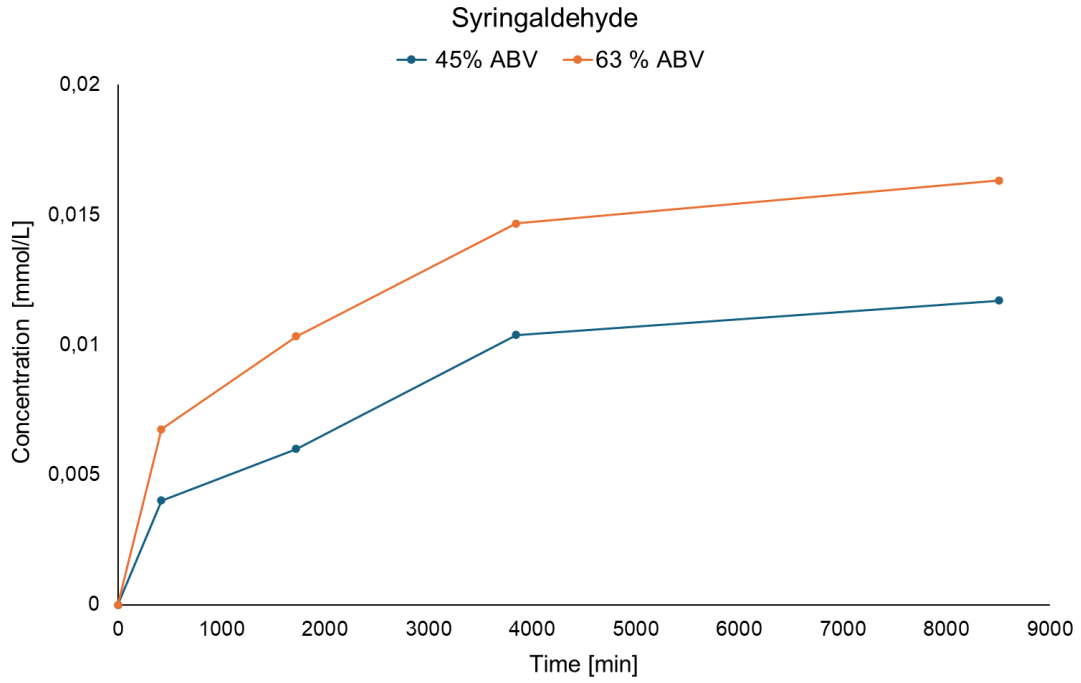

Figure 5.10: Syringaldehyde, ABV effect by comparing G-000 and G-100 samples.

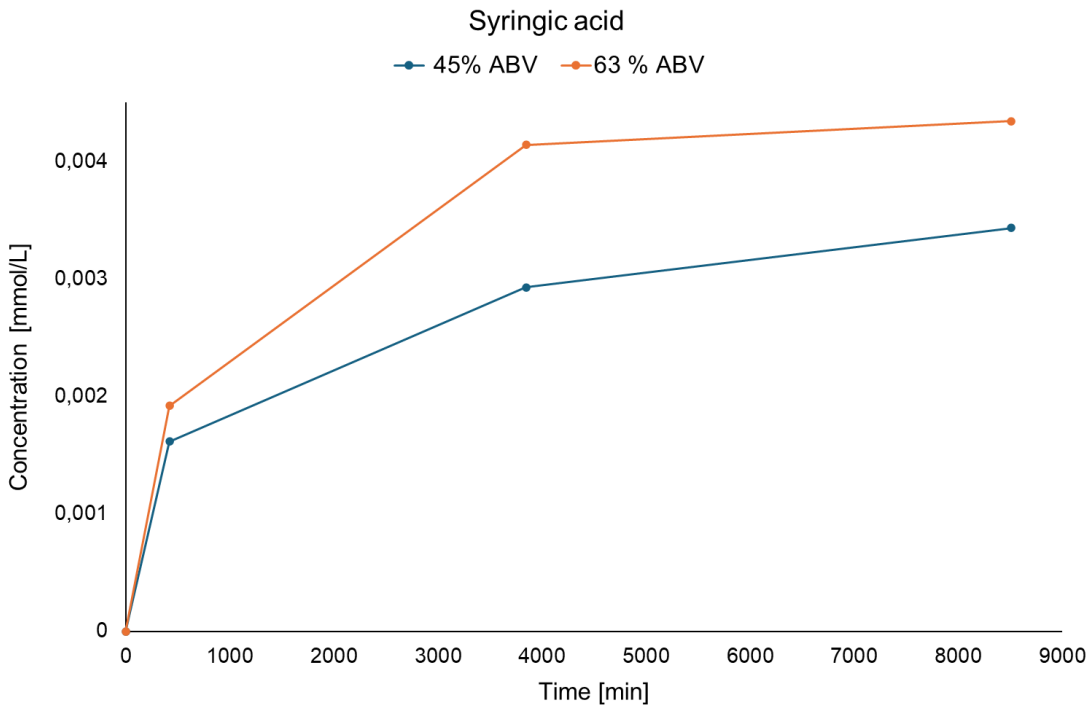

Figure 5.11: Syringic acid, ABV effect by comparing G-000 and G-100 samples.

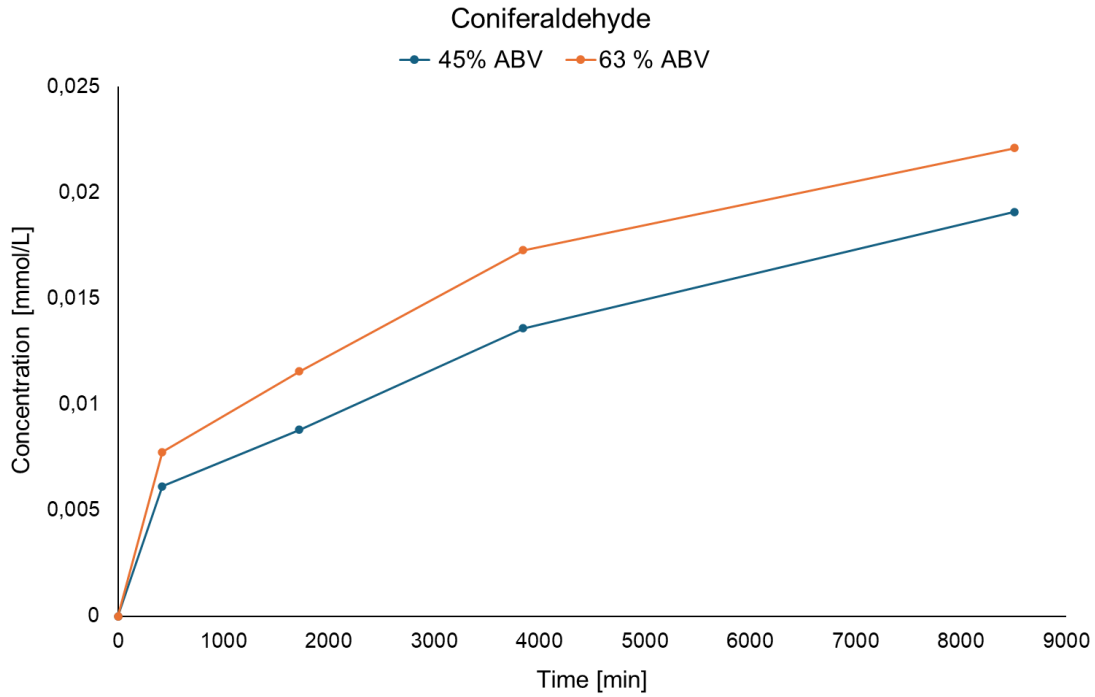

Figure 5.12: Conifer aldehyde, ABV effect by comparing G-000 and G-100 samples.

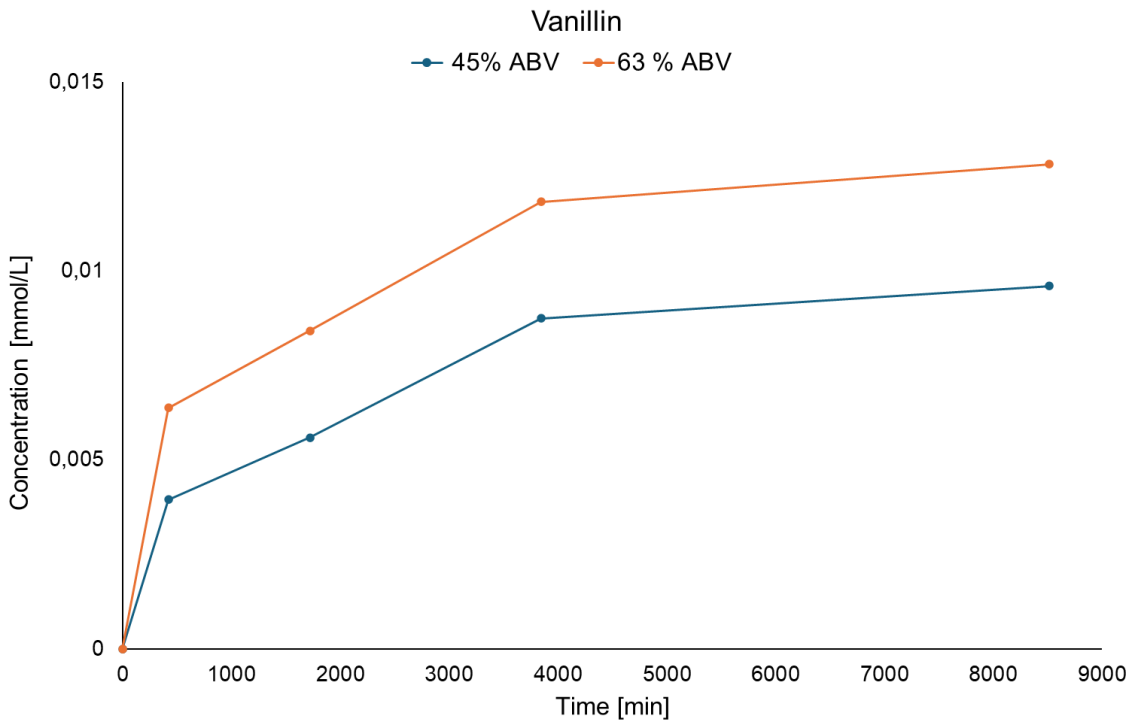

Figure 5.13: Vanillin, research of ABV effect by comparing G-000 and G-100 samples.

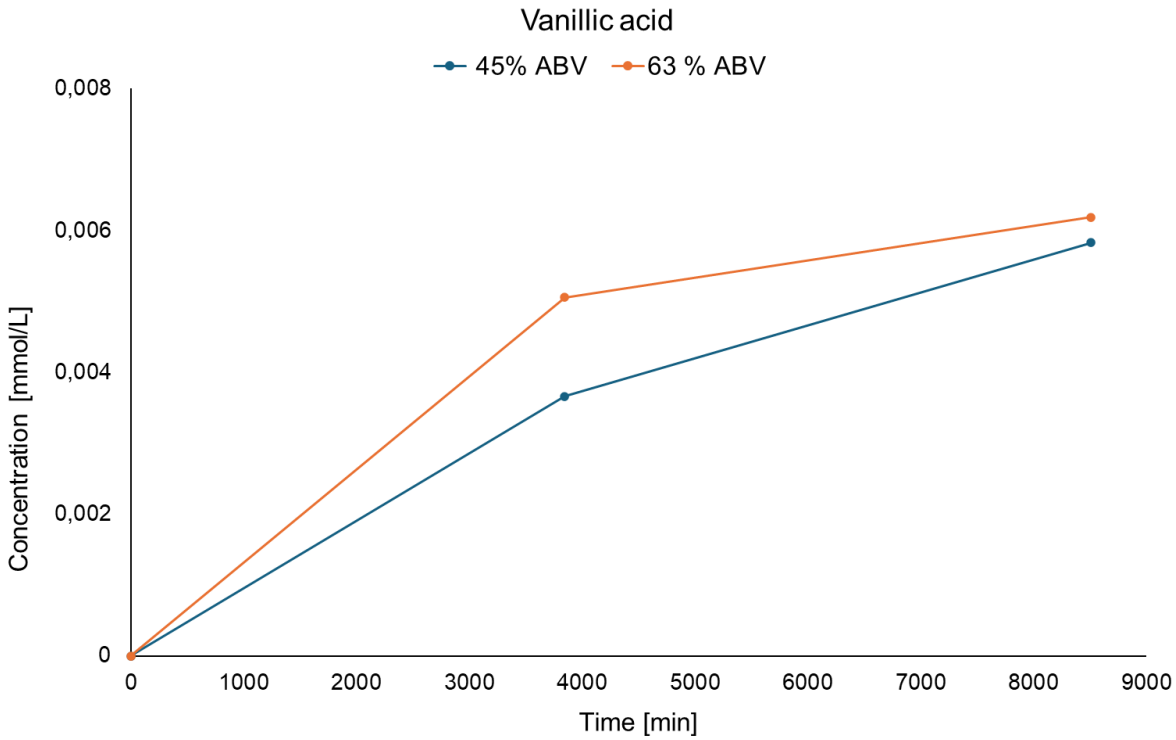

Figure 5.14: Vanillic acid, ABV effect by comparing G-000 and G-100 samples.

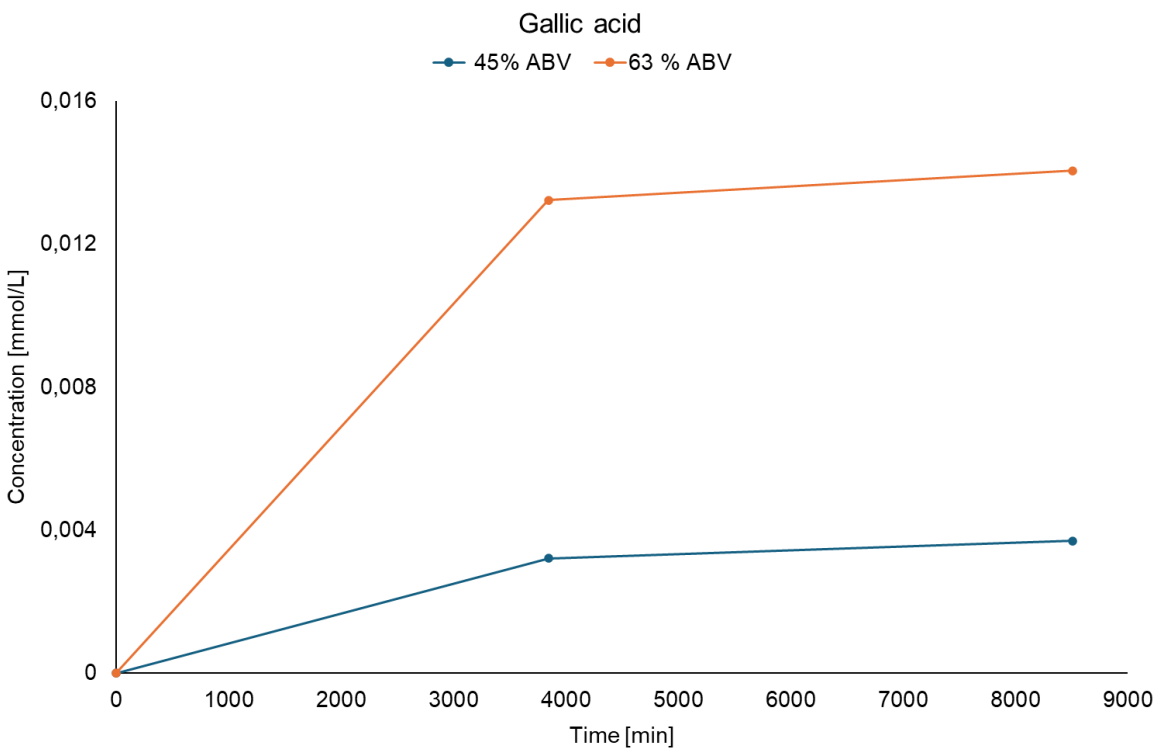

Figure 5.15: Gallic acid, ABV effect by comparing G-000 and G-100 samples.

Overall, it was found that each generic compound's reaction rate rises in direct proportion to the solution's ethanol content. In relation to G-000 points, the data points of sample G-100 seem to be equally pushed upward by a constant number, maintaining the curves' shape. This implies that the kinetic rules of the reactions are not changed because the trend (curve shape) stays the same. Rather, a potential productivity increase is seen for increasing ABV values, most likely as a result of one of the reactants' increased concentrations.

Once the effect of ethyl alcohol on the concentration profiles had been ascertained, in order to remove the variability dictated by at least one parameter of the many considered, it was decided to normalise the concentrations of sample G-000 to the optimal ABV value, which is 63% following Equation 5.3.

$$C_{i_{63\%\,ABV}} = C_{i_{45\%\,ABV}} * \frac{0{,}63}{0{,}45} \tag{5.3}$$

At this point, the experimental data are free of any outliers or undesirable trends and normalised to the same percentage of ABV.

5.2. Model formulation

The next section is dedicated to the goal of fitting experimental data by creating a system of equations that considers the physic-chemical characteristics of whisky maturation and that, by adjusting the key parameters, can most accurately depict the evolution of the concentration measurements over time.

The chapter deals separately with compounds resulting from the ethanolysis of lignin and gallic acid (GA), which is the result instead of the hydrolysis of tannins.

As discussed in Chapter 1.4.2, the former can be divided into two families based on the reaction pattern in which they participate: the coniferyl family, which includes conifer aldehyde (C), vanillin (V), and vanillic acid (VA), and the syringil family, which includes syringaldehyde (S) and syringic acid (SA).

Since the M-500 sample for the syringil and coniferyl families and the M-300 sample for gallic acid were found to have reliable measurements and, consequently, reliable concentration trends over time for each compound under investigation, the numerous attempts made and subject to variation up to the final form of the model were, for the sake of simplicity, carried out on one experiment.

The equations worked out in the various treatments require the use of data from literature searches, which can be checked for completeness in Appendix A.2.

Moreover, despite the configuration of the system used for the experimental trials is the one illustrated in Chapter 4.1.1, for modelling purposes it has been approximated to a single batch system. This simplification is plausible since the time it takes the flow to pass through the reactor is far shorter than the total recirculation time that results hundreds time longer. A calculation of the two characteristic reactor residence and recirculation times can be found in Appendix A.3.

5.2.1. Coniferyl and Syringil families

5.2.1.1. First attempt

As first assumption, it was considered that each compound was independent of each other and solely produced by the ethanolysis of lignin. Accordingly, the material balances on the individual compounds for a batch system operating under isothermal conditions can be written as follows:

$$\frac{dC_S}{dt} = -k_1 C_S^n \tag{5.4}$$

$$\frac{dC_{AS}}{dt} = -k_2 C_{SA}^n \tag{5.5}$$

$$\frac{dC_C}{dt} = -k_3 C_C^n \tag{5.6}$$

$$\frac{dC_V}{dt} = -k_4 C_V^n \tag{5.7}$$

$$\frac{dC_{AV}}{dt} = -k_5 C_{VA}^n \tag{5.8}$$

Where k_i are the kinetic constants, n is the reaction order and C_i is the concentration of the key compounds.

Equations from 5.9 to 5.11 were obtained by linearizing the Equations 5.4 - 5.8 under the premise that n = 0, 1, 2, according to Chapter 4.2.1.1.

- Order n = 0 $$\frac{dC_i}{dt} = k_i \rightarrow C_i = C_i^{\circ} - k_i t \tag{5.9}$$
- Order n = 1 $$\frac{dC_i}{dt} = k_i C_i \rightarrow \ln(C_i) = \ln(C_i^{\circ}) - k_i t \tag{5.10}$$
- Order n = 2 $$\frac{dC_i}{dt} = k_i C_i^2 \rightarrow \frac{1}{C_i} = \frac{1}{C_i^{\circ}} - k_i t \tag{5.11}$$

To determine a first, indicative reaction order for the kinetics of the compounds under study, these were plotted with their corresponding trend lines and R^2 values as shown from Figure 5.16 to Figure 5.20; the more likely reaction order is indicated by R^2 values that are closer to 1.

All compound samples exhibit a greater R^2 for zero order, which leads to the exclusion of the other two alternatives. This could be explained by the reagents lignin and ethanol being present in greater amounts than the whisky congeners, allowing to believe that their concentrations will remain consistent throughout the process. Given this supposition, it's reasonable to have a reaction that is solely dependent on the kinetic constant, which was simple to calculate because it reflects the slope of the straight line that the linearized equation balance depicts.

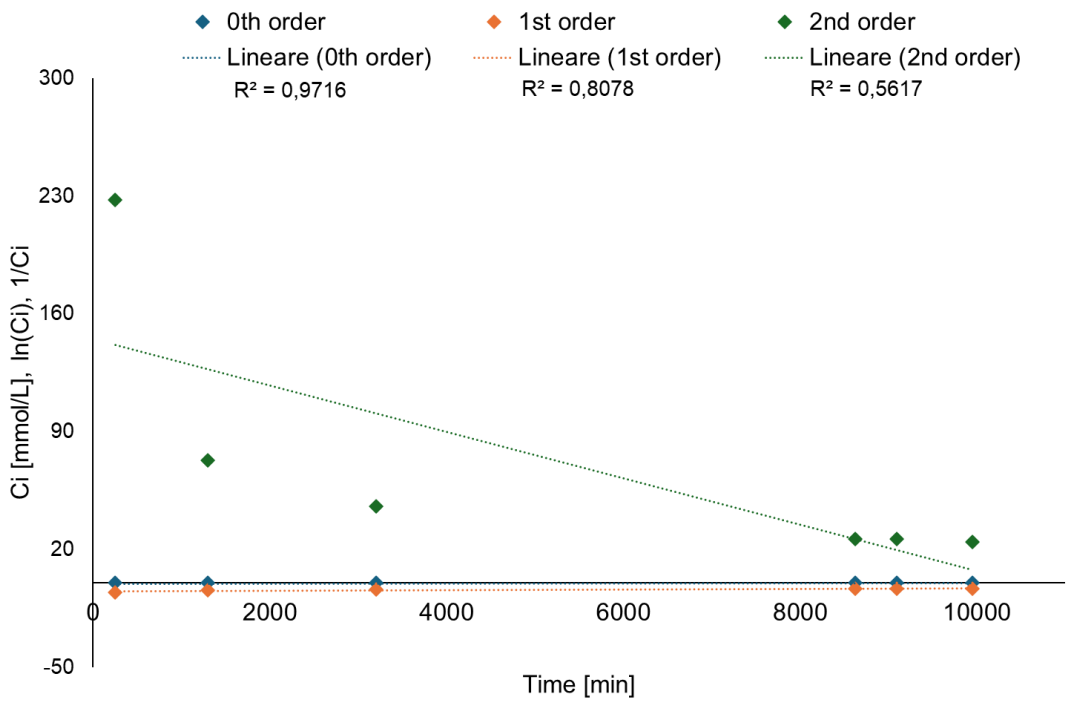

Figure 5.16: Syringaldehyde, M-500 sample, order of reaction research.

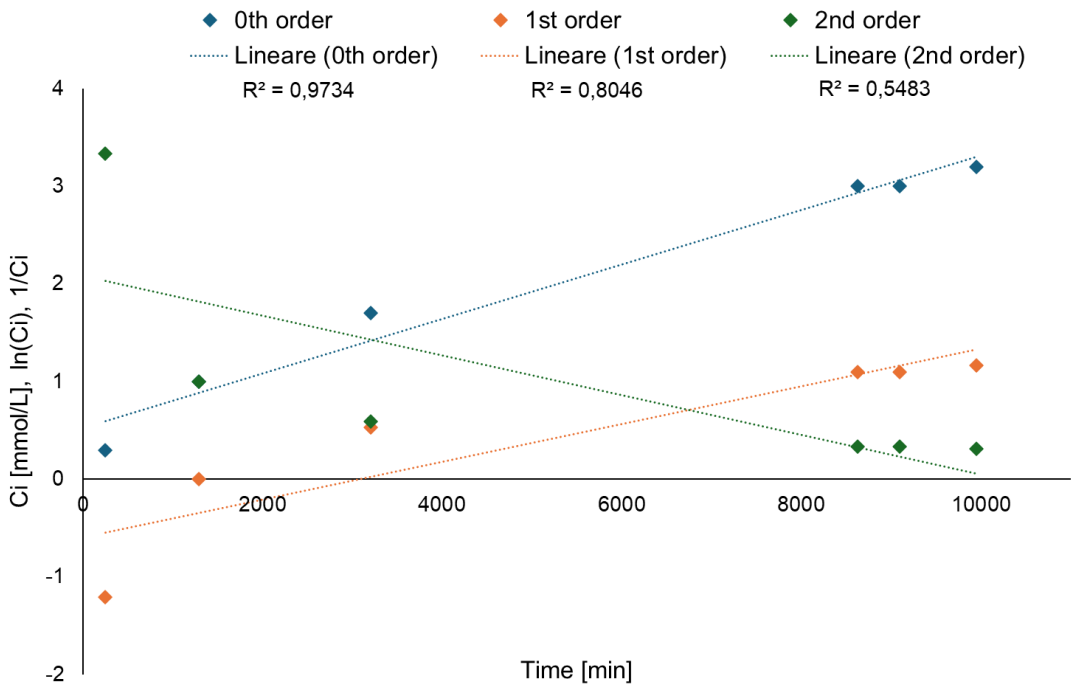

Figure 5.17: Syringic acid, M-500 sample, order of reaction research.

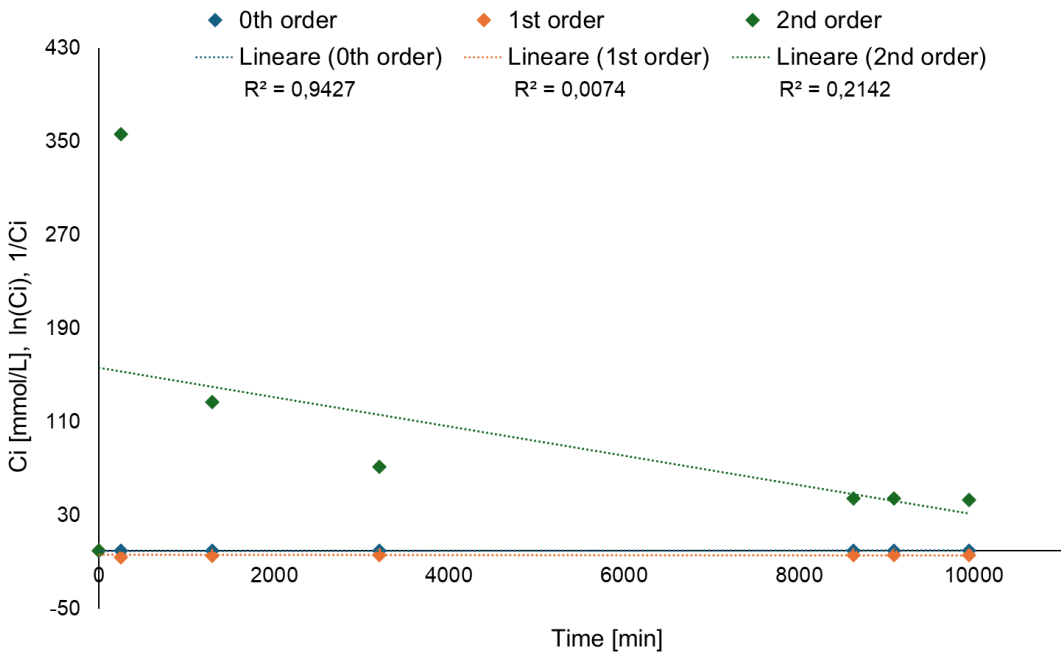

Figure 5.18: Conifer aldehyde, M-500 sample, order of reaction research

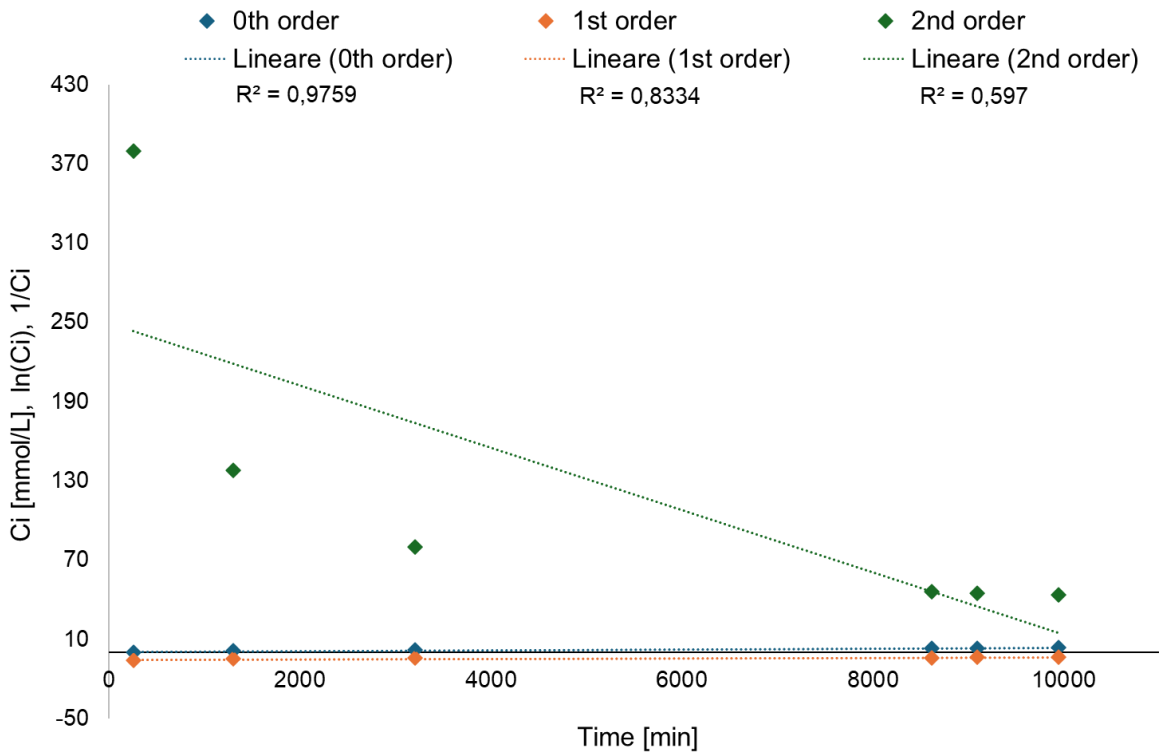

Figure 5.19: Vanillin, M-500 sample, order of reaction research.

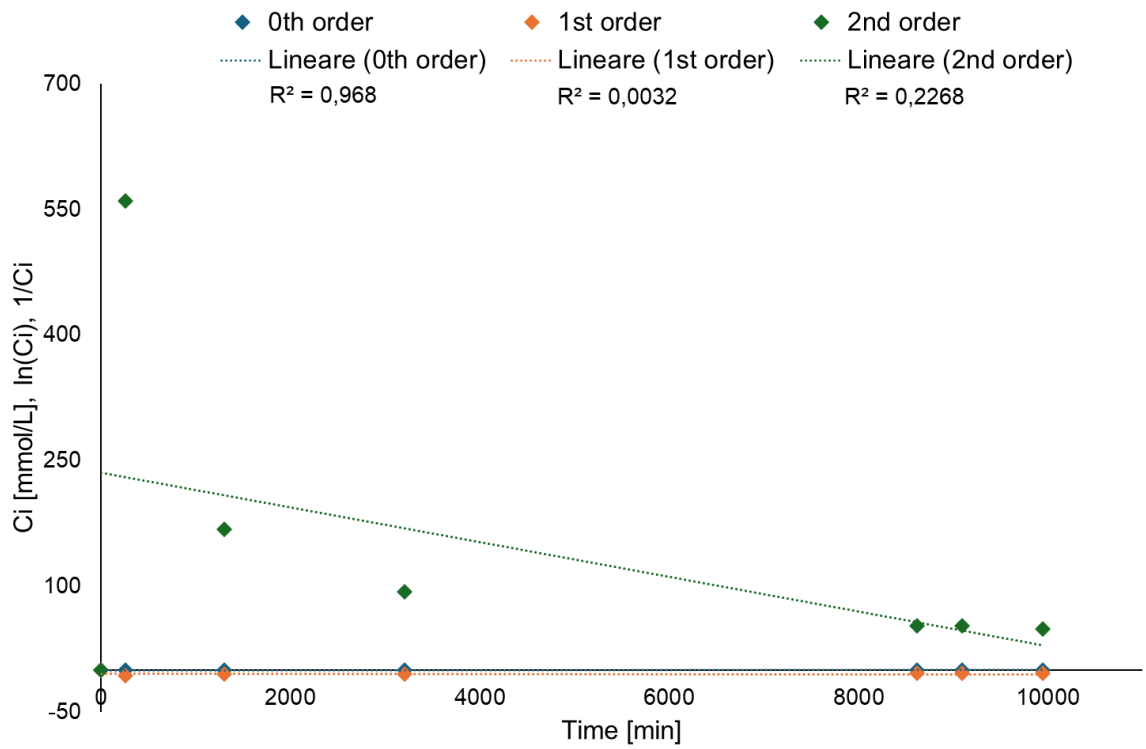

Figure 5.20: Vanillic acid, M-500 sample, order of reaction research.

Table 5.3: Sample M-500, kinetic constants values of the first attempt.

	Syringaldehyde	Syringic acid	Coniferaldehyde	Vanillin	Vanillic acid
$k_i \left[\frac{mmol}{L * min}\right]$	3,76 E-06	1,51 E-06	2,15 E-06	2,17 E-06	1,91 E-06

The Table 5.3 displays the first-attempt values of the kinetic constants derived from this initial and approximate approach to the ripening process's kinetics. This is a highly simplified representation of the actual process, and it will therefore be used solely as a basis for developing further approaches.

5.2.1.2. Second attempt

From this first scenario, the strong simplification of independence between the compounds is removed. The considered congeners belong to a complex reaction scheme in which they are produced and consumed through series reactions as already discussed in Chapter 1.4.2:

$$Lignin + EtOH \rightarrow S + O_2 \rightarrow AS \tag{5.12}$$

$$Lignin + EtOH \rightarrow C + H_2O \rightarrow V + O_2 \ AV \tag{5.13}$$

Different reaction orders have been proposed for the compounds' generation and consumption. According to the first attempt, it is possible to assume that the first aldehydes (S, C) produced by the ethanolysis of lignin have kinetics of order 0. However, compounds that rely on the consumption of the aldehydes themselves, like vanillin and the two syringic and vanillic acids, require to consider their dependence on these same time-varying concentrations, therefore the hypothesis of reactions of order one must be put forth in this scenario.

$$\frac{dC_S}{dt} = k_1 - k_2 C_S \tag{5.14}$$

$$\frac{dC_{AS}}{dt} = k_2 C_S - k_3 C_{AS} \tag{5.15}$$

$$\frac{dC_C}{dt} = k_4 - k_5 C_C \tag{5.16}$$

$$\frac{dC_V}{dt} = k_5 C_C - k_6 C_V \tag{5.17}$$

$$\frac{dC_{AV}}{dt} = k_6 C_V - k_7 C_{AV} \tag{5.18}$$

The model assumed so far, represented by Equations from 5.14 to 5.17, only considers kinetics, no limitations due to mass transfer have been investigated.

A graph comparing the experimental concentration profiles with those derived from solving the mass balances using the Forward Euler method (Chapter 4.2.2.1), expressed by Equation 5.19 – 5.22, had to be created for each sequence of compounds that were produced and consumed in order to visually represent the validity of the advanced assumptions.

$$C_S^{(t)} = C_S^{(t-1)} + \Delta t * (k_1 - k_2 C_S^{(t-1)}) \tag{5.19}$$

$$C_{SA}^{(t)} = C_{SA}^{(t-1)} + \Delta t * (k_2 C_S^{(t-1)} - k_3 C_{SA}^{(t-1)}) \tag{5.20}$$

$$C_C^{(t)} = C_C^{(t-1)} + \Delta t * (k_4 - k_5 C_C^{(t-1)}) \tag{5.21}$$

$$C_V^{(t)} = C_V^{(t-1)} + \Delta t * (k_5 C_C^{(t-1)} - k_6 C_V^{(t-1)}) \tag{5.22}$$

$$C_{VA}^{(t)} = C_{VA}^{(t-1)} + \Delta t * (k_6 C_V^{(t-1)} - k_7 C_{VA}^{(t-1)}) \tag{5.23}$$

The entire duration of the experiment is split between times when the ultrasound machine is turned on and times when it is turned off, as detailed in Chapter 4.1.1. Only in the first case the system perceives a change in the compounds' concentration according to the equations outlined in the formulated model (from Equation 5.19 to 5.23 depending on the considered compound). During the ultrasound off cycles, on the other hand, it appears as though the reaction does not proceed, and the concentration stays constant.

The traditional Euler model, which is used to develop material balances on compounds, had to be modified in order to account for this behaviour.

To illustrate the stepwise trend produced by using the recently described modification of Euler's approach, the concentration profile of syringaldehyde over a shorter time span is displayed below in Figure 5.21, the same graphs for all the other components can be found in Appendix A.5.

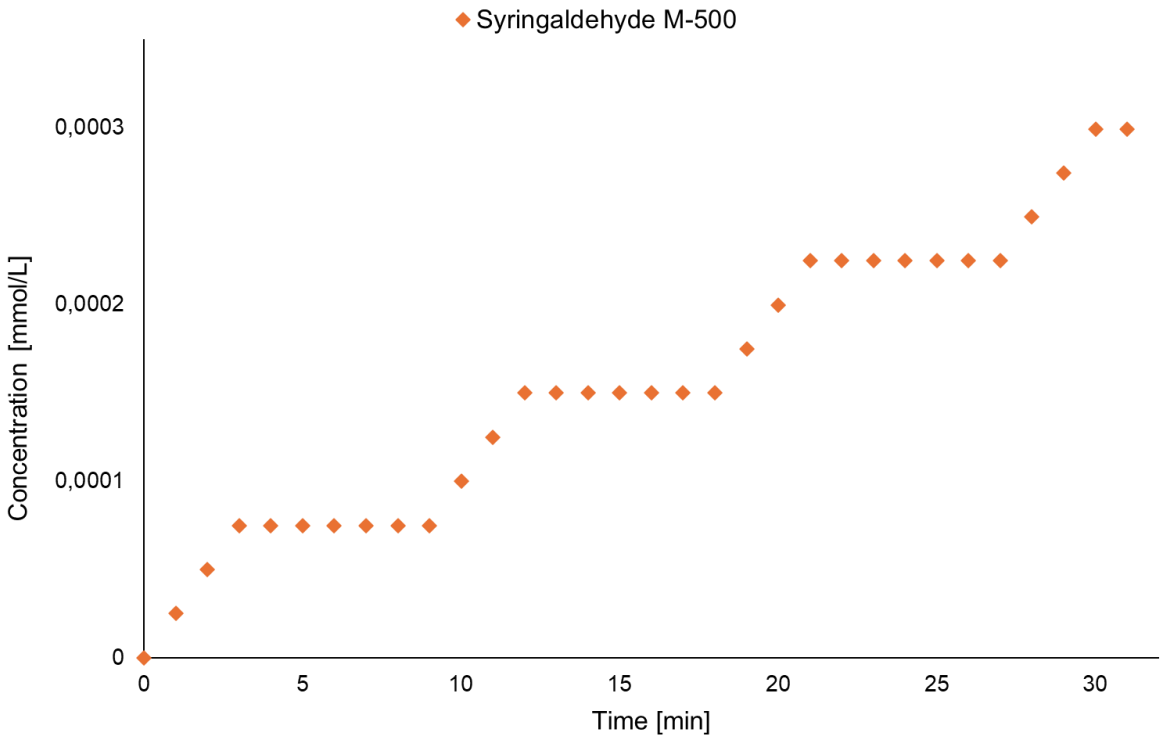

Figure 5.21: Syringaldehyde, sample M-500, step-chart visualization.

Although this will be the approach used for every attempt, the steps trend won't be visible in the overall graphs due to the huge time span considered. Consequently, the function will appear as a continuous line.

At this stage, the goal is to adjust the kinetic parameters in order to fit the experimental values. In this regard the constants evaluated in the first attempt and resumed in Table 1, were initially taken as first guess values for this second trial.

Graphs reported in Figure 5.22 and Figure 5.23 show for the syringil and coniferyl families the concentrations obtained by applying the model introduced so far in comparison with those obtained experimentally.

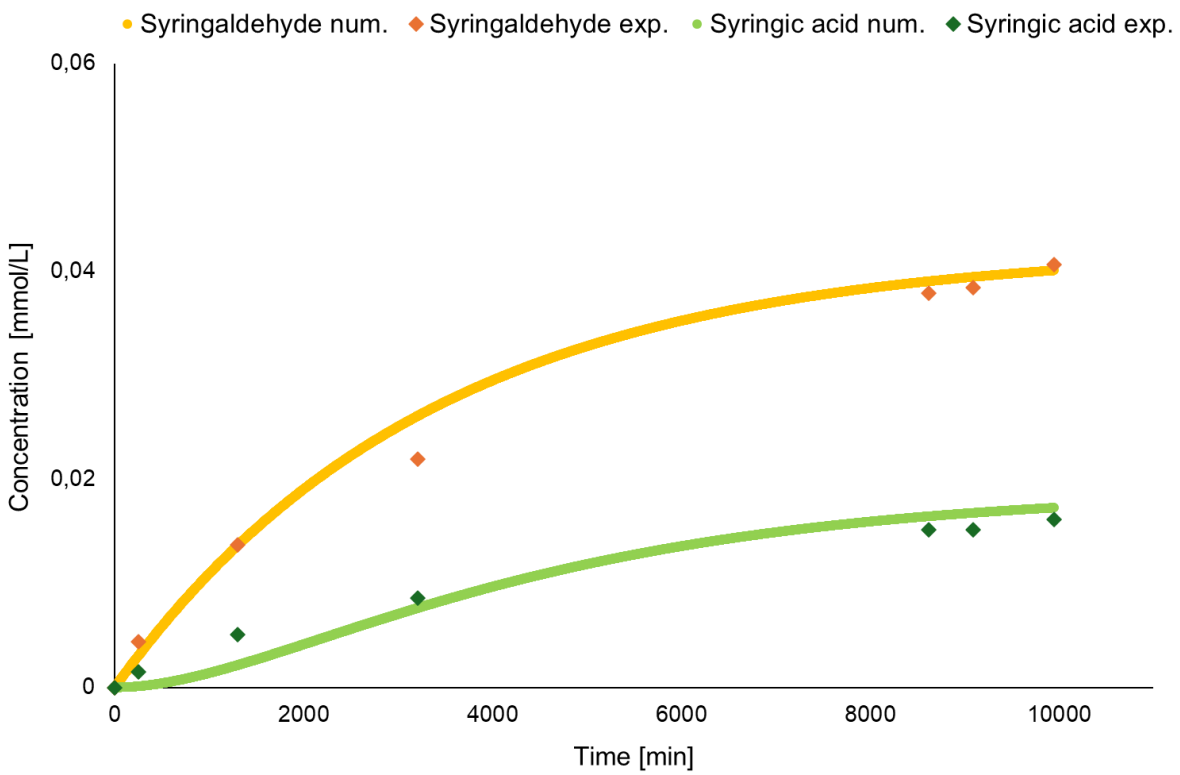

Figure 5.22: Syringil family, M-500 sample, experimental fitting second attempt.

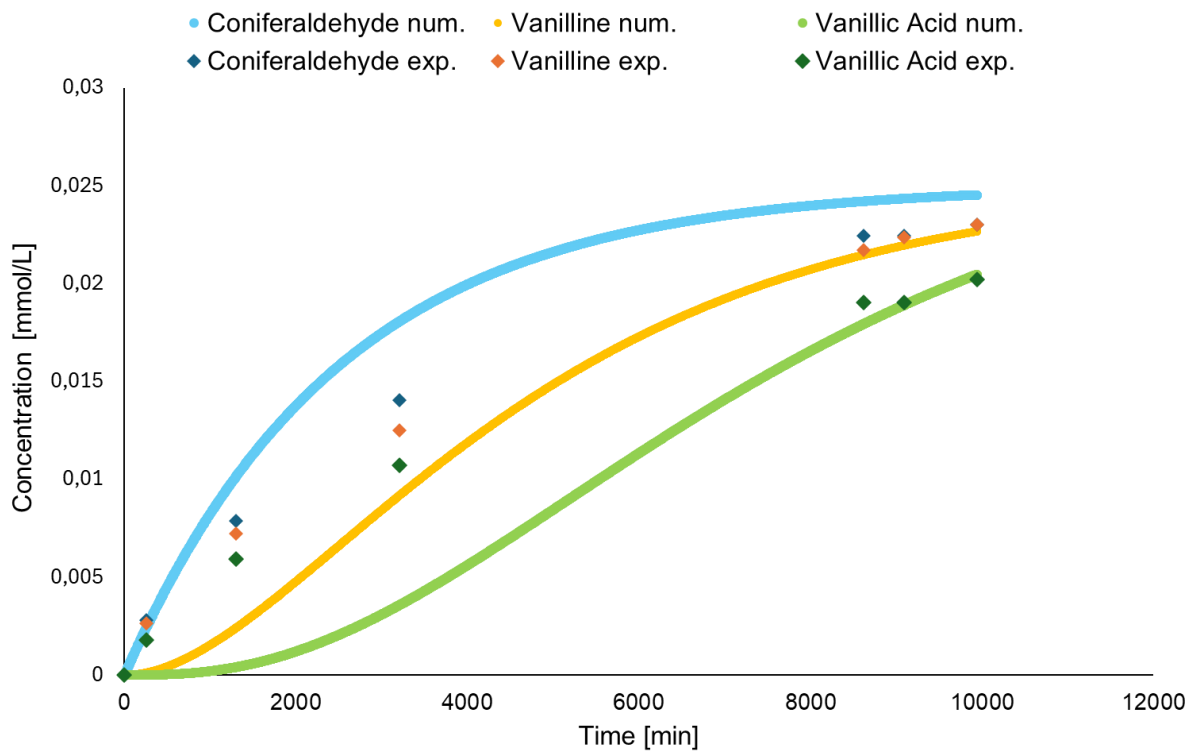

Figure 5.23: Coniferyl family, M-500 sample, experimental fitting second attempt.

Mostly concerning coniferyl family, what emerges, however, is that it is impossible to replicate the trend of the experimental data with a model that only considers the kinetics of the reactions involved, whatever the combination of production and consumption reaction orders and whatever value is assigned to the kinetic constants.

This highlights the need to consider the presence of diffusive phenomena in addition to chemical reactions, which is the starting point in the search for a kinetic model in the hybrid regime.

5.2.1.3. Third attempt

As already explained, the maturation process starts with the reaction of ethanolysis of lignin, one of the most important wood compound; from the results obtained from the previous attempts, it can be stated that a pure chemical regime is not sufficient to describe the process of ageing, so, a hybrid regime has been explored, in which mass transfer phenomena between the solid and the liquid phase are relevant. Among the different possibilities found in literature, the Shrinking Core Model has been found to be the most suitable for the case under study, as discussed in Chapter 4.2.1.2.

According to the model, the ethanol, before reacting with lignin to give aldehydes, has to diffuse through what is called the ash layer, that is the disactivated, so inert, wood layer, that increases in time as the reaction proceeds.

By applying the general Equation 4.14 of SCM to the specific case of ethanol, the ethanolysis reaction rate (Equation 5.24) assumes the shape represented by Equation 5.26 by introducing Equation 5.25:

$$r_1 = k_1 * C_L^{\circ} * C_{EtOH}^{I} \tag{5.24}$$

$$C_{EtOH}^{I} = \left[\frac{\frac{D_{EtOH\,eff}}{\delta} * C^{\circ}{}_{EtOH}}{k_1 C_L^{\circ} + \frac{D_{EtOH\,eff}}{\delta}}\right] \tag{5.25}$$

$$r_1 = k_1 * C_L^{\circ} * \left[\frac{\frac{D_{EtOH\,eff}}{\delta} * C^{\circ}{}_{EtOH}}{k_1 * C_L^{\circ} + \frac{D_{EtOH\,eff}}{\delta}}\right] \tag{5.26}$$

Where k_1 is the kinetic constant of ethanolysis, $D_{EtOH\,eff}$ is the effective diffusion coefficient of ethanol, that accounts, as reported in the Equation 5.27, for the characteristic porosity and tortuosity of the wood matrix.

$$D_{EtOH\,eff} = D_{EtOH} * \frac{\varepsilon}{\tau} \tag{5.27}$$

$C^{\circ}{}_{EtOH}$ and C_L° are, respectively, the initial concentration of ethanol in the bulk and the lignin concentration in the wood, that can be both assumed constant for the reasons explained in the first attempt. This assumption is valid also for the lignin, because, although the ash layer increases in time, the maturation is an extremely low process that makes the consumption of lignin negligible for the time considered in the analysis of this study.

Lastly, δ is the thickness of the ash layer, that can be interpreted as the boundary layer though which the diffusion of ethanol takes place; a good formulation for delta is the one expressed by the Higbie penetration theory, as follows:

$$\delta = \sqrt{12 * D_{EtOH\,eff} * t} \tag{5.28}$$

Initially, only the diffusion of ethanol through the wood matrix has been considered; therefore, the reaction rates for the other compounds are still expressed by the general equation:

$$r_n = k_n\, C_i\, C_j \tag{5.29}$$

Where k_n is the kinetic constant related to the n-reaction, C_i and C_j are the reactant concentrations.

Once the reaction rates for each species have been written, in order to proceed with the construction of the graphs and the research of the experimental fitted values, it is necessary to describe, as for the previous attempts, the concentration profile of the compounds using the equations for the mass balances on a isothermal batch reactor (Equation 5.29, 5.31, 5.33, 5.35, 5.37), discretized according to the Forward Euler method (Equation 5.30, 5.32, 5.34, 5.36, 5.38):

Syringyl group:

$$\frac{dC_S}{dt} = k_1 * C_L^{\circ} * \left[\frac{\frac{D_{EtOH\,eff}}{\delta} * C^{\circ}{}_{EtOH}}{k_1 * C_L^{\circ} + \frac{D_{EtOH\,eff}}{\delta}}\right] * \frac{S_{wood}}{V_{solution}} - k_2 * C_S * C^{\circ}{}_{O_2} \tag{5.29}$$

$$C_S^{(t)} = C_S^{(t-1)} + \Delta t * \left(k_1 * C_L^{\circ} * \left[\frac{\frac{D_{EtOH\,eff}}{\delta} * C^{\circ}{}_{EtOH}}{k_1 * C_L^{\circ} + \frac{D_{EtOH\,eff}}{\delta}}\right] * \frac{S_{wood}}{V_{solution}} - k_2 * C_S^{(t-1)} * C^{\circ}{}_{O_2}\right) \tag{5.30}$$

$$\frac{dC_{AS}}{dt} = k_2 * C_S * C^{\circ}{}_{O_2} - k_3 * C_{AS} * C^{\circ}{}_{EtOH} \tag{5.31}$$

$$C_{AS}^{(t)} = C_{AS}^{(t-1)} + \Delta t * (k_2 * C_S^{(t-1)} * C^{\circ}{}_{O_2} - k_3 * C_{AS}^{(t-1)} * C^{\circ}{}_{EtOH}) \tag{5.32}$$

Coniferyl group:

$$\frac{dC_C}{dt} = k_4 * C_L^{\circ} * \left[\frac{\frac{D_{EtOH\ eff}}{\delta} * C^{\circ}{}_{EtOH}}{k_4 * C_L^{\circ} + \frac{D_{EtOH\ eff.}}{\delta}}\right] * \frac{S_{wood}}{V_{solution}} - k_5 * C_C * C^{\circ}{}_{H_2O} \tag{5.33}$$

$$C_C^{(t)} = C_C^{(t-1)} + \Delta t * \left(k_4 * C_L^{\circ} * \left[\frac{\frac{D_{EtOH\ eff}}{\delta} * C^{\circ}{}_{EtOH}}{k_4 C_L^{\circ} + \frac{D_{EtOH\ eff}}{\delta}}\right] * \frac{S_{wood}}{V_{solution}} - k_5 * C_C^{(t-1)} * C^{\circ}{}_{H_2O}\right) \tag{5.34}$$

$$\frac{dC_V}{dt} = k_5 * C_C * C^{\circ}{}_{H_2O} - k_6 * C_V * C^{\circ}{}_{O_2} \tag{5.35}$$

$$C_V^{(t)} = C_V^{(t-1)} + \Delta t * (k_5 C_C^{(t-1)}\ C^{\circ}{}_{H_2O} - k_3 C_V^{(t-1)} C^{\circ}{}_{O_2}\ ) \tag{5.36}$$

$$\frac{dC_{AV}}{dt} = k_6 * C_V * C^{\circ}{}_{O_2} - k_7 * C_{AV} * C^{\circ}{}_{EtOH} \tag{5.37}$$

$$C_{AV}^{(t)} = C_{AV}^{(t-1)} + \Delta t * (k_6 * C_V^{(t-1)} *\ C^{\circ}{}_{O_2} - k_3 * C_{AV}^{(t-1)} * C^{\circ}{}_{EtOH}) \tag{5.38}$$

At the end of the ethanolysis reaction rate formula is the $\frac{S_{wood}}{V_{solution}}$ ratio. This supports the idea that the reaction occurs on the wood surface wetted by the solution diffused through the delta boundary layer, as suggested by the Shrinking Core Model theory (Chapter 4.2.1.2).

Together with the kinetic constants, it is necessary to estimate a new parameter, that is the diffusion coefficient of ethanol. Actually, as Chapter 2.3 indicates, the effect of ultrasound impacts reaction rates but also the diffusion and transport of matter.

The graph for the M-500 sample is reported in Figure 5.24 for the case of compounds belonging to the syringil family, while the ones related to the coniferyl have not been reported since the model does not allow an estimation of all the parameters (kinetic constants and diffusivity) that permits an acceptable fitting of the experimental values, revealing the limitations of the model introduced in this paragraph.

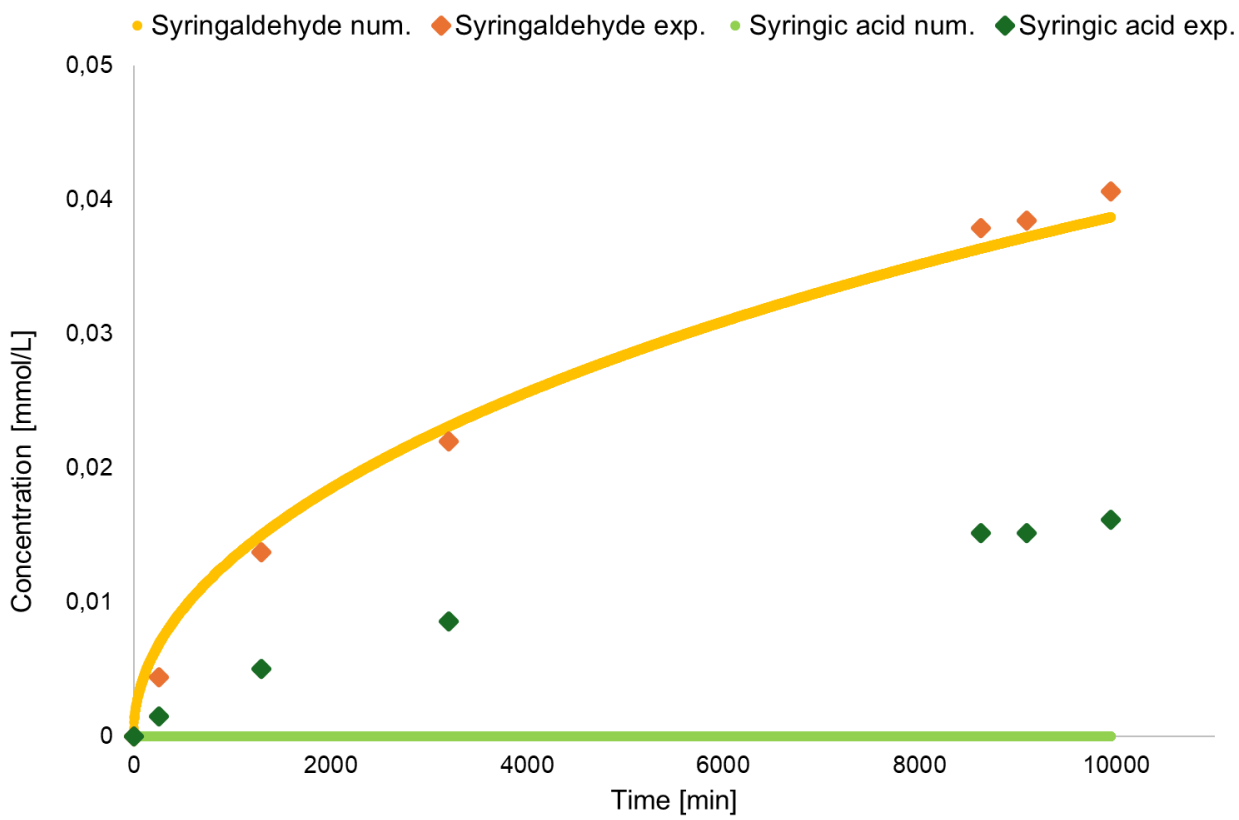

Figure 5.24: Syringil family, M-500 sample, experimental fitting third attempt.

As can be seen, the manipulation of the parameters shows good results for the aldehyde, while reveals the impossibility to find a correspondence with the experimental values for the syringic acid; this represents an important key point, suggesting that the introduction of the shrinking core model for the ethanol, and so accounting for its diffusion in the solid matrix, is the discriminant for the success of the model.

5.2.1.4. Fourth attempt

Starting from the good result obtained from the introduction of the SCM for ethanol, the same logic has been applied to the diffusion of oxygen and water, the reactants involved, respectively, in the production of acids and vanillin. Physically, it means that not only the ethanolysis reaction takes place within the wood matrix, but, once produced, also the aldehyde will not react prior to the diffusion of oxygen or water [118].

The reaction rate to produce the acids, both syringic and vanillic acids have the same path as Equation 5.12 and 5.13 show, is generalized by Equation 5.39; while the one for the production of vanillin from coniferaldehyde is expressed by Equation 5.40.

$$r = k * C_{aldehyde} * C_{O_2}^{I} \ (5.39) \quad \text{and} \quad r = k * C_C * C_{H_2O}^{I} \ (5.40)$$

Where k are the kinetic constants and the $C_{O_2}^{I}$ and $C_{H_2O}^{I}$ are the reactants concentration at the interface.

By expressing the interface concentration of oxygen and water according to the same formulation (Equation 4.14) used for the ethanol with a Shrinking Core Model, new mass balances on each compound are obtained (Equation 5.41, 5.43, 5.45, 5.47, 5.49), together with the equations of the Eulero Forward method (Equation 5.42, 5.44, 5.46, 5.48, 5.50).

Syringil group:

$$\frac{dC_S}{dt} = k_1 * C_L^{\circ} * \left[\frac{\frac{D_{EtOH\,eff}}{\delta} * C^{\circ}{}_{EtOH}}{k_1 * C_L^{\circ} + \frac{D_{EtOH\,eff}}{\delta}}\right] * \frac{S_{wood}}{V_{solution}} - k_2 * C_S * \left[\frac{\frac{D_{O_2\,eff}}{\delta} * C^{\circ}{}_{O_2}}{k_2 * C_S + \frac{D_{O_2\,eff}}{\delta}}\right] * \frac{S_{wood}}{V_{solution}} \tag{5.41}$$

$$C_S^{(t)} = C_S^{(t-1)} + \Delta t * \left(k_1 * C_L^{\circ} * \left[\frac{\frac{D_{EtOH\,eff}}{\delta} * C^{\circ}{}_{EtOH}}{k_1 * C_L^{\circ} + \frac{D_{EtOH\,eff}}{\delta}}\right] * \frac{S_{wood}}{V_{solution}} - k_2 * C_S^{(t-1)} * \left[\frac{\frac{D_{O_2\,eff}}{\delta} * C^{\circ}{}_{O_2}}{k_2 * C_S^{(t-1)} + \frac{D_{O_2\,eff}}{\delta}}\right] * \frac{S_{wood}}{V_{solution}}\right) \tag{5.42}$$

$$\frac{dC_{AS}}{dt} = k_2 * C_S * \left[\frac{\frac{D_{O_2\,eff}}{\delta} * C_{O_2}^{\circ}}{k_2 * C_S + \frac{D_{O_2\,eff}}{\delta}}\right] * \frac{S_{wood}}{V_{solution}} - k_3 * C_{AS} * \left[\frac{\frac{D_{EtOH\,eff}}{\delta} * C^{\circ}{}_{EtOH}}{k_3 * C_{AS} + \frac{D_{EtOH\,eff}}{\delta}}\right] * \frac{S_{wood}}{V_{solution}} \tag{5.43}$$

$$C_{AS}^{(t)} = C_{AS}^{(t-1)} + \Delta t * \left(k_2 * C_S^{(t-1)} * \left[\frac{\frac{D_{O_2\,eff}}{\delta} * C^{\circ}{}_{O_2}}{k_2 * C_S^{(t-1)} + \frac{D_{O_2\,eff}}{\delta}}\right] * \frac{S_{wood}}{V_{solution}} - k_3 * C_{AS}^{(t-1)} * \left[\frac{\frac{D_{EtOH\,eff}}{\delta} * C^{\circ}{}_{EtOH}}{k_3 * C_{AS}^{(t-1)} + \frac{D_{EtOH\,eff}}{\delta}}\right] * \frac{S_{wood}}{V_{solution}}\right) \tag{5.44}$$

Coniferyl group:

$$\frac{dC_C}{dt} = k_4 * C_L^{\circ} * \left[\frac{\frac{D_{EtOH\ eff}}{\delta} * C^{\circ}{}_{EtOH}}{k_4 * C_L^{\circ} + \frac{D_{EtOH\ eff}}{\delta}}\right] * \frac{S_{wood}}{V_{solution}} - k_5 * C_C * \left[\frac{\frac{D_{H_2O\ eff}}{\delta} * C^{\circ}{}_{H_2O}}{k_4 * C_C + \frac{D_{H_2O\ eff}}{\delta}}\right] * \frac{S_{wood}}{V_{solution}} \tag{5.45}$$

$$C_C^{(t)} = C_C^{(t-1)} + \Delta t * \left(k_4 * \left[\frac{\frac{D_{EtOH\ eff}}{\delta} * C^{\circ}{}_{EtOH}}{k_4 * C_L^{\circ} + \frac{D_{EtOH\ eff}}{\delta}}\right] * C_L^{\circ} * \frac{S_{wood}}{V_{solution}} - k_5 * C_C^{(t-1)} * \left[\frac{\frac{D_{H_2O\ eff}}{\delta} * C^{\circ}{}_{H_2O}}{k_4 * C_C^{(t-1)} + \frac{D_{H_2O\ eff}}{\delta}}\right] * \frac{S_{wood}}{V_{solution}}\right) \tag{5.46}$$

$$\frac{dC_V}{dt} = k_5 * C_C * \left[\frac{\frac{D_{H_2O\ eff}}{\delta} * C^{\circ}{}_{H_2O}}{k_4 * C_C + \frac{D_{H_2O\ eff}}{\delta}}\right] * \frac{S_{wood}}{V_{solution}} - k_6 * C_V * \left[\frac{\frac{D_{O_2\ eff}}{\delta} * C^{\circ}{}_{O_2}}{k_6 * C_V + \frac{D_{O_2\ eff}}{\delta}}\right] * \frac{S_{wood}}{V_{solution}} \tag{5.47}$$

$$C_V^{(t)} = C_V^{(t-1)} + \Delta t * \left(k_5 * C_C^{(t-1)} \left[\frac{\frac{D_{H_2O\ eff}}{\delta} * C^{\circ}{}_{H_2O}}{k_5 * C_C^{(t-1)} + \frac{D_{H_2O\ eff}}{\delta}}\right] * \frac{S_{wood}}{V_{solution}} - k_6 * C_V^{(t-1)} \left[\frac{\frac{D_{O_2\ eff}}{\delta} * C^{\circ}{}_{O_2}}{k_6 * C_V^{(t-1)} + \frac{D_{O_2\ eff}}{\delta}}\right] * \frac{S_{wood}}{V_{solution}}\right) \tag{5.48}$$

$$\frac{dC_{AV}}{dt} = k_6 * C_V \left[\frac{\frac{D_{O_2\ eff}}{\delta} * C^{\circ}{}_{O_2}}{k_6 * C_V + \frac{D_{O_2\ eff}}{\delta}}\right] * \frac{S_{wood}}{V_{solution}} - k_7 * C_{AV} \left[\frac{\frac{D_{EtOH\ eff}}{\delta} * C^{\circ}{}_{EtOH}}{k_7 * C_{AV} + \frac{D_{EtOH\ eff}}{\delta}}\right] * \frac{S_{wood}}{V_{solution}} \tag{5.49}$$

$$C_{AV}^{(t)} = C_{AV}^{(t-1)} + \Delta t * \left(k_6 * C_V^{(t-1)} \left[\frac{\frac{D_{O_2\ eff}}{\delta} * C^{\circ}{}_{O_2}}{k_6 * C_V^{(t-1)} + \frac{D_{O_2\ eff}}{\delta}}\right] * \frac{S_{wood}}{V_{solution}} - k_7 * C_{AV}^{(t-1)} \left[\frac{\frac{D_{EtOH\ eff}}{\delta} * C^{\circ}{}_{EtOH}}{k_7 * C_{AV}^{(t-1)} + \frac{D_{EtOH\ eff}}{\delta}}\right] * \frac{S_{wood}}{V_{solution}}\right) \tag{5.50}$$

With the new system of equations, the two additional parameters that need to be manipulated to obtain a good fitting of the experimental values are the oxygen and water diffusion. The graphs related to each compound have been built, and the manipulation of the parameters involved brought to a more precise fitting of the experimental values, as can be seen in the following plots (Figure 5.25 and Figure 5.26) for sample M-500.

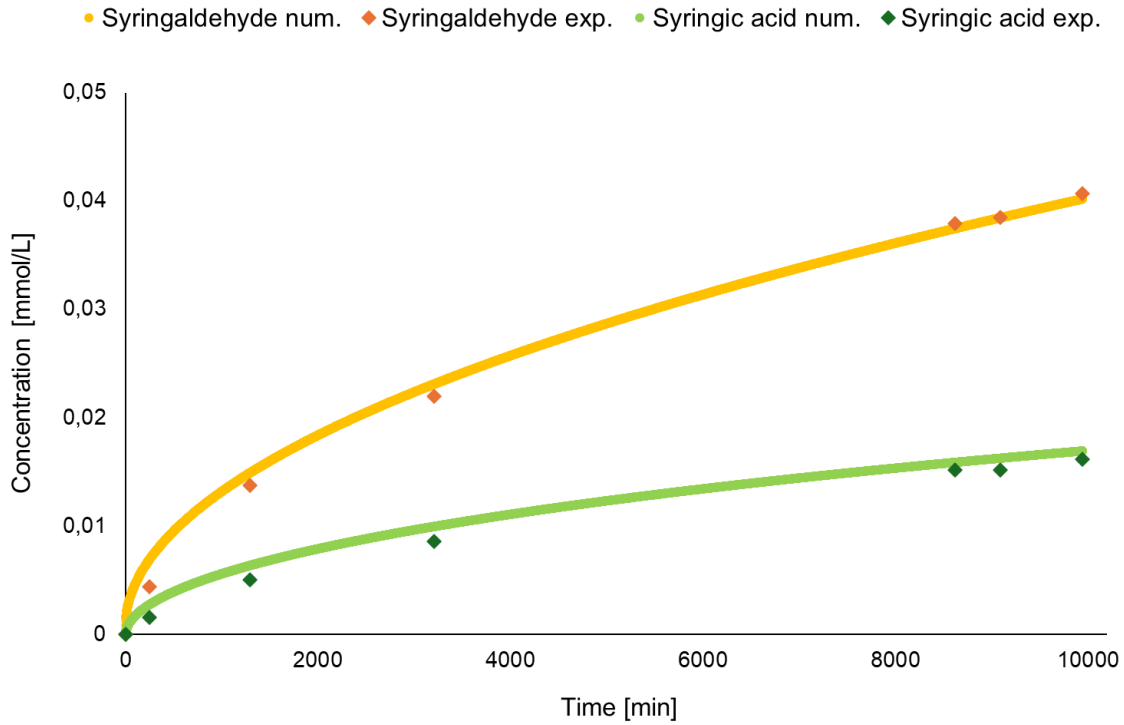

Figure 5.25: Syringil family, M-500 sample, experimental fitting fourth attempt.

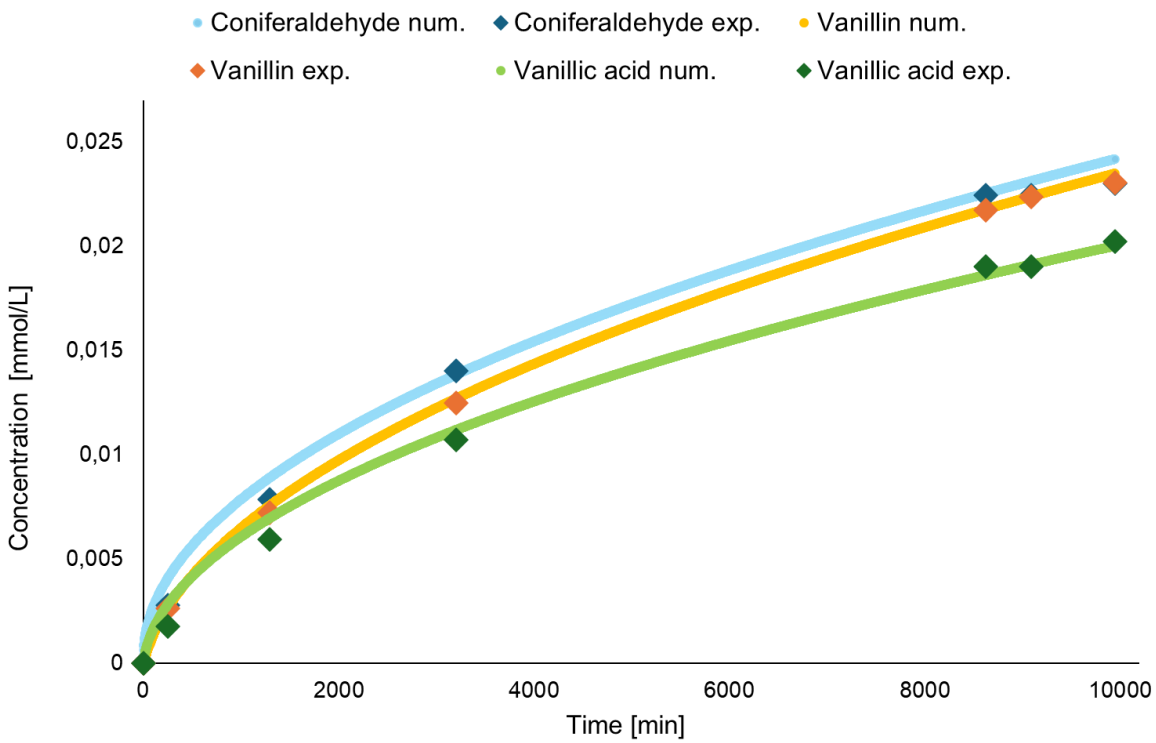

Figure 5.26: Coniferyl family, M-500 sample, experimental fitting fourth attempt.

The Table 5.4 reports the fitted values of all the parameters involved in the system of equations. Without entering in detail about each single parameter, the main consideration regards the consistency of the values obtained, that are extremely low if compared to the ones found in literature having an order of magnitude around 10^{-10}, the specific values for each considered compound can be consulted in the Appendix A.2. Moreover, an increase in these values was expected due to the effect of the ultrasound.

Table 5.4: Sample M-500, manipulated kinetic constants values from the fourth attempt.

Sample M-500	$k_{ethanolysis}\left[\frac{m^4}{mol*s}\right]$	$k_{hydrolysis}\left[\frac{m^4}{mol*s}\right]$	$k_{oxydation}\left[\frac{m^4}{mol*s}\right]$	$k_{esterification}\left[\frac{m^4}{mol*s}\right]$
Syringil	1,67 E-07	/	8,33 E-08	1,16 E-16
Coniferyl	1,67 E-07	1,00 E-06	1,33 E-07	8,33 E-18

Table 5.5: Sample M-500, manipulated diffusivity values from the fourth attempt.

Sample M-500	$D_{EtOH}\left[\frac{m^2}{s}\right]$	$D_{H_2O}\left[\frac{m^2}{s}\right]$	$D_{O_2}\left[\frac{m^2}{s}\right]$
Syringil	9,96E-20	/	8,24E-14
Coniferyl	1,97E-20	1,72E-08	1,06E-13

This last consideration suggests the need to correct the model just developed to try to overcome the mismatch between fitted and expected values.

5.2.1.5. Final attempt

The model of the 4th attempt gives a good fitting of the experimental values, but a further improvement is required to obtain a more realistic order of magnitude of the parameters. This implies a modification of the equations to obtain a more complex

system capable to account for all the phenomena involved in the maturation process and to demonstrate its validity through new fitted parameters that show a greater physical relevance.

Until now it has been assumed that the ethanolysis, hydrolysis and oxidation reactions take place within the wood matrix after the reactants diffusion. In reality, the new products formed on the external surface of the porous matrix partly take part to the successive reactions according to their kinetic scheme, partly diffuse back through the ash layer to accumulate in the bulk. Therefore, the innovation of this attempt is the introduction of the back diffusion phenomenon, which has not been considered before since most of the times it is a quick and negligible step (Chapter 4.2.1.2).

Based on the last considerations, there is the need to introduce a distinction between the compounds found on the external surface of the porous wood matrix and the compounds in the bulk. The experimental values, in fact, are related to the concentration in a liquid phase (moles per litre of solution), and not to the concentration in the wood matrix.

Therefore, for each component it is possible to write two distinctive mass balances, one related to the compound in the solid phase and one to the compound in the liquid phase.

For the solid phase, the variation of a generic component is given by the following terms:

$$\text{Variation} = \text{production} - \text{consumption} - \text{diffusion} \tag{5.51}$$

- The production term is different if considering the aldehydes or the acids: for syringaldehyde and coniferaldehyde, it represents the production obtained from the ethanolysis of lignin, while for vanillin represents the production from the hydrolysis of coniferaldehyde; for the acids, instead, it represents the production coming from the oxidation of syringaldehyde or vanillin, according to the acid considered. All the terms are identical to the ones of the previous attempt and the shrinking core model is applied to justify the diffusion of ethanol, water and oxygen.
- The consumption term for the aldehydes reflects the oxidation of syringaldehyde or vanillin to give the corresponding acid or the hydrolysis of coniferaldehyde to give vanillin; the consumption of the acids is, instead, related to the reaction with the diffused ethanol to give the corresponding esters.

- Lastly, the diffusion of each compound from the solid to the liquid phase represents the additional term.

Specifically, the reaction rates for the production and consumption terms are unchanged, while the diffusion term can be expressed as the generic flux between two phases according to the general expression:

$$N_i = K_c * (C_{i,solid} - C_{i,lqiuid}) \tag{5.52}$$

The mass transfer coefficient, K_c, is expressed as $\frac{D_{i,eff}}{\delta}$, where the effective diffusion coefficient accounts for the porous structure of wood, while the ash layer δ varies in time according to the Equation 5.28 derived from Higbie theory. The driving force is given by the difference in concentration between the solid and the liquid phases.

For the liquid phase, the variation of a generic component is given by the following equation:

$$\text{Variation} = \text{diffusion} \tag{5.53}$$

So, the diffusion term is identical to the one of Equation 5.51 apart from the sign, since the variation of aldehydes or acids in the liquid phase is a function only of the back diffusion in the bulk.

According to the introduced scheme it is possible to write new equations for the mass balances on each component: Equations 5.54, 5.58, 5.62, 5.66, 5.70 refer to congeners mass balances in solid phase with Equations 5.55, 5.59, 5.63, 5.67, 5.71 representing Euler's resolutions , while Equation 5.56, 5.60, 5.64, 5.68, 5.72 refer to congeners mass balances in liquid phase with Equations 5.57, 5.61, 5.65, 5.69, 5.73 representing Euler's resolutions.

Syringaldehyde:

$$\frac{dC_{S\,solid}}{dt} = k_1 * C_L^{\circ} * \left[\frac{\frac{D_{EtOH\,eff}}{\delta} * C^{\circ}{}_{EtOH}}{k_1 * C_L^{\circ} + \frac{D_{EtOH\,eff}}{\delta}}\right] * \frac{S_{wood}}{V_{wood}} - k_2 * C_{S\,solid} * \left[\frac{\frac{D_{O_2\,eff}}{\delta} * C^{\circ}{}_{O_2}}{k_2 * C_{S\,solid} + \frac{D_{O_2\,eff}}{\delta}}\right] * \frac{S_{wood}}{V_{wood}} - \sqrt{\frac{D_{S\,eff}}{12 * t}} * \left(C_{S\,solid} - C_{S\,liquid}\right) * \frac{S_{wood}}{V_{wood}} \tag{5.54}$$

$$C_{S\,solid}^{(t)} = C_{S\,solid}^{(t-1)} + \Delta t * \left(k_1 * C_L^{\circ} * \left[\frac{\frac{D_{EtOH\,eff}}{\delta} * C^{\circ}{}_{EtOH}}{k_1 * C_L^{\circ} + \frac{D_{EtOH\,eff}}{\delta}} \right] * \frac{S_{wood}}{V_{wood}} - k_2 * C_{S\,solid}^{(t-1)} * \left[\frac{\frac{D_{O_2\,eff}}{\delta} * C^{\circ}{}_{O_2}}{k_2 * C_{S\,solid}^{(t-1)} + \frac{D_{O_2\,eff}}{\delta}} \right] * \frac{S_{wood}}{V_{wood}} - \sqrt{\frac{D_{S\,eff}}{12 * t}} * \left(C_{S\,solid}^{(t-1)} - C_{L\,liquid}^{(t-1)} \right) * \frac{S_{wood}}{V_{wood}} \right) \tag{5.55}$$

$$\frac{dC_{S\,liquid}}{dt} = \sqrt{\frac{D_{S\,eff}}{12 * t}} * \left(C_{S\,solid} - C_{S\,liquid} \right) * \frac{S_{wood}}{V_{solution}} \tag{5.56}$$

$$C_{S\,liquid}^{(t)} = C_{S\,liquid}^{(t-1)} + \Delta t * \left(\sqrt{\frac{D_{S\,eff}}{12 * t}} * \left(C_{S\,solid}^{(t-1)} - C_{S\,liquid}^{(t-1)} \right) * \frac{S_{wood}}{V_{solution}} \right) \tag{5.57}$$

Syringic acid:

$$\frac{dC_{SA\,solid}}{dt} = k_2 * C_{S\,solid} * \left[\frac{\frac{D_{O_2\,eff}}{\delta} * C^{\circ}{}_{O_2}}{k_2 * C_{S\,solid} + \frac{D_{O_2\,eff}}{\delta}} \right] * \frac{S_{wood}}{V_{wood}} - k_3 * C_{SA\,solid} * \left[\frac{\frac{D_{EtOH\,eff}}{\delta} * C^{\circ}{}_{EtOH}}{k_3 * C_{SA\,solid} + \frac{D_{EtOH\,eff}}{\delta}} \right] * \frac{S_{wood}}{V_{wood}} - \sqrt{\frac{D_{SA\,eff}}{12 * t}} * \left(C_{SA\,solid} - C_{SA\,liquid} \right) * \frac{S_{wood}}{V_{wood}} \tag{5.58}$$

$$C_{SA\,solid}^{(t)} = C_{SA\,solid}^{(t-1)} + \Delta t * \left(k_2 * C_{S\,solid}^{(t-1)} * \left[\frac{\frac{D_{O_2\,eff}}{\delta} * C^{\circ}{}_{O_2}}{k_2 * C_{S\,solid}^{(t-1)} + \frac{D_{O_2\,eff}}{\delta}} \right] * \frac{S_{wood}}{V_{wood}} - k_3 * C_{SA\,solid}^{(t-1)} * \left[\frac{\frac{D_{EtOH\,eff}}{\delta} * C^{\circ}{}_{EtOH}}{k_3 * C_{AS\,solid}^{(t-1)} + \frac{D_{EtOH\,eff}}{\delta}} \right] * \frac{S_{wood}}{V_{wood}} - \sqrt{\frac{D_{SA\,eff}}{12 * t}} * \left(C_{SA\,solid}^{(t-1)} - C_{SA\,liquid}^{(t-1)} \right) * \frac{S_{wood}}{V_{wood}} \right) \tag{5.59}$$

$$\frac{dC_{SA\,liquid}}{dt} = \sqrt{\frac{D_{AS\,eff}}{12 * t}} * \left(C_{SA\,solid} - C_{SA\,liquid} \right) * \frac{S_{wood}}{V_{solution}} \tag{5.60}$$

$$C_{SA\,liquid}^{(t)} = C_{SA\,liquid}^{(t-1)} + \Delta t * \left(\sqrt{\frac{D_{SA\,eff}}{12 * t}} * \left(C_{SA\,solid}^{(t-1)} - C_{SA\,liquid}^{(t-1)} \right) * \frac{S_{wood}}{V_{solution}} \right) \tag{5.61}$$

Coniferaldehyde:

$$\frac{dC_{C\,solid}}{dt} = k_4 * C_L^{\circ} * \left[\frac{\frac{D_{EtOH\,eff}}{\delta} * C^{\circ}{}_{EtOH}}{k_4 * C_L^{\circ} + \frac{D_{EtOH\,eff}}{\delta}}\right] * \frac{S_{wood}}{V_{wood}} - k_5 * C_C * \left[\frac{\frac{D_{H_2O\,eff}}{\delta} * C^{\circ}{}_{H_2O}}{k_4 * C_C + \frac{D_{H_2O\,eff}}{\delta}}\right] * \frac{S_{wood}}{V_{wood}} - \sqrt{\frac{D_{C\,eff}}{12 * t}} * (C_{C\,solid} - C_{C\,liquid}) * \frac{S_{wood}}{V_{wood}} \tag{5.62}$$

$$C_{C\,solid}^{(t)} = C_{C\,solid}^{(t-1)} + \Delta t * \left(k_4 * C_L^{\circ} * \left[\frac{\frac{D_{EtOH\,eff}}{\delta} * C^{\circ}{}_{EtOH}}{k_4 * C_L^{\circ} + \frac{D_{EtOH\,eff}}{\delta}}\right] * \frac{S_{wood}}{V_{wood}} - k_5 * C_{C\,solid}^{(t-1)} * \left[\frac{\frac{D_{O_2\,eff}}{\delta} * C^{\circ}{}_{O_2}}{k_5 * C_{C\,solid}^{(t-1)} + \frac{D_{O_2\,eff}}{\delta}}\right] * \frac{S_{wood}}{V_{wood}} - \sqrt{\frac{D_{S\,eff}}{12 * t}} * \left(C_{C\,solid}^{(t-1)} - C_{C\,liquid}^{(t-1)}\right) * \frac{S_{wood}}{V_{wood}}\right) \tag{5.63}$$

$$\frac{dC_{C\,liquid}}{dt} = \sqrt{\frac{D_{C\,eff}}{12 * t}} * (C_{C\,solid} - C_{S\,liquid}) * \frac{S_{wood}}{V_{solution}} \tag{5.64}$$

$$C_{C\,liquid}^{(t)} = C_{C\,liquid}^{(t-1)} + \Delta t * \left(\sqrt{\frac{D_{C\,eff}}{12 * t}} * \left(C_{C\,solid}^{(t-1)} - C_{C\,liquid}^{(t-1)}\right) * \frac{S_{wood}}{V_{solution}}\right) \tag{5.65}$$

Vanillin:

$$\frac{dC_{V\,solid}}{dt} = k_5 * C_C * \left[\frac{\frac{D_{H_2O\,eff}}{\delta} * C^{\circ}{}_{H_2O}}{k_5 * C_C + \frac{D_{H_2O\,eff}}{\delta}}\right] * \frac{S_{wood}}{V_{wood}} - k_6 * C_V * \left[\frac{\frac{D_{O_2\,eff}}{\delta} * C^{\circ}{}_{O_2}}{k_6 * C_V + \frac{D_{O_2\,eff}}{\delta}}\right] * \frac{S_{wood}}{V_{wood}} - \sqrt{\frac{D_{V\,eff}}{12 * t}} * (C_{V\,solid} - C_{V\,liquid}) * \frac{S_{wood}}{V_{wood}} \tag{5.66}$$

$$C_{V\,solid}^{(t)} = C_{V\,solid}^{(t-1)} + \Delta t * \left(k_5 * C_C^{(t-1)} * \left[\frac{\frac{D_{H_2O\,eff}}{\delta} * C^{\circ}{}_{H_2O}}{k_5 * C_C^{(t-1)} + \frac{D_{H_2O\,eff}}{\delta}}\right] * \frac{S_{wood}}{V_{wood}} - k_6 * C_{V\,solid}^{(t-1)} * \left[\frac{\frac{D_{O_2\,eff.}}{\delta} * C^{\circ}{}_{O_2}}{k_6 C_{V\,solid}^{(t-1)} + \frac{D_{O_2\,eff.}}{\delta}}\right] * \frac{S_{wood}}{V_{wood}} - \sqrt{\frac{D_{S\,eff}}{12 * t}} * \left(C_{V\,solid}^{(t-1)} - C_{V\,liquid}^{(t-1)}\right) * \frac{S_{wood}}{V_{wood}}\right) \tag{5.67}$$

$$\frac{dC_{V\,liquid}}{dt} = \sqrt{\frac{D_{V\,eff}}{12 * t}} * (C_{V\,solid} - C_{V\,liquid}) * \frac{S_{wood}}{V_{solution}} \tag{5.68}$$

$$C_{V\ liquid}^{(t)} = C_{V\ liquid}^{(t-1)} + \Delta t * (\sqrt{\frac{D_{C\ eff}}{12*t}} * \left(C_{V\ solid}^{(t-1)} - C_{V\ liquid}^{(t-1)}\right) * \frac{S_{wood}}{V_{solution}}) \tag{5.69}$$

Vanillic acid:

$$\frac{dC_{AV}}{dt} = k_6 C_V \left[\frac{\frac{D_{O_2\ eff.}}{\delta} * C^{\circ}{}_{O_2}}{k_6 C_V + \frac{D_{O_2\ eff.}}{\delta}}\right] * \frac{S_{wood}}{V_{wood}} - k_7 C_{AV} \left[\frac{\frac{D_{EtOH\ eff.}}{\delta} * C^{\circ}{}_{EtOH}}{k_7 C_{AV} + \frac{D_{EtOH\ eff.}}{\delta}}\right] * \frac{S_{wood}}{V_{wood}} - \sqrt{\frac{D_{AV\ eff}}{12*t}} * (C_{AV\ solid} - C_{AV\ liquid}) * \frac{S_{wood}}{V_{wood}} \tag{5.70}$$

$$C_{AV\ solid}^{(t)} = C_{AV\ solid}^{(t-1)} + \Delta t * \left(k_6 C_{V\ solid}^{(t-1)} * \left[\frac{\frac{D_{O_2\ eff.}}{\delta} * C^{\circ}{}_{O_2}}{k_6 C_{V\ solid}^{(t-1)} + \frac{D_{O_2\ eff.}}{\delta}}\right] * \frac{S_{wood}}{V_{wood}} - k_7 C_{AV\ solid}^{(t-1)} * \left[\frac{\frac{D_{EtOH\ eff.}}{\delta} * C^{\circ}{}_{EtOH}}{k_7 C_{AV\ solid}^{(t-1)} + \frac{D_{EtOH\ eff.}}{\delta}}\right] * \frac{S_{wood}}{V_{wood}} - \sqrt{\frac{D_{AV\ eff}}{12*t}} * \left(C_{AV\ solid}^{(t-1)} - C_{AV\ liquid}^{(t-1)}\right) * \frac{S_{wood}}{V_{wood}}\right) \tag{5.71}$$

$$\frac{dC_{AV\ liquid}}{dt} = \sqrt{\frac{D_{AV\ eff}}{12*t}} * \left(C_{AV\ solid} - C_{AV\ liquid}\right) * \frac{S_{wood}}{V_{solution}} \tag{5.72}$$

$$C_{AV\ liquid}^{(t)} = C_{AV\ liquid}^{(t-1)} + \Delta t * \left(\sqrt{\frac{D_{AV\ eff}}{12*t}} * \left(C_{AV\ solid}^{(t-1)} - C_{AV\ liquid}^{(t-1)}\right) * \frac{S_{wood}}{V_{solution}}\right) \tag{5.73}$$

The scheme just described is the most comprehensive model for explaining the physic-chemical phenomena that take place during whisky maturation. The introduction of new equations has resulted in an increase in the parameters to be estimated and fit to replicate the trend of the experimental data.

The M-500 sample graphs for the two chemical families are displayed in Figure 5.27 and Figure 5.28 together with Tables 5.5, 5.6 and 5.7 resuming the manipulated parameters.

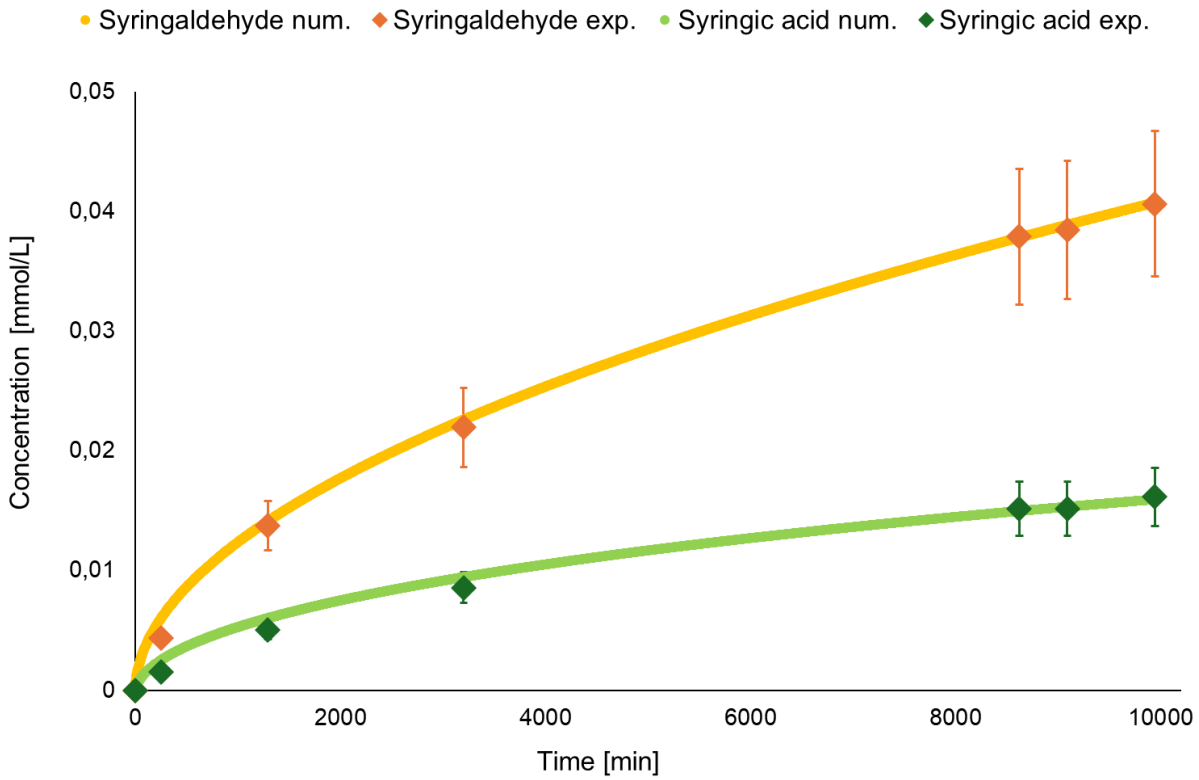

Figure 5.27: Syringil family, M-500 sample, experimental fitting last attempt.

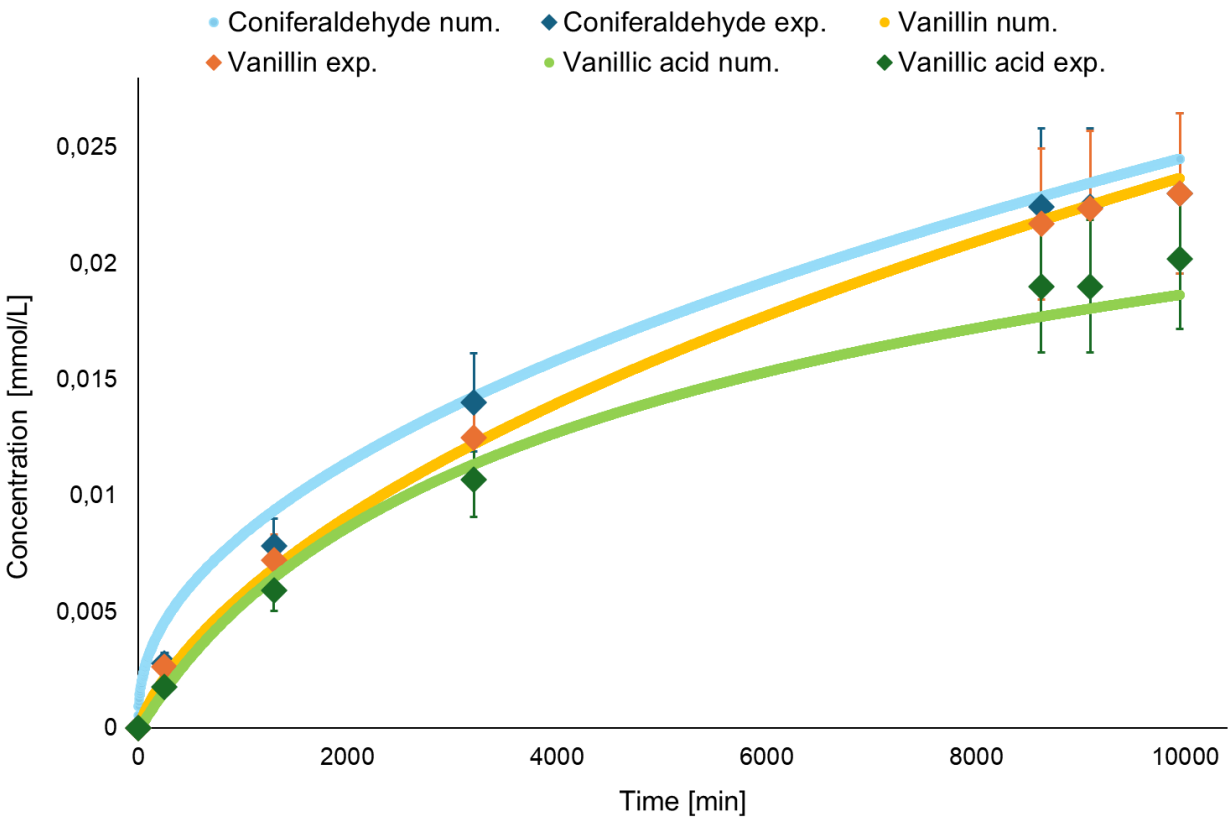

Figure 5.28: Coniferyl family, M-500 sample, experimental fitting last attempt.

Table 5.6: Sample M-500, manipulated kinetic constant values from the last attempt.

Sample M-500	$k_{ethanolysis}\left[\frac{m^4}{mol*s}\right]$	$k_{hydrolysis}\left[\frac{m^4}{mol*s}\right]$	$k_{oxydation}\left[\frac{m^4}{mol*s}\right]$	$k_{esterification}\left[\frac{m^4}{mol*s}\right]$
Syringil	1,33 E-06	/	6,67 E-05	6,67 E-09
Coniferyl	1,67 E-05	2,00 E-02	1,67 E-03	8,33 E-13

Table 5.7: Syringil family, sample M-500, manipulated diffusivity coefficient values from the last attempt.

Sample M-500	$D_{EtOH}\left[\frac{m^2}{s}\right]$	$D_{O_2}\left[\frac{m^2}{s}\right]$	$D_S\left[\frac{m^2}{s}\right]$	$D_{SA}\left[\frac{m^2}{s}\right]$
Syringil	1,43 E-14	1,19 E-07	8,33 E-14	3,33 E-14

Table 5.8: Coniferyl family, sample M-500, manipulated diffusivity coefficient values from the last attempt.

Sample M-500	$D_{EtOH}\left[\frac{m^2}{s}\right]$	$D_{H_2O}\left[\frac{m^2}{s}\right]$	$D_{O_2}\left[\frac{m^2}{s}\right]$	$D_C\left[\frac{m^2}{s}\right]$	$D_V\left[\frac{m^2}{s}\right]$	$D_{VA}\left[\frac{m^2}{s}\right]$
Coniferyl	4,44 E-19	7,82 E-20	1,21 E-12	5,00 E-09	3,33 E-10	5,00 E-11

The graphs constructed for the concentrations of the compounds again fit the experimental values very well. However, despite the apparent success of the model in obtaining higher values for the kinetic and diffusivity parameters than in attempt four, realistic and desirable values remain far off.

5.2.2. Gallic acid

The final section of the model development addresses gallic acid, the sole chemical that has not been considered yet. As previously mentioned in Chapter 5.2.2, this

substance is the result of the hydrolysis of a particular family of tannins, known as gallotannins, that are a component of wood, in the same way of lignin.

Because the mechanism following its production is unclear and poorly defined, it was difficult to construct the compound's kinetic scheme. Nonetheless, research has shown that gallic acid frequently tends to revert to its initial state by a subsequent reaction with the water in solution.

Given that the Shrinking Core Model is quite successful in explaining the behaviour of all other congener reactions, the first attempt tries to assess the same mechanism in relation to tannin hydrolysis and gallic acid consumption.

The system subdivision into solid and liquid sides is also introduced for this scenario to account for the back diffusion of congeners in the liquid phase, in accordance with the most recent arrangements advanced for the syringil and coniferyl cases.

Referring once again to Shrinking Core Model, it was therefore possible to express the reactions in the solid phase of tannins hydrolysis and gallic acid consumption as:

$$r_8 = k_8 * C^{\circ}{}_{tannins} * C^{I}_{H_2O} \tag{5.74}$$

$$r_9 = k_9 * C_{GA} * C^{I}_{H_2O} \tag{5.75}$$

Where k_8 and k_9 are the kinetic constants of hydrolysis of tannins and gallic acid respectively, $C^{\circ}{}_{tannins}$ is the initial concentration of tannins in the wood that can be assumed, for the same reasons as in the case of ethanolysis, to be constant throughout the process, C_{GA} is gallic acid concentration that varies with time and $C^{I}_{H_2O}$ is the water concentration at the interface of the reactive and the ash layers.

Since water must permeate within the deactivated wood layer prior to the reaction, this concentration, like that of the reagents involved in the synthesis of the compounds of the syringil and conferyl groups, is expressed using the formula derived from the SCM (Equation 4.14):

$$C^{I}_{H_2O} = \left[\frac{\frac{D_{H_2O\,eff}}{\delta} * C^{\circ}{}_{H_2O}}{k * C^{\circ}{}_{tannins} + \frac{D_{H_2O\,eff}}{\delta}}\right] \tag{5.76}$$

The term accounting for the back diffusion is given, instead, by Equation 5.77.

$$N_{GA} = \sqrt{\frac{D_{GA\,eff}}{12*t}} * (C_{GA\,solid} - C_{GA\,liquid}) \tag{5.77}$$

Once again, the effective diffusivity of gallic acid considers the porous structure of wood, while the driving force is the concentration gradient of the congener between the solid and liquid phase.

The variation of gallic acid in the solid phase is precisely due to the hydrolysis reaction of the tannins expressed by the Equation 5.74, minus gallic acid consumption (Equation 5.75) and the back diffusion in the liquid phase (Equation 5.77).

The change in the liquid phase, on the other hand, is solely due to the back diffusion of gallic acid (Equation 5.77).

The Equation 5.74, 5.75, 5.76 and 5.77 have been combined to write the usual material balances on the solid (Equation 5.78) and liquid phase (Equation 5.80) on the individual compound, and then developed with Forward Euler method as expressed in Equations 5.79 and 5.81.

$$\frac{dC_{GA\,solid}}{dt} = k_8 * C^{\circ}{}_{tannins} * \left[\frac{\frac{D_{H_2O\,eff}}{\delta} * C^{\circ}{}_{H_2O}}{k_8 * C^{\circ}{}_{tannins} + \frac{D_{H_2O\,eff}}{\delta}}\right] * \frac{S_{wood}}{V_{wood}} - k_9 * C_{GA\,solid} * \left[\frac{\frac{D_{H_2O\,eff}}{\delta} * C^{\circ}{}_{H_2O}}{k_9 * C_{GA\,solid} + \frac{D_{H_2O\,eff}}{\delta}}\right] * \frac{S_{wood}}{V_{wood}} - \sqrt{\frac{D_{GA\,eff.}}{12*t}} * (C_{GA\,solid} - C_{GA\,liquid}) * \frac{S_{wood}}{V_{wood}} \tag{5.78}$$

$$C^{(t)}_{GA\,solid} = C^{(t-1)}_{GA\,solid} + \Delta t * \left(k_8 * C^{\circ}{}_{tannins} * \left[\frac{\frac{D_{H_2O\,eff.}}{\delta} * C^{\circ}{}_{H_2O}}{k_8 * C^{\circ}{}_{tannins} + \frac{D_{H_2O\,eff.}}{\delta}}\right] * \frac{S_{wood}}{V_{wood}} - k_9 * C^{(t-1)}_{GA\,solid} * \left[\frac{\frac{D_{H_2O\,eff.}}{\delta} * C^{\circ}{}_{H_2O}}{k_9 * C^{(t-1)}_{GA\,solid} + \frac{D_{H_2O\,eff.}}{\delta}}\right] * \frac{S_{wood}}{V_{wood}} - \sqrt{\frac{D_{GA\,eff.}}{12*t}} * (C^{(t-1)}_{GA\,solid} - C^{(t-1)}_{GA\,liquid}) * \frac{S_{wood}}{V_{wood}}\right) \tag{5.79}$$

$$\frac{dC_{GA\,liquid}}{dt} = \sqrt{\frac{D_{GA\,eff.}}{12*t}} * (C_{GA\,solid} - C_{GA\,liquid}) * \frac{S_{wood}}{V_{solution}} \tag{5.80}$$

$$C^{(t)}_{GA\,liquid} = C^{(t-1)}_{GA\,liquid} + \Delta t * \left(\sqrt{\frac{D_{GA\,eff.}}{12*t}} * (C^{(t-1)}_{GA\,solid} - C^{(t-1)}_{GA\,liquid}) * \frac{S_{wood}}{V_{solution}}\right) \tag{5.81}$$

The graph for sample M-300 is reported below together with the table reporting the values of the fitted parameters.

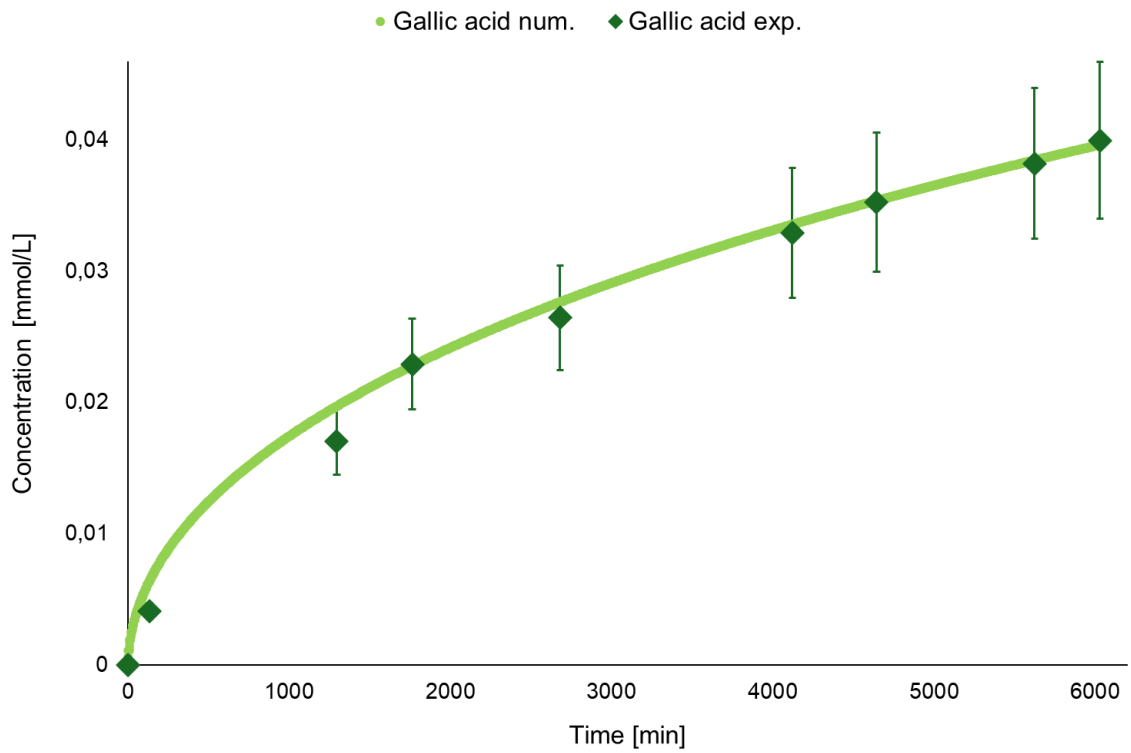

Figure 5.29: Gallic acid, M-300 sample, experimental fitting final attempt.

Table 5.9: Gallic acid, sample M-300, manipulated parameters values from the final attempt.

Sample M-300	$k_{tannins\ hydrolysis}\left[\frac{m^4}{mol * s}\right]$	$k_{GA\ hydrolysis}\left[\frac{m^4}{mol * s}\right]$	$D_{H_2O}\left[\frac{m^2}{s}\right]$	$D_{GA}\left[\frac{m^2}{s}\right]$
Gallic acid	1,67 E-05	1,67 E-06	1,65 E-15	1,67 E-12

Since from the first formulation of the model the shape of the concentration profile appears to be logarithmic and with a trend that seems to reflect well that of the experimental data. In the table are shown the three parameters to be manipulated in case of gallic acid which is the diffusivity coefficient of the compound itself and the two kinetic constants of hydrolysis. However, as in the case of the syringil and coniferyl families, the numbers obtained from fitting the experimental data are low compared to the values found in the literature.

5.3. Results and discussion

Once the structures of the final model have been defined and their validity have been tested and confirmed on sample M-500 for syringil and coniferyl families and M-300 for gallic acid, they have been extended on all the other samples.

This led to the construction of the graphs reported below, in which the error bars have been added to account for the error of experimental measurements dictated by the inaccuracy of the instrument used. This makes the appropriateness of the experimental fitting by the proposed model even more evident.

The mean square error of the concentration values for each compound in each sample has been assessed, and when combined with the graphical representation, it has been made possible to quantify the success of the fitting process in order to better illustrate the validity of the generated model.

5.3.1. Syringil family

The graphs related to the samples of syringil group, together with the estimated value of the overall mean square deviation of the concentration measurements of each compound and for each sample, are reported below.

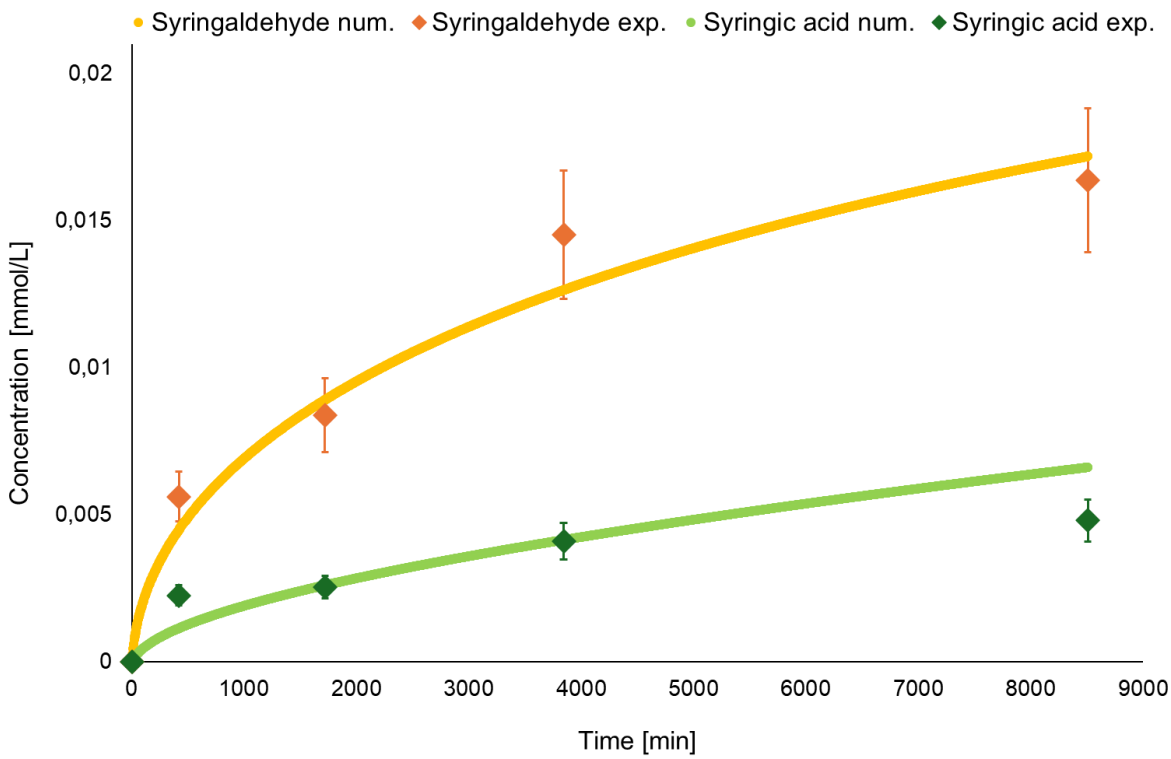

Figure 5.30: Syringil family, G-000 sample, experimental fitting last attempt.

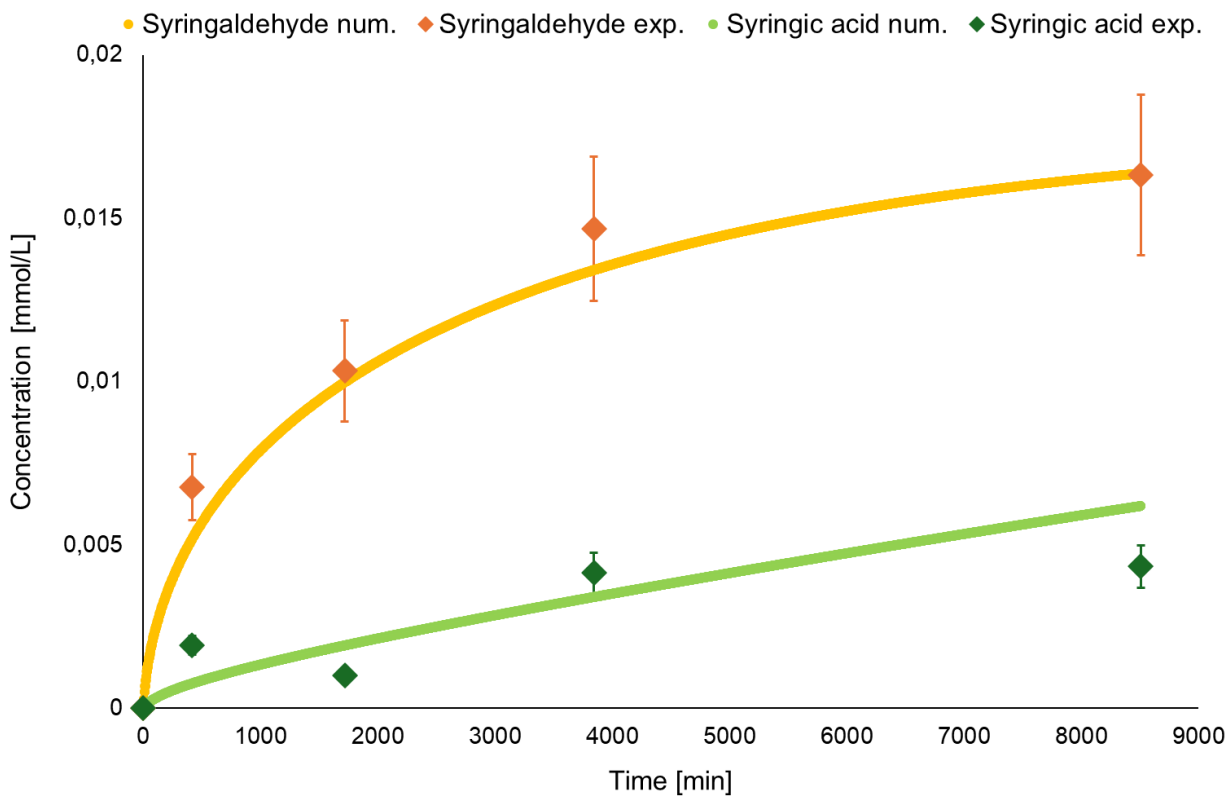

Figure 5.31: Syringil family, G-100 sample, experimental fitting last attempt.

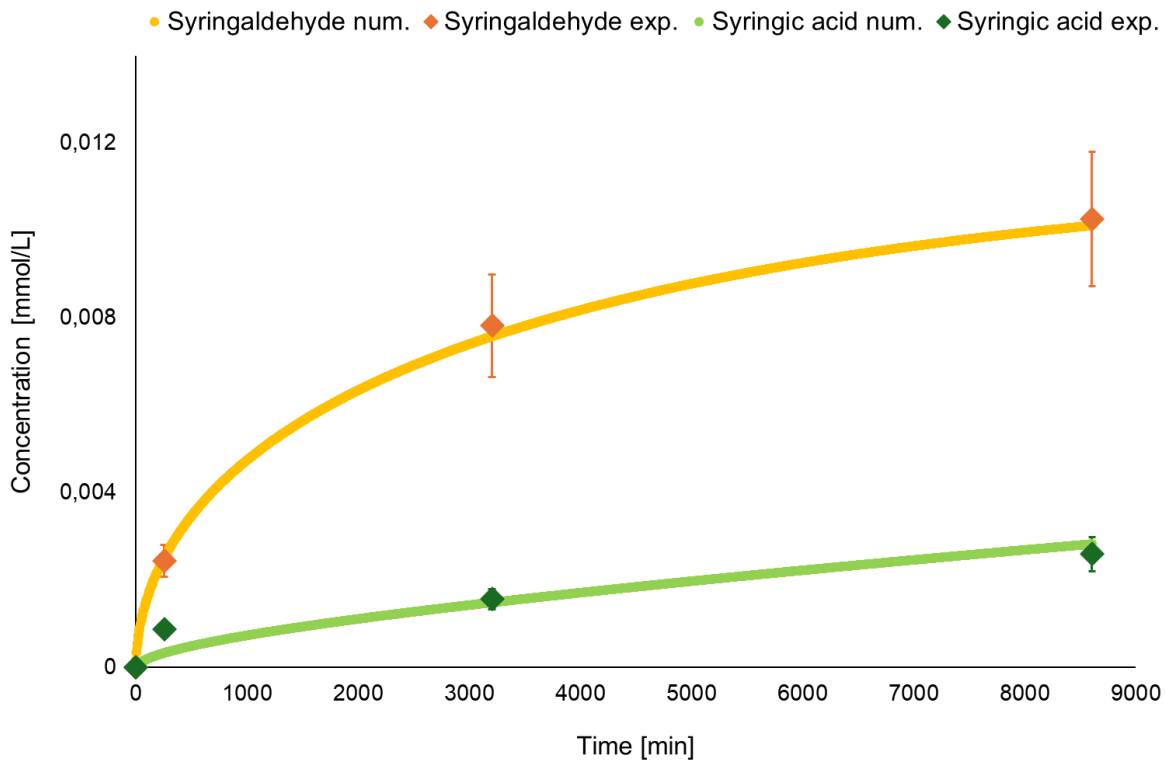

Figure 5.32: Syringil family, G-200 sample, experimental fitting last attempt.

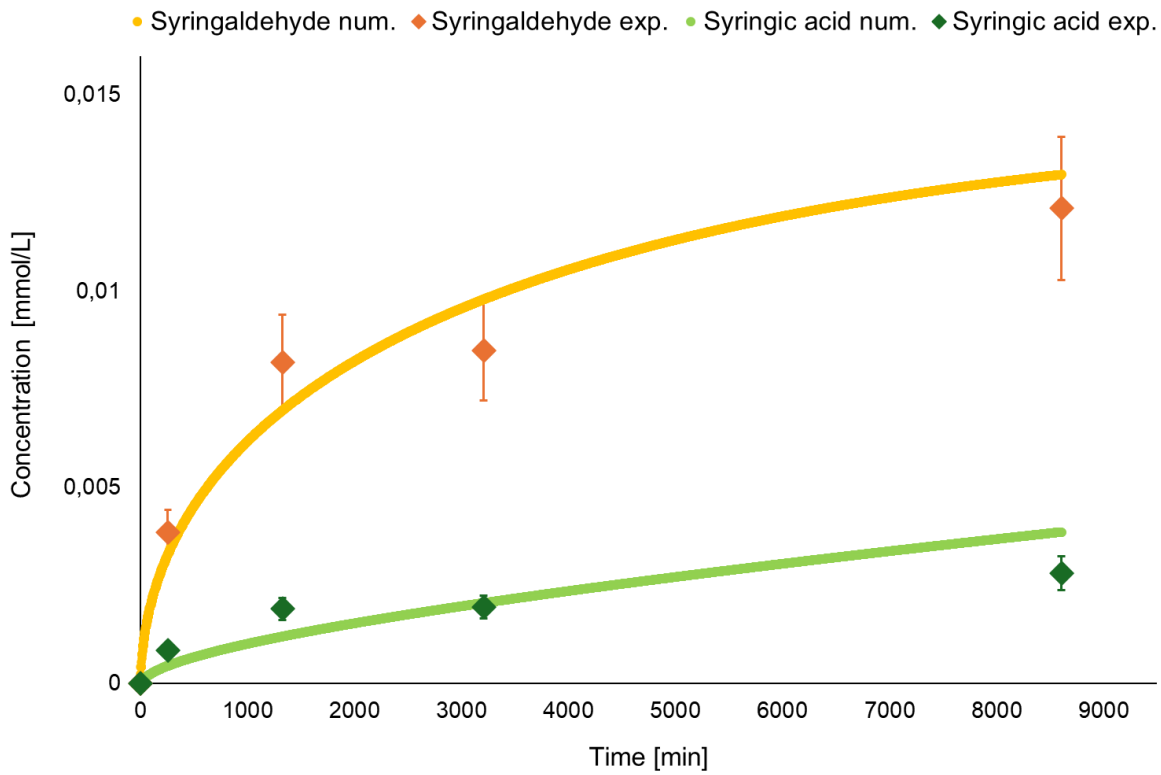

Figure 5.33: Syringil family, G-300 sample, experimental fitting last attempt.

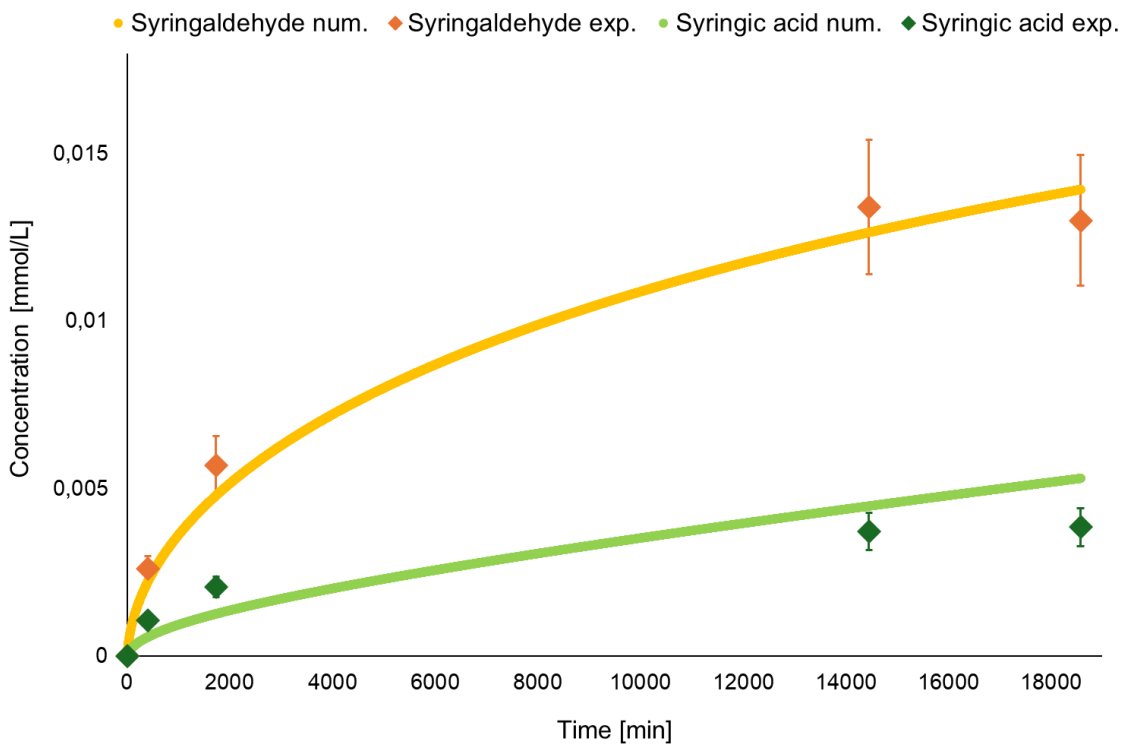

Figure 5.34: Syringil family, G-400 sample, experimental fitting last attempt.

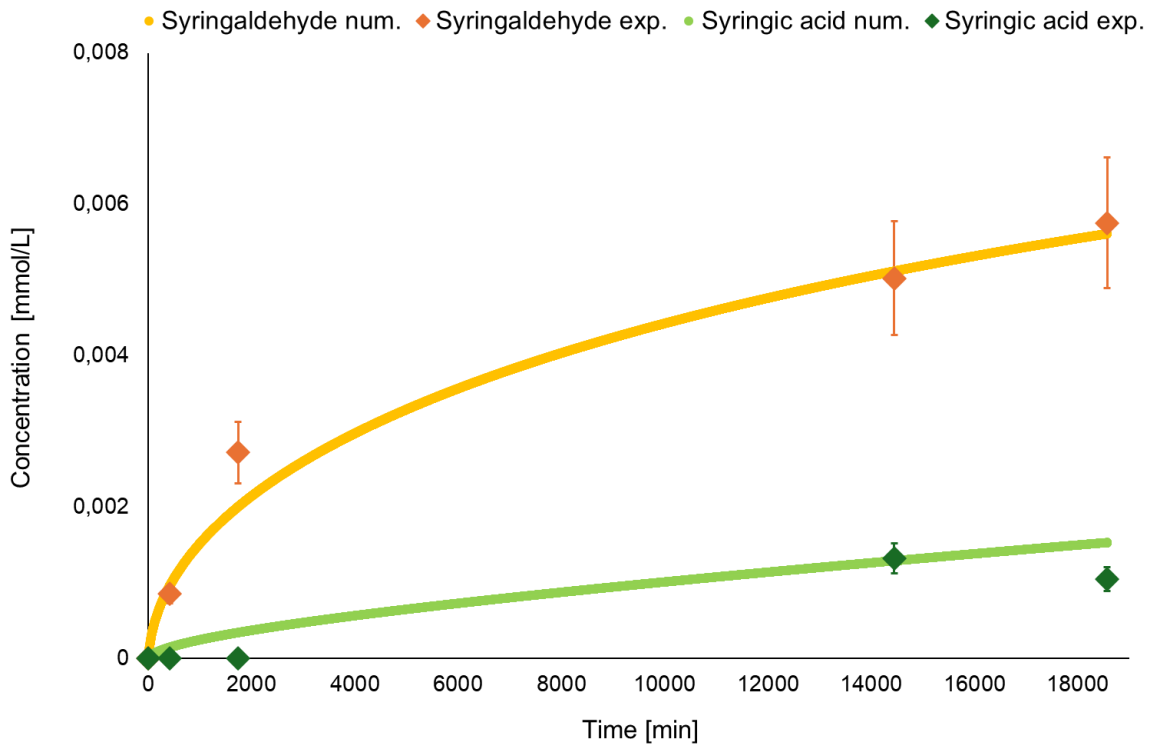

Figure 5.35: Syringil family, G-500 sample, experimental fitting last attempt.

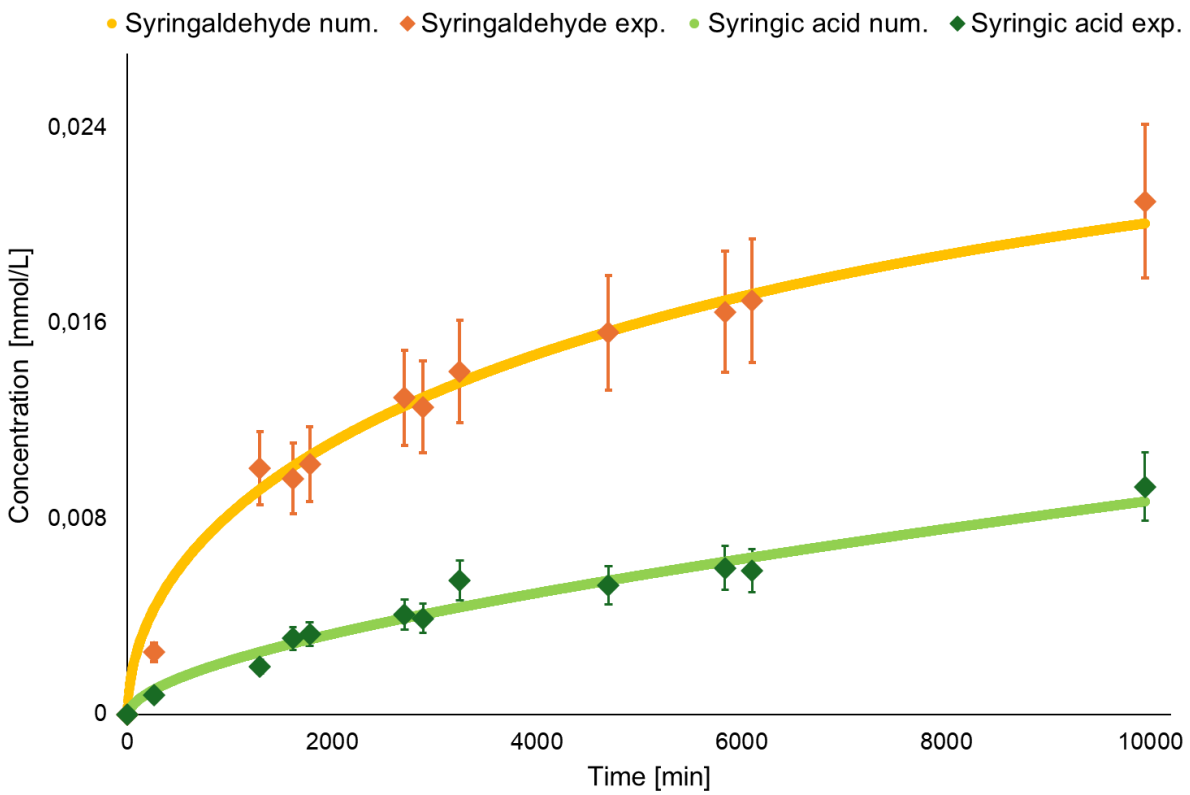

Figure 5.36: Syringil family, G-700 sample, experimental fitting last attempt.

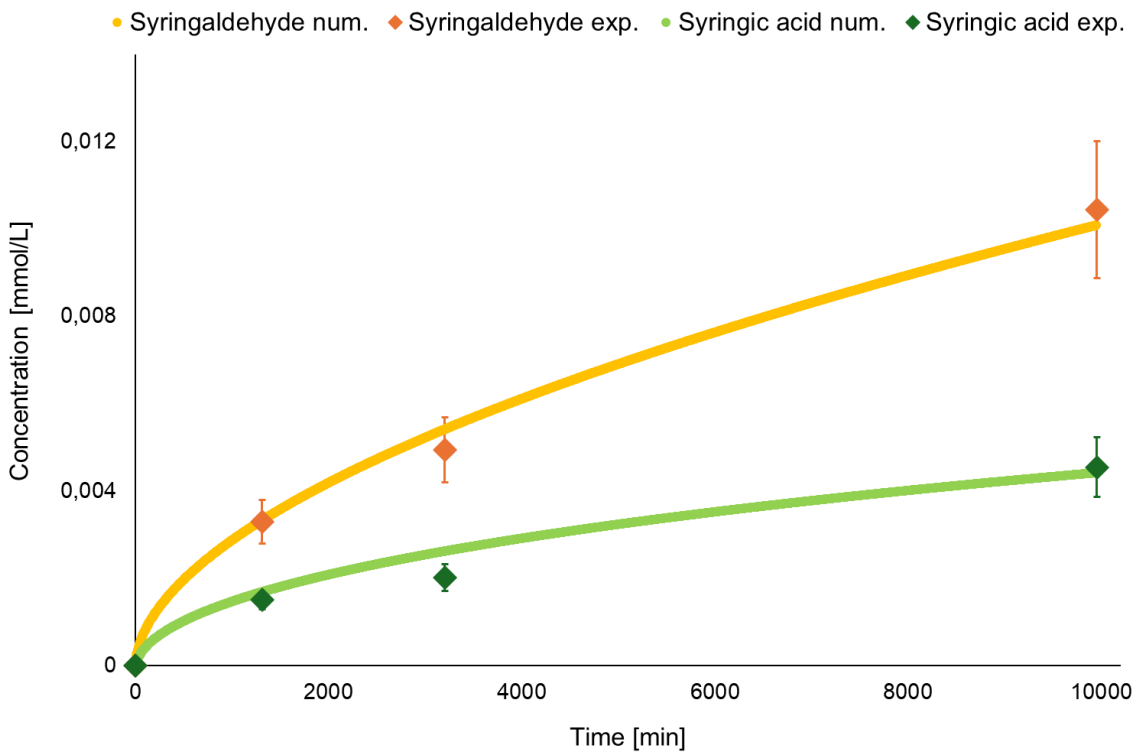

Figure 5.37: Syringil family, G-900 sample, experimental fitting last attempt.

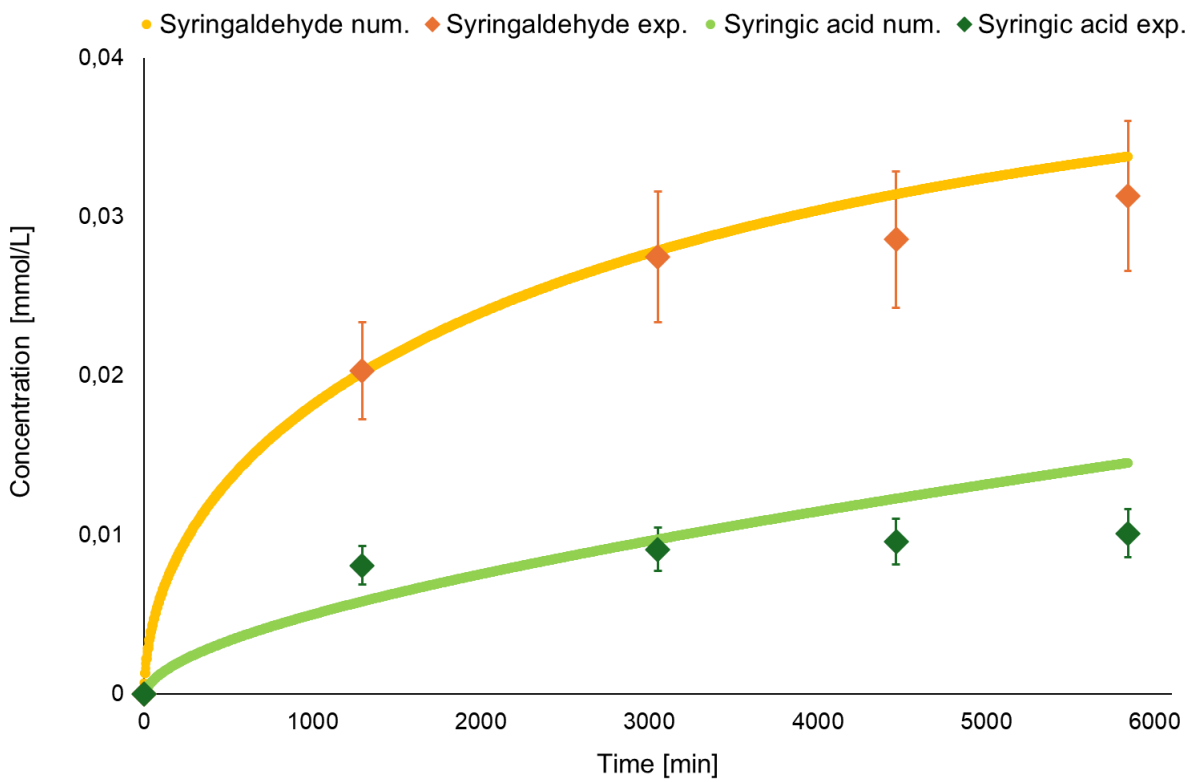

Figure 5.38: Syringil family, M-000 sample, experimental fitting last attempt.

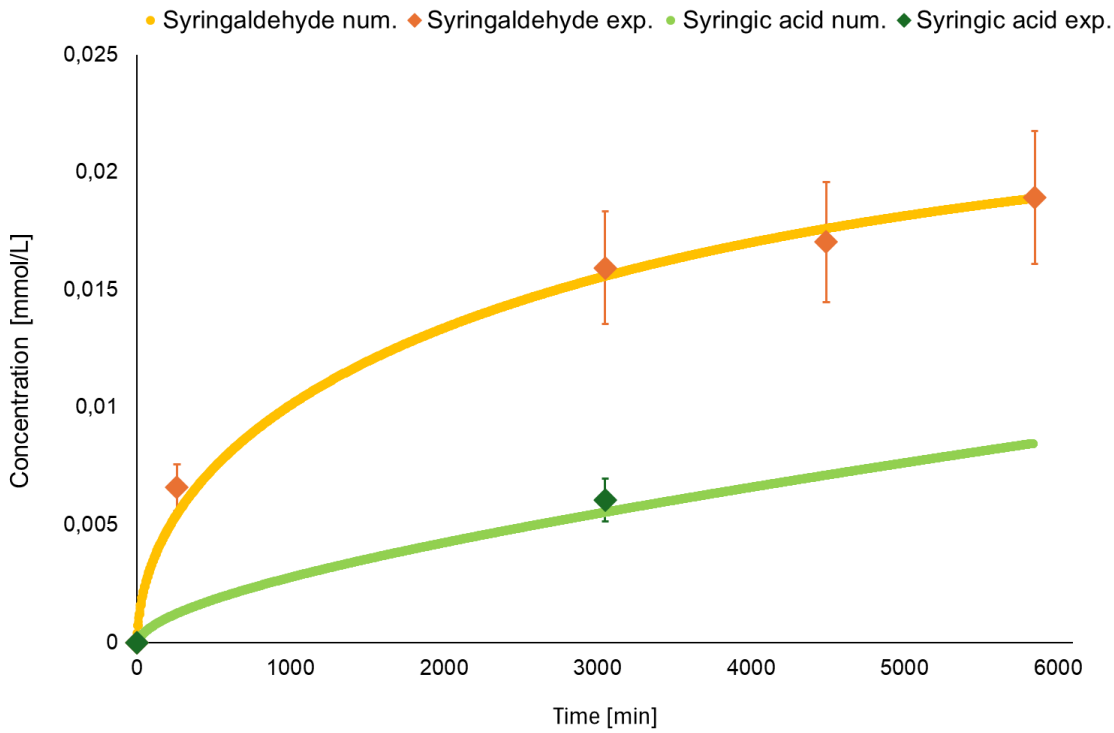

Figure 5.39: Syringil family, M-200 sample, experimental fitting last attempt.

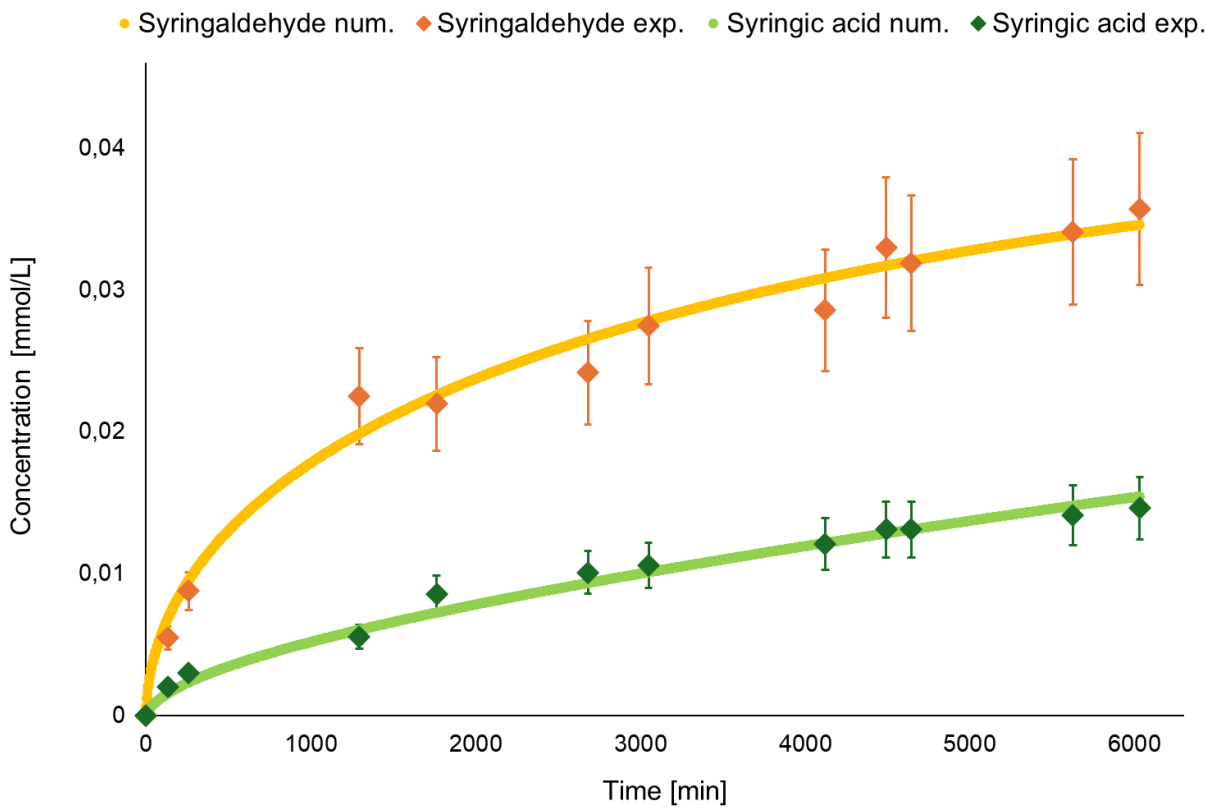

Figure 5.40: Syringil family, M-300 sample, experimental fitting last attempt.

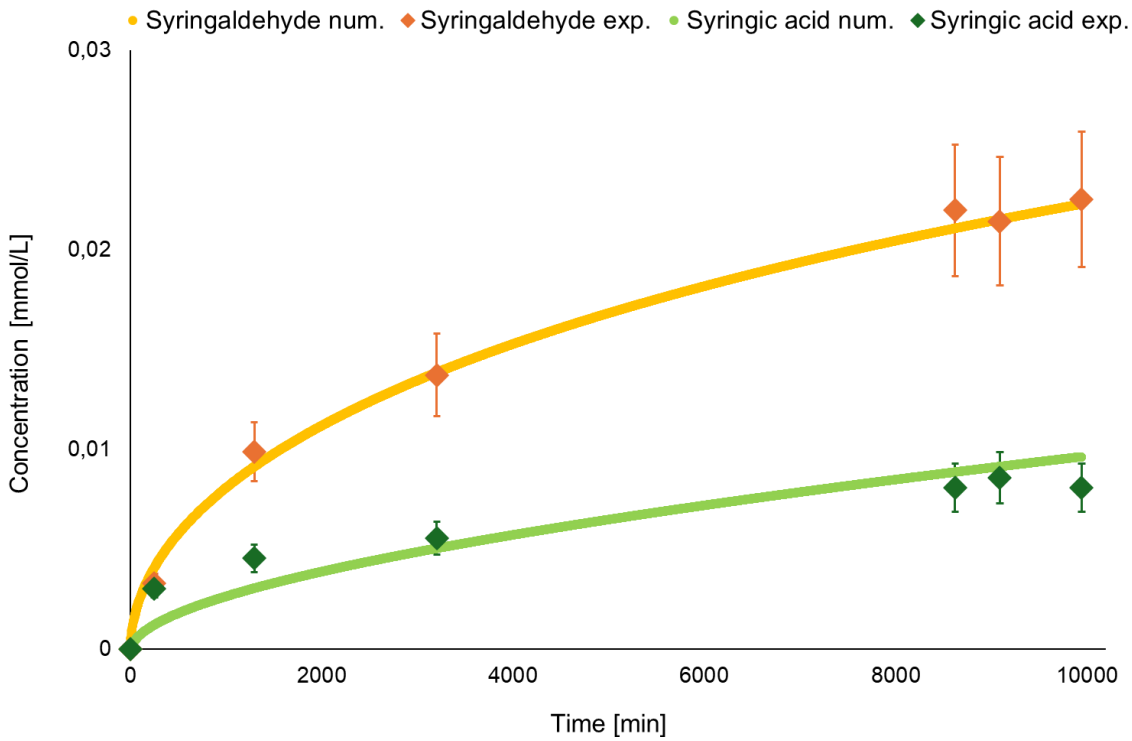

Figure 5.41: Syringil family, M-400 sample, experimental fitting last attempt.

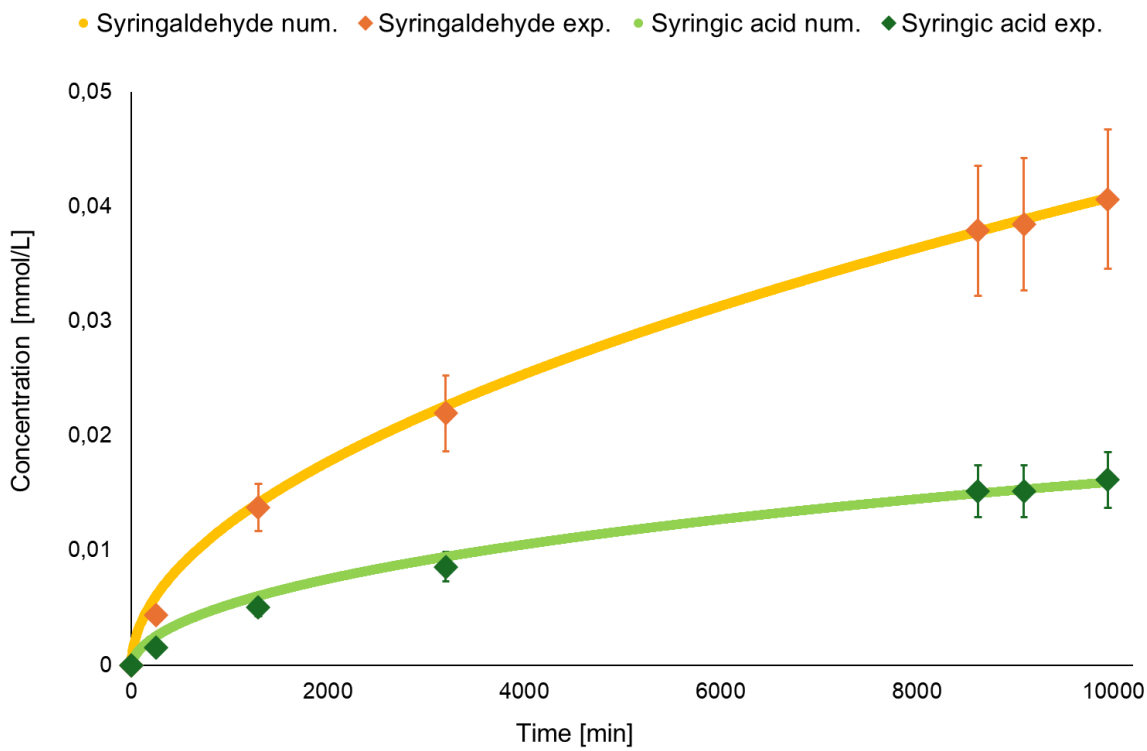

Figure 5.42: Syringil family, M-500 sample, experimental fitting last attempt.

The fitting of the concentrations obtained from the developed model with the experimental values was achieved by manipulating seven parameters, three of which are the kinetic constants of the reactions involved and the remaining four represent the diffusivity values of the reactants migrating through the ash layer. Tables 5.9 and 5.10 reports the values, respectively, for the kinetic constants and for the diffusivities.

Table 5.10: Syringil family, manipulated kinetic constant values from the last attempt.

Sample	$k_1 \left[\frac{m^4}{mol * s}\right]$	$k_2 \left[\frac{m^4}{mol * s}\right]$	$k_3 \left[\frac{m^4}{mol * s}\right]$
G-000	3,33 E-08	1,33 E-04	8,33 E-07
G-100	1,67 E-07	1,33 E-05	1,50 E-06
G-200	1,17 E-06	6,67 E-05	1,50 E-06
G-300	1,50 E-06	1,67 E-04	1,67 E-07
G-400	1,50 E-06	1,33 E-05	1,50 E-06
G-500	1,50 E-06	5,50 E-05	1,50 E-06
G-700	1,50 E-06	1,58 E-03	1,67 E-07
G-900	1,50 E-06	1,00 E-05	4,83 E-09
M-000	1,50 E-06	1,50 E-04	6,67 E-07
M-200	1,50 E-06	5,00 E-05	1,17 E-06
M-300	1,50 E-06	5,00 E-05	1,50 E-06
M-400	8,33 E-07	1,50 E-04	6,67 E-07
M-500	1,33 E-06	6,67 E-05	6,67 E-09

Table 5.11: Syringil family, manipulated diffusion coefficient values from the last attempt.

Sample	$D_{EtOH}\left[\frac{m^2}{s}\right]$	$D_{O_2}\left[\frac{m^2}{s}\right]$	$D_S\left[\frac{m^2}{s}\right]$	$D_{SA}\left[\frac{m^2}{s}\right]$
G-000	1,24 E-14	1,05 E-07	1,50 E-11	5,00 E-12
G-100	1,27 E-14	1,12 E-07	1,67 E-11	2,50 E-12
G-200	1,36 E-14	1,17 E-07	1,43 E-12	5,00 E-14
G-300	1,41 E-14	1,21 E-07	3,33 E-12	1,17 E-13
G-400	1,31 E-14	1,12 E-07	3,33 E-12	2,67 E-12
G-500	1,51 E-14	1,29 E-07	4,67 E-13	6,67 E-14
G-700	1,42 E-14	1,21 E-07	1,67 E-13	1,67 E-14
G-900	1,35 E-14	1,13 E-07	1,25 E-14	1,67 E-14
M-000	1,60 E-14	1,38 E-07	2,17 E-12	2,07 E-13
M-200	1,59 E-14	1,38 E-07	3,67 E-14	3,33 E-15
M-300	1,59 E-14	1,37 E-07	7,30 E-13	8,83 E-14
M-400	1,61 E-14	1,37 E-07	1,42 E-13	2,67 E-14
M-500	1,43 E-14	1,19 E-07	8,33 E-14	3,33 E-14

Overall, it is possible to visualise that the values are around very low orders of magnitude, immediately suggesting a general underestimation by the proposed model.

The way each parameter, being all the others fixed, affects the concentration profile's shape will be described in the lines that follow, beginning with the kinetic constants and moving on to the diffusion coefficients.

k_1 represents the kinetic constant of the ethanolysis of lignin to produce syringaldehyde; for values of orders of magnitude greater than 10^{-4} it seems to be irrelevant in modifying the configuration of the graph, while smaller values cause the initial portion of the aldehyde curve to shift downwards. This initial observation allows to advance the hypothesis that the influence of a chemical regime rather than a diffusive regime prevails on the system at an early stage.

k_2 represents the kinetic constant of the oxidation reaction of syringaldehyde to give syringic acid and, therefore, its manipulation is expected to affect both the aldehyde and acid concentration profile. In particular, higher k_2 values lead to greater acid production and aldehyde consumption; the sensitivity of this parameter becomes decisive starting from values of the order of 10^{-1}; however, for values greater or equal to the unity the curves do not show any substantial modification. The initial section of the acid curve changes only due to a variation of k_2 of at least one order of magnitude, while the final tail of the aldehyde curve is more sensitive and lowers as k_2 increases.

Finally, k_3 represents the kinetic constant of the syringic acid esterification and its manipulation is expected to have a decisive influence on the acid curve. This is what is actually shown graphically: the values of k_3 start to be effectively decisive on the acid curve starting from orders of magnitude of about 10^{-4} , as in the case of k_1. As k_3 increases for one order of magnitude, a downward translation of the syringic acid profile occurs.

Having exhausted the discussion on kinetic constants, the analysis shifts to the diffusion coefficients. Generally, it has been demonstrated that their manipulation leads to alterations in the shapes of the graphs that are more evident than for the kinetic constants. In this regard, finding the right compromise for all the variables involved has been crucial for achieving a good fitting.

D_{EtOH} is responsible for the height of the aldehyde curve and, indirectly, also for the one of the acid, since lower diffusivity values of ethanol lead to lower concentrations of aldehyde, raising the one of the acid; D_{EtOH} is characterized by a high sensitivity, around the order of 10^{-5}, and small changes lead to significant variations in the shape of the profiles.

D_{O_2} has the opposite effect, in fact, higher values of this parameter imply the acid curve increase and the aldehyde curve decrease. It is evident that altering diffusivity values

causes notable changes to the last portion of the curve, supporting the fact that, at the beginning of the process, it is controlled by chemical parameters for brief periods of time, while diffusion parameters predominate at longer periods of time.

D_S, the diffusion coefficient of syringaldehyde, also proved to be an extremely sensitive parameter; even minimal changes of the order of 10^{-8} causes the translation of the concentration profile downwards or upwards.

D_{SA} plays the same role for syringic acid diffusivity; it is even more sensitive than the other diffusivities, since variations of the order of 10^{-8} are decisive on the shape of the concentration profile.

As previously indicated, the model described appears to report parameter values that are too low to be considered realistic, hence generically underestimating the observed chemical-physical processes. At least, the values obtained seem to be consistent for each parameter, consulting them one by one, and for each sample, similar values are noted with a variability of at most a couple of orders of magnitude from the mean value.

The expected increase in kinetic and diffusive parameters dictated by the presence of the ultrasound effect does not appear until this attempt except for the oxygen diffusivity, which its values recover ½ orders of magnitude from the theoretical diffusivity found in literature [119] [120] [121].

5.3.2. Coniferyl family

For the coniferyl group, the graphs related to the samples are reported below:

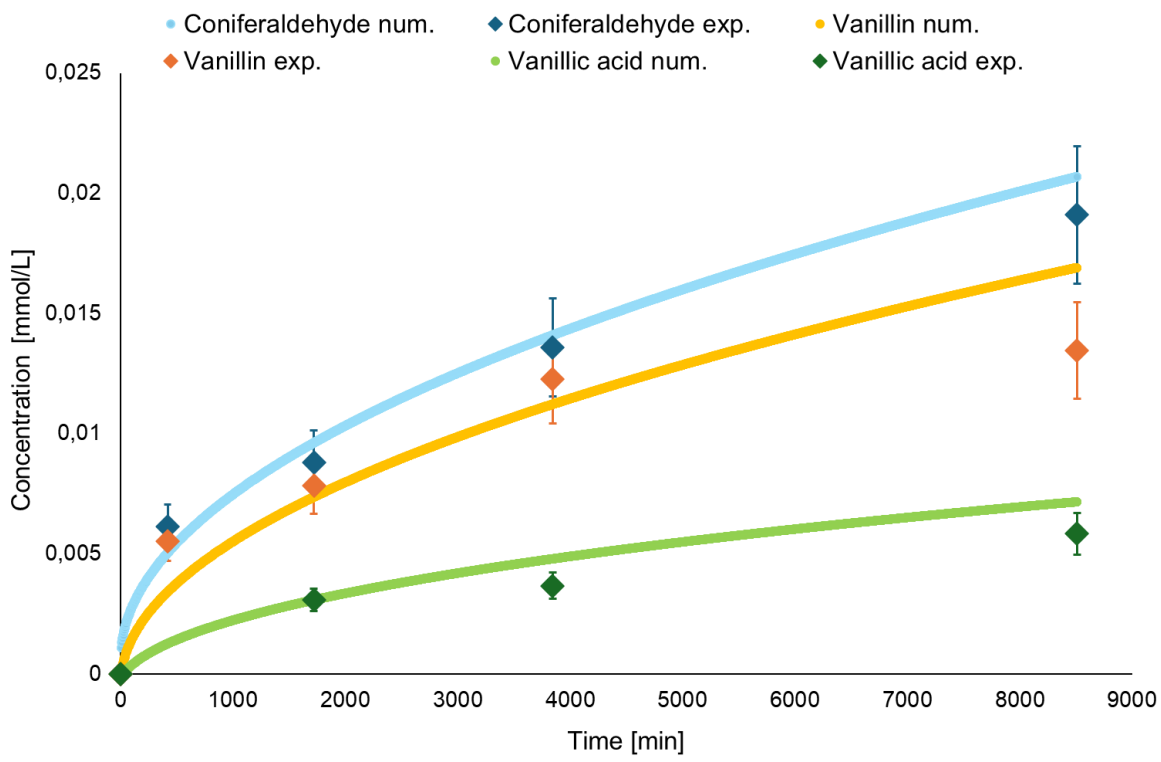

Figure 5.43: Coniferyl family, G-000 sample, experimental fitting last attempt.

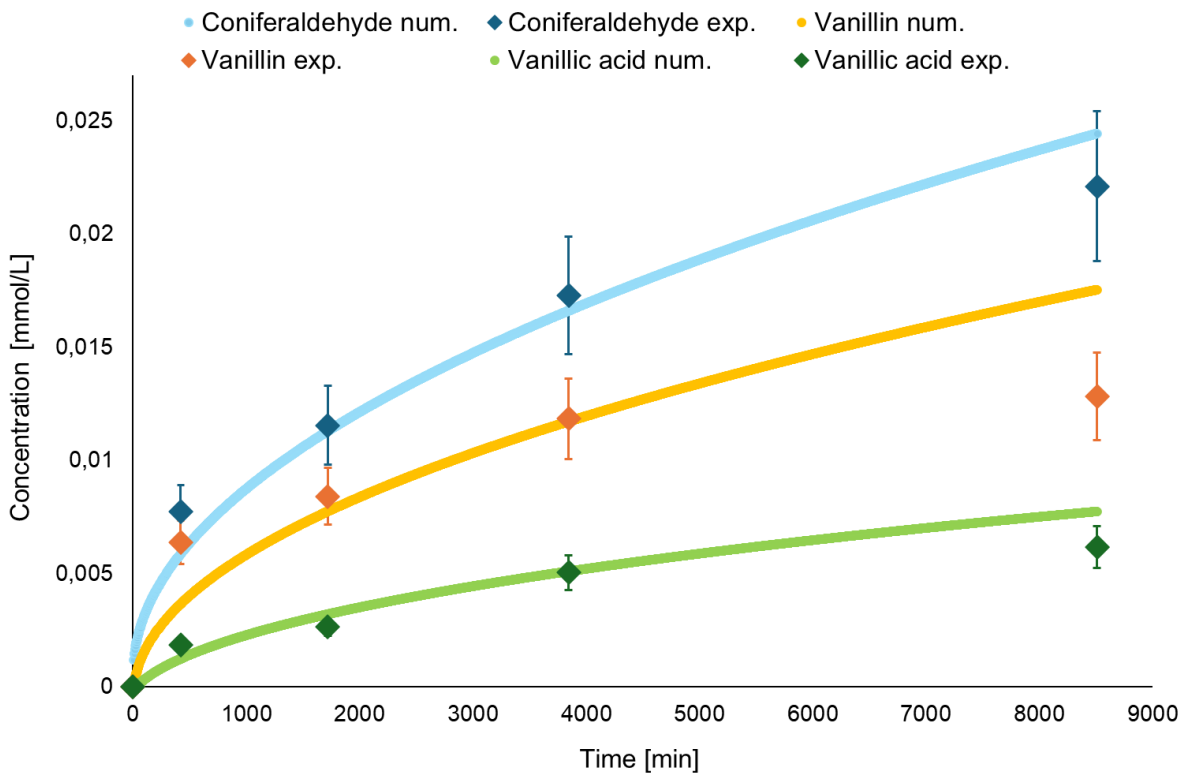

Figure 5.44: Coniferyl family, G-100 sample, experimental fitting last attempt.

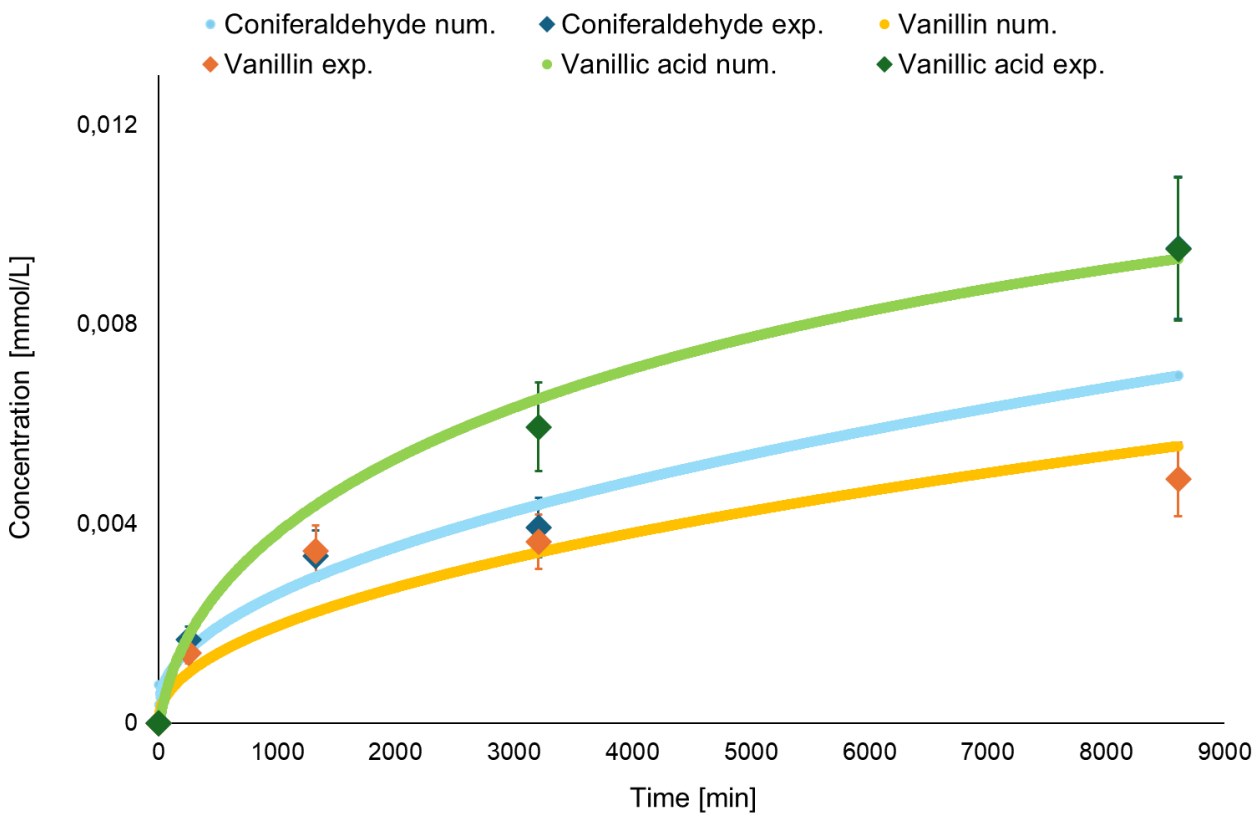

Figure 5.45: Coniferyl family, G-200 sample, experimental fitting last attempt.

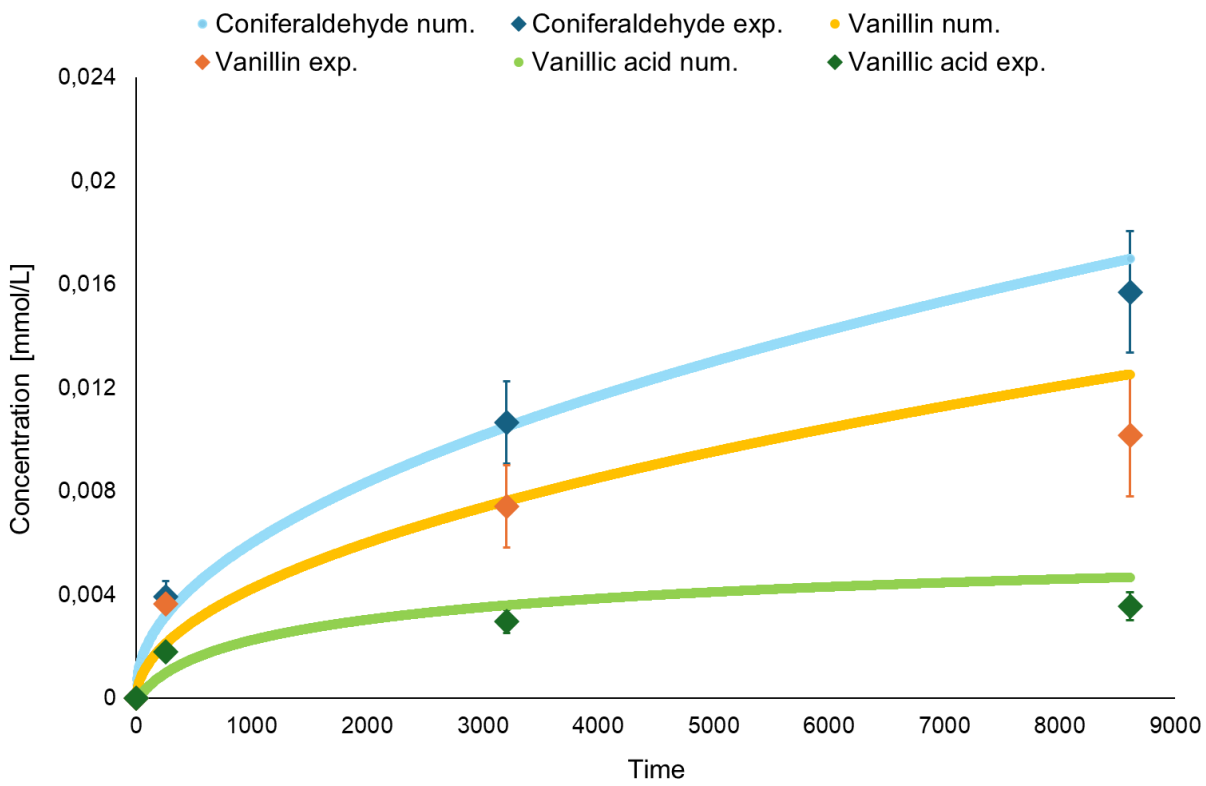

Figure 5.46: Coniferyl family, G-300 sample, experimental fitting last attempt.

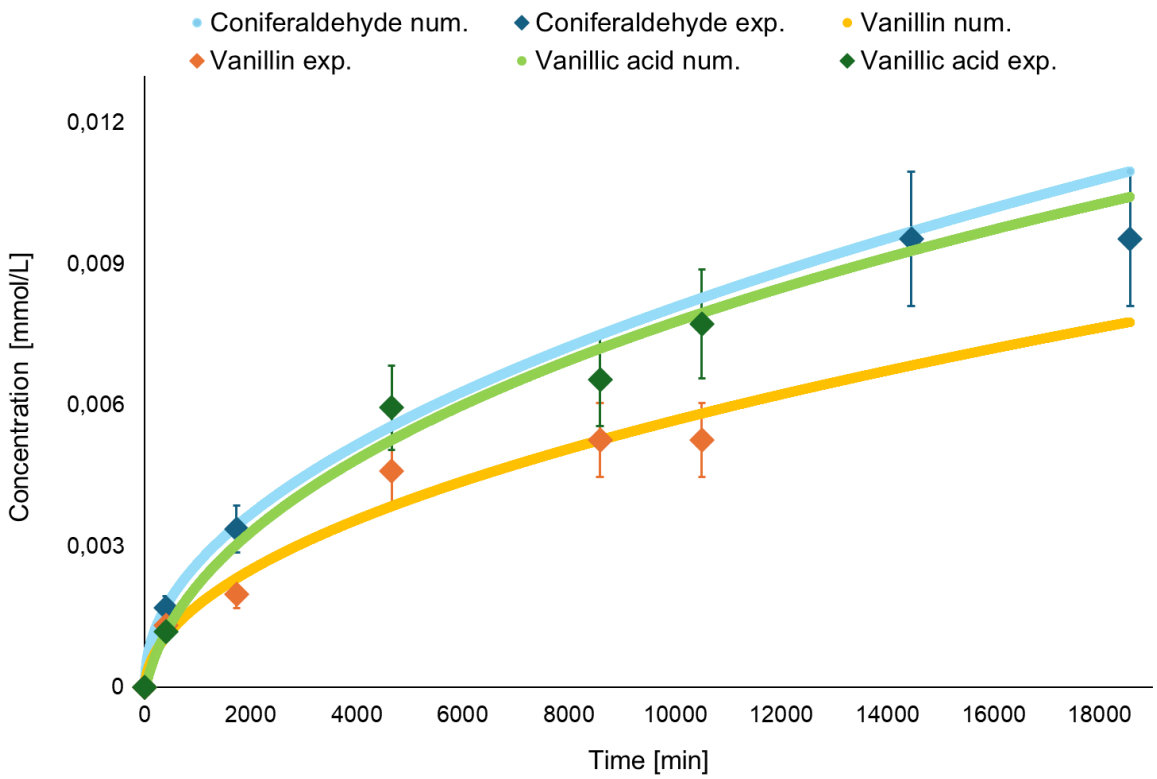

Figure 5.47: Coniferyl family, G-400 sample, experimental fitting last attempt.

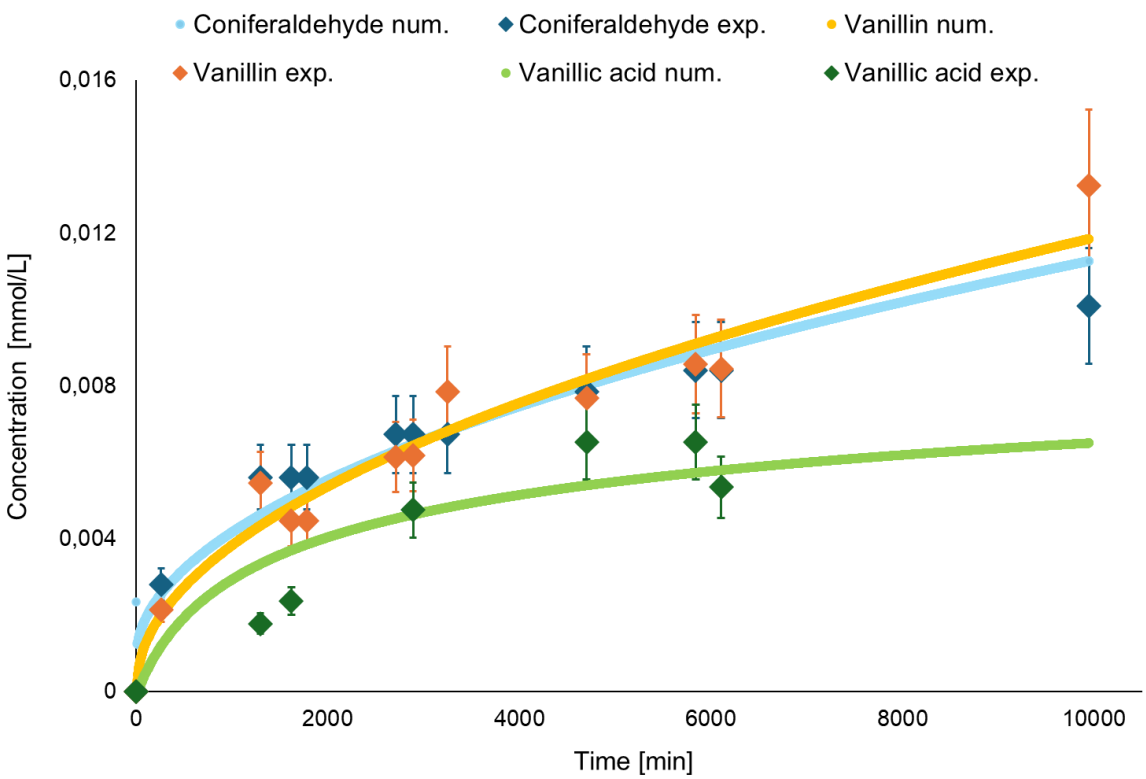

Figure 5.48: Coniferyl family, G-700 sample, experimental fitting last attempt.

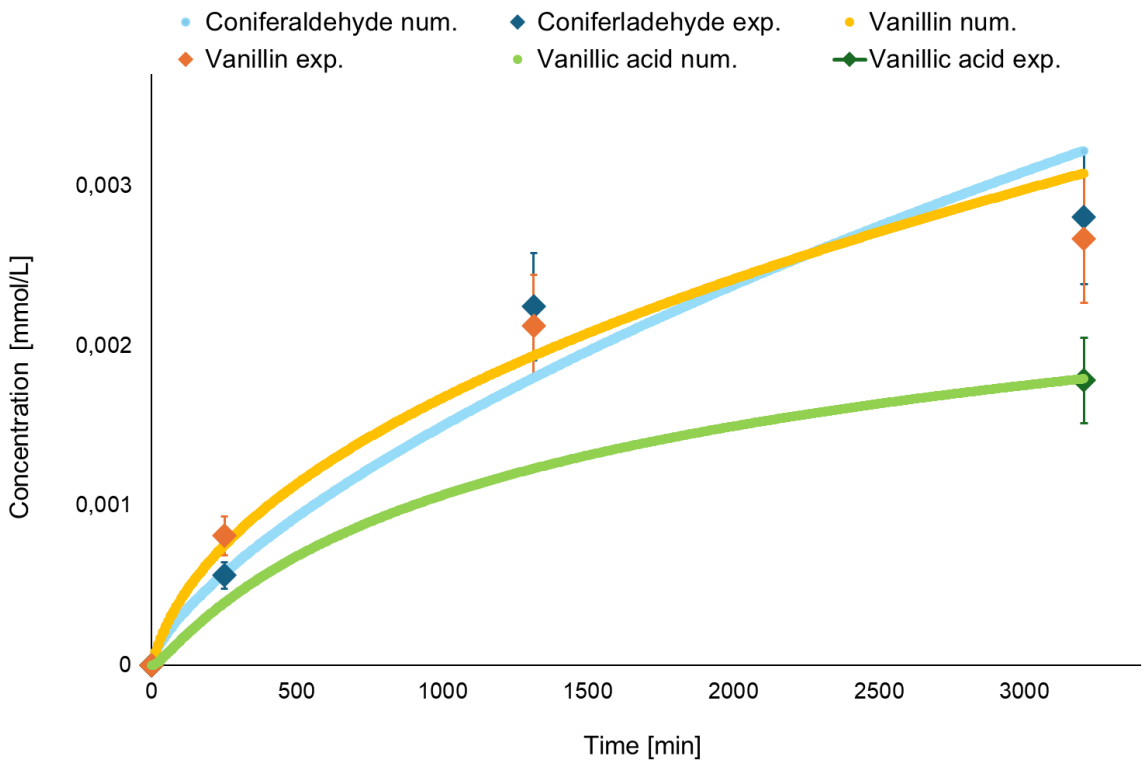

Figure 5.49: Coniferyl family, G-800 sample, experimental fitting last attempt.

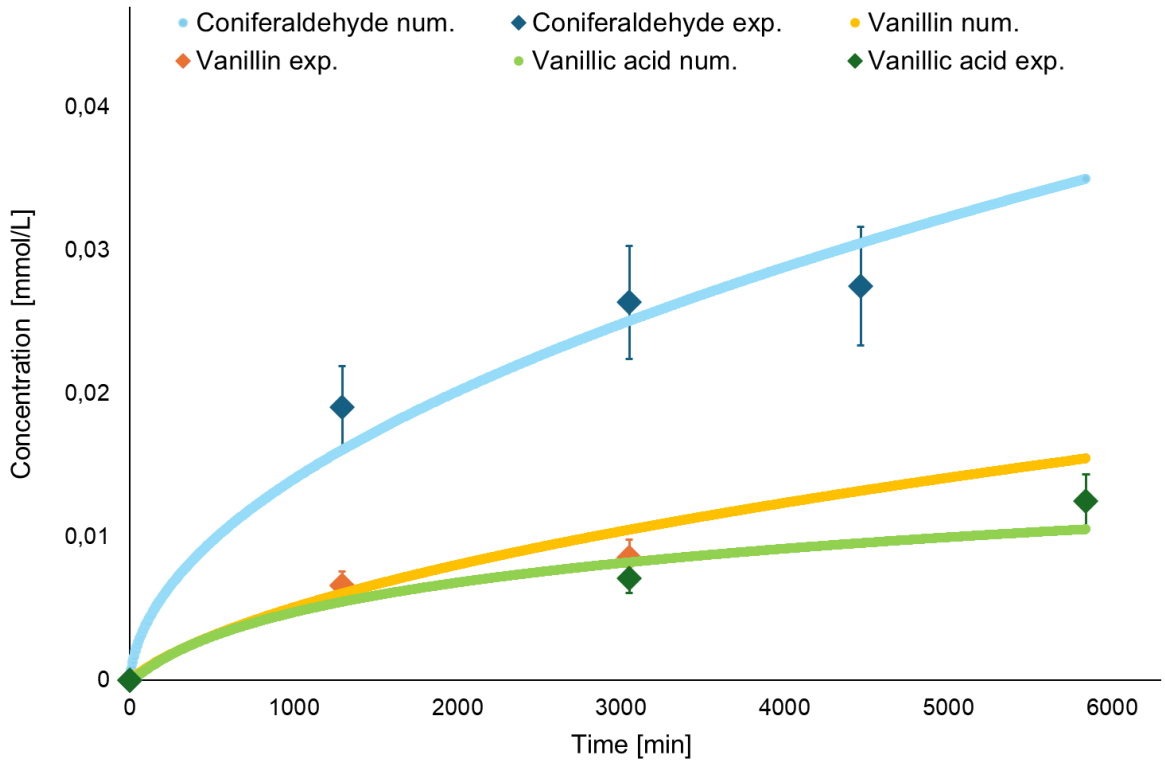

Figure 5.50: Coniferyl family, M-000 sample, experimental fitting last attempt.

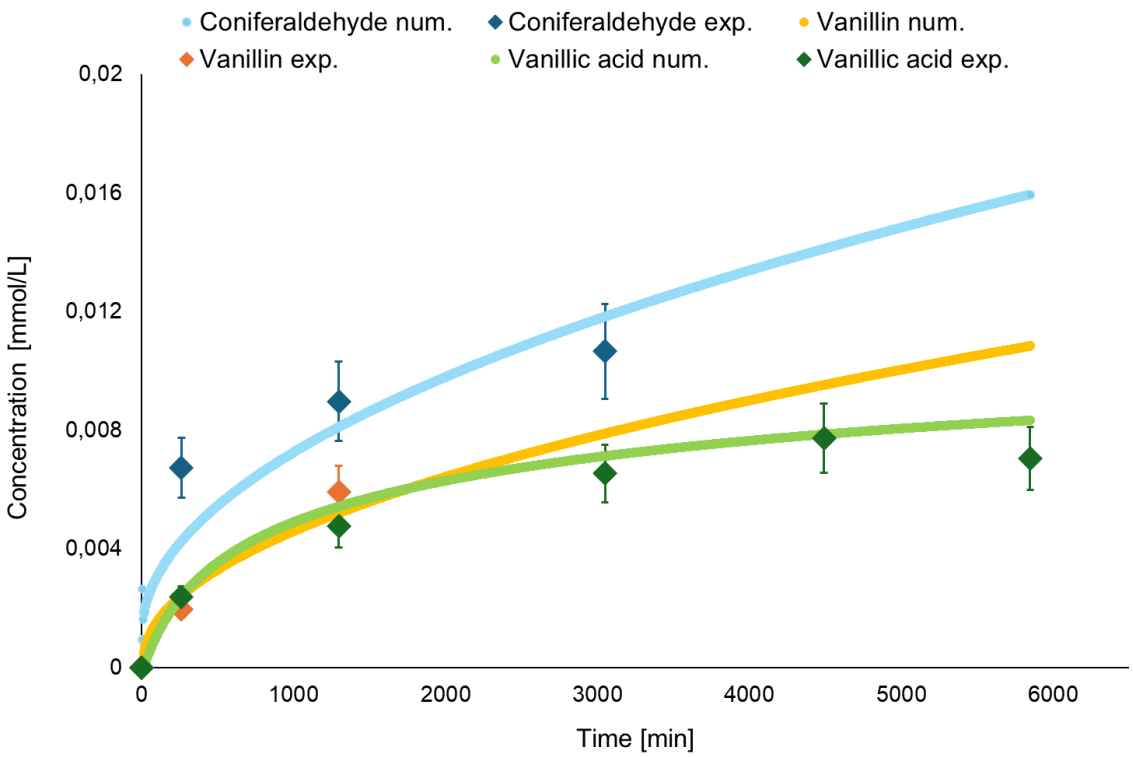

Figure 5.51: Coniferyl family, M-200 sample, experimental fitting last attempt.

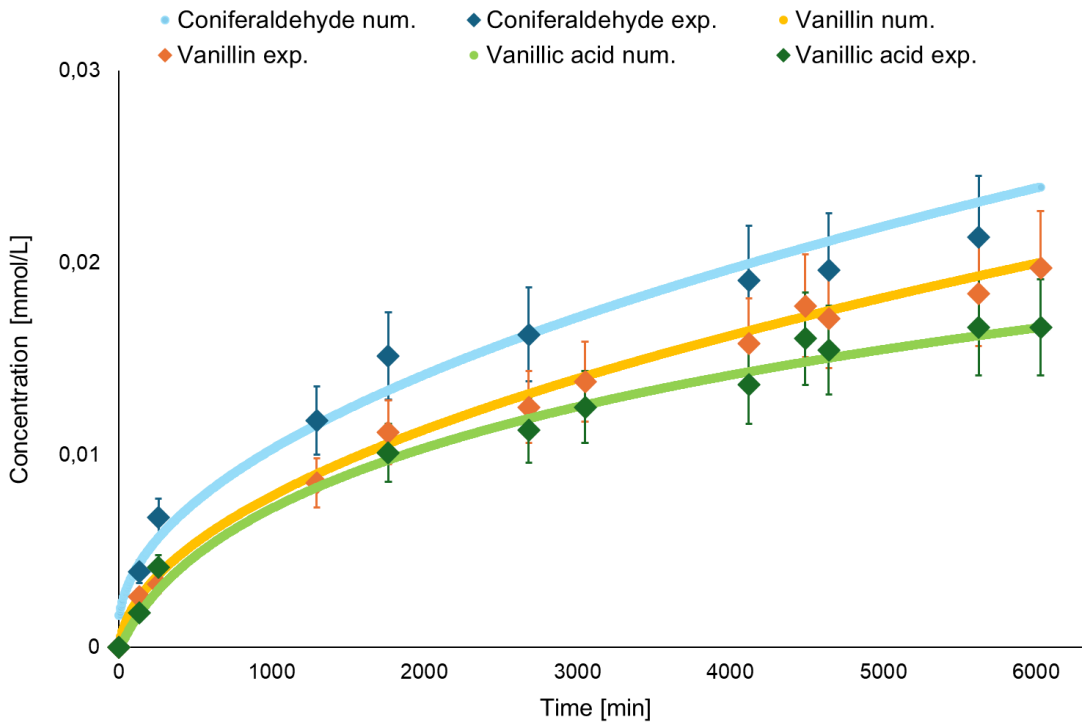

Figure 5.52: Coniferyl family, M-300 sample, experimental fitting last attempt.

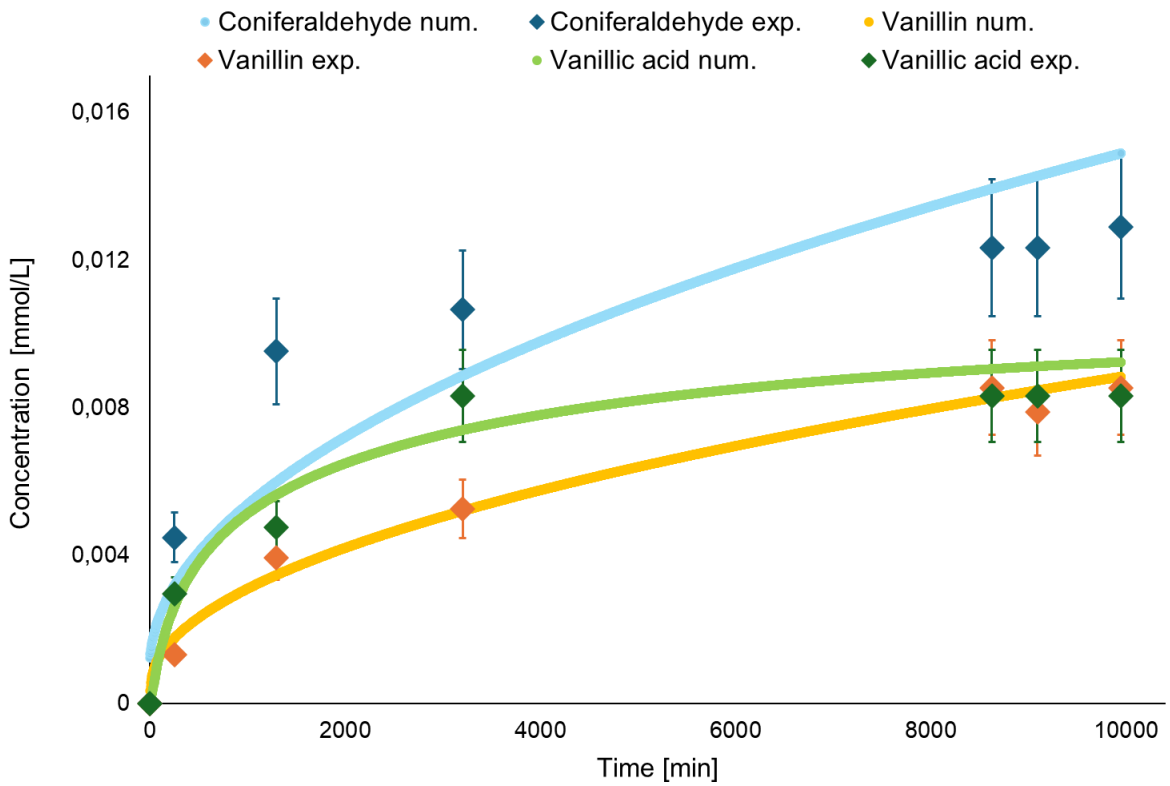

Figure 5.53: Coniferyl family, M-400 sample, experimental fitting last attempt.

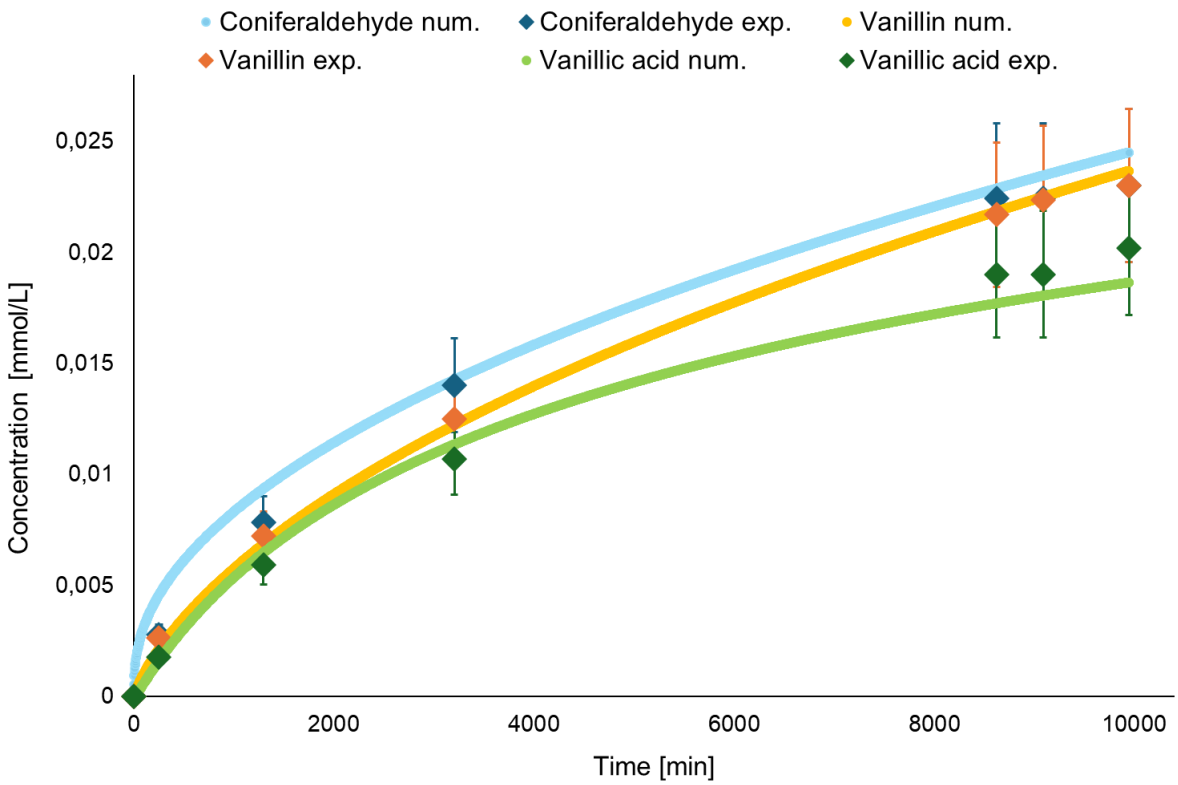

Figure 5.54: Coniferyl family, M-500 sample, experimental fitting last attempt.

The fitting of the experimental values of coniferaldehyde, vanillin and vanillic acid implies the manipulation of ten parameters, that are the four kinetic constants for the reaction rates, three diffusivities of the reactants that must diffuse through the ash layer and three diffusivities of the lignin-congeners that must diffuse back to the bulk phase. Tables 5.11 and 5.12 reports the values, respectively, of the kinetic constants and diffusivities.

Table 5.12: Coniferyl family, manipulated kinetic constant values from the last attempt.

Sample	$k_4 \left[\frac{m^4}{mol * s}\right]$	$k_5 \left[\frac{m^4}{mol * s}\right]$	$k_6 \left[\frac{m^4}{mol * s}\right]$	$k_7 \left[\frac{m^4}{mol * s}\right]$
G-000	1,67 E-05	1,67 E-06	1,67 E-05	6,67 E-13
G-100	1,67 E-05	1,67 E-05	1,67 E-06	6,67 E-13
G-200	1,67 E-05	1,67 E-05	1,67 E-04	3,33 E-12
G-300	1,67 E-05	1,67 E-06	1,67 E-04	6,67 E-12
G-400	1,67 E-05	2,00 E-02	1,67 E-03	5,00 E-13
G-700	1,67 E-05	2,00 E-02	1,67 E-04	6,67 E-12
G-800	1,67 E-05	2,00 E-02	1,67 E-06	1,00 E-11
M-000	1,67 E-05	1,67 E-05	1,67 E-06	1,67 E-12
M-200	1,67 E-05	2,00 E-02	1,67 E-05	6,67 E-12
M-300	1,67 E-05	2,00 E-02	1,67 E-03	1,00 E-12
M-400	1,67 E-05	2,00 E-02	1,67 E-04	1,67 E-11
M-500	1,67 E-05	2,00 E-02	1,67 E-03	8,33 E-13

Table 5.13: Coniferyl family, manipulated diffusion coefficient values from the last attempt.

Sample	$D_{EtOH}\left[\frac{m^2}{s}\right]$	$D_{H_2O}\left[\frac{m^2}{s}\right]$	$D_{O_2}\left[\frac{m^2}{s}\right]$	$D_C\left[\frac{m^2}{s}\right]$	$D_V\left[\frac{m^2}{s}\right]$	$D_{VA}\left[\frac{m^2}{s}\right]$
G-000	1,43 E-14	2,07 E-19	6,62 E-13	1,17 E-06	1,50 E-06	1,50 E-07
G-100	1,77 E-14	2,31 E-19	8,27 E-13	1,17 E-06	1,50 E-06	1,67 E-07
G-200	1,45 E-15	3,73 E-20	5,86 E-13	1,50 E-06	6,67 E-07	1,33 E-07
G-300	4,87 E-15	7,41 E-20	5,86 E-13	1,50 E-06	1,00 E-06	1,17 E-08
G-400	3,41 E-15	6,62 E-20	7,42 E-13	1,33 E-07	1,50 E-06	1,17 E-07
G-700	1,62 E-15	5,32 E-20	1,01 E-12	5,00 E-07	1,67 E-08	2,00 E-10
G-800	1,43 E-15	3,54 E-20	5,86 E-13	1,33 E-09	8,33 E-09	1,17 E-09
M-000	5,58 E-15	6,88 E-20	5,86 E-13	1,00 E-08	1,17 E-09	3,00 E-09
M-200	1,17 E-15	3,35 E-20	6,62 E-13	1,33 E-07	5,00 E-09	3,33 E-10
M-300	2,95 E-15	6,13 E-20	5,86 E-13	1,33 E-07	1,50 E-08	3,33 E-09
M-400	2,44 E-15	7,71 E-20	1,78 E-12	1,00 E-07	3,33 E-08	1,67 E-09
M-500	2,66 E-15	7,82 E-20	1,21 E-12	5,00 E-09	3,33 E-10	5,00 E-11

k_4 represents the kinetic constant for the ethanolysis of lignin to produce coniferladehyde and seems to have no impact on the concentration profile of the components, once the other parameters are fixed. In particular, it shows no significant changes until the 10^{-5} order of magnitude, shows a slight impact between 10^{-6} and 10^{-7}, while bring some changes from 10^{-8} on the coniferaldehyde profile.

k_5 is the kinetic constant for the production of vanillin from coniferaldehyde, and its impact is very similar to k_1, becoming relevant from 10^{-8} on the concentration profile of vanillin.

k_6, instead, represents the kinetic constant for production of vanillic acid from vanillin. The logic behind these parameters is the same for k_1 and k_2, with some differences in the orders of magnitude; it becomes, in fact, slightly relevant from 10^{-5}.

Lastly, k_7 is the constant for the esterification reaction of vanillic acid and it is the only kinetic constant whose values have a greater impact, particularly on the concentration profile of vanillic acid; in this case order of magnitude ranges between 10^{-9} and 10^{-10}; only M-400 sample has a $k_7 = 10^{-8}$, but it is characterized by a strange pattern of the experimental values.

So far, the results obtained for the kinetic constants reveals that, globally, the kinetic scheme involving the components of coniferyl group is not controlled by the chemical reactions rates, while diffusion phenomena have stronger impact; as for the syringil group, the focus is then shifted to the diffusivity parameters.

The values of diffusivity of ethanol and water show a similar behaviour: they have low order of magnitudes, but both D_{O_2} and D_{H_2O} are one order of magnitude bigger for samples G-000 and G-100. However, the main issue regards the extremely low values, that is in contrast to the expected enhancement due to the ultrasound effect; as will be discussed in the final chapter, it is one of the main drawbacks that needs to be further investigated.

The values of diffusivity of oxygen, instead, are characterized by more realistic orders of magnitude, between 10^{-12} and 10^{-13}. The bigger values are related to samples G-700, M-400 and M-500, maybe due to their higher ultrasound times and higher surface to volume ratios.

The enhancement of diffusion phenomena due to the ultrasound effect is more visible on the values of diffusivity for conifer aldehyde, vanillin and vanillic acid. The values for these three compounds range from 10^{-6} and 10^{-11}, so more reasonable values, despite their variability. In particular, diffusivities for the fitted values of samples G-000, G-100, G-200, G-300 and G-400 are higher than the other trials.

The sensitivity analysis of all the parameters involved in the kinetic scheme leads to some conclusions.

The system considered is very complex, since it is composed of four reaction rates in series in a hybrid regime and needs to consider the effect of ten parameters together to obtain a good fitting of the experimental values. The kinetic constants, apart from k_4, show no relevant effect, confirming the dominance of diffusion phenomena. The values of diffusivity for $EtOH$, H_2O and O_2 have the same order of magnitude (with an

acceptance of $\pm$ 1 order of magnitude), confirming the coherence of the model for all the samples considered. The values of D_{EtOH} are extremely low, so further studies on the kinetic scheme and further developments for the model are needed.

5.3.3. Gallic Acid

Lastly, the plots for gallic acid samples have been reported below:

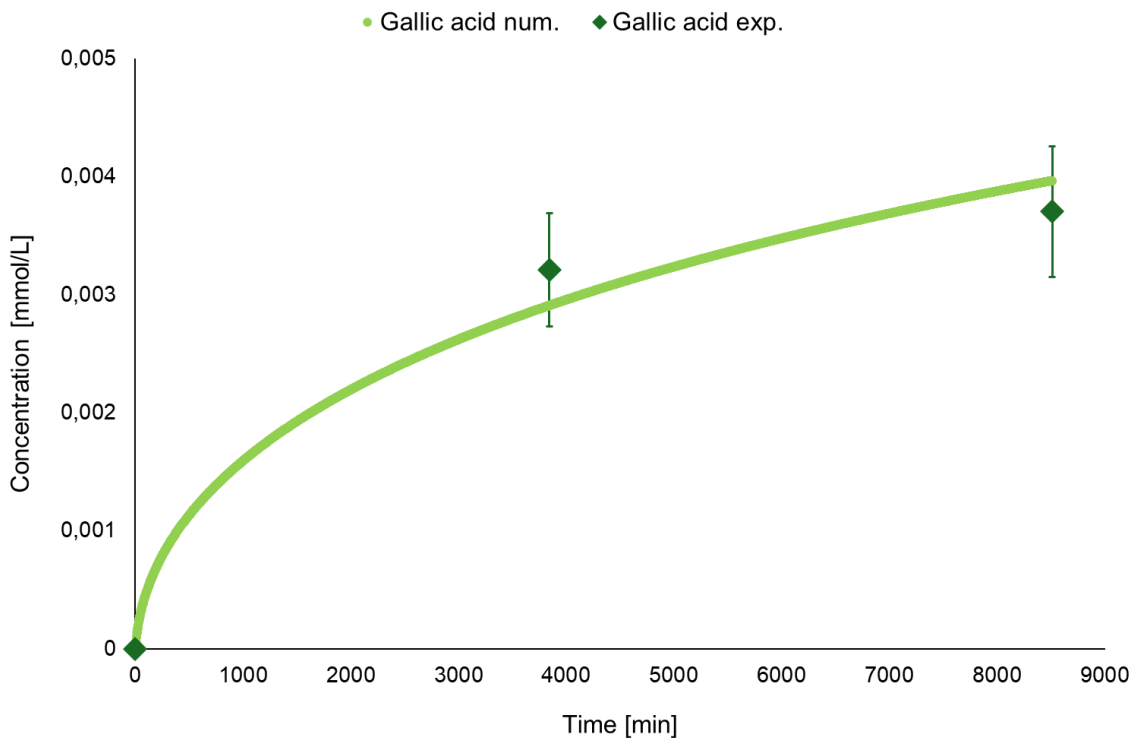

Figure 5.55: Gallic acid, G-000 sample, experimental fitting final attempt.

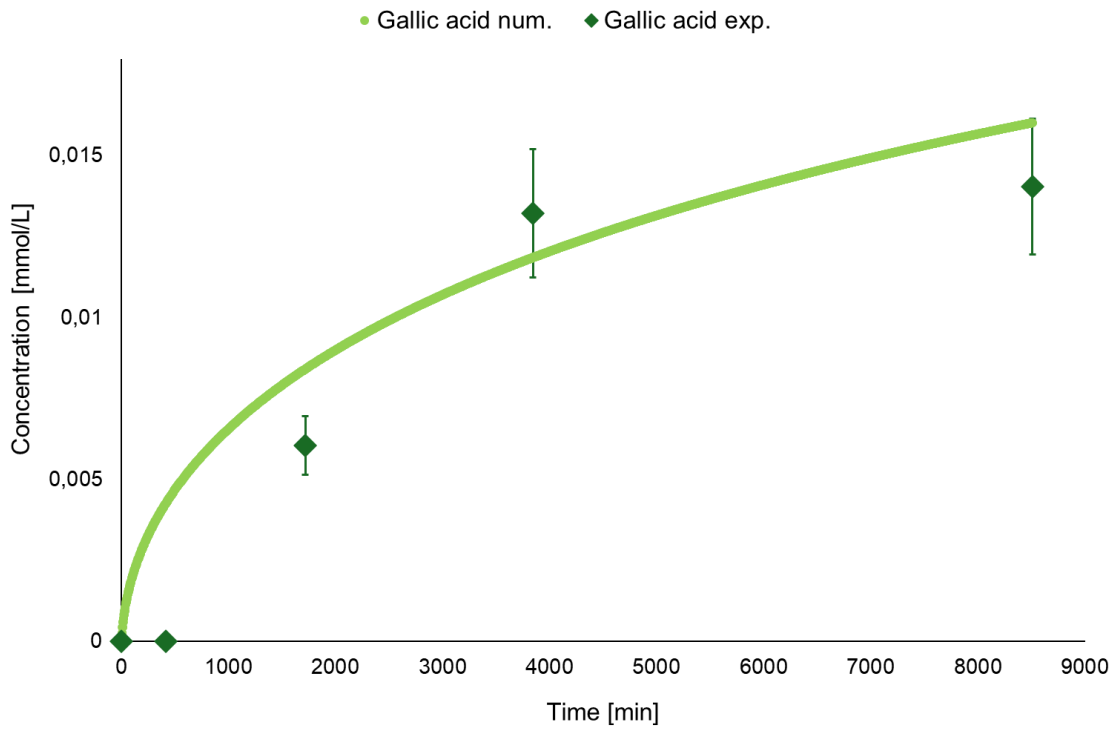

Figure 5.56: Gallic acid, G-100 sample, experimental fitting final attempt.

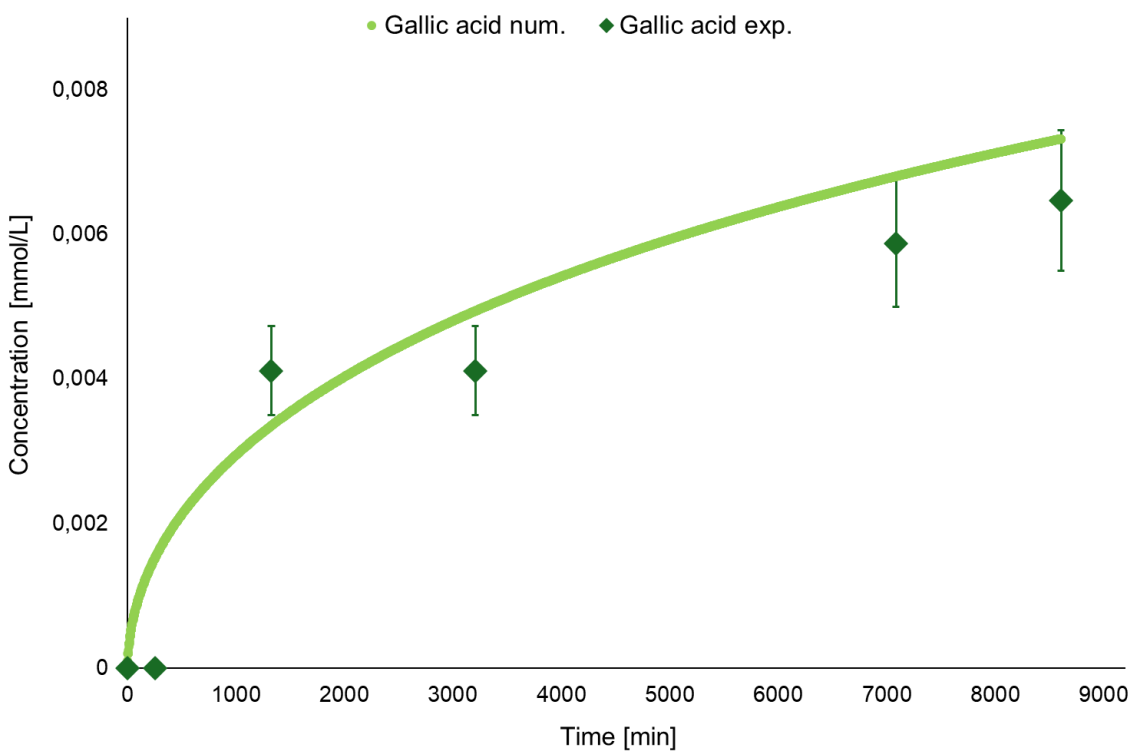

Figure 5.57: Gallic acid, G-300 sample, experimental fitting final attempt.

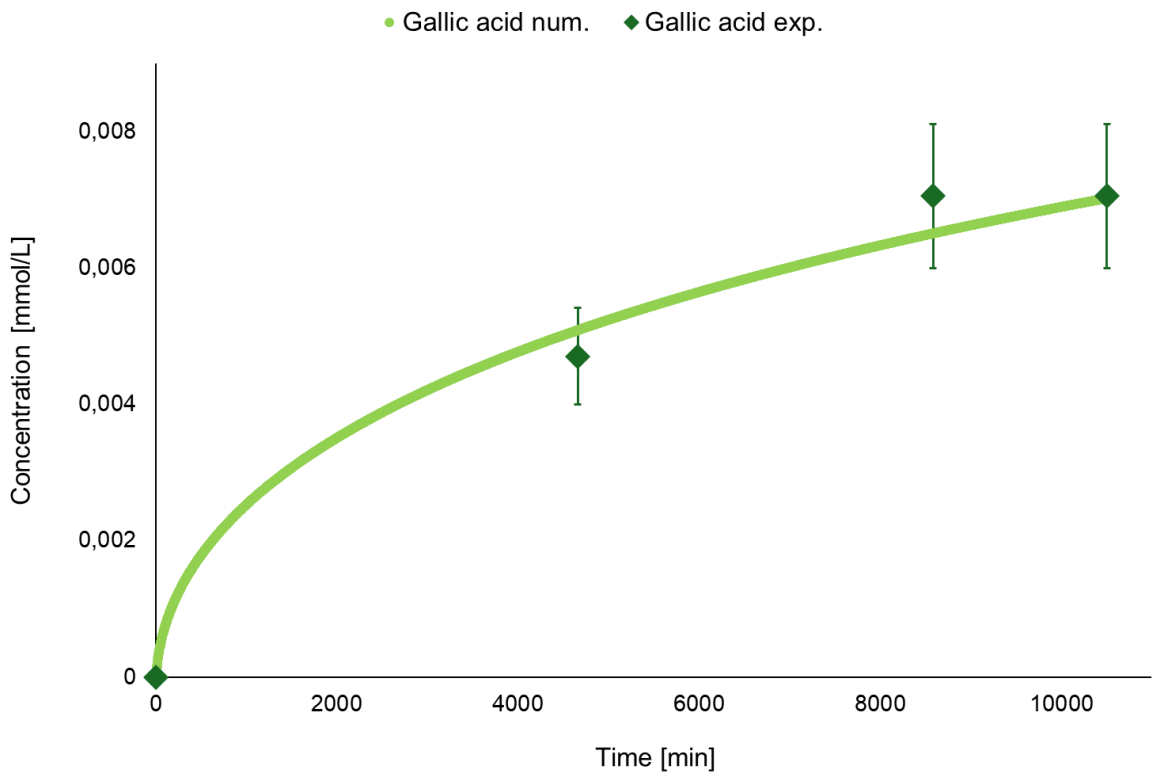

Figure 5.58: Gallic acid, G-400 sample, experimental fitting final attempt.

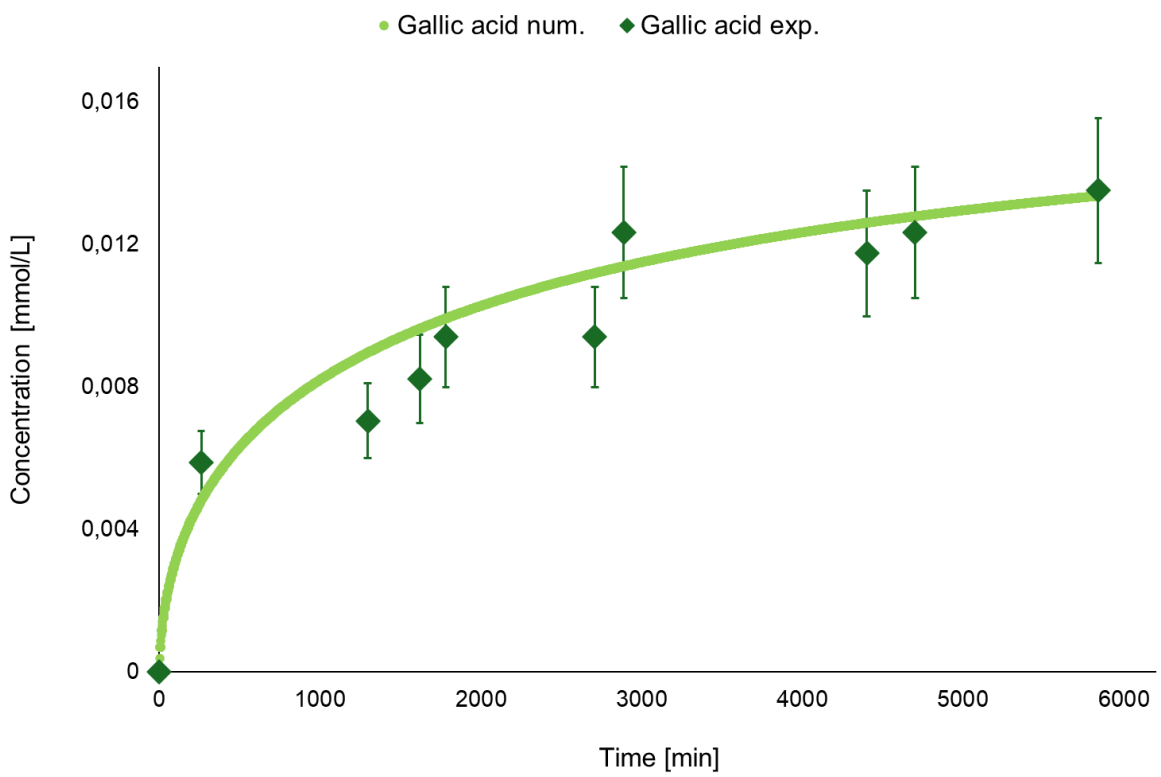

Figure 5.59: Gallic acid, G-700 sample, experimental fitting final attempt.

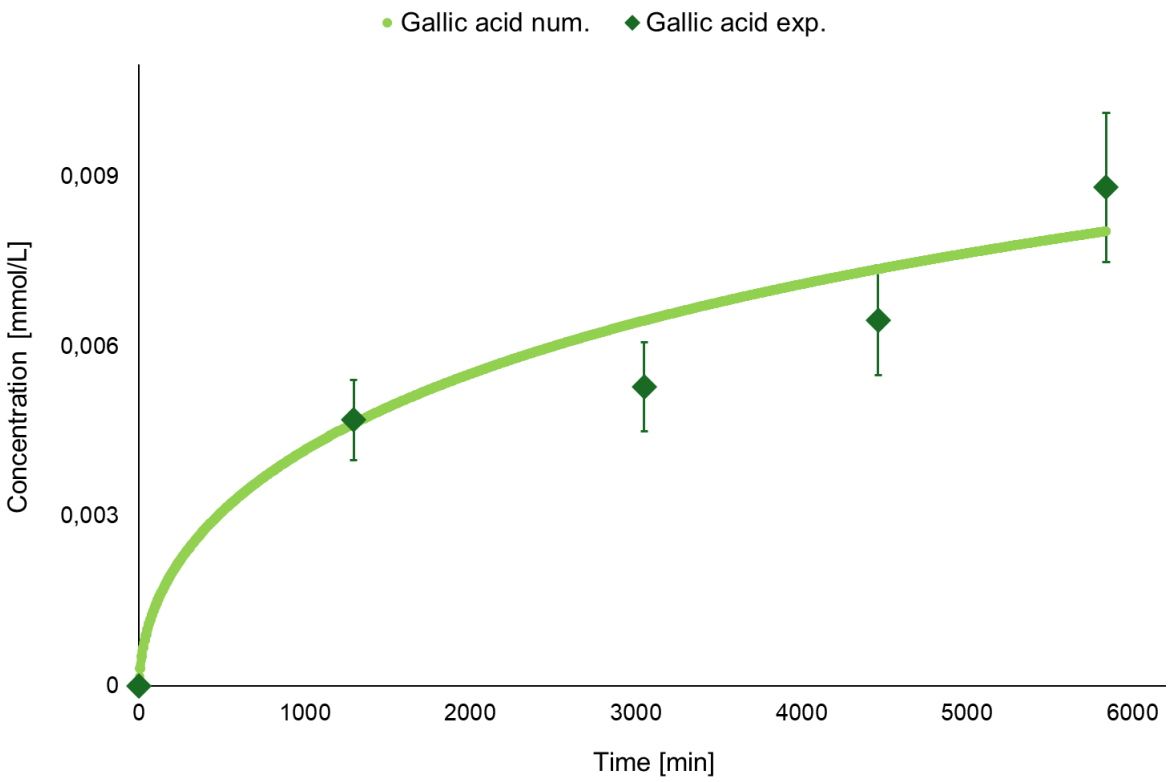

Figure 5.60: Gallic acid, M-000 sample, experimental fitting final attempt.

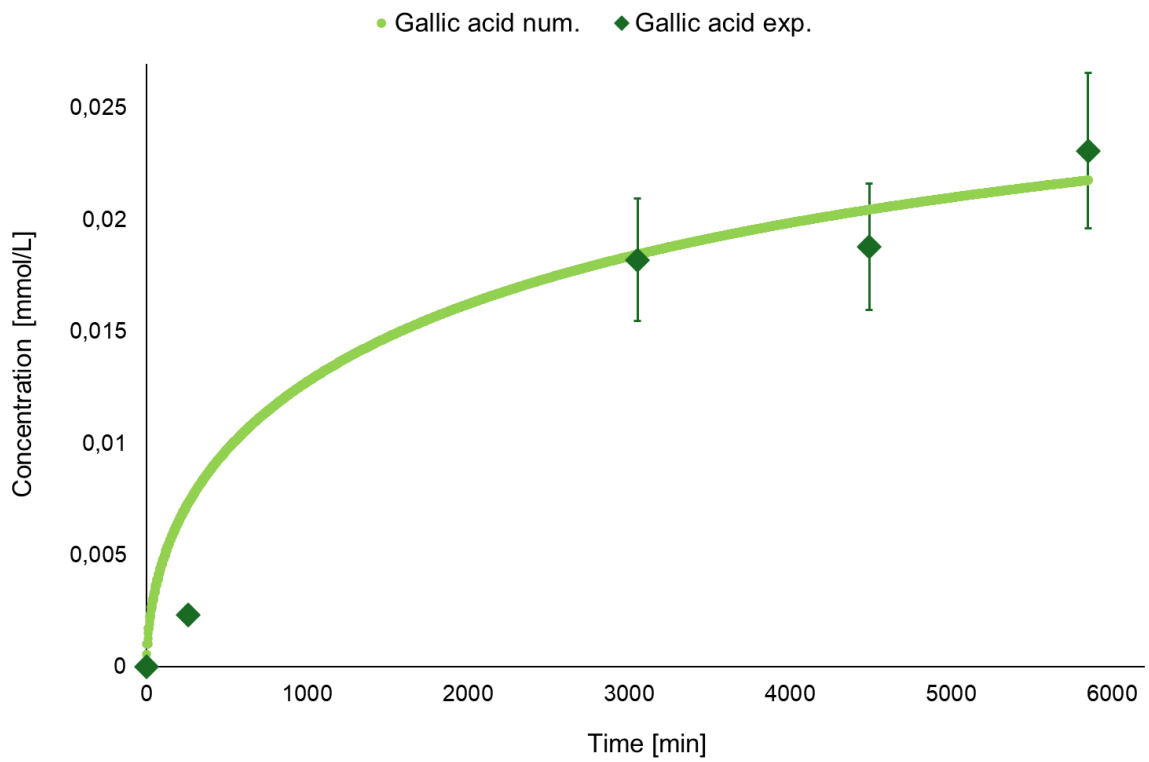

Figure 5.61: Gallic acid, M-200 sample, experimental fitting final attempt.

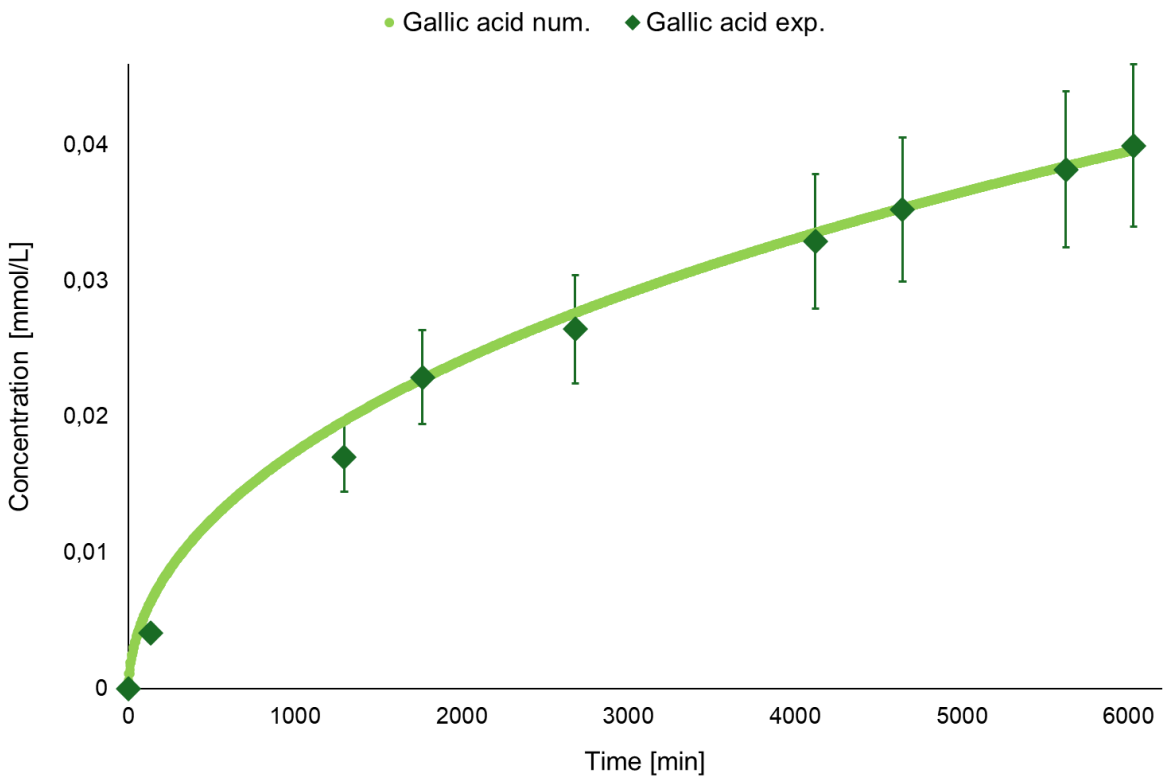

Figure 5.62: Gallic acid, M-300 sample, experimental fitting final attempt.

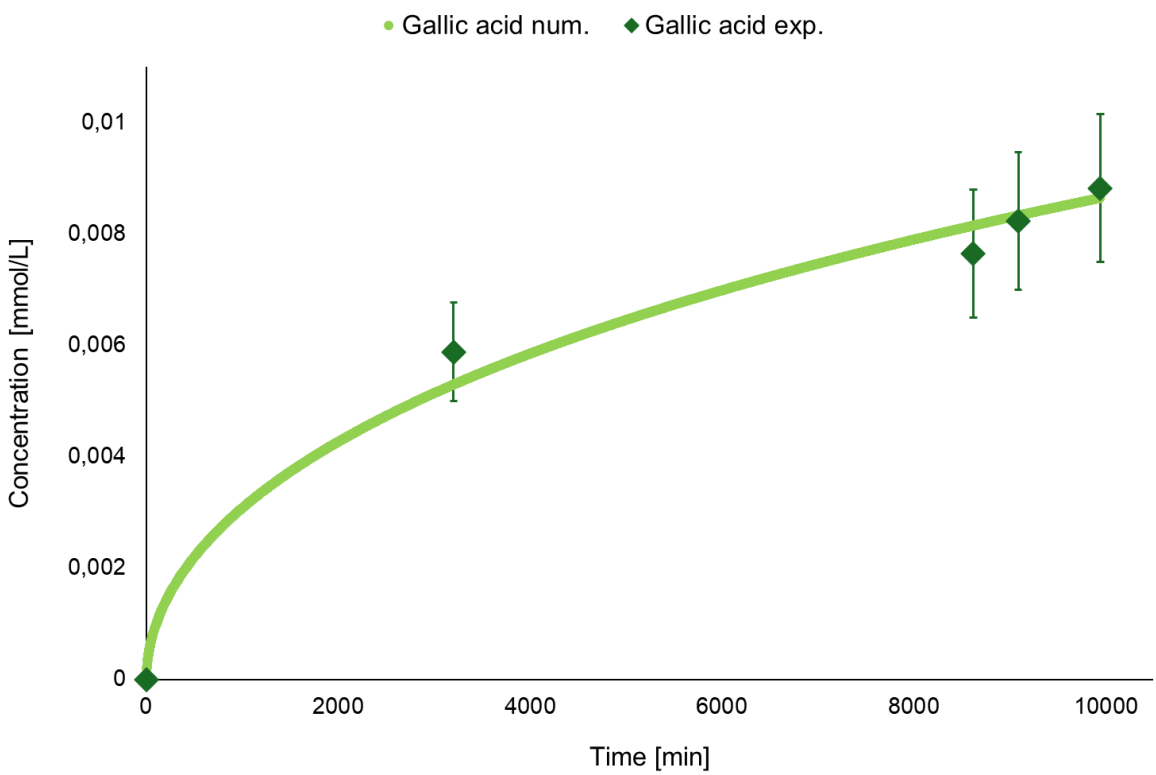

Figure 5.63: Gallic acid, M-400 sample, experimental fitting final attempt.

The system of equations involving gallic acid production and consumption needs the manipulation of four parameters, that are the kinetic constants for tannins hydrolysis and gallic acid hydrolysis and the diffusivity of water and gallic acid. The following table reports the fitted values of the just described parameters.

Table 5.14: Gallic acid, manipulated parameters values from the final attempt.

Sample	$k_8 \left[\frac{m^4}{mol * s}\right]$	$k_9 \left[\frac{m^4}{mol * s}\right]$	$D_{H_2O} \left[\frac{m^2}{s}\right]$	$D_{GA} \left[\frac{m^2}{s}\right]$
G-000	1,67 E-05	1,67 E-07	2,96 E-17	8,33 E-11
G-100	1,67 E-05	1,67 E-06	4,32 E-16	1,00 E-10
G-300	1,67 E-05	1,67 E-06	1,19 E-16	2,33 E-11
G-400	1,67 E-05	8,33 E-07	1,19 E-16	6,67 E-11
G-700	1,67 E-05	1,67 E-06	1,98 E-17	5,17 E-11
M-000	1,67 E-05	1,67 E-06	2,26 E-17	2,33 E-11
M-200	1,67 E-05	1,67 E-07	2,31 E-17	1,50 E-11
M-300	1,67 E-05	1,67 E-06	1,65 E-15	1,67 E-12
M-400	1,67 E-05	1,67 E-06	5,51 E-17	1,67 E-12

The kinetic scheme for gallic acid involves analysing only the compound itself, which is why the parameters to be manipulated are far fewer than in the case of the previous families of compounds. In this case there are two kinetic constants, k_8 for acid production and k_9 for acid consumption, and two diffusion coefficients, specifically for water in the case of tannin hydrolysis and for gallic acid in the case of back diffusion.

k_8 accounts for gallic acid production, therefore higher values lead to higher slopes of the curve. Its sensitivity turned out to be relevant only for orders of magnitude lower

than 10^{-5}, with a minimal contribution to the acid profile once the other parameters are fixed.

k_9 behaves in the same way of k_8 in terms of sensitivity, but with the opposite effect on the acid curve, meaning that higher values bring to lower concentration profile's slopes.

However, the diffusion parameters are much more impactful on the profile of the curves, as for the other groups of compounds. The diffusivity of gallic acid occurs as illustrated in Chapter 5.2.2 in both terms of consumption of the species balance constructed on the solid phase, but also contributes to the only accumulation term in the liquid phase. Overall, the manipulation of this variable causes an upward shift of the curve with a high sensitivity that causes large variations even for small changes of the order of 10^{-7}.

An increase in the diffusivity value of water also corresponds to an upward shift in the acid curve, indeed this term appears in the formation reaction of the congener. Variations in the graph are evident for parameter changes of orders of magnitude around 10^{-4}, demonstrating its high sensitivity.

A pure numerical analysis of the values obtained revealed, once again, a general underestimation of all the chemical-physical phenomena describing the maturation process. However, as in the previous cases, each parameter shows consistent values for each sample, with a deviation of maximum one or two orders of magnitude from the estimated average value.

No parameter, due to the low value compared to literature, confirms the role of ultrasound as an enhancement of the processes in question.

5.4. Further development

Whisky ageing is a complex process involving several chemical compounds interacting each other through various and dynamic mechanisms that are strongly influenced by a multitude of factors.

For this reason, the choice to trace the evolution of congeners over time following a single kinetic scheme for each family may be a strong simplification of the real process, leading to unrealistic and underestimated parameters. Further investigation about the

whole physico-chemical features of the ageing system may lead to a more precise modelling of the process.

Moreover, in accordance with the obtained results, the proposed model must be further refined to ensure the determination of parameters that show more reliable orders of magnitude and that can express the enhancement brought by the effect of ultrasound technology; the use of the Shrinking Core model, in fact, implies a series of assumptions and simplifications that do not allow to consider some of the peculiarities characterising wood in terms of structure (geometry and porosity of the matrix) and composition; in addition, the experimental data used to derive the system of equations are subjected to a certain grade of error, that concur, to a certain extent, to the underestimation of the parameters.

Lastly, the estimation of the activation energies of the kinetic constants for all the reaction rates may be a future challenge; this specific thesis work, in fact, their estimation was not possible since the ageing process is conducted in an isothermal system.

6 Conclusions

The aim of this thesis work was to find a reliable mathematical model capable of simulating the concentration over time of some key chemical compounds that are formed during the maturation of whisky with the application of the ultrasound technology. Ultrasounds, in fact, represent a novel and promising technology in several fields of application; in the food industry, they are used also in the process of maturation of various spirits, among which whisky, whose ageing requires a minimum period of three years to a maximum of thirty, determining several implications in terms of time and costs.

The starting point of this work was the analysis of the experimental data collected in the work of De Taddeo and Ramirez, related to six chemical compounds that impact on the typical taste, flavour and colour of whisky; in particular, syringaldehyde, syringic acid, coniferaldehyde, vanillin and vanillic acid are the products of the degradation of lignin, while gallic acid is formed from the hydrolysis of tannins. The measurements refer to 16 different samples, in which the most important parameters of the accelerated ageing process have been targeted and investigated: wood typology, surface to volume ratio, thermal treatment, ultrasound time and total sonication time.

The first step was to inspect the experimental data with the purpose of removing from the analysis samples or data within a sample, that showed non reliable trends, such as oscillating trends, measurements equal to zero and outliers. After this selection, the model development section highlighted the several attempts made to fit the experimental data, starting with chemical reaction rates expressed as power laws, with kinetic constants as only parameters to fit. However, this first attempt highlighted the impossibility to describe all the phenomena involved in the ageing process with a sole chemical regime.

This last consideration brought to the introduction of a hybrid regime, in which mass transfer phenomena have been considered, finding a good proposal in the Shrinking Core model, used to describe surface reactions that imply the consumption of the so called 'ash layer', represented, in this specific case, by the wood layer where the reactions between wood congeners and the bulk solution reactants take place. Despite the introduction of other parameters to fit, that seem to complicate the whole system, the Shirking Core model allowed to obtain a good fitting of the experimental data,

where the diffusivities of ethanol, water, oxygen and wood congeners revealed to have a stronger impact than the kinetic constants on the profile of the curves.

The work concluded with a modification of the attempt just presented, since the distinction between the compounds in the solid wood matrix and the compounds in the liquid bulk was not considered yet. This implied to consider also the back diffusion of the products just formed from the wood matrix to the liquid phase, without changing the reaction schemes or adding other parameters.

The graphs and the values of the fitted parameters have been reported for all the samples, followed by a sensitivity analysis of these parameters. The kinetic constants showed a minimum or negligible impact for all the reaction schemes, while the values of all diffusivities (ethanol, water, oxygen, wood congeners) are characterised by a high sensitivity, leading to significant changes of the trends with minimal variations, confirming that the whisky aging is substantially under mass transfer control.

However, the results obtained in this work can be improved. The diffusivities of oxygen and wood congeners resulted in order of magnitude comparable to the values usually found in literature, while the ethanol and water diffusivities turned out to have lower orders of magnitude, also in contrast with the expectable enhancement provided by the application of ultrasounds.

To overcome this issue, further developments may concern the investigation of Shrinking Core model variants and the introduction of a more detailed representation of physico-chemical evolution of the system.

Bibliography

[1] Commission regulation, "This document is meant purely as a documentation tool and the institutions do not assume any liability for its contents setting maximum levels for certain contaminants in foodstuffs (Text with EEA relevance)," vol. 1881, no. February 1998, pp. 1–5, 2006, [Online]. Available: https://eur-lex.europa.eu/LexUriServ/LexUriServ.do?uri=CONSLEG:2006R1881:20100701:EN:PDF

[2] Andy Connelly, "The science and art of whisky making," The Guardian. [Online]. Available: https://www.theguardian.com/science/blog/2010/aug/23/science-art-whisky-making

[3] T. J. Kelly, C. O'Connor, and K. N. Kilcawley, "Sources of Volatile Aromatic Congeners in Whiskey," *Beverages*, vol. 9, no. 3, 2023, doi: 10.3390/beverages9030064.

[4] A. C. Power, C. N. Néill, S. Geoghegan, S. Currivan, M. Deasy, and D. Cozzolino, "A brief history of whiskey adulteration and the role of spectroscopy combined with chemometrics in the detection of modern whiskey fraud," *Beverages*, vol. 6, no. 3, pp. 1–13, 2020, doi: 10.3390/beverages6030049.

[5] L. Waterson, "A beginner's guide to Scottish Whisky: history, regions, trails - and the best places to enjoy a drop," lonely planet. [Online]. Available: https://www.lonelyplanet.com/articles/whisky-scotland-introduction

[6] G. H. Miller, *Whisky Science - A Condendsed Distillation*. Springer International Publishing, 2019.

[7] J. Bower, "Scotch whisky: History, heritage and the stock cycle," *Beverages*, vol. 2, no. 2, pp. 1–14, 2016, doi: 10.3390/beverages2020011.

[8] T. C. S. Dolan, *Malt whiskies. Raw materials and processing*. 2003. doi: 10.1016/B978-012669202-0.50019-1.

[9] Russell Inge, *Understanding yeast fundamentals*. 2003.

[10] "The origin of Scotch Whisky." [Online]. Available: https://www.scotchwhiskyexperience.co.uk/about/about-

whisky/history/#:~:text=Whisky has been distilled in,spirits from their surplus barley

[11] J. W. Lehmkuhler and E. S. Vanzant, "INVITED REVIEW: Rise of craft distilleries in the southeastern United States increases bourbon-distillery feedstuffs as supplement for beef cattle," *Appl. Anim. Sci.*, vol. 38, no. 5, pp. 456–465, 2022, doi: 10.15232/aas.2022-02299.

[12] C. Klein, "How Kentucky Became the World's Bourbon Capital," History. Accessed: Mar. 10, 2025. [Online]. Available: https://www.history.com/news/how-kentucky-became-the-worlds-bourbon-capital

[13] R. Moss, "How Bourbon really got its name." [Online]. Available: https://robertfmoss.com/features/How-Bourbon-Really-Got-Its-Name#:~:text=Bourbon%2C the evidence suggests%2C really,hadn't been charred inside

[14] "Bourbon - An American history," Whisky.com. [Online]. Available: https://www.whisky.com/history-bourbon.html#:~:text=Bourbon%2C an American whiskey%2C has,the Whiskey Rebellion in 1794

[15] W. Kew, I. Goodall, D. Clarke, and D. Uhrín, "Chemical Diversity and Complexity of Scotch Whisky as Revealed by High-Resolution Mass Spectrometry," *J. Am. Soc. Mass Spectrom.*, vol. 28, no. 1, pp. 200–213, 2017, doi: 10.1007/s13361-016-1513-y.

[16] C. Brown and I. Duignan, "Understanding the whiskey market - Whiskey market landscape series."

[17] "Whiskey market size & trends," Grand view research. [Online]. Available: https://www.grandviewresearch.com/industry-analysis/whiskey-market

[18] "Whiskey Market: Global Industry Analysis by Market Share, Trend, Size, Competitive Landscape, Regional Outlook and Forecast (2025-2032)," Maximize Market Research.

[19] "Whiskey market analysis by grain type, by quality & by region," Fact.MR. [Online]. Available: https://www.factmr.com/report/4515/whisky-market

[20] A. Swiers, "The Difference Between A Premium And Super Premium Drink," TastingTable. [Online]. Available: https://www.tastingtable.com/1336280/difference-premium-super-drink/

[21] V. L. Espitia-López, F. P. Malpica-Sánchez, H. B. Escalona-Buendía, and J. R. Verde-Calvo, "Innovation and Development in Whisky Production Around the World," *Beverages*, vol. 10, no. 4, pp. 1–14, 2024, doi: 10.3390/beverages10040124.

[22] "Whiskey Market Size & Share, Previsioni della crescita 2025-2034," Global

Market Insights. [Online]. Available: https://www.gminsights.com/it/industry-analysis/whiskey-market

[23] B. C. Smith, C. Sester, J. Ballester, and O. Deroy, "The perceptual categorisation of blended and single malt Scotch whiskies," *Flavour*, vol. 6, no. 1, pp. 1–9, 2017, doi: 10.1186/s13411-017-0056-x.

[24] A. Wanikawa and T. Sugimoto, "A Narrative Review of Sulfur Compounds in Whisk(e)y," *Molecules*, vol. 27, no. 5, 2022, doi: 10.3390/molecules27051672.

[25] A. Wanikawa, "Flavors in Malt Whisky: A Review," *J. Am. Soc. Brew. Chem.*, vol. 78, no. 4, pp. 260–278, 2020, doi: 10.1080/03610470.2020.1795795.

[26] M. J. Delgado-González, M. V. García-Moreno, M. M. Sánchez-Guillén, C. García-Barroso, and D. A. Guillén-Sánchez, "Colour evolution kinetics study of spirits in their ageing process in wood casks," *Food Control*, vol. 119, no. July 2020, 2021, doi: 10.1016/j.foodcont.2020.107468.

[27] J. Espitia-López, H. B. Escalona-Buendía, H. Luna, and J. R. Verde-Calvo, "Multivariate study of the evolution of phenolic composition and sensory profile on mouth of Mexican red Merlot wine aged in barrels vs wood chips," *CYTA - J. Food*, vol. 13, no. 1, pp. 26–31, 2015, doi: 10.1080/19476337.2014.907826.

[28] M. Czerny *et al.*, "Re-investigation on odour thresholds of key food aroma compounds and development of an aroma language based on odour qualities of defined aqueous odorant solutions," *Eur. Food Res. Technol.*, vol. 228, no. 2, pp. 265–273, 2008, doi: 10.1007/s00217-008-0931-x.

[29] R. I. Aylott and W. M. MacKenzie, "Analytical strategies to confirm the generic authenticity of Scotch whisky," *J. Inst. Brew.*, vol. 116, no. 3, pp. 215–229, 2010, doi: 10.1002/j.2050-0416.2010.tb00424.x.

[30] W. T. B. Thomas, H. Bull, A. Booth, R. Hamilton, B. P. Forster, and J. D. Franckowiak, "A practical guide to barley crossing," *Methods Mol. Biol.*, vol. 1900, pp. 21–36, 2019, doi: 10.1007/978-1-4939-8944-7_3.

[31] T. A. Bringhurst, "125th Anniversary Review: Barley research in relation to Scotch whisky production: A journey to new frontiers," *J. Inst. Brew.*, vol. 121, no. 1, pp. 1–18, 2015, doi: 10.1002/jib.192.

[32] T. A. Bringhurst and J. Brosnan, *Scotch whisky: raw material selection and processing*, Second Edi. Elsevier Ltd, 2014. doi: 10.1016/B978-0-12-401735-1.00006-4.

[33] "Base ingredients for whisky production," WhiskyItaly. [Online]. Available: https://www.whiskyitaly.it/it/il-whisky?srsltid=AfmBOorNu1k9HZMdtRL-pEDTy95o4nKkp3nWATOfgLCvZDBbIUD7buGM

[34] "The importance of water," ScotchWhisky.com. [Online]. Available:

https://scotchwhisky.com/magazine/ask-the-professor/8216/the-importance-of-water/

[35] J. L. Sandefur, *T He a Boriginalisation*, no. July. 1998.

[36] A. G. H. Lea and J. R. Piggott, "Second Edition FerlDented Beverage Production," pp. 139–153, 2003.

[37] F. R. Jack, *Whiskies: composition, sensory properties and sensory analysis*. Woodhead Publishing Limited, 2012. doi: 10.1533/9780857095176.3.379.

[38] C. M. Ramsay and D. R. Berry, "Effect of temperature and pH on the formation of higher alcohols, fatty acids and esters in the malt whisky fermentation," *Food Microbiol.*, vol. 1, no. 2, pp. 117–121, 1984, doi: 10.1016/0740-0020(84)90021-2.

[39] D. Naviglio, P. Trucillo, A. Perrone, D. Montesano, and M. Gallo, "Comparison between Conventional Ageing Process in Barrels and a New Rapid Aging Process Based on RSLDE: Analysis of Bioactive Compounds in Spirit Drinks," *Processes*, vol. 12, no. 4, 2024, doi: 10.3390/pr12040829.

[40] "How Whisky Is Made," WhiskyADVOCATE. [Online]. Available: https://whiskyadvocate.com/how-to-make-whisky

[41] "Distilling Whisky: a guide to distillation," The Glenlivet. [Online]. Available: https://www.theglenlivet.com/en/our-community/articles/distilling-whisky/

[42] J. A. Maga, "The contribution of wood to the flavor of alcoholic beverages," *Food Rev. Int.*, vol. 5, no. 1, pp. 39–99, 1989, doi: 10.1080/87559128909540844.

[43] N. Vivas, N. Vivas de Gaulejac, M. F. Bourden-Nonier, C. Mouche, and C. Rossy, "Extraction of phenolics from new oak casks during spirit maturation: impact on spirit colour," *J. Inst. Brew.*, vol. 126, no. 1, pp. 83–89, 2020, doi: 10.1002/jib.586.

[44] M. Stupak, I. Goodall, M. Tomaniova, J. Pulkrabova, and J. Hajslova, "A novel approach to assess the quality and authenticity of Scotch Whisky based on gas chromatography coupled to high resolution mass spectrometry," *Anal. Chim. Acta*, vol. 1042, no. 2018, pp. 60–70, 2018, doi: 10.1016/j.aca.2018.09.017.

[45] G. C. Silvello, A. M. Bortoletto, and A. R. Alcarde, "The barrel aged beer wheel: a tool for sensory assessment," *J. Inst. Brew.*, vol. 126, no. 4, pp. 382–393, 2020, doi: 10.1002/jib.626.

[46] J. R. Piggott, J. M. Conner, and A. Paterson, "Flavour development in whisky maturation," *Dev. Food Sci.*, vol. 37, no. C, pp. 1731–1751, 1995, doi: 10.1016/S0167-4501(06)80261-X.

[47] I. Caldeira *et al.*, "Kinetics of odorant compounds in wine brandies aged in different systems," *Food Chem.*, vol. 211, pp. 937–946, 2016, doi: 10.1016/j.foodchem.2016.05.129.

[48] A. R. Alcarde, L. M. Souza, and A. M. Bortoletto, "Formation of volatile and

maturation-related congeners during the aging of sugarcane spirit in oak barrels," *J. Inst. Brew.*, vol. 120, no. 4, pp. 529–536, 2014, doi: 10.1002/jib.165.

[49] C. Depcik, "Modelling Whisk(e)y, Rum, Cachaca, and Tequila maturation," 2024.

[50] J. R. Mosedale, "Effects of oak wood on the maturation of alcoholic beverages with particular reference to whisky," *Forestry*, vol. 68, no. 3, pp. 203–230, 1995, doi: 10.1093/forestry/68.3.203.

[51] A. Wiehebrink, "Role of Oxygenation in Barrel Aged Spirits," ISC barrels. [Online]. Available: https://www.iscbarrels.com/the-role-of-oxygenation-in-barrel-aged-spirits-part-ii/

[52] M. Waterbury, "How a Warm Climate Transforms Single Malt Flavor," WhiskyADVOCATE. [Online]. Available: https://whiskyadvocate.com/warm-climate-single-malt-whisky-flavor

[53] C. Baraniuk, "How whiskey is shaped by the weather and climate," BBC. [Online]. Available: https://www.bbc.com/future/article/20220826-how-whiskey-is-shaped-by-the-weather-and-climate

[54] C. Roullier-Gall *et al.*, "Influence of regionality and maturation time on the chemical fingerprint of whisky," *Food Chem.*, vol. 323, p. 126748, 2020, doi: 10.1016/j.foodchem.2020.126748.

[55] M. C. Castro, A. M. Bortoletto, G. C. Silvello, and A. R. Alcarde, "Lignin-derived phenolic compounds in cachaça aged in new barrels made from two oak species," *Heliyon*, vol. 6, no. 11, pp. 0–6, 2020, doi: 10.1016/j.heliyon.2020.e05586.

[56] J. M. Conner, A. Paterson, and J. R. Piggott, "Analysis of lignin from oak casks used for the maturation of Scotch whisky," *J. Sci. Food Agric.*, vol. 60, no. 3, pp. 349–353, 1992, doi: 10.1002/jsfa.2740600312.

[57] I. Kögel-Knabner and W. Amelung, *Dynamics, Chemistry, and Preservation of Organic Matter in Soils*, vol. 12. 2013. doi: 10.1016/B978-0-08-095975-7.01012-3.

[58] V. Laverde, A. Marin, J. M. Benjumea, and M. Rincón Ortiz, "Use of vegetable fibers as reinforcements in cement-matrix composite materials: A review," *Constr. Build. Mater.*, vol. 340, no. May, 2022, doi: 10.1016/j.conbuildmat.2022.127729.

[59] S. Dutta, *Lignin Deconstruction: Chemical and Biological Approaches*. Elsevier B.V., 2015. doi: 10.1016/B978-0-444-59567-6.00005-4.

[60] K. Khanbabaee and T. van Ree, "Tannins: Classification and definition," *Nat. Prod. Rep.*, vol. 18, no. 6, pp. 641–649, 2001, doi: 10.1039/b101061l.

[61] K. P. Sharma, "Tannin degradation by phytopathogen's tannase: A Plant's defense perspective," *Biocatal. Agric. Biotechnol.*, vol. 21, no. April, p. 101342,

2019, doi: 10.1016/j.bcab.2019.101342.

[62] K. Kemppainen, M. Siika-aho, S. Pattathil, S. Giovando, and K. Kruus, "Spruce bark as an industrial source of condensed tannins and non-cellulosic sugars," *Ind. Crops Prod.*, vol. 52, pp. 158–168, 2014, doi: 10.1016/j.indcrop.2013.10.009.

[63] S. Cernîşev, "Analysis of lignin-derived phenolic compounds and their transformations in aged wine distillates," *Food Control*, vol. 73, no. 2017, pp. 281–290, 2017, doi: 10.1016/j.foodcont.2016.08.015.

[64] G. D. Yadav and G. P. Fernandes, "Selective synthesis of natural benzaldehyde by hydrolysis of cinnamaldehyde using novel hydrotalcite catalyst," *Catal. Today*, vol. 207, pp. 162–169, 2013, doi: 10.1016/j.cattod.2012.04.052.

[65] V. E. Tarabanko, D. V. Petukhov, and G. E. Selyutin, "New mechanism for the catalytic oxidation of lignin to vanillin," *Kinet. Catal.*, vol. 45, no. 4, pp. 569–577, 2004, doi: 10.1023/B:KICA.0000038087.95130.a5.

[66] L. li Lu, X. yang Lu, and N. Ma, "Kinetics of non-catalyzed hydrolysis of tannin in high temperature liquid water.," *J. Zhejiang Univ. Sci. B*, vol. 9, no. 5, pp. 401–406, 2008, doi: 10.1631/jzus.B0730098.

[67] R. Hemingway and W. E. Hillis, "Behavior of ellagitannins, gallic acid, and ellagic acid under alkaline conditions," 1971, [Online]. Available: https://research.fs.usda.gov/treesearch/8029

[68] B. G. Yasnitskii and I. E. Korobeinikova, "KINETICS OF THE ACIDIC HYDROLYSIS OF TANNIN," 1988.

[69] S. Bjartmar Hylta and E. Lundquist, "Pricing Single Malt Whisky : A Regression Analysis," 2016, [Online]. Available: http://urn.kb.se/resolve?urn=urn:nbn:se:kth:diva-189001

[70] "History of M&H distillery," M&H DISTILLERY. [Online]. Available: https://mh-distillery.com/

[71] R. Kruger, A. Alberti, and A. Nogueira, "Current Technologies to Accelerate the Aging Process of Alcoholic Beverages: A Review," 2022, doi: 10.3390/beverages8040065.

[72] Y. Tao, J. F. García, and D. W. Sun, "Advances in Wine Aging Technologies for Enhancing Wine Quality and Accelerating Wine Aging Process," *Crit. Rev. Food Sci. Nutr.*, vol. 54, no. 6, pp. 817–835, 2014, doi: 10.1080/10408398.2011.609949.

[73] Y. Tao, Z. Zhang, and D. W. Sun, "Experimental and modeling studies of ultrasound-assisted release of phenolics from oak chips into model wine," *Ultrason. Sonochem.*, vol. 21, no. 5, pp. 1839–1848, 2014, doi: 10.1016/j.ultsonch.2014.03.016.

[74] D. N. Daniele Naviglio, "Efficiency of conventional extraction technique

compared to rapid-solid liquid dynamic extraction (RSLDE) in the preparation of bitter liquors and elixirs," *IOSR J. Pharm.*, vol. 04, no. 05, pp. 14–22, 2014, doi: 10.9790/3013-0405014022.

[75] S. Zervos, "Natural and accelerated ageing of cellulose and paper: A literature review," *Cellul. Struct. Prop. Deriv. Ind. Uses*, no. April, pp. 155–203, 2010.

[76] A. C. Chang, "The effects of gamma irradiation on rice wine maturation," *Food Chem.*, vol. 83, no. 3, pp. 323–327, 2003, doi: 10.1016/S0308-8146(03)00050-5.

[77] L. Y. Lin *et al.*, "Acceleration of maturity of young sorghum (kaoliang) spirits by linking nanogold photocatalyzed process to conventional biological aging-a kinetic approach: Accelerated maturation of young spirits," *Food Bioprocess Technol.*, vol. 1, no. 3, pp. 234–245, 2008, doi: 10.1007/s11947-007-0024-z.

[78] G. Duley, S. Poggesi, L. Longhi, E. Longo, and E. Boselli, "How does the application of ultrasound energy influence the ageing of a bottled red wine?," *Appl. Food Res.*, vol. 4, no. 2, p. 100540, 2024, doi: 10.1016/j.afres.2024.100540.

[79] K. S. Ojha, T. J. Mason, C. P. O'Donnell, J. P. Kerry, and B. K. Tiwari, "Ultrasound technology for food fermentation applications," *Ultrason. Sonochem.*, vol. 34, pp. 410–417, 2017, doi: 10.1016/j.ultsonch.2016.06.001.

[80] G. Cravotto and P. Cintas, "Power ultrasound in organic synthesis: Moving cavitational chemistry from academia to innovative and large-scale applications," *Chem. Soc. Rev.*, vol. 35, no. 2, pp. 180–196, 2006, doi: 10.1039/b503848k.

[81] C. Engineering, "Sonochemical reaction engineering Department of Chemical Engineering , Indian Institute of Sci-," vol. 19, no. December, pp. 1055–1076, 1994.

[82] M. J. Delgado-González, M. M. Sánchez-Guillén, M. V. García-Moreno, M. C. Rodríguez-Dodero, C. García-Barroso, and D. A. Guillén- Sánchez, "Study of a laboratory-scaled new method for the accelerated continuous ageing of wine spirits by applying ultrasound energy," *Ultrason. Sonochem.*, vol. 36, pp. 226–235, 2017, doi: 10.1016/j.ultsonch.2016.11.031.

[83] K. A. Dostie and B. A. S. E. Physics, "Design and Modeling of a Sonochemical Reactor Using Geometry , Mode Shapes and Resonance by : A THESIS SUBMITTED IN PARTIAL FULFILLMENT OF THE REQUIREMENTS," *Design*, no. October, 2000.

[84] J. W. Chen and W. M. Kalback, "Effect of ultrasound on chemical reaction rate," *Ind. Eng. Chem. Fundam.*, vol. 6, no. 2, pp. 175–178, 1967, doi: 10.1021/i160022a003.

[85] C. I. D. Red, B. Y. K. A. T. C. Smith, D. Hite, C. State, M. Carlough, and S. C. Corp, "The Effects of Ultrasound and the Diffusion Vkrp Sizing Literature," pp. 21–22.

[86] Y. Yao, "Enhancement of mass transfer by ultrasound: Application to adsorbent regeneration and food drying/dehydration," *Ultrason. Sonochem.*, vol. 31, pp. 512–531, 2016, doi: 10.1016/j.ultsonch.2016.01.039.

[87] A. O. Oladejo, H. Ma, W. Qu, C. Zhou, B. Wu, and X. Yang, "Influence of ultrasound pretreatments on diffusion coefficients, texture and colour of osmodehydrated sweet potato (Ipomea batatas)," *Int. J. Food Sci. Technol.*, vol. 52, no. 4, pp. 888–896, 2017, doi: 10.1111/ijfs.13352.

[88] S. V. Sancheti and P. R. Gogate, "A review of engineering aspects of intensification of chemical synthesis using ultrasound," *Ultrason. Sonochem.*, vol. 36, pp. 527–543, 2017, doi: 10.1016/j.ultsonch.2016.08.009.

[89] N. W. Ingole and S. V. Khedkar, "The Ultrasound reactor technology - A technology for the future," *Int. J. Adv. Eng. Res. Stud.*, vol. II, no. I, pp. 72–75, 2012.

[90] K. S. Suslick, "The Chemical Effects of Ultrasound," *Sci. Am.*, vol. 260, no. 2, pp. 80–86, 1989, doi: 10.1038/scientificamerican0289-80.

[91] M. Gallo, L. Ferrara, and D. Naviglio, "Application of ultrasound in food science and technology: A perspective," *Foods*, vol. 7, no. 10, pp. 1–18, 2018, doi: 10.3390/foods7100164.

[92] S. Nikitenko and F. Chemat, "Ultrasound in Process Engineering," *Green Process Eng.*, no. June 2015, pp. 145–165, 2015, doi: 10.1201/b18533-9.

[93] Y. Tao and D. W. Sun, "Enhancement of Food Processes by Ultrasound: A Review," *Crit. Rev. Food Sci. Nutr.*, vol. 55, no. 4, pp. 570–594, 2015, doi: 10.1080/10408398.2012.667849.

[94] F. Chemat, N. Rombaut, A. G. Sicaire, A. Meullemiestre, A. S. Fabiano-Tixier, and M. Abert-Vian, "Ultrasound assisted extraction of food and natural products. Mechanisms, techniques, combinations, protocols and applications. A review," *Ultrason. Sonochem.*, vol. 34, pp. 540–560, 2017, doi: 10.1016/j.ultsonch.2016.06.035.

[95] H. Kiani, Z. Zhang, A. Delgado, and D. W. Sun, "Ultrasound assisted nucleation of some liquid and solid model foods during freezing," *Food Res. Int.*, vol. 44, no. 9, pp. 2915–2921, 2011, doi: 10.1016/j.foodres.2011.06.051.

[96] G. Cobellis and M. Trabalza, "Critical evaluation of essential oils as rumen modifiers in ruminant nutrition: A review," 2016, doi: 10.1016/j.scitotenv.2015.12.103.

[97] A. F. Rossi, *Optimization of Whisky accelerated aging process*. 2023.

[98] J. Lozano-Sánchez, I. Borrás-Linares, A. Sass-Kiss, and A. Segura-Carretero, *Chromatographic Technique: High-Performance Liquid Chromatography (HPLC).*

2018. doi: 10.1016/b978-0-12-814264-6.00013-x.

[99] M. D. Palamareva, "Liquid Chromatography," vol. Encicloped, 2005, doi: 10.1016/B0-12- 369397-7/00313-7.

[100] A. Fallon, R. F. Booth, and L. D. Bell, *Applications of HPLC in Biochemistry*. 1987.

[101] A. Taha *et al.*, "Ultrasonic emulsification: An overview on the preparation of different emulsifiers-stabilized emulsions," *Trends Food Sci. Technol.*, vol. 105, pp. 363–377, 2020, doi: 10.1016/j.tifs.2020.09.024.

[102] C. Psarra, O. Gortzi, and D. P. Makris, "Kinetics of polyphenol extraction from wood chips in wine model solutions: Effect of chip amount and botanical species," *J. Inst. Brew.*, vol. 121, no. 2, pp. 207–212, 2015, doi: 10.1002/jib.212.

[103] S. Kitanović, D. Milenović, and V. B. Veljković, "Empirical kinetic models for the resinoid extraction from aerial parts of St. John's wort (Hypericum perforatum L.)," *Biochem. Eng. J.*, vol. 41, no. 1, pp. 1–11, 2008, doi: 10.1016/j.bej.2008.02.010.

[104] C. Wiuf and E. Feliu, "Power-law kinetics and determinant criteria for the preclusion of multistationarity in networks of interacting species," *SIAM J. Appl. Dyn. Syst.*, vol. 12, no. 4, pp. 1685–1721, 2013, doi: 10.1137/120873388.

[105] L. O. Explain, W. R. Laws, R. O. An, and S. The, "12.4: Rate Laws ◎," pp. 1–7.

[106] Z. O. Kinetics, D. Form, Z. Order, and R. Law, "Integrated Form of the Zeroth Order Rate Law," no. 3, pp. 3–6, 2021.

[107] I. Reactants, "2.8: Second-Order Reactions," pp. 1–7.

[108] "Oxide growth Thin Solid Films Processing 2014 Oxide growth," 2014.

[109] I. Tudela, P. Bonete, A. Fullana, and J. A. Conesa, "Parameter sensitivity study of the unreacted-core shrinking model: A computer activity for chemical reaction engineering courses," *J. Chem. Educ.*, vol. 88, no. 1, pp. 56–58, 2011, doi: 10.1021/ed100302n.

[110] X. Zhao, R. Wu, and D. Liu, "Evaluation of the mass transfer effects on delignification kinetics of atmospheric acetic acid fractionation of sugarcane bagasse with a shrinking-layer model," *Bioresour. Technol.*, vol. 261, no. January, pp. 52–61, 2018, doi: 10.1016/j.biortech.2018.03.140.

[111] M. D. Pritzker, "Shrinking-core model for systems with facile heterogeneous and homogeneous reactions," *Chem. Eng. Sci.*, vol. 51, no. 14, pp. 3631–3645, 1996, doi: 10.1016/0009-2509(95)00403-3.

[112] H. Ahn and S. Choi, "A comparison of the shrinking core model and the grain model for the iron ore pellet indurator simulation," *Comput. Chem. Eng.*, vol. 97, pp. 13–26, 2017, doi: 10.1016/j.compchemeng.2016.11.005.

[113] A. Galgano and C. Di Blasi, "Modeling wood degradation by the unreacted-core-

shrinking approximation," *Ind. Eng. Chem. Res.*, vol. 42, no. 10, pp. 2101–2111, 2003, doi: 10.1021/ie020939o.

[114] C. C. License and D. Version, "Aalborg Universitet Hydrothermal liquefaction of wood using a modified multistage shrinking-core model Publication date : Hydrothermal liquefaction of wood using a modified multistage shrinking- core model," 2020.

[115] C. Wang, X. Duan, W. Wang, Z. Li, and Y. Qin, "Establishment and verification of a shrinking core model for dilute acid hydrolysis of lignocellulose," *Front. Energy*, vol. 6, no. 4, pp. 413–419, 2012, doi: 10.1007/s11708-012-0212-z.

[116] F. Euler, "1 . 2 : Forward Euler method," pp. 1–16.

[117] J. Ayensa-Jiménez *et al.*, "On the simulation of organ-on-chip cell processes: Application to an in vitro model of glioblastoma evolution," *Adv. Biomech. Tissue Regen.*, pp. 313–341, 2019, doi: 10.1016/B978-0-12-816390-0.00016-9.

[118] T. Schnabel, J. Vrabec, and H. Hasse, "Henry's law constants of methane, nitrogen, oxygen and carbon dioxide in ethanol from 273 to 498 K: Prediction from molecular simulation," *Fluid Phase Equilib.*, vol. 233, no. 2, pp. 134–143, 2005, doi: 10.1016/j.fluid.2005.04.016.

[119] B. Zêzere, I. Portugal, C. M. Silva, and J. R. B. Gomes, "Diffusivities of ketones and aldehydes in liquid ethanol by molecular dynamics simulations," *J. Mol. Liq.*, vol. 371, 2023, doi: 10.1016/j.molliq.2022.121068.

[120] D. E. Bidstrup and C. J. Geankoplis, "Aqueous Molecular Diffusivities of Carboxylic Acids," *J. Chem. Eng. Data*, vol. 8, no. 2, pp. 170–173, 1963, doi: 10.1021/je60017a004.

[121] E. E. Hills, M. H. Abraham, A. Hersey, and C. D. Bevan, "Diffusion coefficients in ethanol and in water at 298K: Linear free energy relationships," *Fluid Phase Equilib.*, vol. 303, no. 1, pp. 45–55, 2011, doi: 10.1016/j.fluid.2011.01.002.

A Appendix

An appendix has been introduced to supplement the chapter on model construction by offering further information that could help with logical path comprehension and in understanding the achieved results.

A.1. Data visualization

In order to simplify and lighten the main discussion, it was decided to leave out a portion of the graphs created for each sample that was being examined. For completeness's sake, all of the missing sample graphs that illustrate how the experimental concentrations of each congener have changed over time are provided here.

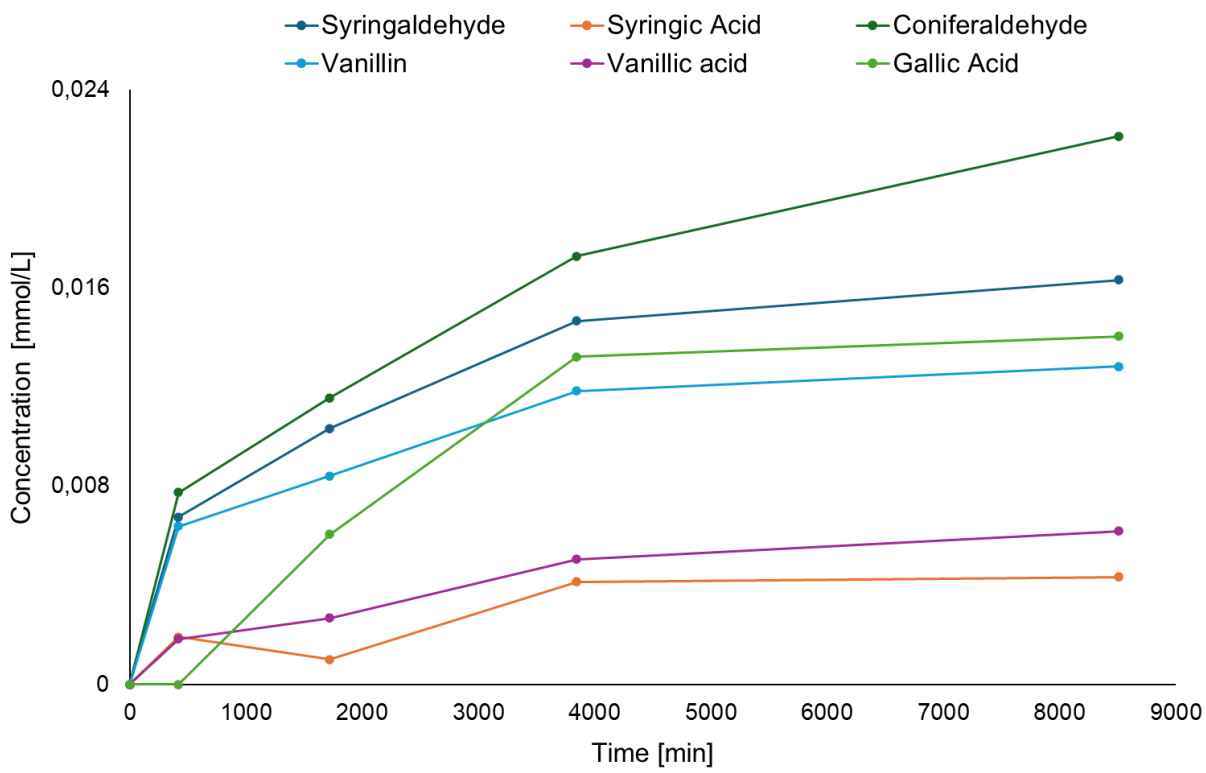

Figure A.1: Sample G-100, experimental concentrations trends.

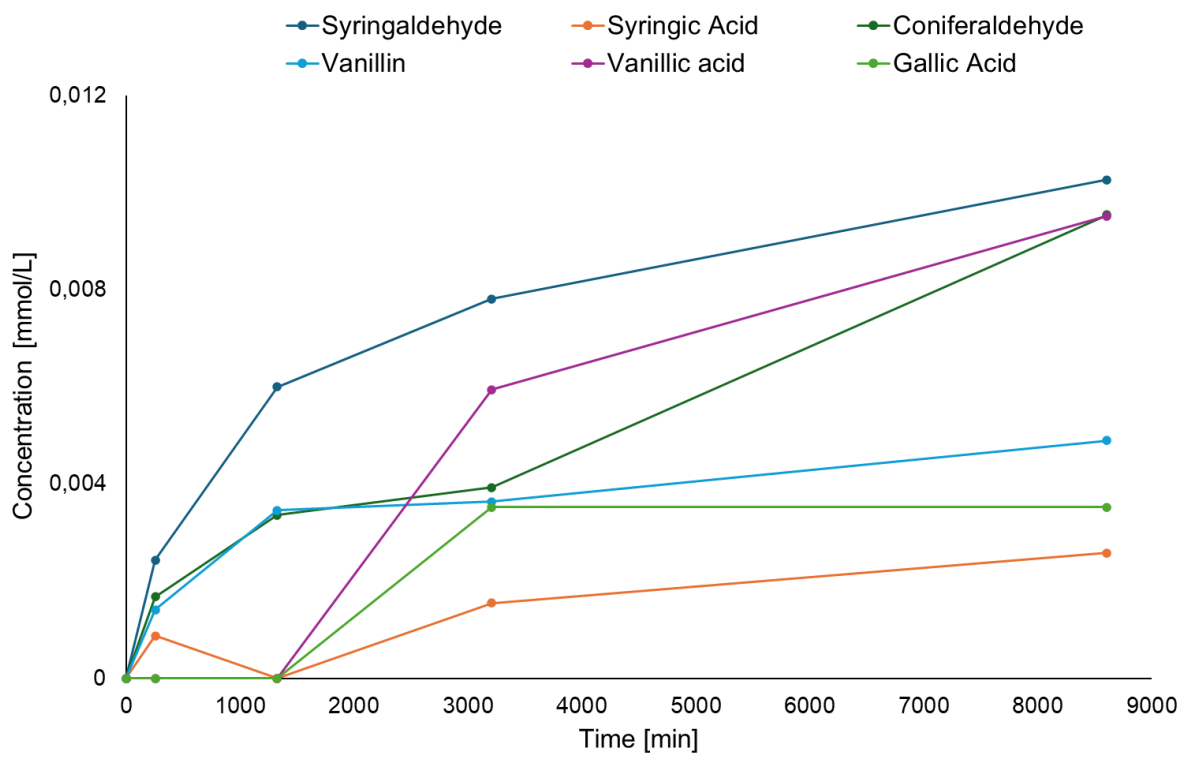

Figure A.2: Sample G-200, experimental concentrations trends.

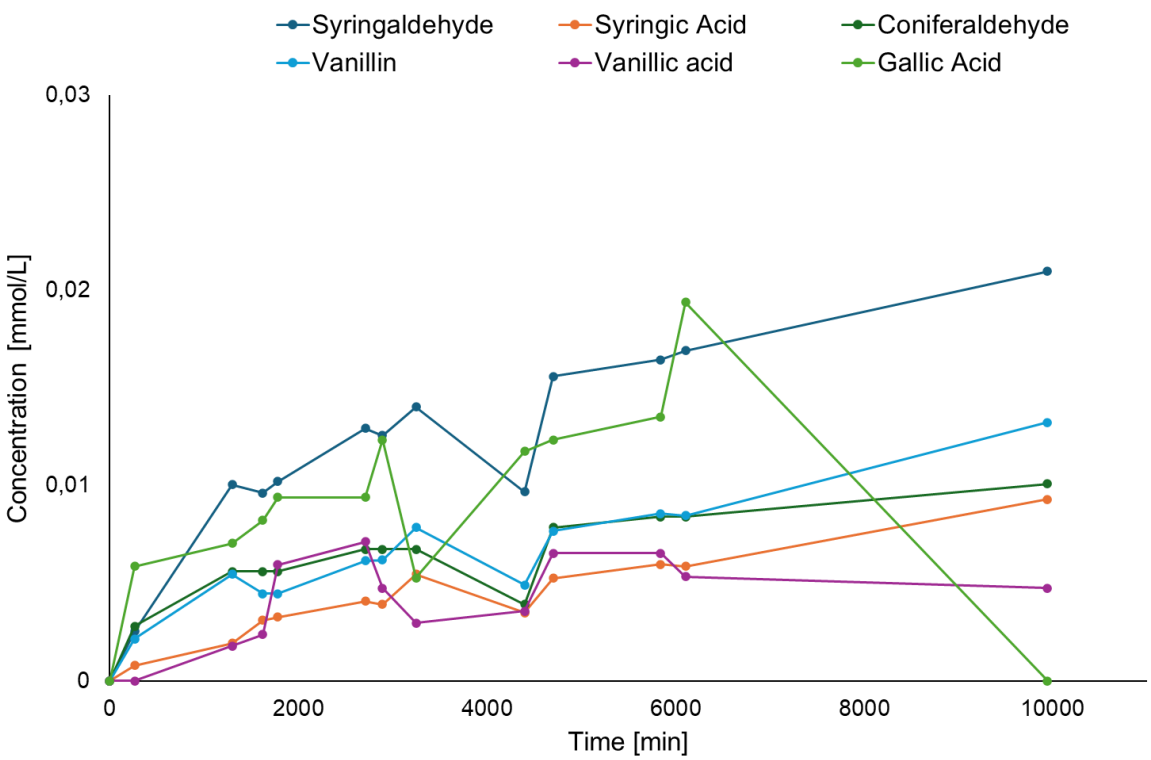

Figure A.3: Sample G-700, experimental concentrations trends.

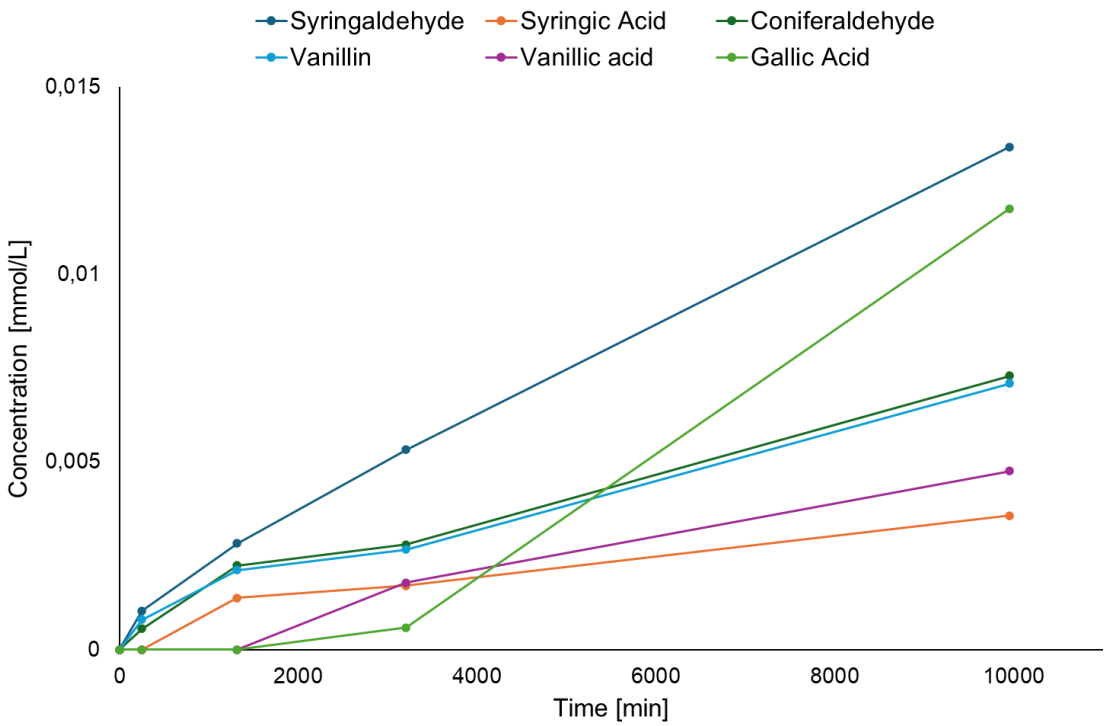

Figure A.4: Sample G-800, experimental concentrations trends.

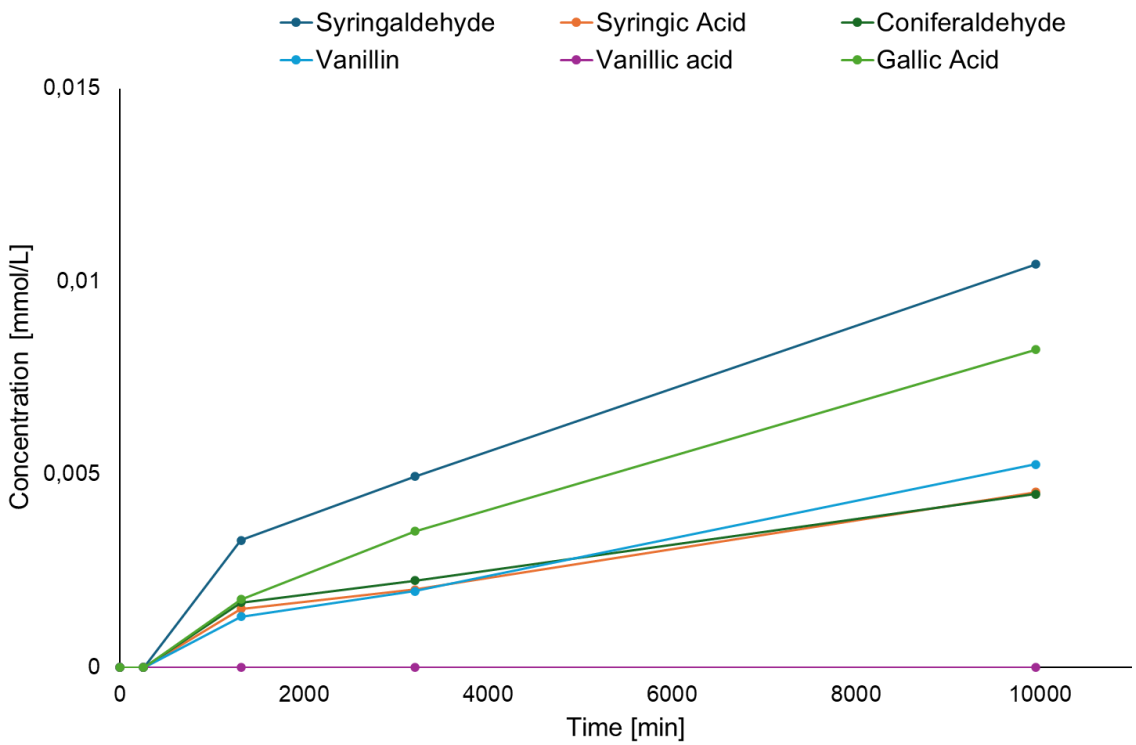

Figure A.5: Sample G-900, experimental concentrations trends.

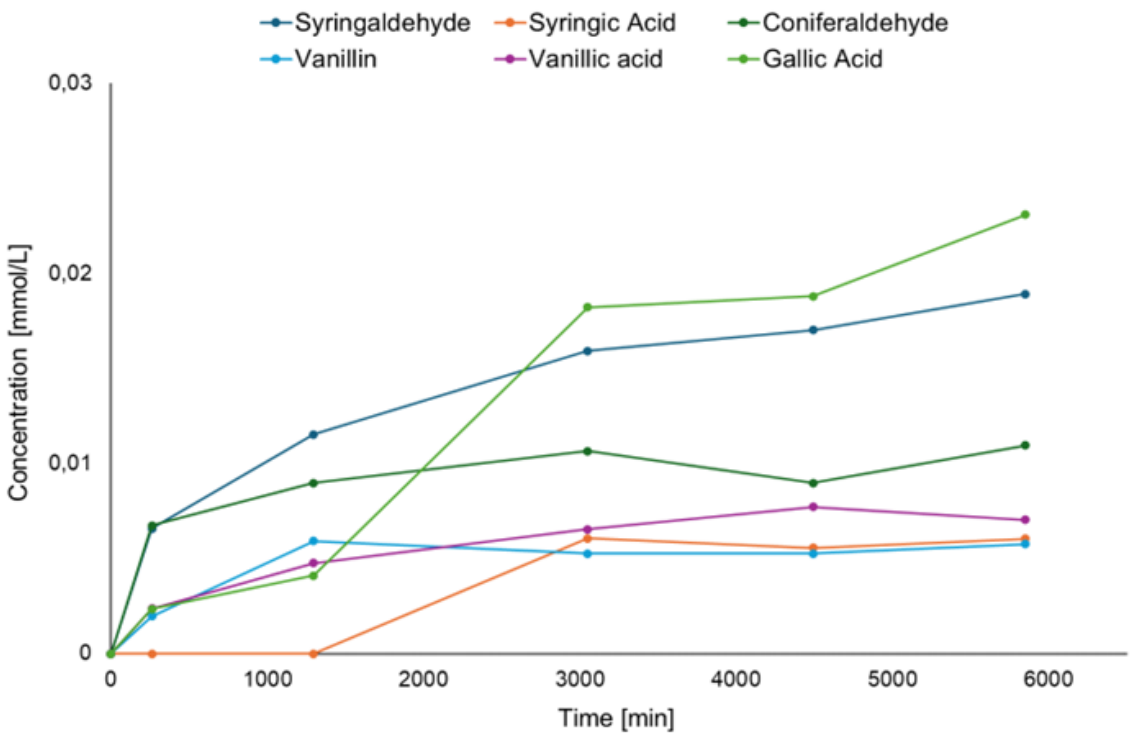

Figure A.6: Sample M-200, experimental concentrations trends.

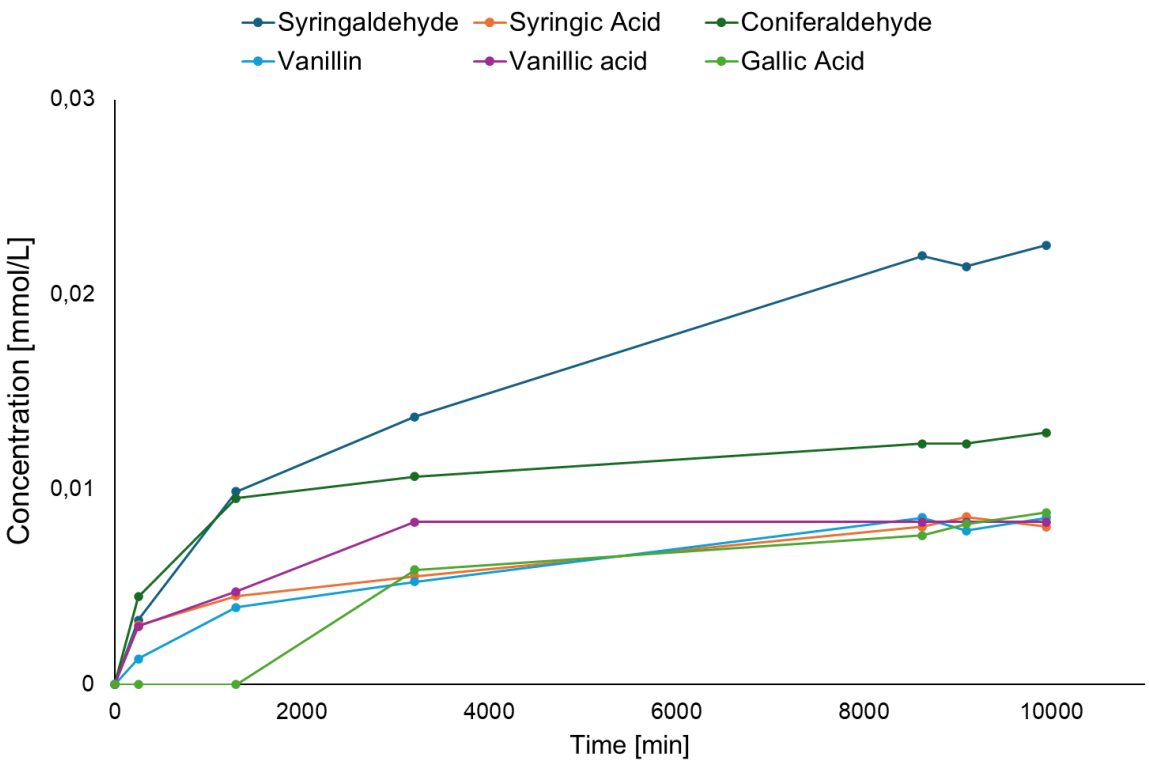

Figure A.7: Sample M-400, experimental concentrations trends.

A.2. Data collection and calculations

This appendix section presents the data, partly taken from literature and partly calculated, used to develop the model and achieve the fitting of the experimental data.

In order to solve the system of equations created to describe the ageing process, it was necessary to set values for the concentrations of ethanol and water in a hydroalcoholic solution.

A.2.1. Solution characterization

In Table A.1 are reported the main parameters of the examined solution, together with the assumed values and their units of measurement.

Table A.A.1: Hydroalcoholic solution parameters.

Parameter	Value
ABV	$0{,}630\ \frac{L_{EtOH}}{L_{solution}}$
ρ_{EtOH}	$0{,}789\ \frac{kg}{L}$
MW_{EtOH}	$46{,}068\ \frac{kg}{kmol}$
V_{EtOH}	$0{,}182\ L$
m_{EtOH}	$0{,}144\ kg$
ω_{EtOH}	0,57401
n_{EtOH}	$0{,}00312\ kmol$
x_{EtOH}	0,34490
C_{EtOH}	$0{,}010789\ \frac{kmol}{L}$
WBV	$0{,}370\ \frac{L_{H_2O}}{L_{solution}}$

ρ_{H_2O}	$0{,}997\ \frac{kg}{L}$
MW_{H_2O}	$18\ \frac{kg}{kmol}$
V_{H2O}	$0{,}10693\ L$
m_{H_2O}	$0{,}10661\ kg$
ω_{H_2O}	0,42599
n_{H_2O}	$0{,}00592\ kmol$
x_{H_2O}	0,65510
C_{H_2O}	$0{,}020493\ \frac{kmol}{L}$
$V_{solution}$	$0{,}289\ L$
$\rho_{solution}$	$0{,}86596\ \frac{kg}{L}$
$MW_{solution}$	$27{,}68077\ \frac{kg}{kmol}$

The following equations illustrate the procedure step by step that has been followed to characterize the solution.

$$V_{EtOH} = ABV * V_{solution} * m_{EtOH} = \rho_{EtOH} * V_{EtOH} \tag{A.1}$$

$$\omega_{EtOH} = \frac{m_{EtOH}}{m_{EtOH}+m_{H_2O}} \tag{A.2}$$

$$WBV = 1 - ABV \tag{A.3}$$

$$V_{H2O} = WBV * V_{solution} \tag{A.4}$$

$$m_{H_2O} = \rho_{H_2O} * V_{H_2O} \tag{A.5}$$

$$\omega_{H_2O} = 1 - \omega_{EtOH} \tag{A.6}$$

$$x_{EtOH} = \frac{\omega_{EtOH}/MW_{EtOH}}{\frac{\omega_{EtOH}}{MW_{EtOH}} + \frac{\omega_{H_2O}}{MW_{H_2O}}} \tag{A.7}$$

$$x_{H_2O} = 1 - x_{EtOH} \tag{A.8}$$

$$n_{EtOH} = \frac{m_{EtOH}}{MW_{EtOH}} \tag{A.9}$$

$$C_{EtOH} = \frac{n_{EtOH}}{V_{solution}} \tag{A.10}$$

$$n_{H_2O} = \frac{m_{H_2O}}{MW_{H_2O}} \tag{A.11}$$

$$C_{H_2O} = \frac{n_{H_2O}}{V_{solution}} \tag{A.12}$$

$$\rho_{solution} = \frac{1}{\frac{\omega_{EtOH}}{\rho_{EtOH}} + \frac{\omega_{H_2O}}{\rho_{H_2O}}} \tag{A.13}$$

$$MW_{solution} = x_{EtOH} * MW_{EtOH} + x_{H_2O} * MW_{H_2O} \tag{A.14}$$

A.2.2. Headspace characterization

For the same purpose a similar approach has been used to determine the concentration of oxygen in the hydroalcoholic solution starting by analysing the air headspace in the reactor.

The Table A.2 displays main parameters assumed for the calculations.

Table A.A.2: Oxygen parameters.

Parameter	Value
P	$1\ atm$
y_{O_2}	0,21
H_{O_2}	$1788{,}386\ atm$
x_{O_2}	0,000119
C_{O_2}	$3{,}72215\ \frac{mmol}{L}$

The concentration of oxygen has been obtained by considering vapour-liquid equilibrium at the interface of solution and air.

$$x_{O_2} = \frac{P * y_{O_2}}{H_{O_2}} \tag{A.15}$$

$$C_{O_2} = \frac{x_{O_2} * \rho_{solution}}{MW_{solution}} \tag{A.16}$$

A.2.3. Wood matrix characterization

Lignin and tannins, two of the main wood constituents, are the reactants of the first hydroalcoholic reactions. At this regard it was necessary to determine their concentration values. Tabel A.3 shows the main parameters concerning wood matrix specs.

Table A.A.3: Wood parameters.

Parameter	Value
ε	0,57
τ	3
$\frac{m_{wood}}{V_{solution}}$	$31\ \frac{g}{L_{solution}}$
MW_{lignin}	$10000\ \frac{kg}{kmol}$
$\frac{m_{lignin}}{V_{solution}}$	$12{,}4\ \frac{g}{L}$
ω_{lignin}	0,40
C_{lignin}	$1{,}24\ \frac{mmol}{L}$
$MW_{tannins}$	$1250\ \frac{kg}{kmol}$
$\frac{m_{tannins}}{V_{solution}}$	$4{,}65\ \frac{g}{L}$
$\omega_{tannins}$	0,15
$C_{tannins}$	$3{,}72\ \frac{mmol}{L}$

In the following lines is reported the procedure referred to a generic i compound used to determine the concentrations of lignin ad tannins.

$$m_i = \omega_i * m_{wood} \tag{A.17}$$

$$C_i = \frac{m_i}{MW_{lignin}} \tag{A.18}$$

A.2.4. Surface to volume parameter

Since according to the Shrinking Core Model, reactions take place on the wood surface between the reactive layer and the consumed ash layer, another key point was to introduce the ratio of wood surface area per wood volume $\left(\frac{S}{V}\right)_{wood}$ into the constructed system of equations.

Starting with the $\frac{S_{wood}}{V_{solution}}$ parameter set by the experiments conducted on the samples under investigation, the procedure for deriving the ratio is illustrated in the equations below.

$$S_{wood} = \frac{S_{wood}}{V_{solution}} * V_{solution} \tag{A.19}$$

$$V_{wood} = \frac{m_{wood}}{V_{solution}} * V_{solution} \tag{A.20}$$

$$\left(\frac{S}{V}\right)_{wood} = \frac{S_{wood}}{V_{wood}} \tag{A.21}$$

The Table A.4 compares $\frac{S_{wood}}{V_{solution}}$ values with the obtained $\frac{S_{wood}}{V_{wood}}$ for each sample.

Table A.A.4: $\frac{S_{wood}}{V_{solution}}$ against $\frac{S_{wood}}{V_{wood}}$ values.

Sample	$\frac{S_{wood}}{V_{solution}}$	$\frac{S_{wood}}{V_{wood}}$
G-000	7,96	192,58
G-100	7,94	192,10
G-200	8,55	206,85
G-300	7,96	192,58
G-400	7,44	180,00
G-500	7,95	192,34
G-600	10,32	249,68
G-700	19,11	462,34
G-800	8,58	207,58
G-900	19,11	462,34
M-000	14,92	360,97
M-100	15,07	364,60
M-200	30,61	740,56
M-300	19,07	461,37
M-400	18,71	452,66
M-500	26,12	631,94

A.2.5. Theoretical diffusion coefficients

In order to have reference values of diffusivity to compare with those obtained from the manipulation of parameters in model development phase, literature researches were carried out. Reference values are given in Table A.5, referring in particular to the diffusivity of the species considered in water or ethanol mixtures. Only orders of magnitude are given, as referred when comparing the numbers obtained from the model.

Table A.A.5: Diffusion coefficients order of magnitudes from literature

Diffusion coefficient	Average value from literature
$D_{EtOH}\left[\frac{m^2}{s}\right]$	**10^{-9}**
$D_{H_2O}\left[\frac{m^2}{s}\right]$	**10^{-5}**
$D_{O_2}\left[\frac{m^2}{s}\right]$	**10^{-9}**
$D_S\left[\frac{m^2}{s}\right]$	**10^{-9}**
$D_{SA}\left[\frac{m^2}{s}\right]$	**10^{-10}**
$D_C\left[\frac{m^2}{s}\right]$	**10^{-9}**
$D_V\left[\frac{m^2}{s}\right]$	**10^{-9}**
$D_{VA}\left[\frac{m^2}{s}\right]$	**10^{-10}**

$D_{GA}\left[\frac{m^2}{s}\right]$	**10^{-10}**

A.3. Residence times evaluation

For the purposes of developing the model, it was necessary to introduce a simplification of the experimental set-up that allowed to consider a single batch system as a first approximation. This was possible because the calculation of residence times in the reactor and recirculation times confirmed that the recycling times are considerably longer than those in the reactor.

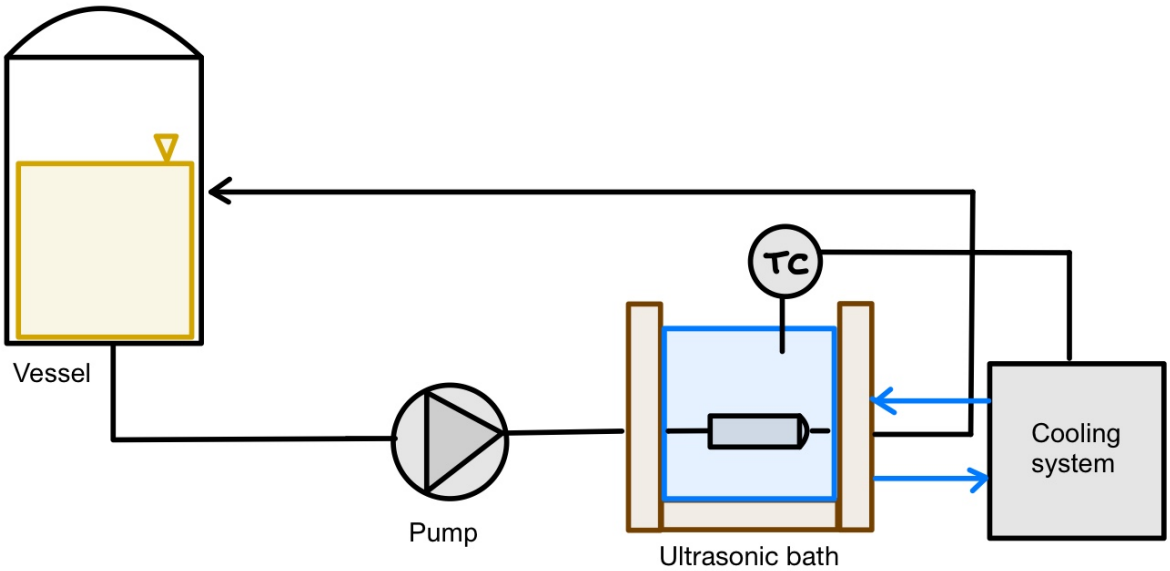

Figure A.8: Experimental set-up.

In the following lines are reported the calculations of the residence times:

$$V_{Reactor} = \frac{\pi d^2}{4} * l = \frac{\pi * 1{,}9^2\ cm^2}{4} * 10{,}5\ cm = 2{,}83\ cm^3 \tag{A.22}$$

$$\tau_{Reactor} = \frac{V_{Reactor}}{\dot{Q}_{whisky}} = \frac{2{,}83}{56}\frac{cm^3}{\frac{cm^3}{min}} = 0{,}051\ min = 3\ sec \tag{A.23}$$

$$\tau_{Recirculation} = \frac{V_{tank}}{\dot{Q}_{whisky}} = \frac{2000}{56}\frac{cm^3}{\frac{cm^3}{min}} = 35{,}7\ min = 2100\ sec \tag{A.24}$$

A.4. Step-charts

Chapter 5.2.1.2 discusses the construction of the step-graph obtained by variation of the classical Forward Euler model. For the sake of completeness of the discussion in the main text, the graphs below demonstrate that the same behaviour has been considered for the concentration evolution of each compound.

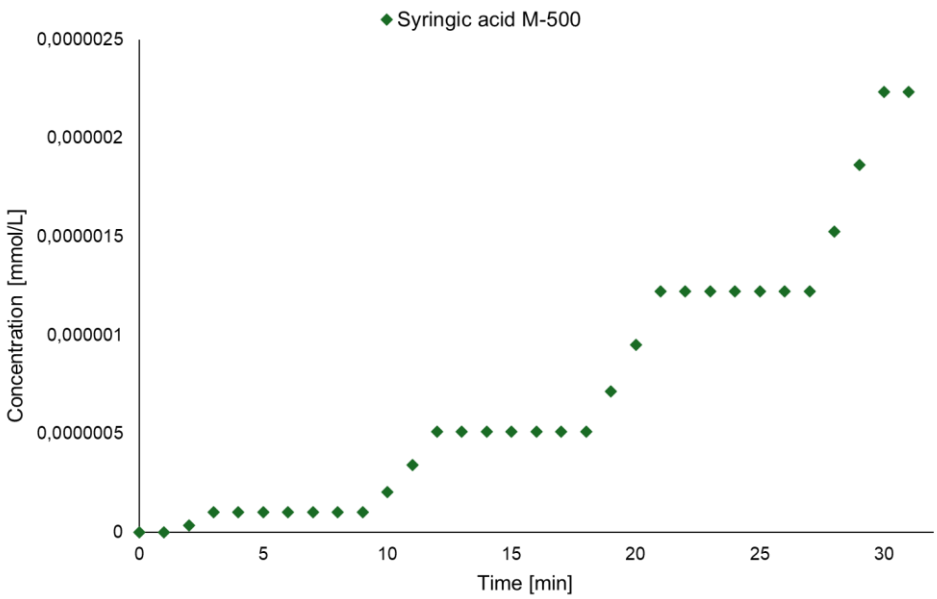

Figure A.9: Syringic acid, sample M-500, step-chart visualization.

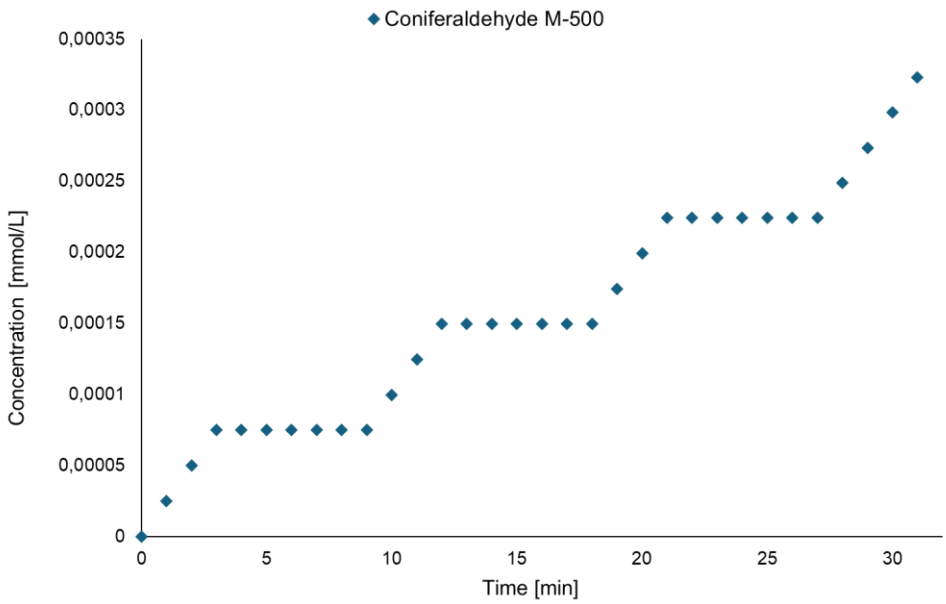

Figure A.10: Coniferaldehyde, sample M-500, step-chart visualization.

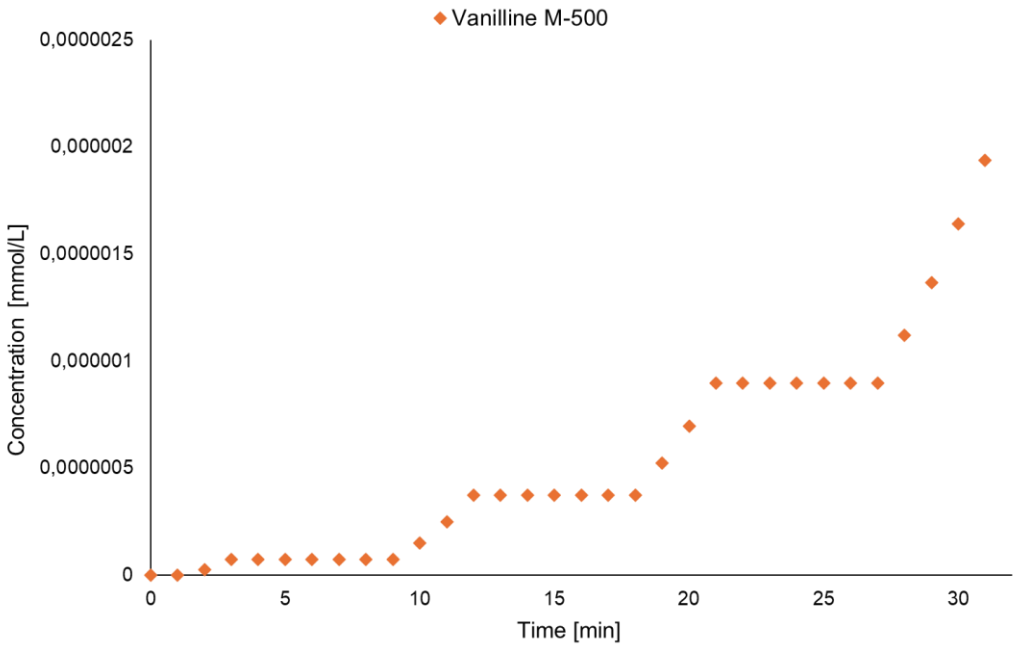

Figure A.11: Vanillin, sample M-500, step-chart visualization.

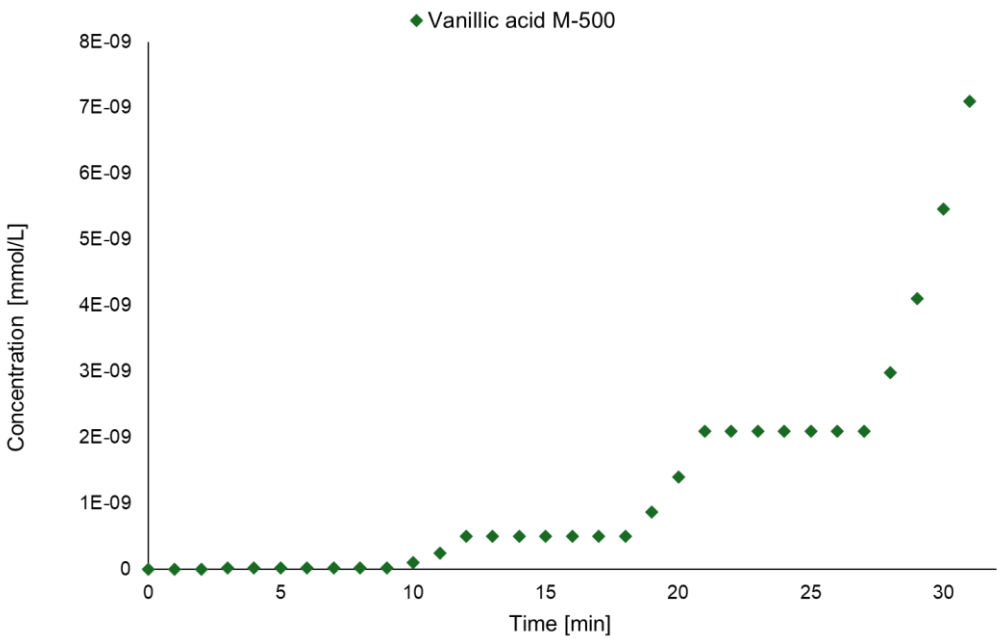

Figure A.12: Vanillic acid, sample M-500, step-chart visualization.

List of Figures

Figure 1.1: Whisky market fragmentation into premium, super-premium and high-end premium. 7
Figure 1.2: Whisky market fragmentation and size. 7
Figure 1.3: Whisky production process scheme. 9
Figure 1.4: Pot still distillation configuration [41]. 13
Figure 1.5: Column still distillation configuration [41]. 14
Figure 1.6: Lignin representation and its phenylpropane units [59]. 20
Figure 1.7: Syringil and Coniferyl reaction scheme [55]. 23
Figure 1.8: Hydrolysis of tannins [66]. 24
Figure 2.1: Ultrasound applications in different frequencies range [79]. 30
Figure 2.2: Schematic representation of the lifetime of a cavitation bubble [83]. 32
Figure 2.3: Sonicated whisky ageing representation [97]. 37
Figure 4.1: Experimental set-up representation. 40
Figure 4.2: Shrinking core system and its five distinctive steps. 45
Figure 4.3: Shrinking core system applied to the key study. 48
Figure 4.4: Representation of Forward Euler method [116]. 49
Figure 5.1: Sample G-000, experimental concentrations trends. 54
Figure 5.2: Sample G-300, experimental concentrations trends. 55
Figure 5.3: Sample M-000, experimental concentrations trends. 55
Figure 5.4: Sample M-300, experimental concentrations trends. 56
Figure 5.5: Sample M-500, experimental concentrations trends. 56
Figure 5.6: Sample M-100, experimental concentrations trends with evident outliers. 57
Figure 5.7: Sample G-600, experimental concentrations trends with evident outliers. 58

Figure 5.8: Sample G-400, experimental concentrations trends with evident outliers. 58
Figure 5.9: Sample G-500, experimental concentrations trends with evident outliers 59
Figure 5.10: Syringaldehyde, ABV effect by comparing G-000 and G-100 samples.... 61
Figure 5.11: Syringic acid, ABV effect by comparing G-000 and G-100 samples..... 61
Figure 5.12: Coniferaldehyde, ABV effect by comparing G-000 and G-100 samples.. 62
Figure 5.13: Vanillin, research of ABV effect by comparing G-000 and G-100 samples. 62
Figure 5.14: Vanillic acid, ABV effect by comparing G-000 and G-100 samples..... 63
Figure 5.15: Gallic acid, ABV effect by comparing G-000 and G-100 samples..... 63
Figure 5.16: Syringaldehyde, M-500 sample, order of reaction research. 66
Figure 5.17: Syringic acid, M-500 sample, order of reaction research. 67
Figure 5.18: Coniferaldehyde, M-500 sample, order of reaction research..... 67
Figure 5.19: Vanillin, M-500 sample, order of reaction research. 68
Figure 5.20: Vanillic acid, M-500 sample, order of reaction research. 68
Figure 5.21: Syringaldehyde, sample M-500, step-chart visualization. 71
Figure 5.22: Syringil family, M-500 sample, experimental fitting second attempt. 72
Figure 5.23: Coniferyl family, M-500 sample, experimental fitting second attempt. .. 72
Figure 5.24: Syringil family, M-500 sample, experimental fitting third attempt..... 76
Figure 5.25: Syringil family, M-500 sample, experimental fitting fourth attempt. 79
Figure 5.26: Coniferyl family, M-500 sample, experimental fitting fourth attempt. ... 79
Figure 5.27: Syringil family, M-500 sample, experimental fitting last attempt. 86
Figure 5.28: Coniferyl family, M-500 sample, experimental fitting last attempt. 86
Figure 5.29: Gallic acid, M-300 sample, experimental fitting final attempt. 90
Figure 5.30: Syringil family, G-000 sample, experimental fitting last attempt. 91
Figure 5.31: Syringil family, G-100 sample, experimental fitting last attempt. 92
Figure 5.32: Syringil family, G-200 sample, experimental fitting last attempt. 92
Figure 5.33: Syringil family, G-300 sample, experimental fitting last attempt. 93
Figure 5.34: Syringil family, G-400 sample, experimental fitting last attempt. 93
Figure 5.35: Syringil family, G-500 sample, experimental fitting last attempt. 94
Figure 5.36: Syringil family, G-700 sample, experimental fitting last attempt. 94

Figure 5.37: Syringil family, G-900 sample, experimental fitting last attempt. 95
Figure 5.38: Syringil family, M-000 sample, experimental fitting last attempt. 95
Figure 5.39: Syringil family, M-200 sample, experimental fitting last attempt. 96
Figure 5.40: Syringil family, M-300 sample, experimental fitting last attempt. 96
Figure 5.41: Syringil family, M-400 sample, experimental fitting last attempt. 97
Figure 5.42: Syringil family, M-500 sample, experimental fitting last attempt. 97
Figure 5.43: Coniferyl family, G-000 sample, experimental fitting last attempt. 102
Figure 5.44: Coniferyl family, G-100 sample, experimental fitting last attempt. 102
Figure 5.45: Coniferyl family, G-200 sample, experimental fitting last attempt. 103
Figure 5.46: Coniferyl family, G-300 sample, experimental fitting last attempt. 103
Figure 5.47: Coniferyl family, G-400 sample, experimental fitting last attempt. 104
Figure 5.48: Coniferyl family, G-700 sample, experimental fitting last attempt. 104
Figure 5.49: Coniferyl family, G-800 sample, experimental fitting last attempt. 105
Figure 5.50: Coniferyl family, M-000 sample, experimental fitting last attempt. 105
Figure 5.51: Coniferyl family, M-200 sample, experimental fitting last attempt. 106
Figure 5.52: Coniferyl family, M-300 sample, experimental fitting last attempt. 106
Figure 5.53: Coniferyl family, M-400 sample, experimental fitting last attempt. 107
Figure 5.54: Coniferyl family, M-500 sample, experimental fitting last attempt. 107
Figure 5.55: Gallic acid, G-000 sample, experimental fitting final attempt. 111
Figure 5.56: Gallic acid, G-100 sample, experimental fitting final attempt. 112
Figure 5.57: Gallic acid, G-300 sample, experimental fitting final attempt. 112
Figure 5.58: Gallic acid, G-400 sample, experimental fitting final attempt. 113
Figure 5.59: Gallic acid, G-700 sample, experimental fitting final attempt. 113
Figure 5.60: Gallic acid, M-000 sample, experimental fitting final attempt. 114
Figure 5.61: Gallic acid, M-200 sample, experimental fitting final attempt. 114
Figure 5.62: Gallic acid, M-300 sample, experimental fitting final attempt. 115
Figure 5.63: Gallic acid, M-400 sample, experimental fitting final attempt. 115
Figure A.1: Sample G-100, experimental concentrations trends. 133
Figure A.2: Sample G-200, experimental concentrations trends. 134
Figure A.3: Sample G-700, experimental concentrations trends. 134
Figure A.4: Sample G-800, experimental concentrations trends. 135

Figure A.5: Sample G-900, experimental concentrations trends. 135
Figure A.6: Sample M-200, experimental concentrations trends..... 136
Figure A.7: Sample M-400, experimental concentrations trends..... 136
Figure A.8: Experimental set-up. 143
Figure A.9: Syringic acid, sample M-500, step-chart visualization. 144
Figure A.10: Coniferaldehyde, sample M-500, step-chart visualization. 144
Figure A.11: Vanillin, sample M-500, step-chart visualization..... 145
Figure A.12: Vanillic acid, sample M-500, step-chart visualization. 145

List of Tables

Table 2.1: Examples of sonicated industrial processes 34

Table 4.1: Units of kinetic constants for different reaction orders..... 43

Table 5.1: Samples operative parameters. 52

Table 5.2: Samples exclusion for each congeners group. 60

Table 5.3: Sample M-500, kinetic constants values from the first attempt. 69

Table 5.4: Sample M-500, manipulated diffusivity values from the fourth attempt ... 80

Table 5.5: Sample M-500, manipulated kinetic constant values from the last attempt. 87

Table 5.6: Syringil family, sample M-500, manipulated diffusivity coefficient values from the last attempt. 87

Table 5.7: Coniferyl family, sample M-500, manipulated diffusivity coefficient values from the last attempt. 87

Table 5.8: Gallic acid, sample M-300, manipulated parameters values from the final attempt. 90

Table 5.9: Syringil family, manipulated kinetic constant values from the last attempt. 98

Table 5.10: Syringil family, manipulated diffusion coefficient values from the last attempt. 99

Table 5.11: Coniferyl family, manipulated kinetic constant values from the last attempt. 108

Table 5.12: Coniferyl family, manipulated diffusion coefficient values from the last attempt. 109

Table 5.13: Gallic acid, manipulated parameters values from the final attempt. 116

Table A.1: Hydroalcoholic solution parameters. 137

Table A.2: Oxygen parameters. 139

Table A.3: Wood parameters. 140

Table A.4: $SwoodVsolution$ against $SwoodVwood$ values 141

Table A.5: Diffusion coefficients order of magnitudes from literature 142

List of symbols

Variable	Description	SI unit
$V_{solution}$	Volume of the solution	[L]
ABV	Alcohol by volume of solution	%
WBV	Water by volume of solution	%
ρ_i	density of a generic compound i	$[Kg/m^3]$
MW_i	Molecular weight of a generic compound i	$[\frac{mg}{mmol}]$
V_i	Volume of a generic compound i	$[m^3]$
m_i	Mass of a generic compound i	$[Kg]$
n_i	Moles of a generic compound i	$[mol]$
ω_i	Massive fraction of a generic compound i	[-]
x_i	Molar fraction of a generic compound i in the liquid phase	[-]
y_i	Molar fraction of a generic compound i in the gas phase	[-]
P	System pressure	bar
T	System temperature	[K]
N	Diffusive flux	$[\frac{mmol}{s}]$
R_S	Surface kinetic reaction rate	$[\frac{mmol}{s*m^2}]$
R	Kinetic reaction rate	$[\frac{mmol}{s*m^3}]$
t	Time	$[s]$
$time_{US}$	Sonication time	$[s]$
$time_{TOT}$	Real time	$[s]$
NC_{ON}	Number of on cycles	[-]
NC_{TOT}	Overall number of cycles	[-]
d	Diameter of the reactor	$[m]$
l	Length of the reactor	$[m]$
$V_{Reactor}$	Reactor volume	$V_{Reactor}$
V_{tank}	Vessel volume	V_{tank}
$\dot{Q}_{whisky}$	Volumetric flow rate of whisky	$[m^3/s]$

$\tau_{Reactor}$	Residence time in the reactor	$[s]$
$\tau_{Recirculation}$	Residence time of a recycle	$[s]$
$C^{\circ}{}_{i}$	Concentration of compound i in the bulk of solution	$[\frac{mmol}{L}]$
C_i^I	Concentration of compound i at the interface	$[\frac{mmol}{L}]$
C_L	Concentration of lignin	$[\frac{mmol}{L}]$
C_{EtOH}	Concentration of ethanol	$[\frac{mmol}{L}]$
C_{O_2}	Concentration of oxygen	$[\frac{mmol}{L}]$
C_A	Concentration of compound A	$[\frac{mmol}{L}]$
C_B	Concentration of compound B	$[\frac{mmol}{L}]$
C_S	Concentration of syringaldehyde	$[\frac{mmol}{L}]$
C_{SA}	Concentration of syringic acid	$[\frac{mmol}{L}]$
C_C	Concentration of coniferaldehyde	$[\frac{mmol}{L}]$
C_V	Concentration of vanillin	$[\frac{mmol}{L}]$
C_{VA}	Concentration of vanillic acid	$[\frac{mmol}{L}]$
C_{GA}	Concentration of gallic acid	$[\frac{mmol}{L}]$
$D_{S,A}$	Diffusion coefficient of compound A through a solid matrix S	$[m^2/s]$
D_{EtOH}	Diffusion coefficient of ethanol	$[m^2/s]$
D_{H_2O}	Diffusion coefficient of water	$[m^2/s]$
D_{O_2}	Diffusion coefficient of oxygen	$[m^2/s]$
D_S	Diffusion coefficient of syringaldehyde	$[m^2/s]$
D_{SA}	Diffusion coefficient of syringic acid	$[m^2/s]$
D_C	Diffusion coefficient of coniferaldehyde	$[m^2/s]$
D_V	Diffusion coefficient of vanillin	$[m^2/s]$
D_{VA}	Diffusion coefficient of vanillic acid	$[m^2/s]$
D_{GA}	Diffusion coefficient of gallic acid	$[m^2/s]$

$D_{EtOH\ eff}$	Effective diffusion coefficient of ethanol	$[m^2/s]$
$D_{H_2O\ eff}$	Effective diffusion coefficient of water	$[m^2/s]$
$D_{O_2\ eff}$	Effective diffusion coefficient of oxygen	$[m^2/s]$
$D_{S\ eff}$	Effective diffusion coefficient of syringaldehyde	$[m^2/s]$
$D_{SA\ eff}$	Effective diffusion coefficient of syringic acid	$[m^2/s]$
$D_{C\ eff}$	Effective diffusion coefficient of coniferaldehyde	$[m^2/s]$
$D_{V\ eff}$	Effective diffusion coefficient of vanillin	$[m^2/s]$
$D_{VA\ eff}$	Effective diffusion coefficient of vanillic acid	$[m^2/s]$
$D_{GA\ eff}$	Effective diffusion coefficient of gallic acid	$[m^2/s]$
δ	Thickness of the ash layer	$[m]$
ε	Wood porosity	$[-]$
τ	Wood tortuosity	$[-]$
S_{wood}	Wood external surface	$[m^2]$
V_{wood}	Wood volume	$[m^3]$
k_1	Kinetic constant of lignin ethanolysis giving syringaldehyde	It depends on the attempt
k_2	Kinetic constant of syringaldehyde oxidation	It depends on the attempt
k_3	Kinetic constant of syringic acid esterification	It depends on the attempt
k_4	Kinetic constant of lignin ethanolysis giving coniferaldehyde	It depends on the attempt
k_5	Kinetic constant of coniferaldehyde hydrolysis	It depends on the attempt
k_6	Kinetic constant of vanillin oxidation	It depends

		on the attempt
k_7	Kinetic constant of vanillic acid esterification	It depends on the attempt
k_8	Kinetic constant of tannins hydrolysis	It depends on the attempt
k_9	Kinetic constant of gallic acid esterification	It depends on the attempt

Acknowledgments
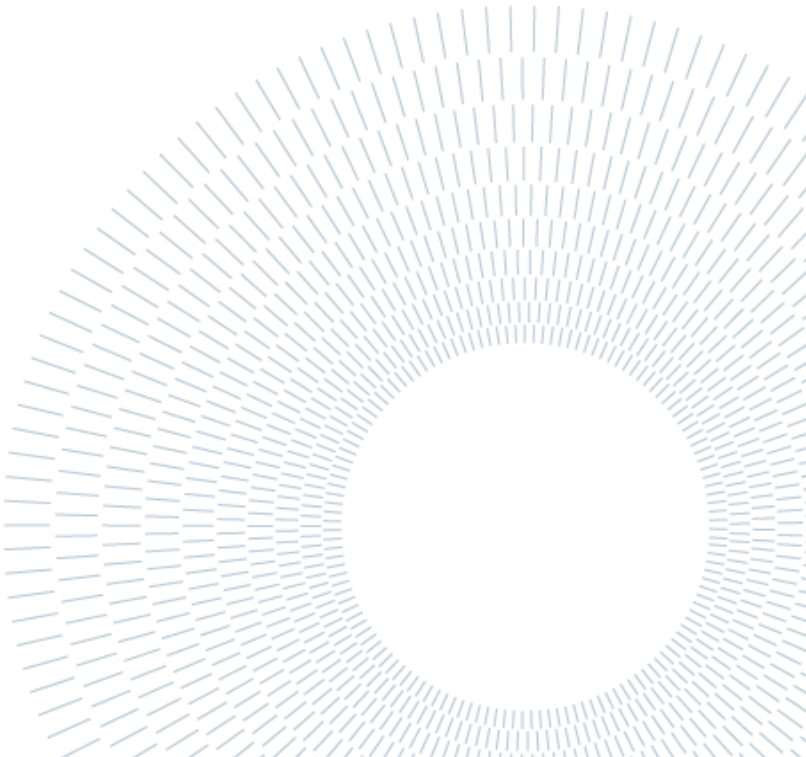
Our sincerest thanks are extended to our project supervisor and mentor, Professor Maurizio Masi, for his encouragement and guidance during the development of this Thesis. His enthusiasm for the topic inspired us to feel the same way.
We would be remiss in not mentioning our parents, relatives and friends who encouraged us in every step of this journey.